UNIVERSIDADE FEDERAL DE PELOTAS
Centro de Ciências Químicas, Farmacêuticas e de Alimentos
Programa de Pós-Graduação em Bioquímica e Bioprospecção

Tese de doutorado

O USO DA TERAPIA FOTODINÂMICA EM LINHAGEM DE MELANOMA METASTÁTICO

Gabriela Klein Couto

Pelotas, 21 de outubro de 2020

Gabriela Klein Couto

O USO DA TERAPIA FOTODINÂMICA EM LINHAGEM DE MELANOMA METASTÁTICO

Tese apresentada ao Programa de Pós-Graduação em Bioquímica e Bioprospecção do Centro de Ciências Químicas, Farmacêuticas e de Alimentos da Universidade Federal de Pelotas, como requisito parcial à obtenção do título de Doutora em Ciências

Orientador: Prof. Dr. Tiago Veiras Collares

Co-Orientador: Profª. Drª. Fabiana Seixas

Pelotas, 21 de outubro de 2020.

Gabriela Klein Couto

O USO DA TERAPIA FOTODINÂMICA EM LINHAGEM DE MELANOMA METASTÁTICO

Tese aprovada, como requisito parcial, para obtenção do grau de Doutora em Ciências, Programa de Pós-Graduação em Bioquímica e Bioprospecção, Centro de Ciências Químicas, Farmacêuticas e de Alimentos, Universidade Federal de Pelotas.
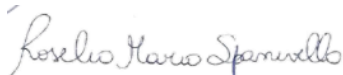
Data da Defesa: 21 de outubro de 2020.

Banca examinadora:

....
Prof. Dr. Tiago Veiras Collares (Orientador)
Doutor em Biotecnologia pela Universidade Federal de Pelotas

....
Prof. Drª. Jenifer Saffi
Doutora em Ciências Biológicas pela Universidade Federal do Rio Grande

do Sul
....
Prof. Drª. Roselia Maria Spanevello
Doutora em Ciências Biológicas pela Universidade Federal do Rio Grande

do Sul
....
Prof. Dr. Bernardo Almeida Iglesias
Doutor em Química pela Universidade de São Paulo

Dedico este trabalho à minha família,
meus pais e meu irmão,
ao meu amor e companheiro de vida Gustavo,
ao pequeno Martín,
ao meu grupo de pesquisa em Biotecnologia do Câncer,
e a todos os pacientes que tanto sofrem com o Melanoma.

AGRADECIMENTOS

"O caminho se faz caminhando..."
(Paulo Freire)

RESUMO

Terapias alternativas têm sido estudadas a fim de otimizar o tratamento de patologias agressivas como o câncer, que é uma das doenças com maior impacto na vida de pacientes. O melanoma é um tipo de câncer de pele que se origina e se desenvolve nos melanócitos. Foram estimados, para o triênio 2020-2022, cerca de 8.450 casos. Quando diagnosticado em estágios iniciais pode ser curado, no entanto, estudos tem demonstrado a disseminação do tumor para outras regiões (metástases) em diagnósticos tardios. A terapia fotodinâmica tem se mostrado uma alternativa promissora neste sentido. Sua ação, para que ocorra o dano celular, é fundamentada em três pontos principais: o uso de sensibilizadores, a luz e a molécula de oxigênio. Atualmente, tem-se buscado novas moléculas que apresentem propriedades ideais para que possam ser utilizadas, como fotossensibilizadores. Neste sentido, as porfirinas têm sido uma classe com interesse fotodinâmico em função de suas características químicas. Esta tese produziu 4 artigos científicos, sendo 2 revisões e 2 artigos originais, os quais avaliaram moléculas com potencial fototerapêutico em linhagem de melanoma e não-tumoral. A metodologia dos artigos originais foi realizada da seguinte forma: Linhagens de células WM1366 (melanoma metastático), CHO (ovário de hamster chinês) e A375 (melanoma metastático) foram cultivadas sob condições ideais e divididas em dois grupos: claro (submetidas a 30 minutos de luz) e escuro (sem exposição a luz). Análises de viabilidade celular, apoptose, ciclo celular, ancoragem molecular, PCR em tempo real e microscopia confocal foram realizadas a fim de respondermos questões como: inibição do crescimento celular, determinação de IC_{50}, identificação do possível mecanismo de morte celular e avaliação da integridade da célula (viabilidade de membrana e integridade do DNA). Cinco diferentes concentrações que variaram de 1,4 a 56 nm foram utilizadas nos diferentes grupos. Nossos resultados demonstram que ambas as porfirinas de platina(II) induzem apoptose por ativação das caspases 3 e 9 via Bax/BCL2. Ainda, indicam que ambas as porfirinas de platina(II) são promissoras como estratégia de administração de medicamentos, uma vez que apresentaram seletividade pelo receptor de LDL, demonstrado pela afinidade com a região N-terminal do ApoB-100 (responsável por carrear o ligante até o receptor de LDL). Somado a isso, análises de arranjo molecular com metais de transição como zinco, cobre e níquel, associados as porfirinas de platina, foram desenvolvidas, a fim de melhorar a ligação das porfirinas à receptores específicos (APOB-100, ERT-B, CAT, SOD e HSA), tornando assim a terapia mais efetiva. Nossos resultados *in vitro* demonstraram que a adição dos íons manteve a inibição da proliferação celular de melanoma metastático. Já os estudos de arranjo molecular mostraram que a adição destes metais melhoraram a força de ligação principalmente com os receptores APOB-100, ERT-B, SOD. Espera-se que os resultados deste trabalho possam contribuir para, futuramente, auxiliar na escolha de uma terapia mais especifica e eficaz contra o melanoma metastático.
Palavras-chave: Porfirinas de platina; fotossensibilizadores; Docking molecular; receptor de LDL; APO B-100; ERT-B, HSA; metais de transição; Câncer.

ABSTRACT

COUTO, Gabriela Klein. **The use of photodynamic therapy in a metastatic melanoma lineage.** 2020. 118f. Thesis (PhD in Biochemistry and Bioprospecting) - Graduate Program in Biochemistry and Bioprospecting of Federal University of Pelotas, 2020.

Alternative therapies have been studied to optimize the treatment of aggressive pathologies such as cancer, which is one of the diseases with the greatest impact on patients' lives. Melanoma is a type of skin cancer that originates and develops in melanocytes. For the period 2020-2022, an estimated 8,450 cases were estimated. When diagnosed in the early stages it can be cured, however, studies have shown the spread of the tumor to other regions (metastases) in late diagnoses. Photodynamic therapy has shown to be a promising alternative in this regard. Its action, for cell damage to occur, is based on three main points: the use of sensitizers, light and the oxygen molecule. Currently, new molecules have been sought that have ideal properties so that they can be used, as photosensitizers. In this sense, porphyrins have been a class with photodynamic interest due to their chemical characteristics. This thesis produced 4 scientific articles, 2 reviews and 2 original articles, which evaluated molecules with phototherapeutic potential in melanoma and non-tumor lineage. The methodology of the original articles was performed as follows: Cell lines WM1366 (metastatic melanoma), CHO (Chinese hamster ovary) and A375 (metastatic melanoma) were grown under ideal conditions and divided into two groups: clear (submitted to 30 minutes light) and dark (without exposure to light). Analyzes of cell viability, apoptosis, cell cycle, molecular anchoring, real-time PCR and confocal microscopy were performed in order to answer questions such as: inhibition of cell growth, determination of IC50, identification of the possible mechanism of cell death and evaluation of the integrity of the cell. cell (membrane viability and DNA integrity). Five different concentrations ranging from 1.4 to 56 nm were used in the different groups. Our results demonstrate that both platinum (II) porphyrins induce apoptosis by activating caspases 3 and 9 via Bax / BCL2. Still, they indicate that both platinum (II) porphyrins are promising as a drug administration strategy, since they showed selectivity for the LDL receptor, demonstrated by the affinity with the ApoB-100 N-terminal region (responsible for carrying the ligand to the LDL receptor). In addition, molecular arrangement analyzes with transition metals such as zinc, copper and nickel, associated with platinum porphyrins, were developed in order to improve the binding of porphyrins to specific receptors (APOB-100, ERT-B, CAT, SOD and HSA), thus making therapy more effective. Our in vitro results demonstrated that the addition of the ions maintained the inhibition of metastatic melanoma cell proliferation. Molecular arrangement studies have shown that the addition of these metals improved the binding strength mainly with APOB-100, ERT-B, SOD receptors. It is hoped that the results of this work may contribute to, in the future, assist in choosing a more specific and effective therapy against metastatic melanoma.

Keywords: Platinum porphyrins; photosensitizers; Molecular docking; LDL receptor; APO B-100; ERT-B, HSA; transition metals; Cancer.

LISTA DE FIGURAS

Figura 7: Representação esquemática das 3 gerações dos fotossensibilizadores utilizados na terapia fotodinâmica. No esquema demonstramos as evoluções de tais compostos. Na primeira geração observamos um número maior de limitações nestes compostos. Estas limitações foram resolvidas, em partes, pelas moléculas de segunda geração, no entanto, atualmente, estão em desenvolvimento moléculas que sejam ainda mais efetivas e seletivas. Fonte: Próprio autor.

Figura 8: Representação esquemática do macrociclo tetrapirrólico comum das porfirinas. Fonte: Enciclopédia Britânica.

ARTIGO 1

Figure 1. Biotechnology and photodynamic therapy in the areas of human / animal health and agriculture.

Figure 2. (A) Examples of most common tetrapyrrole macrocycle molecules used in PDT field and (B) 103 New photosensitizers generation for PDT and PDI application formulated by Luzitin SA, NIOPIK and 104 Pharmacyclics Inc.

ARTIGO 2

Figure 1. Results indicate the number of articles using each screening methodology by decade. The number of articles found for each topic searched is presented on the y axis. Different decades are presented in the x axis. Each bar represents a different screening method (in vitro, in vivo, and in silico) and the combination of more than one screening method: dark blue for in vivo, orange for in vitro, gray for in vivo/in vitro, yellow for in silico and light blue for all the three screening methods (in silico/in vitro/in vivo).

Figure 2. (A) Percentage of trials using different cell lines to form grafts in melanoma murine models for in vivo therapeutic screening. B16 stands for all B16 sublines. Skmel stands for all Skmel sublines. "Others" include UACC-62,

A2058, Na11+, Melanoma xenograft (MEXF), K1735, K1735-M2, HT168-M1, MM96L, Me501, M-14, Me30966, D10, 205, MeWo, VM1, Mel-JD, MEXF 989, WM 266-4, human malignant melanoma (BRO), and M24 cell lines. (B) Percentage of trials using each of the B16 sublines in syngeneic tumor models of melanoma for screening in vivo. Obs.: B16 indicates articles that do not specify a B16 subline.

Figure 3. Software most commonly used for melanoma drug screening. The most commonly used software is MOE (17%), followed by HTS (11%).

Figure 4. The steps necessary for safe, agile, and effective drug screening, which represent important steps for future development of precision medicine.

ARTIGO 3

Fig.1. Structural representation of free-base platinum(II) peripheral porphyrins3-PtTPyP and 4-PtTPyPused in this study. The hexafluorophosphate counter-ionsare omitted for more clarity.

Fig.2. Scheme of treatment protocol of WM1366 cells with 3-PtTPyP and 4-PtTPyP photosensitizers in photodynamic therapy.

Fig. 3. Effect of light action on photosensitizing molecule on cell proliferation. Porphyrin-treated and untreated cells were irradiated for 30 min. Dark group went totally in the dark for the same time. The graph shows the comparison within the light and dark group of 3-PtTPyP and 4-PtTPyP porphyrins. Data are expressed as mean ± SD of three independent times performed in triplicate. Fig. 3A–D: WM1366 cell line was treated with3-PtTPyP (Fig. A and B) and 4-PtTPyP (Fig.C and D) platinum(II) porphyrins at 5 different concentrations. Control group received no treatment with porphyrins. Fig. 3E–F: Effect of light on the photosensitizing molecule on cell proliferation of non-tumor cells. The CHO cell line was treated with3-PtTPyP (Fig. E and G) and4-PtTPyP (Fig. F and H) platinum (II) porphyrins at a concentration above the IC 50 and one below the predetermined IC 50 of each of the molecules. The concentrations used were:

5.62, 4.50 and 2.81 nM for 3-PtTPyP and 5.62, 3.01 and 2.81 for 4-PtTPyP. The concentrations used were: 5.62, 4.50 and 2.81 nM for 3-PtTPyP and 5.62, 3.01 and 2.81 for 4-PtTPyP. For comparison different letters in the chart denote significant difference between the groups. $p < .05$ was considered significant. Table 2 IC50 values of molecules 3-PtTPyPand 4-PtTPyP after 24 h of light exposition against WM1366 line. Porphyrin IC50(nM) 3-PtTPyP4.501 ± 0.58 4-PtTPyP 3.012 ± 0.27.

Fig.4. Molecular docking results. Fig. A and D represent the 3D molecular structure of platinum porphyrins 3-PtTPyP and 4-PtTPyP and their amino acid linkages of the B0582 LDL analog. Fig. B and E demonstrate the binding of platinum porphyrins to the N-terminal region of APO B-100. Fig. C and F demonstrate the similarity of B0582 anchoring of 3-PtTPyP and 4-PtTPyP molecules to the N-terminal region of APO B-100.

Fig.5. (A–F): Morphological analysis after treatment with 3-PtTPyP and 4-PtTPyP photosensitizers. WM1366 cells were stained Texas Red and DAPI - cytoplasm and nucleus, respectively. In the image we can observe a uniform cytoplasm in the control group (Figs. 5A and D) and in the treatments (3-PtTPyPand4-PtTPyP) we observe a reorganization of actin filaments (arrows Fig. 5B). A general thickening of actin fibers in the membrane, ruffling occurred at the border of its plasma membrane (arrows Fig. 5B) and microspikes (arrows Fig. 5C) was observed on the cell surface of some cells. These changes were not identified in dark group cells (Figs. 5D, E and F), respectively.

Fig.6. Induction of apoptosis by porphyrin3-PtTPyP. WM1366 cells were evaluated for apoptosis by annexin V staining under light and dark group conditions at the IC 50 concentration of the compound. The graph (Fig. E) shows the total percentage of apoptotic cells. Figs. A–D show % late and recent apoptosis in each of the groups. Porphyrin 3-PtTPyP with white light dosage had a significant increase in apoptosis when compared to all other groups (**) denotes $p < .007$.

Fig.7. Porphyrin 4-PtTPyP apoptosis induction. WM1366 cells were evaluated for apoptosis by annexin V staining under light and dark group conditions at the IC

50concentration of the compound. The graph (Fig. E) shows the total percentage of apoptotic cells. Figs. A–D show % of late and recent apoptosis in each of the groups. Porphyrin 4-PtTPyP with white light dosage had a significant increase in apoptosis when compared to all other groups (*) denotes $p < .03$.

Fig.8. Platinum(II) porphyrin 3-PtTPyP increased expression of Caspase 3, Caspase 9, P21, BAX, BCL2, MnSOD and GSHR genes in metastatic melanoma line WM1366 24 h after being submitted to white-light irradiation. The gene expression profile was determined by qRT-PCR and the data were normalized using the GAPDH levels. 3-PtTPyPhad a significant increase in the expression of all evaluated genes when compared to the other groups. (****) denotes $p < .0001$, (***) denotes $p < .0005$, (**) denotes $p < .004$, (*) $p < .04$. when compared to the light and dark group of the same molecule. Three independent experiments were performed in triplicate.

Fig. 9. Platinum(II) porphyrin4-PtTPyPincreased expression of Caspase 3, Caspase 9, P21, BAX, BCL2, MnSOD and GSHR genes in metastatic melanoma line WM1366 24 h after being submitted to white-light irradiation. The gene expression profile was determined by qRT-PCR and the data were normalized using the GAPDH levels. 4-PtTPyPhad a significant increase in the expression of all evaluated genes when compared to the other groups. (****) denotes $p < .0001$, (***) denotes $p < .0005$, (**) denotes $p < .004$, (*) $p < .04$. when compared to the light and dark group of the same molecule. Three independent experiments were performed in triplicate.

Fig.10. The platinum(II) porphyrins 3-PtTPyP and 4-PtTPyP did not alter the expression of the iNOS gene (Figs. 10A and B) in the metastatic melanoma line WM1366 and did not induce production of nitric oxide in the cell medium (Fig. 10C) 24 h after submitted to white-light irradiation. The concentration tested was that of the IC50 of each of the molecules. Data are expressed as mean ± SD of three independent times, performed in triplicate. There was no significant difference in the light and dark groups. Fig. 11. The platinum(II) porphyrins 3-PtTPyP and 4-PtTPyP did not alter the cell cycle. The groups had no significant difference in cell cycle arrest.

Fig. 11. The platinum(II) porphyrins **3-PtTPyP** and **4-PtTPyP** did not alter the cell cycle. The groups had no significant difference in cell cycle arrest.

ARTIGO 4

Figure 1. Representative molecular structures of Pt(II) metalloporphyrins used in this study. The counterion hexafluorophosphate (PF6 −) was omitted for more clarity.

Figure 2. Photostability of metalloporphyrin derivatives Zn-4-PtTPyP, Cu-4-PtTPyP and Ni-4-PtTPyP, after irradiation with white-light LED lamp source (100W; 400-800 nm) at a fluence rate of 50 mW/cm2 for different periods of time (0-30 min).

Figure 3. DPBF photo-degradation assay (20 µM) in DMF solution with or without metalloporphyrin derivatives at 2.0 µM, after red-light irradiation (LED array system) at a potency of 26 mW/cm2. The DPBF absorbance was recorded at 416 nm.

Figure 4. Effect of light action on photosensitizing molecule on cell proliferation. Porphyrin-treated and untreated cells were irradiated for 30 minutes. Dark group went totally in the dark for the same time. Comparisons were made within the white-light and dark groups, separately, for each porphyrin. Control group received no treatment with porphyrins. DMSO was the vehicle used to solubilize porphyrins. Data are expressed as mean ± SD of three independent times performed in triplicate. Fig. 4B, 4D and 4F: A375 cell line was treated with Zn-4-PtTPyP (Fig. B), Cu-4-PtTPyP (Fig. D) and Ni-4-PtTPyP (Fig. F) and platinum (II) porphyrins at 6 different concentrations and exposed at photodynamic therapy, for 30 min. Fig. 4A, 4C and 4E: A375 cell line was treated with Zn-4- PtTPyP (Fig. A), Cu-4-PtTPyP (Fig. C) and Ni-4-PtTPyP (Fig. E) and platinum(II) porphyrins at 6 different concentrations, but the groups were kept in the dark. For this evaluation we used the MTT technique. For comparison different letters in the chart denote significant difference between the groups.

Figure 5. A-I – Image of the molecular arrangement of Zn-4-PtTPyP, Cu-4-PtTPyP and Ni-4-PtTPyP porphyrins with the AP-B-100 N-terminal region. In A, D and G we observe the 3D structure of platinum(II) porphyrins with zinc(II), copper(II) and nickel(II), respectively, and their bindings with amino acids. In B, E and H we observe the coupling of porphyrin with zinc(II), copper(II) and nickel(II), respectively and the N-terminal region of Apo B-100. In C, F and I, we can see that the coupling between B0582 and the Apo B-100 region occurs in a similar way to that of zinc(II), copper(II) and nickel(II), respectively derivative. we can observe that the coupling between B0582 and the Apo B-100 region occurs in a similar way to that of zinc(II), copper(II) and nickel(II).

Figure 6. A-I – Image of the molecular arrangement of Zn-4-PtTPyP, Cu-4-PtTPyP and Ni-4-PtTPyP porphyrins with the endothelin B receptor (ERT-B). In A, D and G we observe the 3D structure of platinum(II) porphyrins with zinc(II), copper(II) and nickel(II), respectively, and their bindings with amino acids. In B, E and H we observe the coupling of porphyrin with zinc(II), copper(II) and nickel(II) respectively, and the endothelin B receptor. In C, F and I we can see that the coupling between ET3 and the ERT-B region occurs in a similar way to that of zinc(II), copper(II) and nickel(II) derivative, respectively. we can observe that the coupling between ET3 and the ERT-B region occurs in a similar way for zinc(II), copper(II) and nickel(II).

Figure 7. The HSA steady-state fluorescence emission spectra without and as a function of metalloporphyrin (a) Zn-4-PtTPyP, (b) Cu-4-PtTPyP and (c) Ni-4-PtTPyP, in a Tris-HCl buffer (pH = 7.4). The concentration of HSA is 10 µM and porphyrin concentrations ranged from 0 to 100 µM. Inset: plot of F0/F versus [porphyrin].

Figure 8. A-I – Image of the molecular arrangement of Zn-4-PtTPyP, Cu-4-PtTPyP and Ni-4-PtTPyP porphyrins with the protein Human serum albumin (HSA). In A, D and G we observe the 3D structure of platinum (II) porphyrins with zinc, copper and nickel, respectively, and their bindings with amino acids. In B, E and H we observe the coupling of porphyrin with zinc, copper and nickel, respectively and HAS protein. In C, F and I we can see that the coupling between crystallographic ligand and the HSA protein region occurs in a similar way to that

of zinc, copper and nickel, respectively. we can observe that the coupling between the crystallographic ligand and the HSA protein region occurs in a similar way for zinc, copper and nickel.

Figure 9. In this image, we can see the main common interactions of amino acids and porphyrins. In image A, B and C we see that the most important connections are the same in both porphyrins TYR138 and ARG117, for Zn-4-PtTPyP, Cu-4-PtTPyP and Ni-4-PtTPyP.

DISCUSSÃO

Figura 9: Representação esquemática do mecanismo de morte induzido por apoptose.

Table 4. Molecular anchoring results of the CuZn-SOD (SOD1) enzyme with metalloporphyrins.

Table 5. Molecular anchoring results of the catalase (CAT) enzyme with metalloporphyrins.

Table 6. The HSA-binding parameters with metalloporphyrins Zn-4-PtTPyP, Cu-4-PtTPyP and Ni-4- PtTPyP.

Table 7. Molecular anchoring results of the human serum albumin (HSA) with metalloporphyrins.

Table 8. Amino acid residues participating in the interaction HSA:metalloporphyrin derivatives in the site IB.

LISTA DE ABREVIAÇÕES

OMS – Organização Mundial de Saúde

INCA – Instituto Nacional do Câncer

TFD – Terapia fotodinâmica

EROs – Espécies Reativas de Oxigênio

BCG – *Bacillus Calmette-Guérin*

LDL - Lipoproteínas de baixa densidade

FDA - Food and Drug Administration

BNDS - Banco nacional de desenvolvimento

SUS - Sistema único de saúde

mTHPC - *meta*-tetra(hidroxifenil)clorina

HpD - Derivado de hematoporfirina

Hp – Hematoporfirina

ALA - Ácido 5-aminolevulínico

CH - Ligações metílicas

DNA – Ácido desoxirribonucleico

GPx - Glutationa peroxidase

CAT – Catalase

SOD – Superóxido dismutase

CHO-K1 - Linhagem não tumoral de ovário de hamster chinês

WM1366 – Linhagem de melanoma metastático

A375 – Linhagem de melanoma metastático

SUMÁRIO

1. INTRODUÇÃO

O câncer é uma das doenças com maior impacto na vida de pacientes e familiares na atualidade, sendo uma das principais causas de morte no mundo. No Brasil, para o triênio 2020-2022, foram estimados cerca de 625.370 mil novos casos. Destes, 8.450 são de câncer de pele do tipo melanoma (INSTITUTO NACIONAL DO CÂNCER, 2018a).

O melanoma é um tipo de câncer que se origina e se desenvolve nos melanócitos. Por esse motivo, as lesões geralmente apresentam aspecto de coloração marrom ou preto, entretanto a presença dessa coloração não é exclusiva podendo ser rosada, bege ou branca (BROUSSARD et al., 2018). Apesar de ser menos comum que o câncer de pele não-melanoma de células escamosas e basocelular, o tipo melanoma é considerado mais agressivo (BROUSSARD et al., 2018). Quando detectado em estágios iniciais pode ser curado, no entanto, a disseminação (metástases) para outras regiões é muito frequente quando o diagnóstico é tardio.

O tratamento desta doença é determinado de acordo com o estágio em que se encontra (ORGANIZAÇÃO MUNDIAL DE SAÚDE - OMS, 2017). Geralmente, para os estágios I e II é recomendado a cirurgia para remoção da lesão. Para estágios II e III, imunoterapia, radioterapia ou quimioterápicos podem ser indicados. No estágio mais avançado (IV), no qual a doença já atingiu o perfil metastático, podem ser tratados com radioterapia, imunoterapia, terapia-alvo ou quimioterapia. No entanto, este estágio de caráter mais agressivo é muito difícil de ser tratado com as terapias disponíveis atualmente, e por isso a necessidade da busca de tratamentos mais promissores ou alternativos (AMERICAN CANCER SOCIETY, 2016; SETH et al., 2020).

Neste contexto, terapias alternativas têm sido estudadas a fim de otimizar o tratamento de patologias agressivas como o câncer (AMERICAN CANCER SOCIETY, 2018a). A terapia fotodinâmica (TFD), têm se mostrado uma alternativa promissora neste sentido. Ela tem sua ação fundamentada em três pontos principais, sendo eles: o uso de fotossensibilizadores, a luz e a molécula de oxigênio, para indução do dano celular. Esta terapia caracteriza-se por ser um método minimamente invasivo e seletivo aos tumores, além de apresentar uma diminuição dos efeitos adversos ao paciente (AGOSTINIS et al., 2011;

SAINI; POH, 2013). A sensibilização se dá por meio da absorção da irradiação da fonte de energia luminosa, transferindo essa energia do fotossensibilizador para o oxigênio molecular gerando as espécies reativas de oxigênio (EROs), que são citotóxicas (ABRAHAMSE et al., 2016; HORNE; CRONJÉ, 2017). Essa terapia já tem sido bem estabelecida e com bons resultados em tratamentos como o de acne, antienvelhecimento, verrugas, câncer de pele superficial não-melanoma e hiperplasia sebácea. Além disso, também têm sido utilizada na terapia adjuvante no tratamento de tumores pulmonares, trato respiratório e urinário e tumores neurais (RKEIN; OZOG, 2014).

Atualmente, tem-se buscado novas moléculas que apresentem propriedades ideais para serem utilizadas, como fotossensibilizadores, no tratamento fototerapêutico. Neste sentido, algumas características específicas necessitam ser observadas nessas moléculas a fim de que possam ser utilizadas para este fim. Dentre essas características destacam-se fotoestabilidade potencializada, boa solubilidade em meio fisiológico, alta geração de EROs, seletividade e alta fototoxicidade (O'CONNOR; GALLAGHER; BYRNE, 2009). Moléculas como as porfirinas têm tido grande interesse por parte dos pesquisadores. A estrutura do anel porfirínico é a razão pela qual todos estes derivados absorvem luz a um comprimento de onda próximo dos 400-450 nm, além disso, é uma molécula funcional arquetípicas que desempenha um papel importante em inúmeras áreas de pesquisa científica devido ao seu exclusivo sistema eletrônico e propriedades ópticas (HIROTO; MIYAKE; SHINOKUBO, 2017). Assim, novas moléculas, como as porfirinas contendo complexos periféricos de platina(II) , vêm sendo estudadas com o objetivo de serem candidatas à fotossensibilizadores (TASSO et al., 2017). Tendo em vista os aspectos dissertados anteriormente, somado ao número crescente de casos de câncer de pele no Brasil, é necessário que se faça a busca por compostos e terapias mais efetivas e seguras ao paciente. Acredita-se que a terapia fotodinâmica é um tratamento com potencial que necessita ser mais explorada.

2. REVISÃO BIBLIOGRÁFICA

2 .1 Câncer

O câncer é um termo genérico utilizado para descrever um conjunto de mais de 100 doenças que se caracterizam pelo crescimento anormal e desordenado de células, além de seus limites habituais, que podem invadir partes adjacentes do corpo e / ou espalhar-se para outros órgãos (WHO, 2017) (Figura 1).
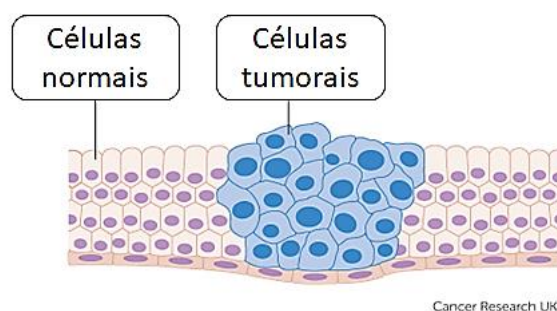
Figura 1. Imagem das células com crescimento normal (núcleo púrpura) e as células com crescimento anormal (núcleo azul). Imagem modificada com licença autoral de Cancer Research UK[*].

Historicamente o câncer é uma doença muito antiga, tendo seus primeiros relatos datados por volta de 8.000 a.C, os quais evidenciaram um osteossarcoma em um dos dedos dos pés de um hominídeo[†]. Ainda neste contexto histórico, Hipócrates, na Grécia Antiga (460-370 a.C), foi criador do termo "carcinoma" que é utilizado até os dias atuais, pois chamou o câncer de "karkino" em função da aparência do tumor ser muito similar com a de um caranguejo da mitologia grega. Assim, existem muitos relatos a cerca desta patologia que é foco de estudo de diversos grupos de pesquisa em todo o mundo (MILLER et al., 2016).

Dados do Instituto Nacional do Câncer (INCA) demostram que o câncer é a segunda principal causa de morte em todo o mundo e indicam que cerca de

---

[*] Licença autoral da Cancer Research UK.
(https://commons.wikimedia.org/wiki/File:Diagram_showing_how_cancer_cells_keep_on_reproducing_to_form_a_tumour_CRUK_127.svg)
[†] Informações retiradas do Portal da Educação
(https://siteantigo.portaleducacao.com.br/conteudo/artigos/fisioterapia/historia-do-cancerdos-escritos-antigos-a-tecnologias-atuais/5559.)

7,6 milhões de pessoas no planeta morrem em decorrência da doença a cada ano. O câncer de pele do tipo não-melanoma lidera os tipos de câncer mais prevalentes do Brasil. Já os cânceres de próstata, pulmão, colorretal, estômago e fígado são os tipos mais frequentes em homens, enquanto os de mama, colorretal, pulmão, colo do útero e o de tireoide são os mais comuns entre as mulheres (INSTITUTO NACIONAL DO CÂNCER, 2018b).

O câncer tem sua origem a partir de uma alteração no DNA da célula, que passa a receber informações incorretas para execução de suas atividades. Tais alterações podem ocorrer em genes especiais, denominados proto-oncogenes, que a princípio são inativos em células normais. Quando ativados, tornam-se oncogenes, responsáveis por transformar as células normais em células cancerosas (INSTITUTO NACIONAL DO CâNCER, 2018a).

Por ser uma doença multifatorial, as possíveis causas desta patologia são as mais variadas, podendo ser externas ou internas ao organismo. Fatores ambientais, comportamentais e genéticos estão diretamente relacionados. Desta forma, o ambiente ao qual a pessoa está diariamente exposta (poluição, defensivos agrícolas, postos de gasolina), seu comportamento (sedentarismo, ingesta de açúcar, carboidratos simples, realização de atividade física) (KLEMENT; KÄMMERER, 2011) e sua carga genética de pré-disposição para determinado tipo de câncer terão ligação não só com o aparecimento do tumor maligno como também com seu potencial de cura (AMERICAN CANCER SOCIETY, 2018b; INCA, 2017).

Dentre os fatores extrínsecos aqueles mais relacionados com o surgimento da doença são: o fumo, a obesidade e as doenças infecciosas. Os homens e as mulheres fumantes expõe-se há inúmeras substâncias carcinogênicas presentes no cigarro como: cianeto, benzeno, nitrosaminas, formaldeído. Já com relação a obesidade o grande problema é a resistência à insulina, pois esta resistência se dá nos tecidos-alvo (fígado, músculo e tecido adiposo) e pelo fato da insulina ser um fator de crescimento celular, a hiperinsulinemia na corrente circulatória pode induzir a um crescimento celular desordenado nos tecidos não-alvo (BRAUNA; BITTON-WORMS; LE ROITH, 2011)[‡].

[‡] Dados da Agência Nacional de Pesquisa para o Câncer.

2.2 Melanoma

A incidência do câncer de pele é a que mais cresce no Brasil. Segundo dados epidemiológicos do INCA o número de casos novos estimados será de 4.200 em homens e de 4.250 em mulheres, totalizando 8.450 novos casos para o triênio 2020-2022. Esses valores correspondem a um risco estimado de 4,03 casos novos a cada 100 mil homens e 3,94 para cada 100 mil mulheres. Na Região Sul, o câncer de pele melanoma é mais incidente quando comparado com as demais regiões, para ambos os sexos (INCA, 2020)

O câncer de pele divide-se em: carcinoma basocelular, epidermóide e melanoma. De todos eles, o melanoma é o menos comum, mas o mais agressivo devido ao seu diagnóstico tardio e com isso chances elevadas de metástase. Sua origem dá-se nos melanócitos (células produtoras de melanina, substância que determina a cor da pele), células que contêm um pigmento chamado melanina, que absorve os raios ultravioletas prejudiciais do sol e tem predominância em adultos brancos (WILLYARD, 2014).

Para um diagnóstico correto é importante que algumas características sejam analisadas nas pintas, na maioria das vezes a regra "ABCDE" pode ser utilizada: Assimetria, Borda, Cor, Diâmetro e Evolução (Figura 2). Dessa forma, manchas que crescem, com formas irregulares e que mudam de coloração devem ser analisadas com cuidado (AMERICAN CANCER SOCIETY, 2018b).
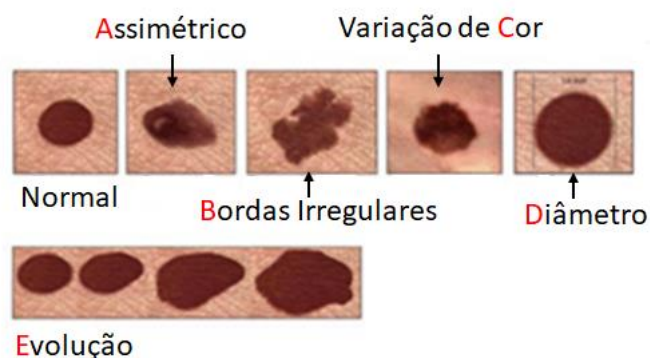
Figura 2: Demonstração visual da regra "ABCDE". Na imagem podemos observar a presença de assimetria, variação de cor, as bordas e diâmetros da pinta e sua evolução de crescimento. Figura adaptada da Sociedade Brasileira de Dermatologia - ano: 2020[§].

[§] https://www.sbd.org.br/dermatologia/pele/doencas-e-problemas/cancer-da-pele/64/

Somado a isso, o diagnóstico é realizado por meio dos estágios, os quais o melanoma se encontra. Nas figuras abaixo (Figura 3 e 4) é possível observar os estágios de Ia/b-IV (tabela 1) sendo que no IV as células tumorais já atingem a corrente sanguínea levando a um perfil metastático (COMPREHENSIVE; NETWORK, 2020).

Tabela 1: Descrição dos estágios de diagnósticos do melanoma.

Estágio	Descrição
Ia	<0,8 mm de espessura sem ulceração.
Ib	<0,8 mm de espessura com ulceração ou 0,8 – 1 mm com ulceração média.
II	>1 mm de espessura
III	Nódulo sentinela positivo
IV	Perfil metastático
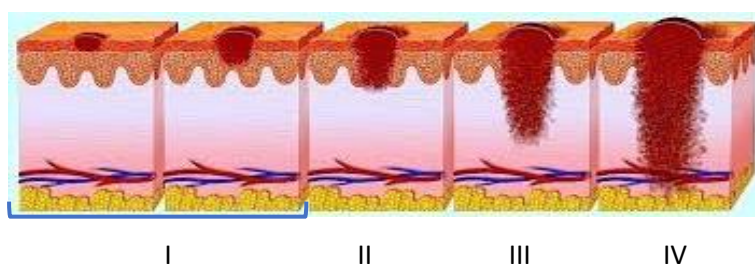
I   II   III   IV

Figura 3: Análise dos estágios do melanoma: I, II, III e IV. Sendo que na última imagem (IV) pode-se observar as células neoplásicas atingindo corrente sanguínea. Imagem modificada de Alexillus (*5 stages of the process and the development of melanoma metastasis to reach the.* Número de identificação da foto: 43968256)[**]

[****] https://www.bigstockphoto.com/pt/image-43968256/stock-photo-stages-of-melanoma
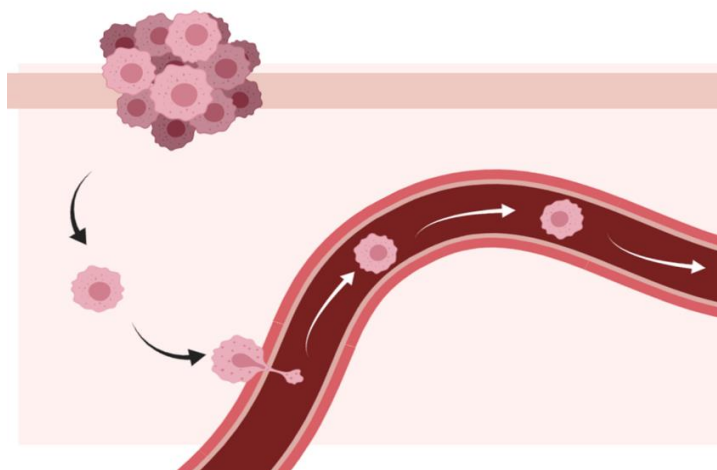
Figura 4: Esquema da metastatização a partir de células oriundas de massa tumoral. Na imagem as células tumorais se desprendem e chegam a corrente sanguínea, fazendo com que a ocorra o espalhamento dessas células de forma sistêmica. Fonte: Próprio autor.

O melanoma tem como principal fator de risco a exposição à radiação ultravioleta do sol. O padrão de exposição pode ser tão importante quanto a quantidade total de radiação ultravioleta que atinge a pele (WILLYARD, 2014). Dessa forma, a maneira mais eficaz para a proteção é o uso do filtro solar e a exposição solar nos horários adequados (antes das 9 h e após as 15 h), podendo variar de acordo com a localização geográfica, conforme o Consenso Brasileiro de Fotoproteção. Ainda, outros fatores parecem estar ligados como: pele fototipo I e II (pele branca muito sensível ou sensível, respectivamente, a queimaduras solares), possuir graves queimaduras solares, a presença de pintas, idade (mais comum nos adultos) e histórico familiar.

2.2.1 Espécies reativas de oxigênio (EROs) e melanoma

As espécies reativas do oxigênio (ERO) são moléculas altamente instáveis e reativas que são capazes de transformar outras moléculas com as quais reagem. Estas espécies são geradas em grande quantidade durante o processo de estresse oxidativo, que afetam moléculas como proteínas, carboidratos, lipídeos e ácido nucleicos. Como exemplo destas espécies

podemos citar: peróxido de hidrogênio, radical superóxido e radical hidroxila. (SILVA; GONÇALVES, 2010).

Espécies reativas e seus derivados são de fundamental importância em razão dos diversos processos fisiológicos que exercem no organismo humano como: a regulação do tônus vascular, a detecção da tensão de oxigênio, a regulação de funções que são controlados pela concentração de oxigênio, o aumento da transdução de sinal a partir de vários receptores de membrana, além de respostas ao estresse oxidativo que irão assegurar a manutenção da homeostase (COUTO et al., 2018; DRÖGE, 2002).

Tais espécies reativas (principalmente as espécies reativas de oxigênio – ERO), são produtos gerados como consequência de reações metabólicas nas mitocôndrias de células eucarióticas. Em células normais, baixas concentrações desses compostos são necessários para a transdução de sinal antes de sua eliminação. No entanto, as células cancerígenas, por apresentarem um metabolismo acelerado, exigem elevadas concentrações de EROs para manter sua alta taxa de proliferação (SOSA et al., 2013).

Acredita-se que no processo do melanoma há envolvimento direto das EROs, estudos recentes confirmaram o importante papel destas espécies em diferentes etapas deste processo de formação desta patologia. A começar pela síntese de melanina que envolve reação redox e acúmulo de ERO, somado a evidência de vários genes mutados que são associados ao melanoma resultantes da atividade EROs. Ainda, estas espécies estão relacionadas ao metabolismo celular, hipóxia e metástase (CANNAVÒ et al., 2019; DENAT et al., 2014; MEIERJOHANN, 2014; WITTGEN; VAN KEMPEN, 2007).

Estudos tem mostrado que células de melanoma são resistentes ao estresse oxidativo. Se níveis elevados de EROs promovem a sobrevivência, proliferação e metástase do câncer, por outro lado, em um nível superior, podem induzir apoptose e senescência celular por meio de danos no DNA (CANNAVÒ et al., 2019).

Um mecanismo de proteção natural para evitar danos oxidativos e promover a sobrevivência celular, são os antioxidantes, moléculas não enzimáticas e enzimáticas como a glutationa peroxidase (GPx), catalase (CAT), superóxido dismutase (SOD), entre outras (CANNAVÒ et al., 2019). Regular o equilíbrio pró-antioxidante poderia ser uma estratégia interessante no tratamento para o melanoma. Principalmente tendo em vista que os medicamentos radio e

quimioterápicos comumente usados influenciam o resultado da diminuição/eliminação do tumor por meio da modulação da ERO.

2.3 Terapia para o melanoma

Segundo o *guideline* do *National Comprehensive Câncer Network* (NCCN) (COMPREHENSIVE; NETWORK, 2020) o tratamento mais adequado do melanoma é determinado de acordo com o estadiamento da doença. Geralmente, para os estágios iniciais (Ia/b e II) a cirurgia para remoção da lesão é recomendada, sendo a análise do linfonodo sentinela recomendada para estágio Ib. Assim, a maioria dos pacientes acabam realizando a cirurgia após a biópsia da lesão. Para maior segurança do paciente, o procedimento cirúrgico é realizado com margens de segurança, ou seja, o cirurgião irá retirar alguns centímetros além da lesão para ter certeza de que todas as células foram removidas. Caso o linfonodo sentinela seja negativo, o paciente deve continuar acompanhando, se positivo paciente deverá receber tratamento específico (COMPREHENSIVE; NETWORK, 2020; SETH et al., 2020).

Para estágio II, após a remoção da lesão, há a recomendação da biópsia do linfonodo sentinela, isso porque o melanoma pode disseminar-se para os gânglios linfáticos. Além disso, testes de imagem também são recomendados. Assim, para os pacientes com linfonodos positivos recomenda-se tratamento com interferon após a cirurgia (COMPREHENSIVE; NETWORK, 2020; SETH et al., 2020)

No estágio III, os linfonodos do paciente já estão comprometidos, dessa forma, devem ser removidos com excisões amplas (lesão e linfonodos) e as opções de tratamento incluem: vacina *Bacillus Calmette-Guérin* (BCG) – como uma forma de imunoterapia, pois aprimora fortemente a resposta imune inespecífica, aumentando a proteção específica e tem demonstrado efeitos clínicos interessantes (LUCIA et al., 2019; NISHIDA et al., 2019), interferon ou interleucina – 2 diretamente na lesão, imunoterapia (como por exemplo, Nivolumabe, Pembrolizumabe, Dafrafenibe e Trametinibe), radioterapia ou quimioterapia. Neste estágio testes de mutação BRAF e exames de imagem também são recomendados. No estágio mais avançado (IV), no qual a doença já atingiu o perfil metastático, podem ser tratados com radioterapia,

imunoterapia, terapia-alvo ou quimioterapia. No entanto, este estágio de caráter mais agressivo é muito difícil de ser tratado com as terapias disponíveis atualmente (COMPREHENSIVE; NETWORK, 2020; SETH et al., 2020)

Além da dificuldade do tratamento, os efeitos adversos aos quais os pacientes acabam tendo que se submeter são extremamente agressivos ao organismo. Com isso, há a necessidade da busca de tratamentos mais promissores e efetivos.

2.4 Terapia fotodinâmica (TFD)

A TFD é uma forma inovadora e não-invasiva de terapia que tem sido utilizada com sucesso em áreas como a ginecologia, urologia, dermatologia e oncologia. Esta terapia tem demonstrado excelentes resultados no tratamento de doenças como acne, psoríase, na inflamação crônica, no tratamento de infecções bacterianas resistentes a medicamentos, bem como diversos tipos de câncer (LUO et al., 2017; SPERANDIO; HUANG; HAMBLIN, 2013).

O uso da fototerapia é ancestral, desde os primórdios os humanos consideravam a aplicação de radiações solares para curas medicinais. Na Grécia antiga, Hipócrates, considerado uma das figuras mais notáveis da história da medicina, incentivou o uso da luz do sol para recuperação de atrofias musculares (EMERSON; MEMBER, 1932). Em 1973 Peter S. Herman, do centro hospitalar universitário de Quebec – Canadá, publicou no periódico LANCET uma *short-communication* alertando que a TFD poderia ser uma nova e interessante abordagem para o tratamento das neoplasias humanas resistentes as terapias convencionais, achados esses demostrados por Diamond e colaboradores ("to existing neoplasms treatment is fascinating . It is mentioned that porphyrins", 1972). A TFD baseia-se na aplicação local ou sistêmica de um composto com propriedades fotossensíveis, denominado fotossensibilizador, que se acumula intensamente em tecidos patológicos (figura 5) (KHARKWAL et al., 2011).
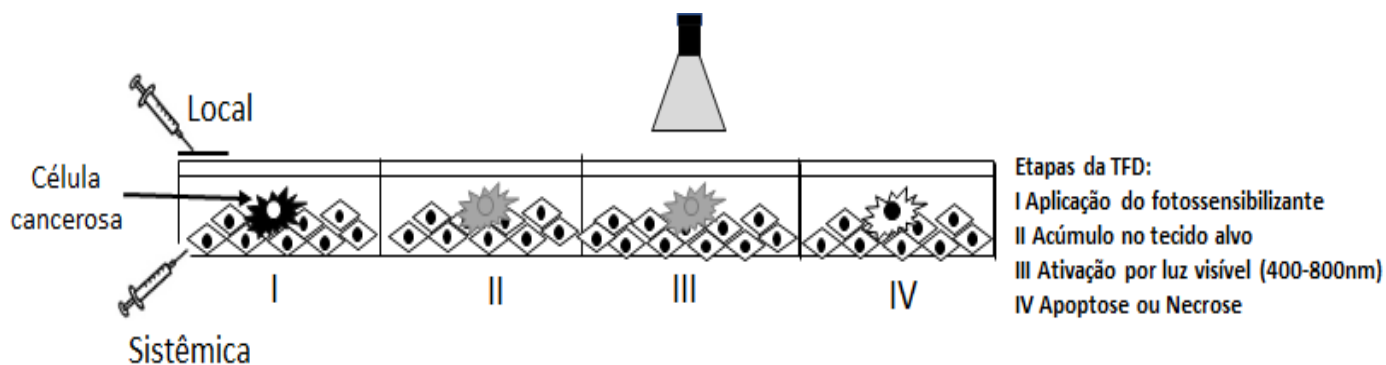
Figura 5: Imagem ilustrativa das etapas envolvidas na aplicação da TFD. Fonte: Próprio autor.

Outro aspecto interessante é que este processo permite a destruição seletiva das células inapropriadas, justamente por serem reações guiadas pela luz (fototóxicas), as quais ocorrem apenas na área de distribuição do fotossensibilizador, somado a isso estas moléculas tem a capacidade de absorver luz no comprimento de onda adequado (VROUENRAETS et al., 2003). Estudos demonstram que fotossensibilizadores acumulam-se em concentrações mais elevadas nas células cancerígenas quando comparados com as células normais (CRUZ et al., 2013; GOMES; NEVES; CAVALEIRO, 2018).

O motivo desta distribuição seletiva pode ser a tendência que os fotossensibilizadores têm de combinar-se, preferencialmente, com lipoproteínas de baixa densidade (LDL) (CRUZ et al., 2013; HAMBLIN; NEWMAN, 1994; KANDA et al., 2019). Há evidências de que células neoplásicas possuam maior captação de LDL e com isso uma maior expressão destes receptores (FIRESTONE, 1994). Esta terapia é bem tolerada pelos pacientes em função de sua ação seletiva. Os protocolos fotodinâmicos são indolores e a simplicidade de sua aplicação permite o uso ambulatorial (KHARKWAL et al., 2011; KWIATKOWSKI et al., 2018).

Apesar do sucesso desta terapia, novos métodos e compostos estão sendo estudados para melhorar seu uso efetivo para esta finalidade. Tem sido pesquisado a associação de eletroporação e nanotecnologia, com o uso de nanocarreadores, objetivando aumentar a concentração local do fotossensibilizador e, também direcioná-lo às células de interesse, o que resulta em melhor eficiência de terapia aplicada (KWIATKOWSKI et al., 2018; SCHMITT; JUILLERAT-JEANNERET, 2012).

2.4.1 TFD e o câncer

A TFD já tem sua aprovação no Food and Drug Administration (FDA), órgão americano responsável por fiscalizar medicamentos. Aqui no Brasil, diversos estudos têm demonstrado excelentes e promissores resultados em linhagens celulares, como em adenocarcinoma de colo de útero, câncer de mama, próstata, entre outros (FONSECA TEIXEIRA; ALVES, 2018; LINARES-ESPINÓS et al., 2018; PELLOSI et al., 2018; SILVA et al., 2018; TASSO et al., 2017).

Ainda, o banco nacional de desenvolvimento (BNDS) está apoiando financeiramente com R$ 3,2 milhões de reais para que TFD seja utilizada em escala comercial e no sistema único de saúde (SUS), oferecendo treinamento e capacitação clínica, facilitando o acesso a medicamentos e equipamentos, e reduzindo os custos da terapia. Este projeto, que está em andamento, envolve 10 países: Brasil, Bolívia, Chile, Equador, El Salvador, Colômbia, Cuba, México, Peru e Venezuela (BUZZÁ et al., 2016). Outro estudo interessante, com pacientes portadores de múltiplos cânceres de pele não-melanoma, foi desenvolvido na Holanda por Horlings e colaboradores utilizando o *meta*-tetra(hidroxifenil)clorina (mTHPC) como fotossensibilizador, o qual demonstrou-se altamente eficaz, com poucos efeitos colaterais (HORLINGS; TERRA; WITJES, 2015).

Com relação a medicamentos que são comercializados, um exemplo é o Foscan® um fotossensibilizador de 2ª geração utilizado na União Europeia desde o ano de 2001 para os seguintes tipos de câncer: cabeça, pescoço, pulmão e cérebro. A formulação contém um único composto ativo, sendo um derivado de clorina (mTHPC), é fotoativado a 652 nm, onde é um ótimo gerador de oxigênio singlete. Sua síntese foi relatada por Bonnett e colaboradores (BONNETT; BERENBAUM, 1989; KNIEBÜHLER et al., 2013).

Outro exemplo é o Metvix®, desenvolvido pela Galderma, indicado - entre outros - para o tratamento de carcinoma basocelular superficial e/ou nodular. A ação deste medicamento se dá pela formação e acúmulo de porfirinas (compostos fotoativos) dentro das células da lesão na área tratada. Quando ativados pela luz, na presença de oxigênio, ocorre a formação de oxigênio singlete, que causa dano aos componentes celulares, em particular às

mitocôndrias e ao DNA. Assim, a ativação pela luz das porfirinas acumuladas conduz a uma reação fotoquímica e consequente fototoxicidade às células- alvo expostas à luz (TASSO et al., 2017).

2.4.2 Mecanismo de ação

A TFD tem seu mecanismo de ação fundamentado em três principais componentes não-tóxicos, sendo eles o uso de sensibilizadores, a luz (com o comprimento de onda adequado) e a molécula de oxigênio, para indução do dano celular, visto que o oxigênio está presente em abundância nos tecidos cancerígenos (BROWN; BROWN; WALKER, 2004; GOMES; NEVES; CAVALEIRO, 2018; SAINI; POH, 2013). Estudos mostram que essa sensibilização pode se dar, principalmente, por dois mecanismos, sendo que ambos são dependentes de moléculas de oxigênio dentro das células (ABRAHAMSE; HAMBLIN, 2016; HORNE; CRONJÉ, 2017; KWIATKOWSKI et al., 2018).

O primeiro estágio dos dois mecanismos é similar: após entrar na célula, a molécula fotossensibilizadora sofre irradiação com um comprimento de onda de luz que coincide com o seu espectro de absorção e é convertida do estado fundamental de energia S_0 para um estado excitado S_n^*, denominado "estado singleto Sn*" pela absorção de fótons. Parte da energia retorna ao estado fundamental e emite fluorescência , e a energia remanescente é direcionada, pela molécula fotossensibilizadora, ao estado triplete excitado T1 – a forma terapêutica adequada do composto (CASTANO; DEMIDOVA; HAMBLIN, 2005; ROBERTSON; EVANS; ABRAHAMSE, 2009).

2.4.2.1 Mecanismo de ação TFD - Tipo I

Estando no estado excitado T1, o fotossensibilizador tem a possibilidade de converter o oxigênio molecular em variadas espécies reativas. Através de um processo de transferência de elétrons neste estado excitado tripleto, temos a formação de espécies radicalares tais como radical hidroxil, radical superóxido, radical hidroperoxil e radical peroxinitrito. Esta cascata de reações

gera estresse oxidativo resultando na destruição de células cancerígenas (DE SILVA et al., 2020; ROBERTSON; EVANS; ABRAHAMSE, 2009).

2.4.2.2 Mecanismo de ação TFD – Tipo II

Além da possibilidade de um fotossensibilizador converter o oxigênio molecular em radicais, o mesmo pode acontecer através de processo de transferência de energia. Desta maneira, o oxigênio molecular que se encontra na forma de triplete ($^3O_2$) passa para singlete ($^1O_2$), gerando assim uma forma altamente reativa. Assim, moléculas de oxigênio singlete são geradas, sendo estas caracterizadas por propriedades oxidantes extremamente fortes (JUZENIENE; MOAN, 2007; NOWAK-STEPNIOWSKA; PERGOL; PADZIK-GRACZYK, 2013). Por este motivo, fotossensibilizantes quando excitados não danificam estruturas celulares, eles reagem apenas com moléculas de oxigênio que se encontram dissolvidas no citoplasma (FONSECA et al., 2006). Tendo em vista este panorama, entende-se que mecanismo do tipo II é o processo mais importante condicionando a eficiência da TFD. No entanto, à medida que o oxigênio se esgota, o mecanismo do tipo I começa a prevalecer (CASTANO; DEMIDOVA; HAMBLIN, 2005). O esquema de ambos mecanismos pode ser observado na figura 6.

Independentemente do tipo de mecanismo, as EROs levam ao foto-dano das proteínas, do DNA, gorduras e outras moléculas na área fotossensibilizada, levando a morte direta de células tumorais. Os diferentes tipos de morte celular dependem de onde o fotossensibilizador encontra-se intracelularmente: danos à mitocôndria podem levar à apoptose, em contrapartida, destruição e a perda da integridade da membrana celular podem induzir necrose, já danos aos lisossomos ou mesmo ao reticulo endoplasmático podem provocar autofagia (KESSEL; OLEINICK, 2010; MEHRABAN; FREEMAN, 2015).
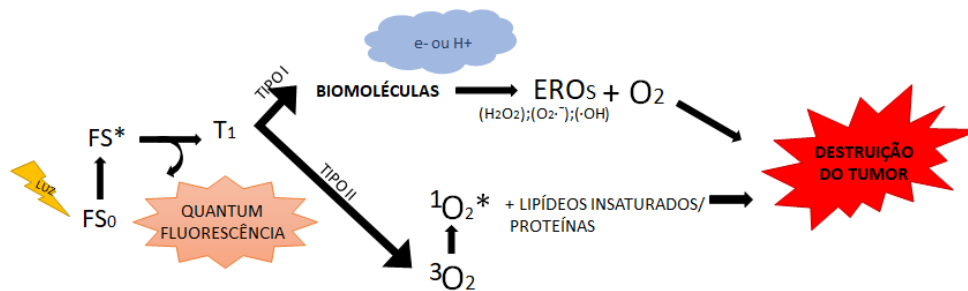
Figura 6: Representação esquemática dos mecanismos de ação da TFD que conduzem à destruição do tecido tumoral por ação do oxigénio singleto (ao combinar-se com lipídeos insaturados/proteínas presentes na membrana plasmática) ou pela formação de espécies reativas de oxigénio. FS -Fotossensibilizador; T_1 – Forma ativa do composto; ERO_S - espécies reativas de oxigénio. Fonte: Próprio autor.

2.4.3 Fotossensibilizadores

Os Fotossensibilizadores são substâncias capazes de absorver luz com um comprimento de onda específico, gerando reações fotoquímicas ou fotofísicas (DE SILVA et al., 2020). Dentre as condições que descrevem um fotossensibilizador ideal, podemos citar: estabilidade à temperatura ambiente, fotossensibilidade apenas na presença de um comprimento de onda específico, absorção máxima na faixa 600 a 800 nm, absorção mínima na faixa de 400 a 600 nm (previne fotossensibilidade excessiva causada pela luz solar), baixa citotoxicidade no escuro e alta seletividade para tecidos neoplásicos (DOBSON; DE QUEIROZ; GOLDING, 2018).

Estes compostos estão descritos em 3 gerações, sendo que a 1ª geração ficou conhecida pelos "derivado de hematoporfirina" (HpD) (ABRAHAMSE; HAMBLIN, 2016). Estes derivados foram obtidos por meio de modificações químicas da primeira porfirina - hematoporfirina (Hp), sendo que a HpD quando comparada com a Hp apresenta melhor seletividade tecidual para tumores. No entanto, surgiram limitações para a sua aplicação clínica como a baixa pureza química e a pobre penetração tecidual em razão da absorção máxima em um comprimento de onda relativamente curto. Somado a isso, após a TFD, o paciente apresentava hipersensibilidade da pele à luz por várias semanas devido a longa meia-vida do fotossensibilizador e seu alto acúmulo na pele. Estas desvantagens levaram à necessidade de investigar novos compostos e iniciou-

se o desenvolvimento de fotossensibilizadores de 2ª geração (CHATTERJEE; FONG; ZHANG, 2008; ZHANG et al., 2018).

Os de 2ª geração incluem derivados de hematoporfirina e fotossensibilizadores sintéticos como: ácido 5-aminolevulínico (ALA), derivados de benzoporfirina, texafirinas, derivados de tiopurina, entre outros (YOON; LI; SHIM, 2013). O uso do ALA mostrou-se uma importante descoberta, pois é um tipo de pró-fármaco que se torna um fotossensibilizador ativo somente após ser transformado na protoporfirina. Por esse motivo, o ALA passou a ser utilizado topicamente ou por via oral em muitas aplicações clínicas (DE ROSA; BENTLEY, 2000; MORTON, 2002). A 2ª geração destas moléculas foi caracterizada por maior pureza química, maior rendimento na formação de oxigênio singleto e melhor penetração em tecidos devido à sua absorção máxima na faixa de comprimento de onda de 650 a 800 nm.

Além disso, eles demonstram menos efeitos colaterais, o que resulta de uma maior seletividade para tecidos cancerígenos e eliminação mais rápida do fotossensibilizador corpo. A principal desvantagem da 2ª geração é a sua pobre solubilidade na água, que é um fator significativamente limitante em sua administração, induzindo dessa maneira, a busca por novos métodos de entrega (NOWAK-STEPNIOWSKA; PERGOL; PADZIK-GRACZYK, 2013) (Figura 7).

Com esse entendimento, os fotossensibilizadores de 3ª geração foram fundamentados na síntese de substâncias com maior afinidade ao tecido tumoral, reduzindo os danos aos tecidos saudáveis circundantes (JOSEFSEN; BOYLE, 2008). Outra demanda que as moléculas de 3ª geração tentam atender é a aplicação clínica como a administração parenteral de fotossensibilizadores, bem como resolver o problema da baixa solubilidade em água (ZHANG et al., 2018).

Novos sistemas de distribuição de medicamentos estão surgindo para aumentar a biodisponibilidade do método fotodinâmico (JOSEFSEN; BOYLE, 2008). Tendo em vista este objetivo, pesquisadores tem combinado moléculas de 2ª geração com outras moléculas focando no receptor-alvo, conjugando, por exemplo, o fotossensibilizador com um anticorpo monoclonal dirigido ao antígeno específico da célula cancerosa (KATAOKA et al., 2017). Estas soluções poderiam permitir um aumento da seletividade e acúmulo do fotossensibilizador nas áreas afetadas, reduzindo as doses do medicamento, mantendo efeitos

terapêuticos satisfatórios (KATAOKA et al., 2017; SAVELLANO; HASAN, 2003) (Figura 7).

Com relação a baixa solubilidade, Muehlmann et al. propuseram um novo fotossensibilizador de terceira geração, que se apresenta como um sistema composto pelo fotossensibilizador hidrofóbico de cloreto de alumínio-ftalocianina (AlPc) associado a nanopartículas de poli (metil-vinil éter-anidrido maleico) dispersíveis em água. O estudo obteve resultados eficazes nas linhagens tumorais testadas (MUEHLMANN et al., 2014).
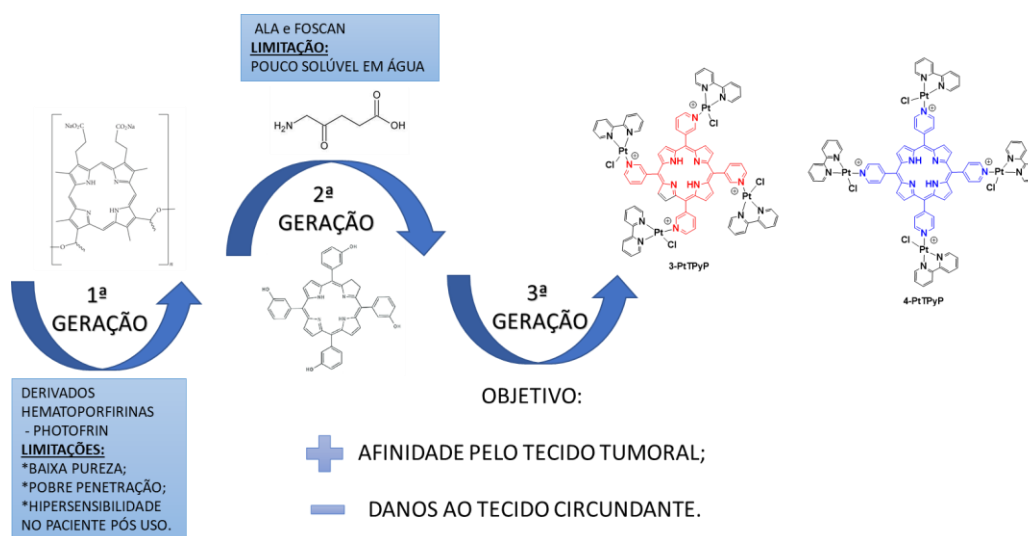
Figura 7: Representação esquemática das 3 gerações dos fotossensibilizadores utilizados na terapia fotodinâmica. No esquema demonstramos as evoluções de tais compostos. Na primeira geração observamos um número maior de limitações nestes compostos. Estas limitações foram resolvidas, em partes, pelas moléculas de segunda geração, no entanto, atualmente, estão em desenvolvimento moléculas que sejam ainda mais efetivas e seletivas. Fonte: Próprio autor.

2.4.4 Porfirinas

As porfirinas pertencem a uma classe de moléculas orgânicas com uma estrutura geral de macrociclo tetrapirrólico contendo 18 elétrons (formado por quatro anéis pirrólicos), consiste em quatro unidades de pirrol e quatro átomos de carbono em ponte, ligados por ligações metílicas (-CH-) (HIROTO; MIYAKE; SHINOKUBO, 2017). Como representantes desta classe de compostos temos o

grupo heme, que contém íons ferro(II), a clorofila, que contém íons magnésio(II) e os pigmentos biliares. Dessa forma, são responsáveis por funções como: transporte de oxigênio e armazenamento (hemoglobina e mioglobina), transporte de elétrons (citocromos) e coleta de energia luminosa (clorofila) (MILGROM, 1997). Elas possuem pigmentação de cor púrpura. A estrutura em anel da porfirina é a razão pela qual todos os derivados porfíricos absorvem luz a um comprimento de onda próximo dos 400-450 nm, dando-lhes a sua cor característica (Figura 8) (MILGROM, 1997).
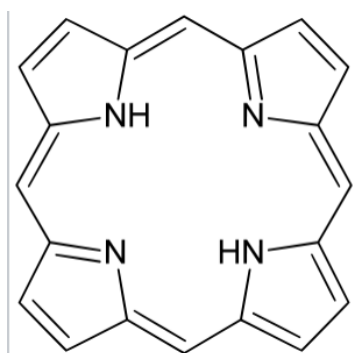
Figura 8: Representação esquemática do macrociclo tetrapirrólico comum das porfirinas. Fonte: Enciclopédia Britânica.

A biossíntese de porfirinas é regulada nos eucariotos superiores pela concentração do produto heme, o qual serve como inibidor por retroalimentação dos passos iniciais da via de síntese (LEHNINGER, 2009). A concentração do hemo em eucariontes regula a sua síntese por um mecanismo de feedback negativo. Em humanos, a desregulação deste sistema por deficiência de uma das enzimas da via de síntese de porfirinas causa uma doença popularmente conhecida como porfirias (LEHNINGER, 2009).

O interesse dos químicos orgânicos e inorgânicos pelas porfirinas deu-se, em função de que a porfirina é uma molécula funcional arquetípicas que desempenha um papel importante em inúmeras áreas de pesquisa científica devido ao seu exclusivo sistema eletrônico e propriedades ópticas (HIROTO; MIYAKE; SHINOKUBO, 2017; KADISH; CAEMELBECKE; ROYAL, 2000). Dentre essa ampla variedade de áreas podemos citar: fotossíntese, biocatálise relacionada ao P450, células fotovoltaicas, agentes terapêuticos fotodinâmicos,

sondas de bioimagem, quimiossensores, entre outros (KADISH; CAEMELBECKE; ROYAL, 2000).

2.4.5 Platina e seus derivados na área médica

A platina é um metal de transição denso, maleável, dúctil, altamente não reativo, branco prateado. Possui excelente resistência à corrosão, é estável a altas temperaturas e possui propriedades elétricas estáveis. Seu nome é derivado do termo espanhol *platino,* que significa "pequena prata" (LØKSE, 2018). Este metal foi descrito pelos europeus no início do século XVI, mas foi ter uma investigação mais aprofundada com Antônio de Ulloa em 1748, quando este publicou um relatório sobre o "novo metal" atraindo, assim, a curiosidade de cientistas (MAUSKOPF; MCDONALD; HUNT, 1984).

Atualmente diversos são os usos conhecidos da platina, ela pode ser encontrada em equipamentos de laboratório, pode ser usada como conversores catalíticos, eletrodos elétricos, joias, equipamentos odontológicos, entre outros. Por ser um metal pesado, a exposição a curto prazo a sais de platina pode causar irritação nos olhos, nariz e garganta e a exposição a longo prazo pode causar alergias respiratórias e cutâneas (MEEKS; LA NIECE; ESTÉVEZ, 2002). De maneira geral, compostos de platina são encontrados em apenas dois estados de oxidação estável: Pt(II) e Pt(IV). Os derivados de platina(II) são os mais comuns e se encontram em uma configuração estrutural quadrática-planar de seus compostos, sendo estes compostos difíceis de serem oxidados a Pt(IV). Já os derivados de platina(IV) são mais raros mas não menos importantes. Normalmente são estáveis em uma configuração geométrica octaédrica, com sua esfera de coordenação contendo átomos mais duros (por exemplo, oxigênio) para estabilizar o centro metálico. Sais de platina(IV) podem ser facilmente reduzidos a compostos de platina(II), principalmente em meio fisiológico.

Agentes antineoplásicos à base de platina(II), como cisplatina, oxaliplatina e carboplatina foram desenvolvidos ao longo dos anos e demonstraram possuir um boa efetividade contra alguns tumores (WHEATE et al., 2010). Nesta revisão, dentre os derivados de platina(II), daremos destaque a cisplatina.

A cisplatina teve sua descoberta datada de 1845 e liberada para uso médico em 1978/1979(FISCHER; ROBIN GANELLIN, 2006). Faz parte da lista de medicamentos essenciais da Organização Mundial da Saúde (OMS, 2013). Este medicamento tem sua administração por via intravenosa como infusão de curta duração em solução salina normal para tratamento de malignidades sólidas e hematológicas, como por exemplo: câncer de pulmão de pequenas células, carcinoma de células escamosas da cabeça e pescoço, câncer de ovário, câncer de colo do útero, bexiga, testículos, linfoma (INSTITUTO NACIONAL DEL CANCER, 2016). Como mecanismo de ação, temos que a cisplatina interfere na replicação do DNA, matando as células de proliferação mais rápida, que em teoria são cancerígenas. Essa atividade antitumoral é atribuída à ligação ao DNA, com formação de adutos, originando ligações intra e intercadeias que induzem alterações estruturais. O seu efeito citotóxico é, dessa maneira, causado pela inibição da transcrição e replicação, o que leva a indução da apoptose (ROCHA et al., 2018; WANG; LIPPARD, 2005).

Mesmo sendo uma alternativa de tratamento com resposta inicial alta para vários tipos de câncer, alguns pacientes acabam recidivando com a doença resistente à cisplatina. Neste contexto, diferentes mecanismos de resistência à cisplatina foram propostos, incluindo: alterações na captação celular e efluxo do fármaco, aumento da desintoxicação do fármaco, inibição da apoptose e aumento do reparo do DNA(STORDAL; DAVEY, 2007).

Dessa forma, sabendo que derivados de platina(II) apresentam uma resposta promissora ao tratamento de alguns tipos de câncer, mas atualmente observamos pacientes resistentes a tal tratamento, torna-se necessária a busca por novos derivados de platina(II) que consigam desempenhar o tratamento de forma mais efetiva, segura e com menos resistência.

3. OBJETIVO

3.1 Objetivo geral

Bioprospectar fotossensibilizadores para terapia fotodinâmica no tratamento do melanoma metastático.

3.2 Objetivos específicos

- Elucidar o estado da arte da terapia fotodinâmica, bem como sua aplicação na biotecnologia e ciências biológicas;
- Verificar a forma de *screening* de novas moléculas na terapia do melanoma;
- Avaliar o potencial antitumoral de porfirinas tetra-catiônicas contendo complexos periféricos de platina(II) (**3-PtTPyP** e **4-PtTPyP**) na linhagem celular de melanoma metastático (WM1366);
- Avaliar o efeito citotóxico destas porfirinas (**3-PtTPyP** e **4-PtTPyP**) em linhagem não tumoral de ovário de hamster chinês (CHO-K1) como controle da terapia proposta e identificar o mecanismo de morte celular;
- Investigar a adição de metais de transição como zinco **(Zn-4-PtTPyP),** cobre **(Cu-4-PtTPyP)** e níquel **(Ni-4-PtTPyP)** a porfirina de platina(II) no potencial antitumoral, bem como na seletividade na linhagem celular de melanoma metastático;
- Elucidar o tempo de exposição à terapia fotodinâmica induzida pelos compostos nas linhagens tratadas;
- Demonstrar mecanismos de seletividade dos compostos em estudo;
- Observar a integridade da célula, como viabilidade de membrana e integridade do DNA, após tratamento com os compostos;

4. RESULTADOS

Esta Tese originou 4 artigos científicos que se interligaram ao longo deste estudo. Em um momento inicial buscamos entender, por meio da nossa *invited review*, o estado da arte da terapia fotodinâmica, sua inserção na bioprospecção de novas moléculas e sua relação com a biotecnologia e as ciências biológicas. Dentre os principais achados deste artigo de revisão, destacamos: (i) a diminuição os efeitos adversos relacionados a terapia convencional; (ii) a melhora da resistência dos quimioterápicos tradicionais, como a doxorrubicina; (iii) a terapia fotodinâmica como uma opção viável e eficaz para um tratamento de melhor qualidade. Nossa busca ainda correlacionou a TFD com a nanotecnologia na melhora da forma de entrega, absorção da luz e para aplicação no diagnóstico do câncer (COUTO et al., 2020a).

Posteriormente, observamos a importância de implementarmos estudos *in silico* a triagem de nossas moléculas candidatas a testes *in vitro* para avaliação de efeito antitumoral. Ferramentas *in silico* mostraram-se de grande valor para triagem inicial de novas moléculas, pensando em uma abordagem mais racional do *screening* de novos compostos. Além disso, a possibilidade da precisão na previsão de interações entre as moléculas e seus receptores, além da economia de tempo e dinheiro, é de grande valia, pois a escolha das moléculas para testes subsequentes pode se dar de forma mais efetiva (COUTO et al., 2019).

Após um primeiro *screening*, avaliamos a ação antitumoral de porfirinas de platina(II). Nossos resultados indicaram que as porfirinas 3-PtTPyP e 4-PtTPyP apresentam atividade seletiva antitumoral na linhagem de melanoma metastático estudada, sugerindo que o principal mecanismo de morte se deu por apoptose por meio da ativação das caspases 3 e 9 via Bax/BCL2. Somado a isso é importante citar que ambas não foram tóxicas na linhagem celular não-tumoral e também nos grupos que não receberam incidência de luz (grupos escuros). Ainda, a avaliação *in silico* indicou que ambas as porfirinas de platina(II) foram promissoras como estratégia de liberação do fármaco, apresentando afinidade para a região N-terminal da ApoB-100, o que também pode estar explicando o fato da preferência pelas células tumorais (COUTO et al., 2020b).

Ao longo do estudo do uso das porfirinas de platina(II) na TFD investigamos também as consequências (possível melhora do efeito antitumoral

e seletividade) da inclusão de íons como o zinco, cobre e níquel à porfirina 4-PtTPyP e sua ação na ligação com os receptores apolipoproteína B (APO B-100) e receptor de endotelina (ERT-B), albumina do soro humano (HSA) e antioxidantes como superóxido dismutase (SOD) e catalase (CAT). Nossos resultados sugerem que, principalmente, porfirinas Zn-4-PtTPyP e Ni-4-PtTPyP podem inibir a proliferação celular de melanoma metastático quando exposto ao sistema fotodinâmico. Além disso, o estudo *in silico* indicou que ao adicionarmos metais de transição ocorreu uma potencialização da afinidade destas porfirinas à região N-terminal de ApoB-100 (KLEIN COUTO et al., 2020).

Neste contexto, a afinidade para o receptor de ERT-B foi avaliada pelo fato deste estar superexpresso em patologias como o câncer. Dessa forma, manejar a atividade deste receptor torna-se interessante. Nossas porfirinas ligaram-se de forma superior ao controle (ET3) utilizado neste estudo. Indicando que, a atividade proliferativa, metastática e antiapoptótica relacionadas a este receptor estavam comprometidas. Com isso, as metaloporfirinas mostraram-se de forma promissora como um antitumoral e na estratégia de seletividade, entrega e inibição de metástase tumoral (KLEIN COUTO et al., 2020).

Antioxidantes como a SOD são conhecidos por serem importantes para o tratamento de patologias como câncer. As células tumorais, dependem, de certa forma, do ambiente altamente instável e mutagênico do estresse oxidativo é por isso que o manejo de espécies antioxidantes é interessante (ANDRISIC et al., 2018). As metaloporfirinas apresentaram uma forte ligação *in silico* com o receptor da SOD, com destaque para Zn-4-PtTPyP e Ni-4-PtTPyP, indicando a possibilidade destas porfirinas suprimirem a malignidade de células de melanoma humano (KLEIN COUTO et al., 2020).

Por fim, entendemos que a TFD pode ser extrapolada e ganhar espaço nas mais diferentes áreas de estudo, e encorajamos seu uso em diferentes áreas biológicas, inclusive sendo sugerida para potencializar o tratamento do câncer.

Os resultados que fazem parte desta tese de doutorado estão apresentados sob forma de artigo. Os itens materiais e métodos, resultados, discussão e referências bibliográficas encontram-se no próprio manuscrito.

4.1 Capítulo 1 (Artigo 1) - **Perspectives of photodynamic therapy in Biotechnology (invited review)**

O Manuscrito foi Publicado no **Journal of Photochemistry & Photobiology, B: Biology. F.I: 4.38**

Invited Review

Perspectives of photodynamic therapy in biotechnology

Gabriela Klein Couto[a], Fabiana Kommling Seixas[a], Bernardo Almeida Iglesias[b], Tiago Collares[a],*

[a] Molecular and Cellular Oncology Research Group, Cancer Biotechnology Laboratory, Technological Development Center, Federal University of Pelotas, Pelotas, Brazil
[b] Laboratory of Bioinorganic and Porphyrinoid Materials, Chemistry Department, Federal University of Santa Maria, Santa Maria, Brazil

ARTICLE INFO

ABSTRACT

Photodynamic therapy (PDT) is a current and innovative technique that can be applied in different areas, such as medical, biotechnological, veterinary, among others, both for the treatment of different pathologies, as well as for diagnosis. It is based on the action of light to activate photosensitizers that will perform their activity on target tissues, presenting high sensitivity and less adverse effects. Therefore, knowing that biotechnology aims to use processes to develop products aimed at improving the quality of life of human and the environment, and optimizing therapeutic actions, researchers have been used PDT as a tool of choice. This review aims to identify the impacts and perspectives and challenges of PDT in different areas of biotechnology, such as health and agriculture and oncology. Our search demonstrated that PDT has an important impact around oncology, minimizing the adverse effects and resistance to chemotherapeutic to the current treatments available for cancer. Veterinary medicine is another area with continuous interest in this therapy, since studies have shown promising results for the treatment of different animal pathologies such as Bovine mastitis, Malassezia, cutaneous hemangiosarcoma, among others. In agriculture, PDT has been used, for example, to remove traces of antibiotics of milk. The challenges, in general, of PDT in the field of biotechnology are mainly the development of effective and non-toxic or less toxic photosensitizers for humans, animals and plants. We believe that there is a current and future potential for PDT in different fields of biotechnology due to the existing demand.

1. Introduction

Photodynamic therapy (PDT) has been an interesting ally in different areas of knowledge. Its mechanism of action is based on the application of photosensitizers activated locally or systemically by light with an oxygen source, at an appropriate wavelength, and from this application occurs the generation of reactive oxygen species (ROS - singlet oxygen and radical species), responsible for triggering the expected results [1]. Studies in the field of human and animal health, especially dermatology, oncology, urology, microbiology, parasitology [2–4] and agriculture [5,6] has been demonstrating how eclectic and interesting this therapy can be (Fig. 1).

In this sense, biotechnology that aims to use cellular and biomolecular processes to develop technologies and products, aiming to improve life and health on the planet, has a total interest in developing products that may use tools that can be more effective and less aggressive either to humans, animals and plants [7]. For this reason, PDT has been widely used in the field of biotechnological treatments for the most different pathologies, such as method of choice for treatment of age-related macular degeneration and is appreciated as minimally invasive therapeutic procedure to treat skin, esophageal, head and neck, lung, and bladder cancers with high cure rates, low side effects, and excellent cosmetic outcome [8].

Still, in this context, it would be very interesting to think of molecules that could be marked and activated by light directly on the tissue of interest, for diagnostic purposes, for example, tetrapyrrole macrocycles (Fig. 2) [2,9]. Fig. 2A highlights some molecules with their effectiveness highlighted, for example, the mixture of oligomers Photofrin®, which is a photosensitizer used in photodynamic therapy and radiotherapy and for the treatment of lung carcinoma and esophageal cancer [10]. Foscan®, a drug-based on a tetra-(3-hydroxyphenyl)chlorin (temoporfin), is a photosensitizer commercialized in Europe and widely used in photodynamic therapy for the treatment of head and neck carcinoma [11]. Other chlorophyll derivatives, such as Chlorin e6, Visudyne® and Tookad®, are also used in the treatment of cancer by photodynamic action [12,13]. A new generation of photosensitizers for application in PDT has also shown success in this area (Fig. 2B), as is the case with Redaporfin®, a third-generation bacteriochlorin derivative used in the treatment of cancer and produced by Luzitin SA (Coimbra - Portugal) [14] and the Lutex® derivative (Lutrin/Antrin) based on a lutetium texafirin structure (Texas-shaped porphyrin) that exhibited an excellent response in preclinical breast cancer studies and prostate [15,16].
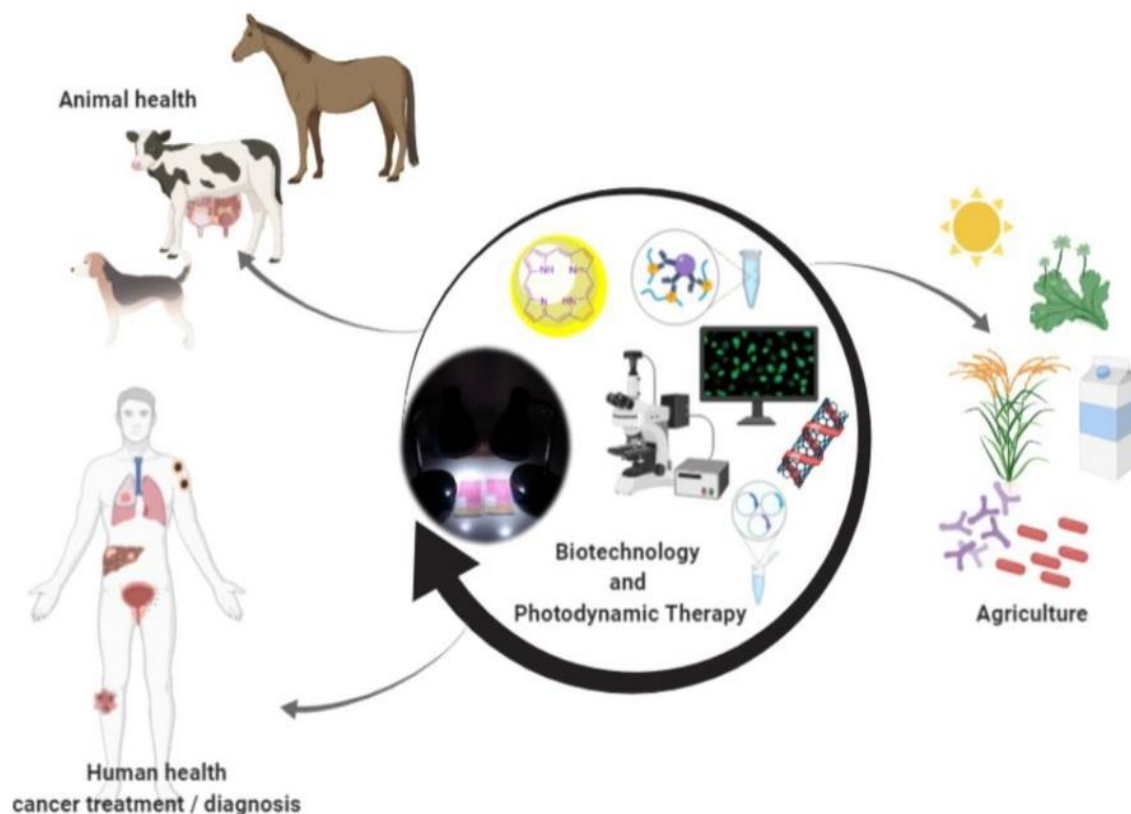
Fig. 1. Biotechnology and photodynamic therapy in the areas of human/animal health and agriculture.

In this context, we could also think of molecules that could not only diagnose but also treat the patient simultaneously. We are at the frontier of knowledge and the development of such forms of treatment/diagnosis [17].

Another area that has shown interest in PDT is that of bioprospecting, after all, have as precept is the systematic search for organisms, genes, enzymes, compounds, processes and parts from living beings that have economic potential and lead to the development of a product [18]. We know that one of the greatest difficulties in the management of photosensitizers is linked to the fact of low solubility in water, the most appropriate vehicle for future formulations [19]. Thus, due to this high hydrophobicity, encapsulation approaches have been considered to minimize the formation of inactive aggregates in an aqueous environment. [20].

The vast majority of controlled delivery systems are based on nanoparticles (NP) or other nanostructures [21]. NPs, which usually range in size from 1 to 100 nm, reveal unique physical and chemical properties and are being explored for photosensitizers in order to optimize current treatment regimes in PDT [22]. Still, it is important to mention that in addition to the NPs (most commonly used) the encapsulation of the photosensitizer can occur through a system of micelles, liposomes, biodegradable NPs, conjugating the photosensitizer with hydrophobic polymers such as polyethylene glycol (PEG) [19].

These modifications end up bioprospect old and new photosensitizers which end up optimizing their specificity, selectivity, increasing their action time, leading to a better biological response.

Thus, the areas of biotechnology and bioprospecting are closely related, showing a special interest in photodynamic processes, due to the advantages it presents. Thus, this perspective aimed to assess the impact of PDT on biotechnology, the main goals and challenges within this field in the current scenario.

2. Impacts of Photodynamic therapy at Biotechnology

In this session we will address the impacts that the PDT has on the different areas of knowledge of biotechnology. We chose to cover the areas of human and veterinary health and agriculture. We also added a topic specifically involving cancer, as it is the area of study of our research group.

2.1. Photodynamic Therapy and Biotechnology and Health

The use of phototherapy is ancestral, from the beginning of time humans consider utilize the application of solar radiation for medicinal cures. In ancient Greece, Hippocrates encourages the use of sunlight to recover from muscular atrophies []. The first evidence of the use of PDT in this area dates back to 1988 when Schneckenburger et al. discussed the fluorescence properties of photosensitizers used in photodynamic therapy in the field of medicine and biology. In this paper, they still highlight the importance of PDT for biotechnology, emphasizing that until the present moment (1988), few works had been done in the application of fluorescence methods in this field. Until that moment the development of biotechnological products was concentrated in compounds with fluorescent properties [24].

Currently, product development and the number of studies in this area have considerably increased. The main focus of using PDT in the area of biotechnology has been human and animal health. Areas such as dermatology, oncology, urology are of great interest in this type of treatment, since the adverse effects are infinitely less than those of conventional therapies [25–27].

In human medicine, PDT represents an alternative, well-known and recognized treatment option for several indications, as mentioned above. In the medical veterinary area, the steps are slower. Few treatments are available for pets and large pets. The main indication in this area is for skin tumors in cats. Other possible indications are urinary tract neoplasms in dogs and equine sarcoid (common tumors in horses) [28] and canine otitis [29].

Dobson et al. published a review in 2018 in order to verify a possible new scenario for the veterinary PDT. However, even though it is promising, the area advances in this treatment at a slow pace. According to
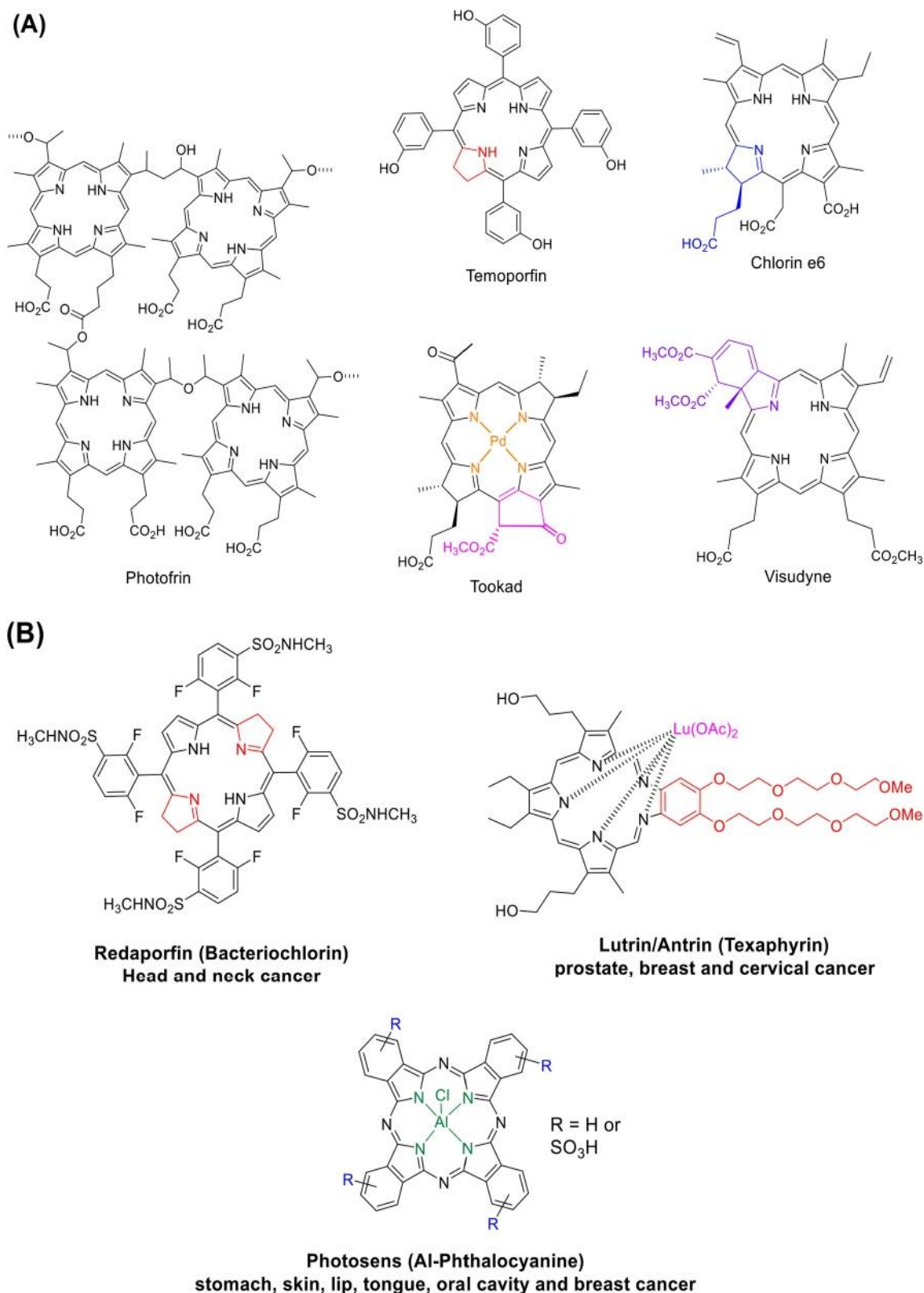
Fig. 2. (A) Examples of most common tetrapyrrole macrocycle molecules used in PDT field and (B) New photosensitizers generation for PDT and PDI application formulated by Luzitin SA, NIOPIK and Pharmacyclics Inc.

them, there are few professionals qualified to perform such treatment and the cost of treatment is still high [17].

If the treatment still does not reach the veterinary clinics, for the reasons already mentioned, research in this area, on the other hand, has sought alternatives and new photosensitizers for this therapy. Searches of databases such as PubMed and Science Direct have shown this interest on the part of researchers. As in the research of human health, the

veterinary area has focused more on lines aimed at the treatment of cancer, with slightly focus in clinic microbiology [30,31]. In a recent study Rocha et al. (2019) used PDT to fight cutaneous hemangiosarcoma in dogs, a malignant neoplasm that often occurs in this species [32]. A treatment with PDT, in this pathology, is very interesting since it can avoid mutilating surgeries, being seen as an alternative therapy and possible efficacy.

In the veterinary field, we also observed studies in the ophthalmological area [33], dermatology such as the treatment of Malassezia infection [34], in the treatment of bovine mastitis, a disease that leads to a significant drop in milk production, added to the fact that treatments with conventional antibiotics can leave residues in the milk [35], among other areas.

Thus, investing time, energy and money in this field of knowledge seems to be a good and future strategy since, especially in the veterinary area, there is still a lot of space for new developments and research. The creation of new biotechnological products and the re-positioning of strategies will be essential in the near future.

2.2. Photodynamic Therapy and Biotechnology and Agriculture

The scientific evidence in the field of PDT is very vast in the area of health, however, it comes in a constant growth in agriculture. Improvements in milk and food are among the focuses of this treatment. In a recent study (2020) Chen et al. evaluated 5-aminolevulinic acid (5-ALA) which is a promising bio-stimulant, food nutrient and photo-dynamic drug (widely used in the treatment of some types of cancer) with wide applications in modern agriculture and phototherapy. The objective of this study was to improve the yield in addition to establishing a solid technological base for the large-scale commercialized bioproduction of 5-ALA [6]. In this study in question, increase the biosynthesis of 5-ALA more economically increase the prospects for industrialization in the form of a sustainable and environmentally friendly process.

For biotechnology field, improving efficiency and productive capacity is of great importance for the productive sector. After all, agricultural biotechnology includes a range of breeding tools and techniques, which alter living organisms, or parts of them, to produce or modify products, improve plants or animals, or develop microorganisms for specific agricultural uses.

Another perspective of studies in this area, is the fact of improving the cultivation of plants that produce metabolites that can be used as photosensitizers in PDT. As is the case with *Hypericum perforatum* (St. John's wort) which has valuable secondary metabolites for treatment with PDT and depression [5].

In addition to improvements in food, it is possible to try to reduce the bacteria in milk, through a photoinactivation performed with the aid of PDT, in this case, antimicrobial photodynamic therapy (aPDT) [36,37]. The interesting thing about this technique is that because it does not use conventional antibiotic therapy, milk does not have traces of antibiotics in the final product, which can lead to possible bacterial resistance. It is important to note that antibiotics are widely used in the dairy industry to fight disease and improve animal performance [38]. Thus, alternative treatments for the pathologies that affect these animals, such as mastitis, are considered of great value for agricultural biotechnology.

2.3. Photodynamic Therapy and Biotechnology and Cancer

In section 2.1 we covered PDT in the field of biotechnology related to health. As we mentioned, studies in this area are vast. However, the number of researchers focused on the search for cancer treatments draws attention. There are numerous treatment strategies, here we can mention the use of recombinant *Mycobacterium bovis* BCG [39] and also the use of pyrazoline with the hydrogen and chlorine substituents for bladder cancer [40], for example. Because it is a less aggressive and more targeted therapy, it is easy to understand this interest. This is a therapy that is already available for the treatment of different types of cancer worldwide, mainly for non-melanoma skin cancer [41].

The researchers' current search has focused on the discovery of new photosensitizers (PS). These are fundamental pieces for the success of the therapy, after all PS are excited by a specific wavelength, triggering the whole mechanism of action. New drug distribution systems are emerging to increase the bioavailability of the photodynamic method [42]. These solutions could allow an increase in selectivity and accumulation of photosensitizer in the affected areas, reducing the doses of the medication, maintaining satisfactory therapeutic effects [43,44].

Our research group has started studied tetra-cationic porphyrins containing peripheral platinum(II) complexes [45–47] as candidates for photosensitizers for the treatment of metastatic melanoma, an extremely aggressive type of skin cancer that is diagnosed late and does not respond well to the treatments currently available. Our results have shown promising, in which we observed not only an anti-tumor activity in the studied metastatic melanoma strains, with a concentration of porphyrins on the nanomolar scale, but also a selective distribution in tumor tissues. These findings demonstrate an alternative therapy with less adverse effects and more targeted [48].

In a search in databases such as science direct when we search for the words "photodynamic therapy" and "cancer", we have 1129 articles published in 2020 alone, while in PubMed we found 1124 publications in the years 2019–2020, demonstrating how vast and interesting is this area. Lung cancer [49], glioma [50], breast [51], melanoma [48], has been in great demand.

In addition to the unpleasant adverse effects on the patient, the fact that resistance to conventional chemotherapy is also on the biotechnology radar, aiming at the development of more effective and less novice products for patients [52]. Khdair et al. evaluated the combination of doxorubicin with methylene blue, for PDT, a drug widely used in the treatment of different types of cancer, with PDT. This combination was evaluated precisely because doxorubicin has significant resistance to patients [53].

In a comparative way we have numerous studies focused on the area of oncology in order to improve the therapy of this pathology, reducing the adverse effects, increasing the adherence to the treatment, decreasing the resistance to the chemotherapies existing in the market [54–56]. In the literature, we found some reviews that evaluated the viability of PDT, such as that of Yang et al. who demonstrated that this therapy is a viable and effective option for better quality treatment for future cancer patients [57]. In contrast, El-Hussein et al. in their review article explored the combined use of chemotherapy and PDT in the treatment of lung cancer, demonstrating how this approach can be the last resort for many patients who have been diagnosed with this type of cancer [58].

Still, in this context of PDT for cancer magnetic nanocomposites (photosensitizers associated with magnetic nanoparticles) seem interesting for the treatment of pathologies as complex and heterogeneous as this one [59–61]. For example, we cite the study by Choi et al. which proposed to develop multifunctional magnetic nanoparticles conjugated with a photosensitizer (PS) and molecules directed to cancer, in order to reach an improvement in the penetration of light *in vivo*, as well as the efficiency of targeting cancer cells. In this work, the central magnetic nanoparticles (Fe_3O_4) were covalently linked with chlorine e6 (Ce6) as a PS and folic acid (FA). The group obtained good results of cell death *via* apoptosis, however, *in vivo* studies are necessary to verify its biological effects for clinical applications [61].

On the other hand, Chiang et al. developed a photosensitive and magnetic satellite nucleus (TCSN) in order to increase the damage induced by the incidence of light to tumor cells. The results of the studies showed that with this technique an increase in the therapeutic window by magnetic enrichment and bimodal phototherapy, which could serve as an advanced extracorporeal strategy to remove the circulating tumor cells, cells that often end up causing metastases [62].

PDT can also contemplate that diagnosis and therapy can together to fight cancer. It was what Fan et al. proposed in their study, where they successfully developed a distinct three-layer nanostructured particle responsive to tumor acidity (S-NP) that encapsulates the photosensitizer chlorin e6 (Ce6) and that Gd(III) derivatives to be used in precision PDT guided by dual model image - fluorescence / magnetic resonance (MR) [63].

In the vast field of PDT, biotechnology and cancer, we still need to move forward and focus efforts against more deeply located tumors, since against superficial tumors such as basal cell skin cancer, PDT has a good response [64]. In order to develop options for PDT *in vivo*, Rodrigues et al. evaluated the success of a nano-emulsion containing aluminum-phthalocyanine (AlPc-NE) as a mediator of photodynamic therapy (PDT-AlPc-NE) against breast adenocarcinoma tumors grafted into mice (BALB/c). The study was concerned with evaluating the development of lung metastases, as well as the growth of the mammary tumor. The results show that the application of PDT-AlPc-NE eradicated transplanted tumors in all treated animals. In addition, known animals free of detectable metastases in the lungs [65].

2.4. Techniques Consolidated in PDT

Still within the context of the PDT, it is important to mention consolidated techniques in the area, as PDT and biotechnology become even more connected. Techniques such as photosensitizing doping. Interesting studies in this area have been developed over time, such as that of Shen et al. which conjugated doped polymer nanoparticles with photosensitizer incorporating poly-oxyethylene nonylphenol ether (CO-520) in them. Thus obtaining nanoparticles of poly[9,9-dibromohexylfluorene-2,7-ylenethylene-*alt*-1,4-(2,5-dimethoxy)phenylene] (PFEMO) doped with *meso*-tetra(phenyl)porphyrin (TPP) incorporated in *CO*-520 with stability characteristics and low cytotoxicity in the dark, in addition to efficiency in the generation of singlet oxygen species, improving PDT activity in cancer cells. This modification allowed simultaneous monitoring *in vivo* by fluorescence images of two photons during the photodynamic treatment [66].

In addition to the oncology area, we observed impressive results against Leishmania, using PDT doping. These results were demonstrated in the study by Nadhman et al. which developed biocompatible silver PEGylated zinc oxide nanoparticles. These nanoparticles performed well, with high production of singlet oxygen and hydroxyl radicals, the leading producers of ROS, in addition to low toxicity in the dark [67]. Interesting answers, according to the authors, not only for leishmaniasis but for the treatment of cancer and other infections.

Correlating PDT and immunological therapies are also medical strategies of interest against cancer. For example, we quote Ramírez-García et al. who proposed to integrate these techniques with upward converting nanoparticles (UCNPs) in order to improve the diagnosis of cancer. Ramírez-García demonstrated that as UCNPs convert deep infrared light (NIR) into higher energy emissions, they allow the observation of images and detection of malignant cells, in addition to the simultaneous transfer of energy to activate photosensitizers [68]. In this study, they used nanocomposites conjugated with the monoclonal antibody trastuzumab to treat HER2 positive breast cancer, obtaining significant positive results.

Drug delivery techniques with photosensitizers are of paramount importance in addition to being widely applied around oncology. The use of nanoparticles makes it possible to reach a target, focusing on specific receptors, increasing the selectivity of photodynamic therapy [69]. As we mentioned earlier, in order to improve the delivery system, in addition to NPs we can find polysomes, biodegradable NPs, micelles, among others [19], without forgetting that photosensitizers must remain in a monomeric form to be photoactive [70]. We draw attention here to liposomes, which are considered one of the most efficient vehicles for transporting hydrophobic molecules in an aqueous medium to the target tissue, usually the scenario that we find in front of PDT treatments [71].

These vesicles with one or more concentric phospholipid bilayers, end up becoming biocompatible depending on their lipid composition. [19,72]. In addition, the particle size, being nanometric (between 60 and 120 nm), ends up giving a high delivery capacity of the therapeutic agent. All these properties make this type of system effective vehicles for delivering PDT drugs [73]. As an example, Hematoporphyrin (Hp)

or its derivative (HpD) and Photofrin® (a partially purified form of HpD) were the first photosensitizers to be encapsulated in liposomes based on L-α-di-palmitoylphosphatidylcholine (DPPC) [74].

In this context of Drug delivery, polymeric micelles appear as nanocarriers of well-known drugs and used in the diagnosis and pharmacotherapy of several diseases [75]. This type of vehicle is composed of amphiphilic polymers that "self-conform" in nanostructures with sizes ranging between 10 and 200 nm and that contain an internal hydrophobic core, in which drugs that are poorly soluble in water can be trapped, providing excellent distribution and stability to these hydrophobic compounds [76,77].

In this universe, such techniques can be combined, as in the study by Zhang et al. which developed a drug delivery system for photosensitized doped nanoparticles, self-monitored and self-administered in order to diagnose, treat and monitor the delivery and distribution of drug molecules [78]. In this study the researchers used two possible drugs for the treatment of cancer, curcumin and *meso*-tetra(4-pyridyl) porphyrin (H_2TPyP) being co-doped in the curcumin matrix. In this context, H_2TPyP was used as a PDT drug. As a result the researchers observed that the combined drugs provided a fluorescent imaging and tracking system in real time *in vitro* and *in vivo* with high therapeutic efficiency of cancer [78].

Medicines like Photofrin, a photosensitizer know for PDT have been the subject of studies in the field of nanotechnology. As for example, Lamch et al. who studied the use of polymeric micelles based on Pluronic P123 (EO 20 PO 65 -EO 20, PM 5800 Da) and F127 (EO 100 -EN 69 -EO 100, PM 12600 Da), in order to improve the efficiency of Photofrin® in cell line of ovary resistant to traditional drugs and breast deficient in caspase-3. These cells were treated with Photofrin® in free and encapsulated form, showing as results an improved photodynamic activity with good efficiency, in the groups treated with the encapsulated drug [79].

We know that photosensitizers, in general, have limitations such as low water solubility [80], which makes its subsequent *in vivo* administration difficult. In this sense, nanotechnology can be a great ally. Muehlmann et al. proposed a new third generation photosensitizer, which is presented as a system composed of the hydrophobic photosensitizer of aluminum chloride-phthalocyanine (AlPc) associated with nanoparticles of poly(methyl-vinyl ether-maleic anhydride) dispersible in water. They evaluated this photosensitizer in breast tumor and non-tumor cells *in vitro*, obtaining effective results in the tumor lines tested [81].

Much of the studies in the area of PDT is directed to the treatment of diseases such as cancer [47,81–85], however, we can observe an interesting development of biotechnological bioprospecting, in relation to this therapy in the industrial area that meets agriculture, food, environment, converging for the elaboration of new processes and bioproducts [86–88]. As an example, we highlight the Photodynamic Inactivation Device (PID) developed by Foggiato et al. in order to use it for microbial reduction or disinfection of solid surfaces for clinical orthodontic instruments, and thus, to propose a low cost and non-toxic alternative for the disinfection of biomedical devices as non-critical instruments, allowing its use also in the food industry [88].

In this context of industrial bioprospecting, we see an important demand regarding foodborne microbial diseases, as they are considered a worldwide public health problem, since they are directly related to food security. The chemical and thermal procedures traditionally applied to control microbial growth in the food industry can alter the food matrix and lead to antimicrobial resistance, thus, changes in this area are desired [89,90]. Thus, antimicrobial PDT becomes an attractive alternative for the control of foodborne pathogenic bacteria, as it is less likely to cause antimicrobial resistance and does not promote undesirable nutritional and sensory changes in the food matrix [91].

Still in the food area, Kim et al. evaluated the effect of the 405 ± 5 nm light-emitting diode (LED) on food preservation. This effect was evaluated against bacteria such as *Escherichia coli* O157:H7,

Listeria monocytogenes and *Salmonella* spp. The study showed excellent results, in which LED lighting effectively inactivated 97–99% of these microorganisms. of the sleeve surface at refrigerated temperature, being, however, less effective for L. *monocytogenes* and *E. coli* O157:H7 at room temperature. Another result interesting was that the quality of the mango fruit when cut was not influenced by the LED, even after long exposure, regardless of the storage temperature [92]. Examples like this show us that PDT tends to arouse industrial interest, since it can be marketed as a highly efficient, non-thermal sterilization technology.

In addition to the food industry, product development based on PDT has been developed. Rocha et al. proposed the creation of a microemulsion mouthwash based on curcumin to disinfect the oral cavity in combination with PDT. The formulation developed by the group was tested against biofilms of *Candida albicans*, methicillin-resistant *Staphylococcus aureus* (MRSA) and *Escherichia coli*, remaining stable after 60 days of storage. As a result, they observed a significant reduction ($p < 0,05$) of UFC.mL^{-1} in all microorganisms tested after treatment combining PDT and curcumin microemulsion. [93].

3. Challenges and Perspectives of Photodynamic Therapy in Biotechnology

The challenges of PDT in the field of biotechnology are the development of effective and non-toxic or less toxic photosensitizers for humans, animals and plants. The focus should be on third generation molecules, which include the characteristics necessary for the functioning of the PDT, with increased and selectivity in the generation of reactive oxygen species and efficiency.

Results in clinical practice demonstrate how interesting the therapy is, including financially for biotechnology. One of the factors that generate greater interest in this therapy is the possibility of avoiding resistance to photosensitizers, differently from what occurs in conventional chemotherapy.

Currently, the difficulty in treating large tumor masses and the limited depth of treatment are the main limitations of PDT. The fact that visible light can penetrate tissues with a depth of no more than 5–10 mm ends up restricting the application of therapy to more superficial lesions, being, up to the present moment, molecules that have absorption in a lower energy region (for example, red or near infrared regions) the most suitable.

Regarding costs, comparatively between PDT and conventional chemotherapy, both are similar, being high - still - to patients. If the area of cancer still has challenges to be overcome, in agriculture, on the other hand, the therapy will be shown to be a little more accessible for the treatment of cases of mastitis, for example, and for direct improvement in the quality of milk to patients. Treatments of interest on the biotechnological scale to improve the population's diet.

We believe that there is current and future potential for photodynamic therapy in different fields of biotechnology, due to the already existing demand. It needs more effective treatments, with less adverse effects, targeted, with less incidence of resistance (to drugs and microorganisms) both in the area of human and animal health, as well as in the agricultural area.

Declaration of Competing Interest

The authors declare that they have no known competing financial interests or personal relationships that could have appeared to influence the work reported in this paper.

References

[1] S. Kwiatkowski, B. Knap, D. Przystupski, J. Saczko, E. Kędzierska, K. Knap-Czop, J. Kotlińska, O. Michel, K. Kotowski, J. Kulbacka, Photodynamic therapy – mechanisms, photosensitizers and combinations, Biomed. Pharmacother. 106 (2018) 1098–1107, https://doi.org/10.1016/j.biopha.2018.07.049.

[2] A.T.P.C. Gomes, M.G.P.M.S. Neves, J.A.S. Cavaleiro, Cancer, photodynamic therapy and porphyrin-type derivatives, An. Acad. Bras. Cienc. 90 (2018) 993–1026, https://doi.org/10.1590/0001-3765201820170811.

[3] R. Saini, C.F. Poh, Photodynamic therapy: a review and its prospective role in the management of oral potentially malignant disorders, Oral Dis. 19 (2013) 440–451, https://doi.org/10.1111/odi.12003.

[4] T.M.A.L. Parente, E.L. de Rebouças, V.C.V. dos Santos, F.C.B. Barbosa, I.C.J. Zanin, Serratia marcescens resistance profile and its susceptibility to photodynamic antimicrobial chemotherapy, Photodiagn. Photodyn. Ther. (2016), https://doi.org/10.1016/j.pdpdt.2016.04.007.

[5] A. Sobhani Najafabadi, M. Khanahmadi, M. Ebrahimi, K. Moradi, P. Behroozi, N. Noormohammadi, Effect of different quality of light on growth and production of secondary metabolites in adventitious root cultivation of *Hypericum perforatum*, Plant Signal. Behav. (2019), https://doi.org/10.1080/15592324.2019.1640561.

[6] J. Chen, Y. Wang, X. Guo, D. Rao, W. Zhou, P. Zheng, J. Sun, Y. Ma, Efficient bioproduction of 5-aminolevulinic acid, a promising biostimulant and nutrient, from renewable bioresources by engineered Corynebacterium glutamicum, Biotechnol. Biofuels. (2020), https://doi.org/10.1186/s13068-020-01685-0.

[7] S. Bhatia, D. Goli, Chapter 1 History, Scope and Development of Biotechnology, (2018), https://doi.org/10.1088/978-0-7503-1299-8ch1.

[8] K. Plaetzer, M. Berneburg, T. Kiesslich, T. Maisch, New Applications of Photodynamic Therapy in Biomedicine and Biotechnology, Biomed. Res. Int. (2013), https://doi.org/10.1155/2013/161362.

[9] B. Habermeyer, R. Guilard, Some activities of PorphyChem illustrated by the applications of porphyrinoids in PDT, PIT and PDI, Photochem. Photobiol. Sci. (2018), https://doi.org/10.1039/c8pp00222c.

[10] T. Sheng, Y. Ong, T.M. Busch, T.C. Zhu, Reactive oxygen species explicit dosimetry to predict local tumor growth for Photofrin-mediated photodynamic therapy, Biomed. Opt. Express (2020), https://doi.org/10.1364/boe.393524.

[11] K.J. Lorenz, H. Maier, Squamous cell carcinoma of the head and neck : PPPPhotodynamic therapy with Fos®can, HNO. 56 (2008) 402–409, https://doi.org/10.1007/s00106-007-1573-1.

[12] J. Kim, Y. Um jo, K. Na, photodynamic therapy with smart nanomedicine, Arch. Pharm. Res. 43 (2020) 22–31, https://doi.org/10.1007/s12272-020-01214-5.

[13] S.A. McFarland, A. Mandel, R. Dumoulin-White, G. Gasser, Metal-based photosensitizers for photodynamic therapy: the future of multimodal oncology? Curr. Opin. Chem. Biol. 56 (2020) 23–27, https://doi.org/10.1016/j.cbpa.2019.10.004.

[14] A.C.S. Lobo, L.C. Gomes-da-Silva, P. Rodrigues-Santos, A. Cabrita, M. Santos-Rosa, L.G. Arnaut, Immune Responses after Vascular Photodynamic Therapy with Redaporfin, J. Clin. Med. (2019), https://doi.org/10.3390/jcm9010104.

[15] T.D.M, J.L. Sessler, Texaphyrins: a new approach to drug development, J. Porphyrins Phthalocyanines 5 (2001) 134–142.

[16] M.S. Blumenkranz, K.W. Woodburn, F. Qing, S. Verdooner, D. Kessel, R. Miller, Lutetium texaphyrin (lu-tex): a potential new agent for ocular fundus angiography and photodynamic therapy, Am J. Ophthalmol. (2000), https://doi.org/10.1016/S0002-9394(99)00462-6.

[17] J. Dobson, G.F. de Queiroz, J.P. Golding, Photodynamic therapy and diagnosis: principles and comparative aspects, Vet. J. (2018), https://doi.org/10.1016/j.tvjl.2017.11.012.

[18] N.L. Saccaro, A regulamentação de acesso a recursos genéticos e repartição de benefícios: Disputas dentro e fora do Brasil, Ambient. e Soc. (2011), https://doi.org/10.1590/s1414-753x2011000100013.

[19] M.Q. Mesquita, C.J. Dias, S. Gamelas, M. Fardilha, M.G.P.M.S. Neves, M.A.F. Faustino, An insight on the role of photosensitizer nanocarriers for photodynamic therapy, An. Acad. Bras. Cienc. (2018), https://doi.org/10.1590/0001-3765201720170800.

[20] L. Tang, J. Cheng, Nonporous silica nanoparticles for nanomedicine application, Nano Today (2013), https://doi.org/10.1016/j.nantod.2013.04.007.

[21] D.K. Chatterjee, L.S. Fong, Y. Zhang, Nanoparticles in photodynamic therapy: an emerging paradigm, Adv. Drug Deliv. Rev. 60 (2008) 1627–1637, https://doi.org/10.1016/j.addr.2008.08.003.

[22] K.I. Ogawara, K. Higaki, Nanoparticle-based photodynamic therapy: current status and future application to improve outcomes of cancer treatment, Chem. Pharm. Bull. (2017), https://doi.org/10.1248/cpb.c17-00063.

[24] H. Schneckenburger, H.K. Seidlitz, J. Eberz, New trends in photobiology. Time-resolved fluorescence in photobiology, J. Photochem. Photobiol B Biol. (1988), https://doi.org/10.1016/1011-1344(88)85033-4.

[25] T. Garg, N. Jain, G. Rath, A.K. Goyal, Nanotechnology-based photodynamic therapy: concepts, advances, and perspectives, Crit. Rev. Ther. Drug Carrier Syst. (2015), https://doi.org/10.1615/CritRevTherDrugCarrierSyst.2015011645.

[26] L.Q. Soares Lopes, A.P. Ramos, P.M. Copetti, T.V. Acunha, B.A. Iglesias, R.C. Vianna Santos, A.K. Machado, M.R. Sagrillo, Antimicrobial activity and safety applications of meso-tetra(4-pyridyl)platinum(II) porphyrin, Microb. Pathog. (2019), https://doi.org/10.1016/j.micpath.2018.12.038.

[27] G.G. Rossi, K.B. Guterres, C.H. da Silveira, K.S. Moreira, T.A.L. Burgo, B.A. Iglesias, M.M.A. de Campos, Peripheral tetra-cationic Pt(II) porphyrins photo-inactivating rapidly growing mycobacteria: first application in mycobacteriology, Microb. Pathog. (2020), https://doi.org/10.1016/j.micpath.2020.104455.

[28] J. Buchholz, H. Walt, Veterinary photodynamic therapy: A review, Photodiagn. Photodyn. Ther. (2013), https://doi.org/10.1016/j.pdpdt.2013.05.009.

[29] I.B. Seeger, Ries MG, Gressler AS, LT, S.A. Botton, C. JF, In vitro antimicrobial photodynamic therapy using tetra-cationic porphyrins against multidrug-resistant bacteria isolated from canine otitis, Photodiagn. Photodyn. Ther. (2020), https://doi.org/10.1016/j.pdpdt.2020.101982.

[30] A.I. Musani, J.K. Veir, Z. Huang, T. Lei, S. Groshong, D. Worley, Photodynamic

therapy via navigational bronchoscopy for peripheral lung cancer in dogs, Lasers Surg. Med. (2018), https://doi.org/10.1002/lsm.22781.

[31] T. Osaki, S. Hibino, I. Yokoe, H. Yamaguchi, A. Nomoto, S. Yano, Y. Mikata, M. Tanaka, H. Kataoka, Y. Okamoto, A basic study of photodynamic therapy with glucose-conjugated chlorin e6 using mammary carcinoma xenografts, Cancers (Basel) (2019), https://doi.org/10.3390/cancers11050636.

[32] M.S.T. Rocha, C.M. Lucci, J.A.M. dos Santos, J.P.F. Longo, L.A. Muehlmann, R.B. Azevedo, Photodynamic therapy for cutaneous hemangiosarcoma in dogs, Photodiagn. Photodyn. Ther. (2019), https://doi.org/10.1016/j.pdpdt.2019.05.026.

[33] E.A. Giuliano, J. Ota, S.A. Tucker, Photodynamic therapy: basic principles and potential uses for the veterinary ophthalmologist, Vet. Ophthalmol. (2007), https://doi.org/10.1111/j.1463-5224.2007.00578.x.

[34] W.R. Kim, S.G. Bae, T.H. Oh, Photodynamic therapy of red and blue lights on Malassezia pachydermatis: An in vitro study, Pol. J. Vet. Sci. (2018), https://doi.org/10.24425/119037.

[35] L.H. Moreira, J.C.P. de Souza, C.J. de Lima, M.A.C. Salgado, A.B. Fernandes, D.I.K. Andreani, A.B. Villaverde, R.A. Zângaro, Use of photodynamic therapy in the treatment of bovine subclinical mastitis, Photodiagn. Photodyn. Ther. (2018), https://doi.org/10.1016/j.pdpdt.2017.12.009.

[36] A. Galstyan, U. Dobrindt, Determining and unravelling origins of reduced photo-inactivation efficacy of bacteria in milk, J. Photochem. Photobiol B Biol. (2019), https://doi.org/10.1016/j.jphotobiol.2019.111554.

[37] F.P. Sellera, C.P. Sabino, M.S. Ribeiro, R.G. Gargano, N.R. Benites, P.A. Melville, F.C. Pogliani, In vitro photoinactivation of bovine mastitis related pathogens, Photodiagn. Photodyn. Ther. (2016), https://doi.org/10.1016/j.pdpdt.2015.08.007.

[38] S.P. Oliver, S.E. Murinda, Antimicrobial resistance of mastitis pathogens, Vet. Clin. North Am. - Food Anim. Pract. (2012), https://doi.org/10.1016/j.cvfa.2012.03.005.

[39] K.R. Begnini, C. Rizzi, V.F. Campos, S. Borsuk, E. Schultze, V.C. Yurgel, F. Nedel, O.A. Dellagostin, T. Collares, F.K. Seixas, Auxotrophic recombinant Mycobacterium bovis BCG overexpressing Ag85B enhances cytotoxicity on superficial bladder cancer cells in vitro, Appl. Microbiol. Biotechnol. (2013), https://doi.org/10.1007/s00253-012-4416-2.

[40] J.W. Tessmann, J. Buss, K.R. Begnini, L.M. Berneira, F.R. Paula, C.M.P. de Pereira, T. Collares, F.K. Seixas, Antitumor potential of 1-thiocarbamoyl-3,5-diaryl-4,5-di-hydro-1H-pyrazoles in human bladder cancer cells, Biomed. Pharmacother. (2017), https://doi.org/10.1016/j.biopha.2017.07.060.

[41] Instituto Nacional Del Cancer, Tipos de tratamiento - National Cancer Institute, 6 Abril, (2017).

[42] L.B. Josefsen, R.W. Boyle, Photodynamic therapy: novel third-generation photo-sensitizers one step closer? Br. J. Pharmacol. 154 (2008) 1–3, https://doi.org/10.1038/bjp.2008.98.

[43] M.D. Savellano, T. Hasan, Targeting cells that overexpress the epidermal growth factor receptor with polyethylene glycolated BPD verteporfin photosensitizer im-munoconjugates, Photochem. Photobiol. 77 (2003) 431–439, https://doi.org/10.1562/0031-8655(2003)0770431TCTOTE2.0.CO2.

[44] H. Kataoka, H. Nishie, N. Hayashi, M. Tanaka, A. Nomoto, S. Yano, T. Joh, New photodynamic therapy with next-generation photosensitizers, Ann. Transl. Med. 5 (2017), https://doi.org/10.21037/atm.2017.03.59 183–183.

[45] J.A.S.C, J.P.C.T. Leandro, M.O. Lourenço, Bernardo A. Iglesias, Patrícia M.R. Pereira, Henrique Girão, Rosa Fernandes, Maria G.P.M.S. Neves, Synthesis, characterization and biomolecule-binding properties of novel tetra-platinum(ii)-thiopyridylporphyrins, Dalton Trans. 44 (2015).

[46] V.A. Oliveira, B.A. Iglesias, B.L. Auras, A. Neves, H. Terenzi, Photoactive: Meso-tetra(4-pyridyl)porphyrin-tetrakis-[chloro(2,2'bipyridine)platinum(II)] derivatives recognize and cleave DNA upon irradiation, Dalton Trans. 46 (2017) 1660–1669. doi:https://doi.org/10.1039/c6dt04634g.

[47] T.T. Tasso, T.M. Tsubone, M.S. Baptista, L.M. Mattiazzi, T.V. Acunha, B.A. Iglesias, Isomeric effect on the properties of tetraplatinated porphyrins showing optimized phototoxicity for photodynamic therapy, Dalton Trans. 46 (2017) 11037–11045, https://doi.org/10.1039/c7dt01205e.

[48] G.K. Couto, B.S. Pacheco, V.M. Borba, J.C.R. Junior, T.L. Oliveira, N.V. Segatto, F.K. Seixas, T.V. Acunha, B.A. Iglesias, T. Collares, Tetra-cationic platinum(II) porphyrins like a candidate photosensitizers to bind, selective and drug delivery for metastatic melanoma, J. Photochem. Photobiol B Biol. (2020), https://doi.org/10.1016/j.jphotobiol.2019.111725.

[49] S. Pramual, K. Lirdprapamongkol, V. Jouan-Hureaux, M. Barberi-Heyob, C. Frochot, J. Svasti, N. Niamsiri, Overcoming the diverse mechanisms of multidrug resistance in lung cancer cells by photodynamic therapy using pTHPP-loaded PLGA-lipid hybrid nanoparticles, Eur. J. Pharm. Biopharm. (2020), https://doi.org/10.1016/j.ejpb.2020.02.012.

[50] X. Wang, Z. Li, Y. Ding, K. Wang, Z. Xing, X. Sun, W. Guo, X. Hong, X. Zhu, Y. Liu, Enhanced photothermal-photodynamic therapy for glioma based on near-infrared dye functionalized Fe3O4 superparticles, Chem. Eng. J. (2020), https://doi.org/10.1016/j.cej.2019.122693.

[51] M.M. Deken, M.M. Kijanka, I. Beltrán Hernández, M.D. Slooter, H.S. de Bruijn, P.J. van Diest, P.M.P. van Bergen en Henegouwen, C.W.G.M. Lowik, D.J. Robinson, A.L. Vahrmeijer, S. Oliveira, Nanobody-targeted photodynamic therapy induces significant tumor regression of trastuzumab-resistant HER2-positive breast cancer, after a single treatment session, J. Control. Release (2020), https://doi.org/10.1016/j.jconrel.2020.04.030.

[52] S. Zhen, X. Yi, Z. Zhao, X. Lou, F. Xia, B.Z. Tang, Drug delivery micelles with ef-ficient near-infrared photosensitizer for combined image-guided photodynamic therapy and chemotherapy of drug-resistant cancer, Biomaterials (2019), https://doi.org/10.1016/j.biomaterials.2019.119330.

[53] A. Khdair, Di Chen, Y. Patil, L. Ma, Q.P. Dou, M.P.V. Shekhar, J. Panyam, Nanoparticle-mediated combination chemotherapy and photodynamic therapy overcomes tumor drug resistance, J. Control. Release (2010), https://doi.org/10.1016/j.jconrel.2009.09.004.

[54] D.R. Mokoena, B.P. George, H. Abrahamse, Enhancing breast cancer treatment using a combination of cannabidiol and gold nanoparticles for photodynamic therapy, Int. J. Mol. Sci. (2019), https://doi.org/10.3390/ijms20194771.

[55] T. Michy, T. Massias, C. Bernard, L. Vanwonterghem, M. Henry, M. Guidetti, G. Royal, J.L. Coll, I. Texier, V. Josserand, A. Hurbin, Verteporfin-loaded lipid nanoparticles improve ovarian cancer photodynamic therapy in vitro and in vivo, Cancers (Basel) (2019), https://doi.org/10.3390/cancers11111760.

[56] X. Wang, G. Ramamurthy, A.A. Shirke, E. Walker, J. Mangadlao, Z. Wang, Y. Wang, L. Shan, M.D. Schluchter, Z. Dong, S.M. Brady-Kalnay, N.K. Walker, M. Gargesha, G. MacLennan, D. Luo, R. Sun, B. Scott, D. Roy, J. Li, J.P. Basilion, Photodynamic therapy is an effective adjuvant therapy for image-guided surgery in prostate cancer, Cancer Res. (2020), https://doi.org/10.1158/0008-5472.CAN-19-0201.

[57] M. Yang, T. Yang, C. Mao, Enhancement of photodynamic cancer therapy by phy-sical and chemical factors, Angew. Chem. Int. Ed. (2019), https://doi.org/10.1002/anie.201814098.

[58] P.M.-K. Ahmed El-Hussein, Sello L. Manoto, Saturnin Ombinda-Lemboumba, Ziya A. Alrowaili, A Review of Chemotherapy and Photodynamic Therapy for Lung Cancer Treatment, Anti Cancer Agents Med. Chem. (2020), https://doi.org/10.2174/1871520620666200403144945.

[59] G. Tan, W. Li, J. Cheng, Z. Wang, S. Wei, Y. Jin, C. Guo, F. Qu, Magnetic iron oxide modified pyropheophorbide-a fluorescence nanoparticles as photosensitizers for photodynamic therapy against ovarian cancer (SKOV-3) cells, Photochem. Photobiol. Sci. (2016), https://doi.org/10.1039/c6pp00340k.

[60] P.V. Ostroverkhov, A.S. Semkina, V.A. Naumenko, E.A. Plotnikova, P.A. Melnikov, T.O. Abakumova, R.I. Yakubovskaya, A.F. Mironov, S.S. Vodopyanov, A.M. Abakumov, A.G. Majouga, M.A. Grin, V.P. Chekhonin, M.A. Abakumov, Synthesis and characterization of bacteriochlorin loaded magnetic nanoparticles (MNP) for personalized MRI guided photosensitizers delivery to tumor, J. Colloid Interface Sci. (2019), https://doi.org/10.1016/j.jcis.2018.10.087.

[61] K.H. Choi, K.C. Nam, G. Cho, J.S. Jung, B.J. Park, Enhanced photodynamic antic-ancer activities of multifunctional magnetic nanoparticles (Fe3O4) conjugated with chlorin e6 and folic acid in prostate and breast cancer cells, Nanomaterials (2018), https://doi.org/10.3390/nano8090722.

[62] C.S. Chiang, Y.C. Kao, T.J. Webster, W.C. Shyu, H.W. Cheng, T.Y. Liu, S.Y. Chen, Circulating tumor-cell-targeting Au-nanocage-mediated bimodal phototherapeutic properties enriched by magnetic nanocores, J. Mater. Chem. B (2020), https://doi.org/10.1039/d0tb00501k.

[63] F. Fan, Y. Yu, F. Zhong, M. Gao, T. Sun, J. Liu, H. Zhang, H. Qian, W. Tao, X. Yang, Design of tumor acidity-responsive sheddable nanoparticles for fluorescence/mag-netic resonance imaging-guided photodynamic therapy, Theranostics (2017), https://doi.org/10.7150/thno.18557.

[64] R.K. Horlings, J.B. Terra, M.J.H. Witjes, MTHPC mediated, systemic photodynamic therapy (PDT) for nonmelanoma skin cancers: case and literature review, Lasers Surg. Med. 47 (2015) 779–787, https://doi.org/10.1002/lsm.22429.

[65] M.C. Rodrigues, L.G. Vieira, F.H. Horst, E.C. de Araújo, R. Ganassin, C. Merker, T. Meyer, J. Böttner, T. Venus, J.P.F. Longo, S.B. Chaves, M.P. Garcia, I. Estrela-Lopis, R.B. Azevedo, L.A. Muehlmann, Photodynamic therapy mediated by alumi-nium-phthalocyanine nanoemulsion eliminates primary tumors and pulmonary metastases in a murine 4T1 breast adenocarcinoma model, J. Photochem. Photobiol B Biol. (2020), https://doi.org/10.1016/j.jphotobiol.2020.111808.

[66] X. Shen, L. Li, H. Wu, S.Q. Yao, Q.H. Xu, Photosensitizer-doped conjugated polymer nanoparticles for simultaneous two-photon imaging and two-photon photodynamic therapy in living cells, Nanoscale (2011), https://doi.org/10.1039/c1nr11104c.

[67] A. Nadhman, S. Nazir, M. Ihsanullah Khan, S. Arooj, M. Bakhtiar, G. Shahnaz, M. Yasinzai, PEGylated silver doped zinc oxide nanoparticles as novel photo-sensitizers for photodynamic therapy against Leishmania, Free Radic. Biol. Med. (2014), https://doi.org/10.1016/j.freeradbiomed.2014.09.005.

[68] G. Ramírez-García, E. De La Rosa, T. López-Luke, S.S. Panikar, P. Salas, Controlling trapping states on selective theranostic core@shell (NaYF4:Yb,Tm@TiO2-ZrO2) nanocomplexes for enhanced NIR-activated photodynamic therapy against breast cancer cells, Dalton Trans. (2019), https://doi.org/10.1039/c9dt00482c.

[69] J. Shi, P.W. Kantoff, R. Wooster, O.C. Farokhzad, Cancer nanomedicine: Progress, challenges and opportunities, Nat. Rev. Cancer (2017), https://doi.org/10.1038/nrc.2016.108.

[70] M.R. Hamblin, L.Y. Chiang, S. Lakshmanan, Y.Y. Huang, M. Garcia-Diaz, M. Karimi, A.N. De Souza Rastelli, R. Chandran, Nanotechnology for photodynamic therapy: A perspective from the Laboratory of Dr. Michael R. Hamblin in the Wellman Center for Photomedicine at Massachusetts General Hospital and Harvard Medical School, Nanotechnol. Rev. (2015), https://doi.org/10.1515/ntrev-2015-0027.

[71] O. Medina, Y. Zhu, K. Kairemo, Targeted liposomal drug delivery in Cancer, Curr. Pharm. Des. (2005), https://doi.org/10.2174/1381612043383467.

[72] A. Salvati, S. Ristori, J. Oberdisse, O. Spalla, G. Ricciardi, D. Pietrangeli, M. Giustini, G. Martini, Small angle scattering and zeta potential of liposomes loaded with octa(carboranyl)porphyrazine, J. Phys. Chem. B (2007), https://doi.org/10.1021/jp0731710.

[73] A. Sneider, R. Jadia, B. Piel, D. VanDyke, C. Tsiros, P. Rai, Engineering remotely triggered liposomes to target triple negative breast cancer, Oncomedicine (2016), https://doi.org/10.7150/oncm.17406.

[74] J.D. Spikes, A preliminary comparison of the photosensitizing properties of por-phyrins in aqueous solution and liposomal systems, Adv. Exp. Med. Biol. (1983), https://doi.org/10.1007/978-1-4684-4406-3_17.

[75] S.D. Li, L. Huang, Pharmacokinetics and Biodistribution of Nanoparticles, in: Mol. Pharm. (2008), https://doi.org/10.1021/mp800049w.

[76] E. Kahraman, A. Karagöz, S. Dinçer, Y. Özsoy, Polyethylenimine modified and non-modified polymeric micelles used for nasal administration of carvedilol, J. Biomed. Nanotechnol. (2015), https://doi.org/10.1166/jbn.2015.1915.

[77] M.A. Moretton, C. Hocht, C. Taira, A. Sosnik, Rifampicin-loaded "flower-like" polymeric micelles for enhanced oral bioavailability in an extemporaneous liquid fixed-dose combination with isoniazid, Nanomedicine (2014), https://doi.org/10.2217/nnm.13.154.

[78] J. Zhang, Y.C. Liang, X. Lin, X. Zhu, L. Yan, S. Li, X. Yang, G. Zhu, A.L. Rogach, P.K.N. Yu, P. Shi, L.C. Tu, C.C. Chang, X. Zhang, X. Chen, W. Zhang, C.S. Lee, Self-monitoring and self-delivery of photosensitizer-doped nanoparticles for highly effective combination cancer therapy in vitro and in vivo, ACS Nano (2015), https://doi.org/10.1021/acsnano.5b02513.

[79] C.A.A.W.K. LAMCH Ł, KULBACKA J, PIETKIEWICZ J, ROSSOWSKA J, DUBIŃSKA-MAGIERA M, Preparation and characterization of new zinc(II) phthalocyanine - Containing poly(l-lactide)-b-poly(ethylene glycol) copolymer micelles for photodynamic therapy, J. Photochem. Photobiol. B Biol. 160 (2016) 185–197.

[80] J. Zhang, C. Jiang, J.P. Figueiró Longo, R.B. Azevedo, H. Zhang, L.A. Muehlmann, An updated overview on the development of new photosensitizers for anticancer photodynamic therapy, Acta Pharm. Sin. B 8 (2018) 137–146, https://doi.org/10.1016/j.apsb.2017.09.003.

[81] L.A. Muehlmann, B.C. Ma, J.P.F. Longo, M.F. de M. Almeida Santos, R.B. Azevedo, Aluminum-phthalocyanine chloride associated to poly(methyl vinyl ether-co-maleic anhydride) nanoparticles as a new third-generation photosensitizer for anticancer photodynamic therapy, Int. J. Nanomedicine (2014), https://doi.org/10.2147/IJN.S57420.

[82] J.P.F. Longo, S.P. Lozzi, A.R. Simioni, P.C. Morais, A.C. Tedesco, R.B. Azevedo, Photodynamic therapy with aluminum-chloro-phtalocyanine induces necrosis and vascular damage in mice tongue tumors, J. Photochem. Photobiol. B Biol. (2009), https://doi.org/10.1016/j.jphotobiol.2008.11.003.

[83] G. Klein Couto, J.C. Rodrigues, B.S. Pacheco, L. Damé Simões, J.D. Paschoal, F.K. Seixas, T.V. Acunha, B.A. Iglesias, T. Collares, Zinc(II), copper(II) and nickel(II) ions improve the selectivity of tetra-cationic platinum(II) porphyrins in photodynamic therapy and stimulate antioxidant defenses in the metastatic melanoma lineage (A375), Photodiagn. Photodyn. Ther. (2020), https://doi.org/10.1016/j.pdpdt.2020.101942.

[84] A. Fonseca Teixeira, J.R. Alves, Title: Low power blue LED exposure increases effects of doxorubicin on MDA-MB-231 breast cancer cells, Photodiagn. Photodyn. Ther. (2018), https://doi.org/10.1016/j.pdpdt.2018.07.016.

[85] V. Monge-Fuentes, L.A. Muehlmann, J.P.F. Longo, J.R. Silva, M.L. Fascineli, R.B. Azevedo, P. de Souza, F. Faria, I.A. Degterev, A. Rodriguez, F.P. Carneiro, C.M. Lucci, P. Escobar, R.F.B. Amorim, Photodynamic therapy mediated by acai oil (Euterpe oleracea Martius) in nanoemulsion: a potential treatment for melanoma, J. Photochem. Photobiol. B Biol. (2017), https://doi.org/10.1016/j.jphotobiol.2016.12.002.

[86] S. Bruno, D. Coppola, G. Di Prisco, D. Giordano, C. Verde, Enzymes from marine polar regions and their biotechnological applications, Mar. Drugs. (2019), https://doi.org/10.3390/md17100544.

[87] M.G. Pessôa, K.A.C. Vespermann, B.N. Paulino, M.C.S. Barcelos, G.M. Pastore, G. Molina, Newly isolated microorganisms with potential application in biotechnology, Biotechnol. Adv. (2019), https://doi.org/10.1016/j.biotechadv.2019.01.007.

[88] A.A. Foggiato, D.F. Silva, R.C.F.R. Castro, Effect of photodynamic therapy on surface decontamination in clinical orthodontic instruments, Photodiagn. Photodyn. Ther. (2018), https://doi.org/10.1016/j.pdpdt.2018.09.003.

[89] M.A. Desta Sisay, A review on major food borne bacterial illnesses, J. Trop. Dis (2015), https://doi.org/10.4172/2329-891x.1000176.

[90] E.P.C. Lai, Z. Iqbal, T.J. Avis, Combating antimicrobial resistance in foodborne microorganisms, J. Food Prot. (2016), https://doi.org/10.4315/0362-028X.JFP-15-023.

[91] A.F. Silva, A. Borges, E. Giaouris, J.M. Graton Mikcha, M. Simões, Photodynamic inactivation as an emergent strategy against foodborne pathogenic bacteria in planktonic and sessile states, Crit. Rev. Microbiol. (2018), https://doi.org/10.1080/1040841X.2018.1491528.

[92] M.J. Kim, C.H. Tang, W.S. Bang, H.G. Yuk, Antibacterial effect of 405 ± 5 nm light emitting diode illumination against Escherichia coli O157:H7, Listeria monocytogenes, and Salmonella on the surface of fresh-cut mango and its influence on fruit quality, Int. J. Food Microbiol. (2017), https://doi.org/10.1016/j.ijfoodmicro.2016.12.023.

[93] M.P. Rocha, A.L.M. Ruela, L.P. Rosa, G.P.O. Santos, F.C.S. Rosa, Antimicrobial Photodynamic therapy in dentistry using an oil-in-water microemulsion with curcumin as a mouthwash, Photodiagn. Photodyn. Ther. (2020), https://doi.org/10.1016/j.pdpdt.2020.101962.

Os resultados que fazem parte desta tese de doutorado estão apresentados sob forma de artigo. Os itens materiais e métodos, resultados, discussão e referências bibliográficas encontram-se no próprio manuscrito.

4.2 Capítulo 2 (Artigo 2) - **The Melding of Drug Screening Platforms for Melanoma (review)**

O artigo foi publicado na revista **Frontiers in Oncology. F.I: 4.848**

The Melding of Drug Screening Platforms for Melanoma

Gabriela Klein Couto[1], Natália Vieira Segatto[2], Thaís Larré Oliveira[2], Fabiana Kömmling Seixas[2], Kyle M. Schachtschneider[3,4,5] and Tiago Collares[2*]

[1] Research Group in Molecular and Cellular Oncology, Postgraduate Program in Biochemistry and Bioprospecting, Cancer Biotechnology Laboratory, Center for Technological Development, Federal University of Pelotas, Pelotas, Brazil, [2] Biotechnology Graduate Program, Molecular and Cellular Oncology Research Group, Laboratory of Cancer Biotechnology, Technology Development Center, Federal University of Pelotas, Pelotas, Brazil, [3] Department of Radiology, University of Illinois at Chicago, Chicago, IL, United States, [4] Department of Biochemistry & Molecular Genetics, University of Illinois at Chicago, Chicago, IL, United States, [5] National Center for Supercomputing Applications, University of Illinois at Urbana-Champaign, Urbana, IL, United States

The global incidence of cancer is rising rapidly and continues to be one of the leading causes of death in the world. Melanoma deserves special attention since it represents one of the fastest growing types of cancer, with advanced metastatic forms presenting high mortality rates due to the development of drug resistance. The aim of this review is to evaluate how the screening of drugs and compounds for melanoma has been performed over the last seven decades. Thus, we performed literature searches to identify melanoma drug screening methods commonly used by research groups during this timeframe. *In vitro* and *in vivo* tests are essential for the development of new drugs; however, incorporation of *in silico* analyses increases the possibility of finding more suitable candidates for subsequent tests. *In silico* techniques, such as molecular docking, represent an important and necessary first step in the screening process. However, these techniques have not been widely used by research groups to date. Our research has shown that the vast majority of research groups still perform *in vitro* and *in vivo* tests, with emphasis on the use of *in vitro* enzymatic tests on melanoma cell lines such as SKMEL and *in vivo* tests using the B16 mouse model. We believe that the union of these three approaches (*in silico, in vitro,* and *in vivo*) is essential for improving the discovery and development of new molecules with potential antimelanoma action. This workflow would provide greater confidence and safety for preclinical trials, which will translate to more successful clinical trials and improve the translatability of new melanoma treatments into clinical practice while minimizing the unnecessary use of laboratory animals under the principles of the 3R's.

Keywords: drug screening, melanoma, *in silico*, *in vitro*, *in vivo*, cancer, 3R, B16 melanoma

INTRODUCTION

The global incidence of cancer is rapidly rising and remains a leading cause of death worldwide (1), highlighting the need for ongoing research focused on the discovery and development of new drug candidate molecules as well as new treatments. According to the World Health Organization (WHO), about 8.8 million people die of cancer each year (2). With regard to Brazil, around 600,000 new cancer cases are expected for the biennium 2018–2019 (3). This is partially due to the increased incidence of Melanoma in recent years (4). Not only does melanoma represents one of the fastest growing forms of cancer, but its advanced metastatic forms carry high mortality rates due to their development of resistance to drugs traditionally used to treat melanoma (5).

In order to determine the optimal treatment strategy, melanoma patients must be evaluated and classified into stages. For stages 0 and I, surgery for tumor excision is generally the preferred treatment option. For stage II, or stage I with positive sentinel lymph node biopsy, adjuvant treatment with interferon is preferred. For stage III where the tumor has already metastasized to the lymph nodes, surgery with wide excision in addition to adjuvant treatment with interferon is preferred. If the patient does not respond, the remaining options include: bacillus Calmette-Guérin (BCG) immunotherapy, interleukin-2 (intralesional), radiotherapy, imiquimod application, and chemotherapy (see **Table 1** for a list of the most commonly used chemotherapeutics for melanoma treatment). Stage IV melanomas are especially difficult to treat. Chemotherapy with dacarbazine and temozolomide may be used individually or in combination with interleukin-2 and/or interferon. In recent years, therapies such as immunotherapy and targeted therapies have proven to be more effective than the traditional chemotherapy (21). Although early-stage melanoma can be treated with surgery, advanced (metastatic) disease is difficult to cure and treatment options are unsatisfactory, highlighting the urgent need for novel treatment strategies (22).

For new drugs to be available for commercialization, they must first go through the necessary steps mandated by regulatory agencies such as the Food and Drug Administration (FDA)[1], namely: Discovery and development; preclinical trials, clinical trials, and FDA review. Research and development of new antimelanoma molecules occurs in several ways. Some research groups develop or acquire software in order to test thousands of molecules, aiming to select the most promising candidates for the next tests (*in vitro/in vivo*). This development process is known as "*in silico* test" (23, 24). In addition to predicting safety and toxicity, these tests can predict interactions between molecules and their receptors, saving time and money during the process of drug screening. Other groups choose to test some molecules *in vitro* and then select their candidates for future *in vivo* and *ex vivo* trials. Both of these approaches follow the 3R principle: "reduction, replacement, and refinement" of animal use. In order to adhere to this principle, it is important to continuously review and optimize the way screening of new candidate drugs is performed. In addition, a robust initial screening of these molecules provides strong candidates for subsequent preclinical and clinical testing.

The objective of this review is to analyze the methods used to screen new drug candidate molecules over the last seven decades using articles published during this period (**Figure 1**). As the use of *in silico* and *ex vivo* methodologies are not as widespread compared with *in vivo* and *in vitro* methodologies, this review is divided into three major sessions according to the chronological order in which these different screening approaches were first utilized.

---

[1]https://www.fda.gov/patients/drug-development-process/step-5-fda-post-market-drug-safety-monitoring

Section I
In vitro Drug Assays for Melanoma

In vitro drug screening assays for melanoma are mostly performed to evaluate the cytotoxic potential of new compounds for cancer cell lines and to characterize target mechanisms of action. Several mechanisms have been identified in melanoma regression, including apoptosis pathways, necrosis, and autophagy (25). In addition to cytotoxicity, immune mechanisms are also involved in the therapeutic efficacy against metastatic melanoma, corroborating the use of intralesional BCG as an immunotherapeutic agent (26, 27).

The need to conduct animal research based on 3Rs principle has strengthened the development of novel and more robust *in vitro* models able to better mimic *in vivo* human conditions. Tumor biology is extensively diverse in terms of genetics, pigmentation, morphology, metabolism, and immune microenvironment. A variety of screening techniques have been developed tin an attempt to address this variability. Combination therapies have been clinically employed; however, resistance to therapy has propelled the search for low-cost and rapid screening techniques that allow for selection of new and more effective compounds (28).

In this section, we aim to show the evolution of *in vitro* techniques employed for melanoma drug screening, ranging from conventional assays to novel models for the discovery of more efficient targets.

Cell Lines

Most melanoma cell lines used for *in vitro* drug screening are derived from humans. In addition, some studies have explored the use of cells obtained directly from both primary and metastatic tumor biopsies to characterize the potential of novel drugs *in vitro* (29–32). The establishment and analysis of primary melanoma cell cultures is important to investigate tumor heterogeneity in the era of personalized medicine. However, the need to preserve biopsy samples for histological diagnosis may limit their use for *in vitro* drug screening.

Mutations involved in human melanoma progression are commonly observed in *BRAF/NRAS* and *TP53* resulting in altered regulation of the RAS RAF-MEK-ERK and ARF-p53 pathways, respectively (33). As expected, the most commonly used melanoma cell lines harbor many of these mutations (**Table 2**). In addition, as metastatic melanoma is the most aggressive type of skin cancer, cell lines derived from metastatic tumors (**Table 2**) are routinely employed to evaluate drugs targeting cell migration and invasiveness (34).

Both pigmented and non-pigmented melanoma cell lines have been used to identify drugs capable of improving therapeutic efficacy and avoiding resistance related to melanin's scavenger ability (35). Amelanotic cell lines, especially A375 and SKMEL-28, have been employed for this purpose (36, 37). Sharma et al. demonstrated improved efficacy of a hypericin-based therapy following depigmentation of melanotic and amelanotic cell lines (UCT Mel-1 and A375, respectively) with a tyrosinase-inhibitor, suggesting the melanogenesis process represents a promising target for treating metastatic melanoma (36).

TABLE 1 | Chemotherapeutics most commonly used for treatment of melanoma.

| chemotherapy | *In vitro* tests | | | *In vivo* tests | | | Monkey | Clinical tests | Approval date[a] | Company | References |
	Institute	Cell line	Human blood	Mouse/ camundongos	Rabbit	Dogs /monkey					
Dacarbazine[d] (also called DTIC)	-American Cancer Society; -Brazilian Ministry of Health; - National Cancer Institute.	Information not found.	Analysis of human peripheral blood lymphocytes	Carcinogenicity	Risk for Pregnancy	Information not found.	Information not found.	PHASE II and III	May.27.1975/ FDA	BAYER HLTHCARE	(6–9)
Temozolomide[d]	-American Cancer Society; -Brazilian Ministry of Health.	Information not found.	Clastogenic analysis in human lymphocytes	– Carcinogenicity; –Toxicology profile.	Toxicology profile.	–Testicular atrophy was observed; –Toxicology studies were performed.	Information not found.	PHASE III and IV	Aug.11.1999/ FDA	MERCK SHARP DOHME	(9, 10)
Nab- paclitaxel[b]	American Cancer Society.	CHO cell line –mutagenicity test	clastogenic analysis in human lymphocytes.	– Genotoxicity; –Risk for pregnancy.	Information not found.	Information not found.	Information not found.	PHASE II and III	Dec. 29, 1992/ FDA	HQ SPCLT PHARMA	(11–13)
Cisplatin[c]	-American Cancer Society; -Brazilian Ministry of Health.	–Mutagenic test; – Chromosomal abnormalities in cell lines.	Information not found.	–Drug is teratogenic, embryotoxic, carcinogenic and leukemogenic; –Regression of tumors in mice was observed.	Information not found.	Information not found.	Information not found.	PHASE III	Dec. 19, 1978 /FDA	HQ SPCLT PHARMA	(14)
Carboplatin[d]	American Cancer Society.	Genotoxicity assessment	Information not found.	–Evaluation of the lethal dose; –Investigation of toxic effects; –Risk for pregnancy.	Information not found.	–A lethal dose was evaluated; –Investigation of toxic effects.	Information not found.	PHASE II and III	March 3, 1989 /FDA	Uninformed	(15–17)

(Continued)

TABLE 1 | Continued

| chemotherapy | Institute | In vitro tests | | In vivo tests | | | Monkey | Clinical tests | Approval date[a] | Company | References |
		Cell line	Human blood	Mouse/ camundongos	Rabbit	Dogs /monkey					
Vinblastine[d]	American Cancer Society	– Mutagenicity; –There is no information on clastogenicity.	Information not found.	–Risk of Mutagenicity; –There is no information on clastogenicity; – Degenerative changes were observed in germ cells, in animal studies.	Information not found.	Information not found.	Information not found.	PHASE II and III	Nov. 5, 1965/FDA	Uninformed	
Nivolumab[d]	American Cancer Society	In vitro assays: -Specific memory response antigen in vitro.	Tests carried out: –Mixed lymphocytic reaction; -Stabilization of enterotoxin B by Staphylococcal of PBMCs; -Suppression assay with regulatory T cells	Transgenic mice were immunized for antibody-screening test			- Pharmacokinetics, toxicity and immunogenicity of nivolumab in cynomolgus monkeys; -Imunization of SK-MEL-3 melanoma cells and surface antigen of hepatitis B virus in cynomolgus monkeys.	PHASE III	Dec. 22, 2014 /FDA	BRISTOL MYERS SQUIBB	(18)
Ipilimumab[d]	American Cancer Society		–To evaluate potential action was tested on human lymphocytes; –Evaluate immunotherapy action.	Risk assessment in pregnancy.	Information not found.	Information not found.	-Evaluation of risk pregnancy; –Post abnormalities cement; –Toxicological tests.	PHASE I, II and III	March 25, 2011/FDA	BRISTOL MYERS SQUIBB	(19, 20)

[a] http://drugcentral.org; [b] https://media.celgene.com/content/uploads/sites/19/Abraxane_Bula_Profissional.pdf; [c] http://pfizer.com.br/sites/g/files/g10027021/f/product_attachments/PlatamineCS_PS.pdf; [d] https://dailymed.nlm.nih.gov/dailymed/drugInfo.cfm?setid=f073b58e-56d6-4c8d-a2ce-b37719402d77&audience=consumer; http://www.bccancer.bc.ca/drug-database-site/Drug%20Index/Vinblastine_monograph_1Feb2015.pdf; https://clinicaltrials.gov/ct2/show/NCT00213278.
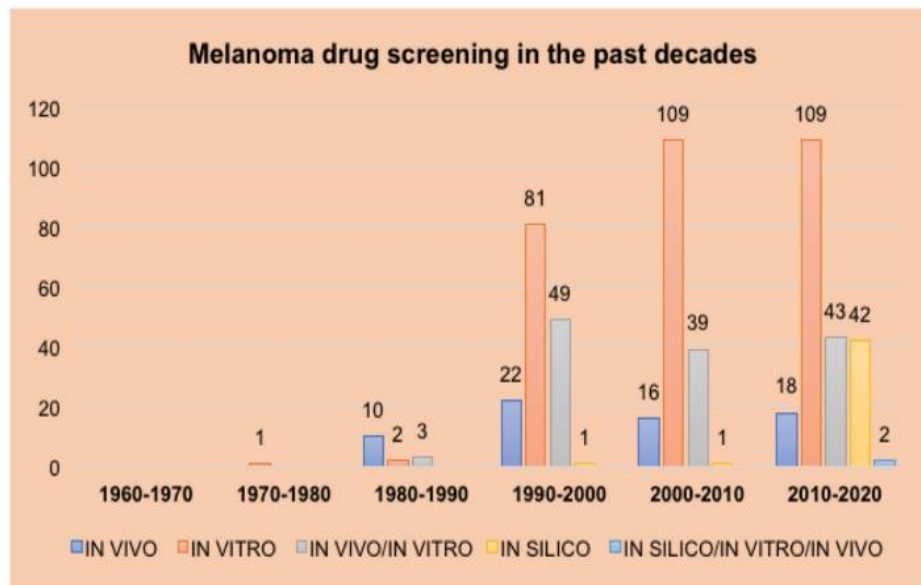
FIGURE 1 | Results indicate the number of articles using each screening methodology by decade. The number of articles found for each topic searched is presented on the y axis. Different decades are presented in the x axis. Each bar represents a different screening method (*in vitro*, *in vivo*, and *in silico*) and the combination of more than one screening method: dark blue for *in vivo*, orange for *in vitro*, gray for *in vivo/in vitro*, yellow for *in silico* and light blue for all the three screening methods (*in silico/in vitro/in vivo*).

Murine melanoma is mainly represented by studies using the metastatic B16F10 cell line. The B16F10 cell line retains wild-type copies of *TP53*, *NRAS*, and *BRAF*, although it does harbor deletions of tumor suppressor genes associated with the INK4a/ARF pathway (38). B16 cell lines are frequently employed to induce tumors in murine models for *in vivo* drug screening, which is discussed in detail below.

Conventional Assays

The most common assays used for screening drugs for melanoma treatment, as well as for other cancers, are employed to evaluate enzyme activity. Other techniques have been used to determine mechanisms of cytotoxicity, including membrane damage, DNA synthesis blockade, production of reactive oxygen species (ROS, and drug uptake (39).

Assays primarily based on tetrazolium compounds have been used since the 1980s to determine cell viability. These compounds, such as 3- (4,5-dimethylthiazol-2-yl)−2,5-diphenyl tetrazolium bromide (MTT) and 3-(4,5-dimethylthiazol-2-yl)-5-(3-carboxymethoxyphenyl)-2- (4-sulfophenyl)-2H-tetrazolium (MTS), are used as substrates in colorimetric assays to determine the activity level of mitochondrial enzymes. These techniques are often used as initial steps for novel molecule screening. However, there are several disadvantages associated with tests based on detection of mitochondrial enzymatic activity, including the fact that reprogramming of melanoma cells is frequently accompanied by a metabolic switch that uses glycolysis rather than oxidative phosphorylation for energy production, and that tetrazolium compounds can be reduced by other mechanisms independent of enzymatic catalysis, which can lead to a biased result (40). Thymidine incorporation assays are a direct method to measure DNA synthesis during cell division that have

been used extensively since the 80s in studies reporting drug evaluation for melanoma (41). However, assays based on isotype incorporation are reported to be more sensitive and reliable than indirect methods to assess cell viability, such as MTT and clonogenic assays (29).

A more recent study used the activity of an acid phosphatase enzyme to determine melanoma cell viability after treatment with kinase inhibitors (42). Kinase proteins are involved in several process that are deregulated in cancers, including melanoma (43). Using Sk-Mel-28 and Sk-Mel-2 cell lines, which harbor *BRAF* and *NRAS* mutants, respectively, the authors screened 160 compounds of which 20 demonstrated the ability to inhibit growth rates by more than 50%. Among them, fascaplysin, a CDK4 inhibitor, demonstrated the ability to induce apoptosis and inhibit growth using a clonogenic assay. CDK4 deregulation due to a lack of expression of the tumor suppressor p16INK4a is associated with 82% of melanoma metastases (44). These results demonstrate that kinase-targeted screening assays are a promising strategy for identification of novel, targeted therapeutics for metastatic melanoma. Other studies employed for preliminary drug screening for melanoma are based on ATP detection through a luminescent signal produced by the luciferase reaction (45, 46).

The production of melanin by melanocytes occurs through activity of a tyrosinase enzyme in an organelle called melanosome (47). It is well established that melanin can contribute to therapeutic evasion and resistance by acting as a chelator agent (48–50). Tyrosinase-targeted drugs may promote melanocyte depigmentation and consequently improve therapeutic susceptibility (36). Thus, the melanogenesis process has also been explored as a therapeutic target since the 90's (48, 51, 52). *In vitro* techniques to evaluate tyrosinase activity have been employed.

TABLE 2 | Human melanoma cell lines most frequently used for *in vitro* drug screening studies.

Human melanoma cell lines	Genetic characteristics*	Pigmentation*
LOX-IMVI[#]	*BRAF* ValGlu (600)	Amelanotic
Malme-3M[#]	*BRAF* ValGlu (600) CDKN2A deletion	Pigmented
SKMEL-2[#]	*NRAS* GlnArg (61) *TP53* GlySer (245)	Amelanotic
SKMEL-5[#]	*BRAF* ValGlu (600)	Amelanotic
SKMEL-28	*BRAF* ValGlu (600) *CDK4* ArgCys (24) *EGFR* ProSer (753) *PTEN* ThrAla (167) *TP53* LeuArg (145)	Amelanotic
UACC-62	*BRAF* ValGlu (600) PTEN insertion; frameshift (248)	**
UACC-257	*BRAF* ValGlu (600) CDKN2A deletion	**
M14[#]	*BRAF* ValGlu (600) *TP53* GlyGlu (266)	Amelanotic
WM1366	*NRAS* GlnLeu (61)	
A375	*BRAF* ValGlu (600)	Amelanotic
SKMEL-1[#]	*BRAF* ValGlu (600) *CTNNB1* SerCys (33)	Pigmented

Data obtained from PubMed, ATCC and ExPASy databases.
#Derived from metastatic sites.
*** Information not described.*

Riley *et al.* screened a group of phenolic compounds with side-chain variations for melanogenesis-targeted cytotoxicity (51). The authors evaluated tyrosinase mediated oxidation of phenols to quinones using oximetry and spectrophotometry, in addition to the relation with inhibition of thymidine incorporation as a measure of cell viability. Phenols with lipophilic sidechains demonstrated increased melanocytotoxic potential, highlighting the importance of screening organelle-specific drug targets. More recent works have accessed tyrosinase activity using L-dihydroxyphenylalanine (L-DOPA), a precursor for melanin biosynthesis, as a substrate (48, 53).

Studies from as early as the 80s were already seeking to develop screening techniques to detect anti-proliferative or anti-invasiveness drugs for melanoma (34, 54). A membrane invasion culture system (MICS) was developed using a basement-membrane-like structure to evaluate the ability of a drug to block invasiveness, a desirable characteristic to fight against metastasis. Using the A375 metastatic cell line, its ability to invade Matrigel-filters in MICS chambers was measured after drug exposure by staining and counting cells that remained trapped on the filters. After evaluation of 26 compounds in different dosages, 15 combinations demonstrated more than 60% inhibition of invasion compared to untreated cells. Compounds were previously characterized based on their non-cytotoxic profile in established concentrations through clonogenic assays to ensure that cells would remain viable, i.e., retaining their ability

to metastasis (34). A fluorometric assay was developed in the early 90's to screen compounds for anti-proliferative potential based on the ability of cytoplasmatic esterase to metabolize the substrate 4-methylumbelliferyl heptanoate (MUH) in viable cells. The results of this assay correlated with results obtained using the thymidine incorporation method. The test was further validated using cisplatin and vindesine treatments on SK Mel-28 and StML-12 melanoma cell lines (54).

Aiming to improve selectivity, studies from the last decade have explored the potential of photodynamic therapy in melanoma (48, 55–57). Such studies have also employed uptake assays to assess the internalization of photosensitizers by tumor cells. Internalization experiments are commonly based on fluorescent microscopy, confocal microscopy, fluorometry, and spectrophotometry (48, 55, 56). Following preliminary screenings, other *in vitro* techniques are typically utilized to better characterize compounds with promising characteristics for melanoma treatment, including (i) flow cytometry (FC) to detect phosphatidylserine residues that are externalized in apoptotic cells (58) and to assess cell cycle distribution (59); (ii) enzymatic assays to detect caspase activity (60); (iii) TUNEL staining to measure DNA damage (60); and (iv) western blot to detect expression of kinase proteins (60, 61).

Unfortunately, due to the extensive diversity of melanoma tumors and mechanisms involved in cell death processes, it is difficult to elect a single test to predict effective drugs. Moreover, most novel screening approaches described in the literature do not use positive and negative clinical samples nor a single standard treatment as a reference to determine the potential predictive value of new *in vitro* screening techniques, making it difficult to compare the efficacy of these methodologies. Thus, our group has employed a combination of several *in vitro* approaches to determine the potential efficacy of novel targets, including characterization of cell death processes, cell cycle, cytotoxic mechanisms, production of reactive oxygen species, and clonogenic ability (62–66). We believe that the incorporation of multiple techniques results in a more reliable result that could be extrapolated for further *in vivo* tests.

Molecular Approaches

Molecular tools have also played an important role in co-localization studies, which are used to evaluate intracellular targets of new anti-tumor compounds. Kleemann et al. employed organelle-targeted GFP and/or YFP-plasmids to characterize location of hypericin in A375, 501mel, and UCT Mel-1 melanoma cell lines (48). Our group has also been working to characterize possible mechanisms of action of BCG-based immunotherapy against metastatic melanoma using reporter recombinant BCG strains (data not published). We have also employed the construction of recombinant BCG strains to serve as potentially stronger immunotherapeutic agents against bladder cancer, with promising results demonstrated through *in vitro* approaches (67, 68). We are currently evaluating the efficacy of this strategy for melanoma treatment.

High-throughput screening based on a gene trap strategies was also developed and validated for malignant melanoma using the A375 cell line harboring a *BRAF* driver mutation

(V600E) (69). The approach consists of detecting the inhibition of oncogenic pathways by drugs using a promoterless reporter system that becomes active and emits an "on" signal when integrated in specific loci. Identification of gene traps in relevant oncogenic pathways was performed using known BRAF and MEK inhibitors, vemurafenib and trametinib, respectively. Of the 6000 compounds initially screened, 40 were identified as MAPK pathway inhibitors using this approach.

3D Models

Melanoma progression evolves from a radial growth phase (RGP) to a vertical growth phase (VGP), the stage in which most cases are diagnosed (70). Tumors in the VGP stage are associated with increased metastatic potential and poor prognosis. Moreover, the melanoma microenvironment consists of a network of cells, including fibroblasts, immune cells, endothelial cells, and transformed melanocytes (71). Conventional tests based on detection of enzyme activity do not effectively mimic this complexity. Thus, more complex systems are urgently needed to better understand and mimic the tumor microenvironment, especially for metastatic melanoma, which is often associated with resistance to therapy.

A 3D platform was developed to screen a series of chemotherapeutic drugs using B16-F10 melanoma cell line as a model (72). The platform combines a 3D extracellular matrix with gold electrodes that sense the electrical response after drug exposure. The microfluidic device was able to detect changes in the response of drug-susceptible and drug tolerant B16-F10 cells after carboplatin exposure. Considering that intra- and inter-tumor variability can result in varying levels of chemoresistance for individual tumor cell clones, this kind of approach could emerge as an ideal solution for personalized screening of multiple drugs at once.

Spheroid models have also been developed for evaluation of novel drugs (73). The organotypic 3D model resembles cutaneous melanoma metastasis and represents a more reliable strategy than 2D methods. Vörsmann et al. developed melanoma spheroids of about 500 μm in size using SBCL 2 (RGP stage), WM 115 (VGP stage), and 451-LU (metastatic) cells mixed with collagen I and fibroblasts to form an *in vitro* skin model (74). Using the 3D model, the authors observed an improvement in the therapeutic effect of TRAIL + cisplatin and reduced efficacy of TRAIL + UVB, which is incongruent with what was observed when using a 2D culture system. Three-dimensional models represent a more suitable tool for drug screening for metastatic melanoma. As the metastatic process involves cytoskeletal reorganization and loss of adhesion receptors, destabilizing the cellular interactions with the extracellular matrix, these targets can also be explored to characterize novel anti-melanoma drugs. Changes in cytoskeletal organization have been investigated using fluorescence staining and tubulin polymerization assays; however, this work has been done predominately using 2D models (75). Combining 3D model systems with these evaluations represents a powerful new method for new drug discovery, allowing for investigation of distinct processes contributing to invasion, migration, and metastasis.

Because of these results, we believe it is important to consider the effects of cell-cell interactions in co-culture experiments and the mechanism of action for immune cells when screening potential of new drug targets. Moreover, further investigation of tumor microenvironment is another important factor to be considered when testing therapies against melanoma, especially in the case of metastatic disease. Our group is currently focused on determining the response induced by novel compounds using melanoma cells co-cultured with immune cells, and characterizing pathways activated by these agents.

We also highlight that although *in vitro* assays provide important information regarding the cytotoxic potential of new compounds being screened, they fail to mimic the complex environment of a living animal. Therefore, *in vivo* screening following initial *in vitro* validation of the most promising anti-melanoma compounds represents an essential and rational step in the development and approval of new melanoma drugs, in accordance with the need to reduce, replace and refine animal experimentation and to better select drug candidates. Moreover, the huge tumor variability observed clinically requires the use of a combination of techniques for screening, including the use of different cell lines representative of various genetic, metabolic, and physiologic phenotypes to minimize bias when testing new drugs.

Section II
In vivo Models of Melanoma

Animal models are important tools for elucidating the effectiveness of new biomedical compounds and therapies. In fact, in order for a new biomedical product to enter human clinical trials and be approved for commercialization, the treatment must first be tested for efficacy and safety in at least two different animal models (76). Therefore, *in vivo* testing in animal models is a critical step in the screening of new potential compounds with antimelanoma activity. therapies for melanoma.

Since the rise of spontaneous melanoma is extremely rare in animal models, exceptions being three swine lines that develop spontaneous forms of malignant melanoma: the Sinclair miniature white pig (77), the Munich miniature swine troll (78) and the Melanoma bearing Libechov minipigs (MeLiM) (79), it is necessary to induce tumor formation in order to create biological models of melanoma. This induction can be performed using several approaches, including genetic engineering, graft transplantation, and viral/physical/chemical induction. Graft transplantations consist of either xenograft or allograft (syngeneic) depending on whether the donor tumor originates from a different or the same species, respectively (80).

The most widely used preclinical model is the murine model. Some of their characteristics, like small size, well-known genetics, easy handling, and inexpensiveness make them the ideal choice for drug screening. Specifically, for melanoma, graft transplantation using B16 murine melanoma cells represent the most widely used animal model. Of the articles published between 1980 and 2018 involving *in vivo* screening of potential antimelanoma molecules, 70% of them used mice bearing B16 grafts for their *in vivo* evaluations (**Figure 2A**). In this section of the review, we will discuss the most widely used melanoma animal models for *in vivo* screening of drugs and compounds.
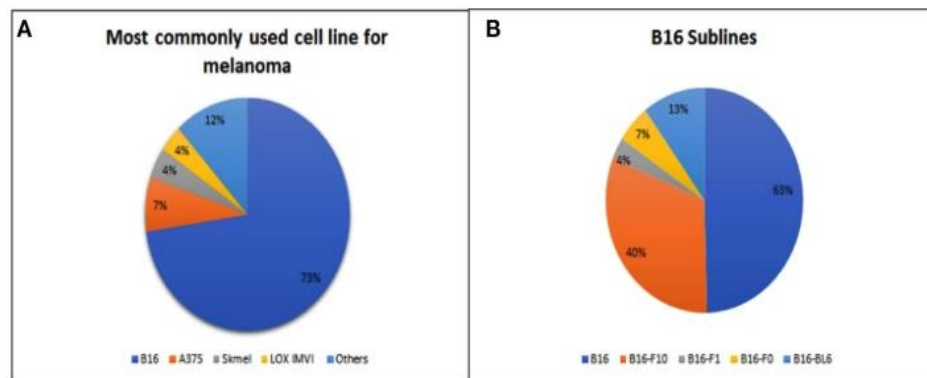
FIGURE 2 | (A) Percentage of trials using different cell lines to form grafts in melanoma murine models for *in vivo* therapeutic screening. B16 stands for all B16 sublines. Skmel stands for all Skmel sublines. "Others" include UACC-62, A2058, Na11+, Melanoma xenograft (MEXF), K1735, K1735-M2, HT168-M1, MM96L, Me501, M-14, Me30966, D10, 205, MeWo, VM1, Mel-JD, MEXF 989, WM 266-4, human malignant melanoma (BRO), and M24 cell lines. **(B)** Percentage of trials using each of the B16 sublines in syngeneic tumor models of melanoma for screening *in vivo*. Obs.: B16 indicates articles that do not specify a B16 subline.

B16 Syngenic Mouse Model

As mentioned before, the most widely used pre-clinical animal model for melanoma drug screening is the B16 syngenic mouse model, mainly due to its well-known genetics and histological characteristics similar to human melanoma. In addition, because this animal model possess a functional immune system, syngeneic transplantations are frequently used to evaluate immunotherapies and interactions between tumor and immune cells (81). Synergistic transplantation of B16 murine melanoma cells into C57BL/6 mice involves inoculation of mice with the same genetic background of the host animal. It is one of the most advantageous experimental models for testing large numbers of drugs in order to select specific compounds for their antimelanoma activity and has been vastly used for this purpose over the past decades. The inoculation can be performed subcutaneously (SC), intraperitoneally (IP), or intravenously (IV) depending on whether the formation of a solid or metastatic tumor is desired.

Several studies use the B16 murine melanoma model to evaluate compounds. Some examples date back from the 80's, where Miura et al. tested the antimelanoma and melanocytotoxic effects of phenolic and catecholic compounds. Among nine compounds tested, 4-S-cysteaminylphenol (CAP) resulted in an increase in the life span of solid melanoma-bearing mice and inhibited the growth of the melanoma tissue (82). In addition the glutamine analog L-glutamic acid γ-monohydroxamate (GAH) was tested and proved to considerably increase survival of mice bearing solid B16 melanoma tumors in a schedule-dependent matter (83). Finally, the anti-tumor properties of Cy 233, a new nitrosoureido sugar, was investigated and demonstrated long-term survival of mice bearing B16 solid tumors across all schedules of treatment (84). Together, these studies represent examples of successful *in vivo* evaluation of melanoma treatments using the B16 syngenic mouse model.

More recently, 16K hPRL, a potent inhibitor of angiogenesis was shown to inhibit tumor growth in a subcutaneous B16F10 mouse melanoma model using a gene transfer method based on cationic liposomes (85). TPI-1, a SHP-1-targeted anti-cancer agent, inhibited the growth of B16 melanoma tumors in ∼83%

of treated mice at a tolerated oral dose in a T cell-dependent manner (86). A systematic study testing MPTQ, a compound containing a novel tetracyclic condensed quinoline ring system, was carried out to evaluate its antitumor efficacy against B16 murine melanoma. In this study, both single and multiple IP doses displayed high levels of activity against the SC grafted B16 melanoma, significantly increasing survival and inhibiting tumor growth (87). Finally, *in vivo* investigation of dipotassium-trioxohydroxytetrafluorotriborate's antitumor effects in a B16-F10 melanoma tumor model demonstrated reduced tumor growth compared to controls (88).

The methodology to obtain and utilize the widely used B16 solid tumor model is well established. The subcutaneous (or sometimes intraperitoneal) injection of about 1×10^5 cells/mouse in C57BL/6J strain mice results in palpable tumor within 5 to 10 days that grow to 1 cm^3 in 14 to 21 days (89). The results are obtained by comparing the tumor size of the treated groups against the control.

B16 Artificial Metastatic Mouse Model

The use of models that mimic invasiveness are important in melanoma drug discovery since melanomas are characterized by their high aggressiveness and ability to metastasize to distant organs (90). Metastatic melanoma is incurable in most cases, presenting a 5-year survival rate lower than 5% (91). Therapeutic options available today for the treatment of advanced melanoma are largely ineffective (5, 92), highlighting the importance of continued improvement in metastatic melanoma treatment through the screening of new compounds for anti-metastatic activity. In this context, IV injection of B16 cells to obtain pulmonary metastases has been used for the past decades in order to investigate the effect of new molecules on metastatic formations. Several studies have performed IV injection of B16-F10 cells into the tail vein of mice, which allows the cells to travel throughout the body and invade other organs, resulting in distant melanoma metastases (93–96).

Using this model, Sharma et al. demonstrated that 7t8OG was able to reduce the number of lung metastases observed in 89–99% of mice harboring B16 metastatic tumors (93). The

antimelanoma activity of molecules produced by *Streptomyces griseoluteus* was also evaluated using this approach. One of the tested molecules demonstrated a dose-dependent antimetastatic activity *in vivo*, however, none of them showed activity against solid melanoma tumor models *in vivo* (94). A liposome-based formulation of ET-18-OCH3 was also shown to be more effective in reducing lung tumor nodules in metastatic B16/F10 melanoma bearing mice than non-liposome-based formulations (97).

In more recent studies, B16-F10 tumor-bearing mice with pulmonary metastases were used to screen potential antimelanoma molecules and evaluate their antimetastatic activity, including a specific inhibitor of thrombin, recombinant hirudin with stealthy liposomal vinblastine (98), a heterodimer recombinant (r) IL-7/HGFb that was cloned and expressed as a single-chain hybrid cytokine (95), nanoencapsulated alkanoid Camptothecin (CPT) (99), interferon alpha (100), an aqueous extract from the root of *Platycodon grandiflorum* (96), berberine (101), and RAM, an RGD-non-peptide Analog-Molecule that markedly reduced up to 80% of lung metastases development (102). In addition, the antimetastatic activity of the theophylline analog 7-(2-hydroxyethyl)theophylline (HET) (103), peptides corresponding to conserved complementary determining regions from different immunoglobulins (104), carbamoylphosphonates (CPOs) (105), and C4-benzazole naphthalimide derivatives (106) were also screened using this model.

In addition, the ability of the topoisomerase I inhibitor MONCPT to reduce melanoma metastasis was tested using the B16-F10 metastatic mouse model. However, instead of using the regular B16 cell line, they employed a slightly different approach through the use of a B16-F10 cell line expressing green fluorescent protein (B16-F10-GFP). These cells were also injected subcutaneously in order to evaluate the antitumor effect of the molecule in solid melanoma tumors. The use of B16-F10-GFP recombinant cells allowed the investigators to visualize the resulting tumors using a fluorescent macro-imaging system and fluorescence stereomicroscope. The number of metastatic nodules on the lung surface were counted under fluorescence stereomicroscope to quantify the pulmonary metastases. MONCPT markedly reduced pulmonary metastases in a dose-dependent matter and inhibited tumor growth in the B16-F10 xenograft model (107).

Another alternative approach is to use the melanotic subline B16F10-Nex2, which was developed from B16-F10 cells by the Experimental Oncology Unit (UNONEX) and is characterized by low immunogenicity and moderate virulence. It can form lethal subcutaneous tumors, while pulmonary nodules are formed only when injected IV (108). Three studies have used this subline to produce a lung metastatic melanoma model for screening of potential melanoma treatments. The first evaluated the effect of fastuosain, a cysteine proteinase from *Bromelia fastuosa*. After treatment, very few lung metastatic nodules were detected (108). In another study, FTY720, a compound already approved by the Food and Drug Administration for treatment of patients with multiple sclerosis, was found to limit metastatic melanoma growth (109). Finally, Bechara et al tested the *in vitro* antitumor activity of a Biphosphinic Palladacycle Complex (BPC), followed

by *in vivo* studies demonstrating BPC protects mice against metastatic melanoma (110).

The methodology to obtain and utilize B16 artificial metastatic mouse models is also well established. An IV injection of 2×10^5 cells on C57BL/6J mice results in the establishment of visible pulmonary tumor nodules within 3 days. In order to determine the antimetastatic effects of a given drug, the number of lung metastases are counted and compared to a control group.

One big advantage of this model is the extremely rapid formation of lung metastases. However, this is only possible because this model does not mimic the actual events required for metastasis of primary tumors, since the first steps of metastasis (localized invasion and intravasation into the blood vessels) are bypassed when cells are injected directly into the mouse bloodstream (111). This represents the biggest disadvantage when utilizing the B16 artificial metastatic model. To overcome this, B16 sublines with enhanced metastatic ability have been isolated and used to form spontaneous metastases in mice. Despite these limitations, the B16-F10 artificial metastatic mouse model is still a valuable model to test the ability of compounds to inhibit formation of metastatic nodules.

B16 Sublines

It is well known that primary malignant tumors consist of a heterogeneous population of cells rather than a homogeneous cellular mass (112). Therefore, it is rational to think that subpopulations within a cell line can present different and unique characteristics from one another. Likewise, the B16 lineage has sublines that present different characteristics. Due to their specific characteristics, each subline is ideal to study different aspects of melanoma. Some sublines, like B16-F1, have a low potential for lung colonization and are useful for studying primary tumor growth (113), while others, for example B16-F10, display a high potential for pulmonary metastasis and are ideal for *in vivo* metastatic studies. The rapid growth and fast development of B16-F10 tumors typically leads to death within 2 to 4 weeks after SC injection into mice (114). Therefore, the ideal subline to use depends on the experimental design and expected activity of the compounds being screened.

There are also some populations of melanoma B16 cells with enhanced metastatic ability. These populations have been identified, selected, and isolated *in vitro* to established sublines characterized by their enhanced invasive properties. One example is the B16–BL6 melanoma cell line, a highly metastatic murine tumor cell. The BL6 variant subline was selected and isolated *in vitro* from B16-F10 cells. It displays greater invasiveness when injected SC or intramuscular (IM) compared to its parental line (B16-F10). However, the variant subline is less efficient than the parent B16-F10 line in producing experimental metastases after IV injection, probably because B16-F10 cells are already highly metastatic when injected IV (115). Similar to its parental cell line, the B16-BL6 can also be used to form solid tumors, and has been used to test novel melanoma treatments, including N-Benzyladriamycin-14-valerate, a novel lipophilic anthracycline with greater *in vivo* antitumor activity than doxorubicin (116), SBF-1, a synthetic

steroidal glycoside (117), and surface-charged nanostructured lipid carriers (NLCs) (118).

In addition to B16-BL6, the Mmb16 cell line represents another metastatic B16 subclone (119, 120). It has been used to demonstrate significant antitumoral activity of combination IL-12 and paclitaxel therapy (120), as well as the efficacy of systemic infusion of recombinant human macrophage-colony-stimulating factor in combination with local treatment with human recombinant tumor necrosis factor cx and mouse recombinant interferon (119).

One of the advantages of using B16 sublines with enhanced metastatic ability instead of the parental B16-F10 lines is the ability of these sublines (B16-Bl6 and Mmb16) to form spontaneous lung metastases when inoculated SC or IP. The spontaneous lung metastasis model represents a highly valuable model because B16-Bl6 and Mmb16 cells have to go through all the initial events required for primary tumor metastasis (111, 121), therefore mimicking the metastatic process that occurs clinically. This is in contrast to methods consisting of artificial injection of cells directly into the animal vein. However, it is a much more time-consuming process and therefore not as frequently used.

Other B16 variations include the B16-F0 and B16-F1 cell lines, which are derived from C57Bl/6 mice[2]. But, overall, these sublines are not used as frequently as the B16-F10 cell line (**Figure 2B**). In fact, B16-F10 is the most widely used of all available sublines for *in vivo* xenograft modeling.

Several characteristics make the B16 an ideal experimental model in drug screening. For instance, it utilizes a well-characterized cell line and tumors are rapidly developed after B16 inoculation. Also, syngeneic transplantations are frequently used to test immunotherapies (81), which represents a major advantage of this model over xenografts because it allows the evaluation of interactions between tumor and immune cells present in the tumor microenvironment. In fact, models with functional immune systems are essential to test immunotherapies that aim to stimulate the body's immune system to target and attack melanoma cells. One example is the melanin-mediated cancer immunotherapy strategy, which consists of transdermal vaccination using a MN patch loaded with B16F10 whole tumor lysate, which resulted in increased survival of C57BL/6J mice (122). The B16-F10 model was also used to test a synergistic immunotherapy strategy targeting both the immunoinhibitory receptor programmed cell death protein 1 and the immunosuppressive enzyme indoleamine 2,3-dioxygenase. Using this model, the antitumor effect of this treatment was demonstrated, including enhanced effective T cell immunity and reduced immunosuppression in the local site (123). In addition, the use of an *in situ* formed immunotherapeutic biorresponsive fibrin gel was able to control local tumor recurrence after surgery as well as the development of distant tumors by 'awaking' the host innate and adaptive immune systems (124).

However, an obvious disadvantage of B16 syngeneic models is the use of murine cell lines instead of human cells, which have shown to display several differences compared to

human melanomas in terms of hallmarks of cancer, including expression of adhesion proteins, growth factor production, and antiapoptotic mechanisms (114). In addition, even though distinct sublines are available, B16 cells were originally isolated from a single inbred mouse strain and therefore do not possess the range of genetic variation observed clinically. Some authors even propose that B16 models should not be used because the data obtained from them can lead to false conclusions. Instead, they recommend using murine models that better recapitulate human melanoma, such as genetically modified mouse models (114).

Additional Murine Cell Lines

Although the B16 allogenic tumor model deserves special attention as it is the most widely used melanoma model for *in vivo* drug screening, other murine cells are also available to be inoculated into mice to form graft tumor models. These include K1735 and its subclone K1735-M2, both derived from C3H/HeN mice (86, 94), and the Cloudman S-9 cell line, obtained from the DBA/2 mouse (113, 125), in addition to a variety of other cell lines not addressed here.

These lines have also been used to evaluate new compounds with potential antimelanoma activity. In one study, TPI-1 analogs were tested, with analog TPI-1a4 found to inhibit growth of K1735 melanoma tumors in mice (86). In a screening of actinomycetes for substances with solid antitumor activity, a structure named U-77863 obtained from *Streptomyces griseoluteus* (strain WS6724) exhibited a dose-dependent antimetastatic activity *in vivo* in both K1735-M2 and B16-F10 murine melanoma models (94). Lastly, vitalethine was evaluated in mice inoculated with the uniformly fatal Cloudman S-91 melanoma cell line, displaying substantially diminished tumor sizes as well as increased survival (125). However, these murine cell lines are not as well characterized, and their use for melanoma drug screening is uncommon compared to the B16 cell line.

Cell Line Xenograft Models

Xenograft models developed using human cancer cell lines have been widely used in research to answer questions ranging from the efficacy of new therapies to elucidation of the mechanisms underlying tumor biology. This scenario is no different for melanoma, where xenograft models are widely used for the study of metastases and drug screening (126). Consistent with the methodologies employed to obtain solid tumors in syngeneic models, an amount of $\pm 2 \times 10^6$ human cells are injected usually SC into immunodeficient mice to generate xenograft models of human melanoma.

The biggest difference in injecting either mouse or human cells into mice in order to form grafts is that human cells lines need to be injected into immunosuppressed or imunocompromised mice to avoid rejection by the host immune system. These models are called xenograft models, meaning that the tumor donor and the host animal belong to different species. Severe compromised imunodeficiency (SCID) and athymic nude mice are the most commonly used animals for this purpose. They both lack an efficient immune system, limiting the ability of these mice

---

[2]Information extracted from: https://www.atcc.org

to recognize and reject the human cells, allowing the injected human cells to grow in the mouse model and form tumors. More specifically, nude athymic (nu/nu) mice are T-cell deficient (127) and SCID mice are both T and B-cells deficient (128).

A375 is one of the most commonly used human cell lines for mouse xenograft development and subsequent compound screening. In nude mice bearing well-developed human A375 melanoma xenografts, administration of 125I-labeled ZME and ZME-gelonin was tested for its antimelanoma activity in solid and metastatic tumor models. The results showed suppression of tumor growth and a 213% increase in mean survival time in the immunotoxin group compared to the control group (129). Other compounds, including 4-substituted methoxybenzoyl-aryl-thiazoles (SMART) (130), YM-201627 (131), and the organopalladium compound tris (dibenzylideneacetone) dipalladium (Tris DBA) (132) were tested using A375 melanoma xenografts. Other generally used human cell lines include the Skmel sublines and LOX human amelanotic melanoma cell line.

Although used frequently for compound screening, cell line xenograft models are poorly pre-dictive of clinical outcomes, as evidence by the high proportion of drugs demonstrating efficacy in these models that ultimately fail in clinical trials (133). This is mainly due to establishment of melanoma cell lines under artificial conditions during cell culture growth and *in vivo* passaging over several years resulting in selection of clones that are no longer representative of the original tumor (80). To overcome this, the use of primary mela-noma cells for xenograft development has also been reported and will be addressed in the next section of the review.

In addition, these models do not possess a functional immune system, which precludes their use in immunotherapy studies. Despite these disadvantages, xenografts are widely used due to the ability to produce tumors using human melanoma cells. In mice, these melanoma cells can interact with the bloodstream, lymphatic vessels, and tissue stroma, providing valuable information regarding compound effectiveness in this context. (134).

As discussed in this section, all *in vivo* graft models have advantages and disadvantages. Therefore, to obtain results translatable to preclinical and clinical trials, we believe that compounds should be tested simultaneously in more than one murine model. The data obtained in each model (syngeneic and xenograft) would complement each other, since the advantages of one model usually represent disadvantages of another. In addition, the use of genetically modified mouse models that better reflect the human disease could help address questions not possible using graft models.

New Models
In order to improve the process of screening compounds with potential antimelanoma activity, a number of research groups have worked to develop new models with various pros and cons, which are discussed in depth below.

Patient-Derived Tumor Xenograft (PDTX)
Several studies have demonstrated that PDTX models are more suitable for mimicking human tumors than traditional cell line xenografts (135, 136). The goal of PDTX models is to promote personalized medicine by allowing the animal model to bear human tumor cells originated from actual patients. This platform allows scientists to test and evaluate efficacy of drugs and therapies on the patient's own cells. PDTX models have led to discovery of drug resistance mechanisms common found in metastatic melanoma patients and are also useful for identifying combination therapy regimens that could prevent drug resistance (135). PDTX models are also heterogeneous in nature and therefore more closely reflect tumors observed clinically.

To develop PDTX models, tumor cells are obtained from a surgically resected clinical tumor sample. The tumor mass serves as the raw material from which small specimens are obtained. These specimens are then transplanted SC into immunodeficient mice to produce tumors derived from the patient's malignant cells (136). However, this is a time consuming and technically challenging technique, with palpable tumors developing between 3 to 9 months, with many mice failing to develop tumors, which represents its biggest disadvantage of this model (135, 136).

Although this approach allows for more personalized drug discovery and has a huge potential in melanoma drug screening, it hasn't been widely employed to date. One example using PDTX models for drug screening is the work of Hollingshead et al. describing the preclinical basis for further development of 17-dimethyl aminoethylamino-17-demethoxygeldanamycin hydrochloride (17-DMAG, NSC 707545). In this work, four melanoma xenografts (MEXF 276, MEXF 462, MEXF 514, and MEXF 989) were derived from clinical surgical specimens and directly implanted into nude mice aiming to perform the *in vivo* efficacy studies (137).

Genetic Engineered Mouse Models (GEMM) of Melanoma
Cancer is a multifactorial diseases trigged by genetic perturbations in genes related mostly to cell proliferation, cell cycle, and apoptosis (138). In this context, elucidating the genetic underlying melanoma development is an essential step to fully understand the disease and improve melanoma treatment. To this end, genetically engi-neered mouse models (GEMMs) have been vastly used to investigate the effect of genetic alterations in the processes of melanoma initia-tion, progression, and metastasis (139).

GEMMs are mostly used to unravel the molecular mechanisms related to melanoma development and drug resistance rather than in the drug screening process itself. However, they have been very useful for elucidating gene function and identifying key targets for therapeutics. Examples of genetic engineering models (GEMs) for melanoma are showed in **Table 3**.

Zebrafish and Porcine Models
Another model that is of interest for melanoma drug screening is the zebrafish (*Danio rerio*) embryonic model because it allows the investigation of antitumor drug properties within 1 week, in addition to being suitable for toxicity screenings. The optical transparency of the zebrafish also provides the unique opportunity to monitor fluorescently labeled cancer cell growth

Animal	Gene modified	Function/goal	References
Zebrafish	$BRAF^{V600E}$; p53-deficient	Study the genetic basis of melanoma initiation and development,	(140)
Zebrafish	$NRAS^{Q61K}$; p53-deficient	Study the genetic basis of melanoma pathogenesis	(141)
Zebrafih	$HRAS^{G12V}$	Study the molecular basis of melanoma formation and progression	(142)
Zebrafish	$HRAS^{G12V}$	Provide a link between kita expressing melanocyte progenitors and melanoma and offer the advantage of a larval phenotype suitable for large scale drug and genetic modifier screen	(143)
Zebrafish	$GNAQ^{Q209P}$; p53-deficient	Study the correlation between oncogenic GNAQQ209P mutation and sustained ERK1/2-MAPK activation	(144)
Mouse	$HRAS^{G12V}$; p53-deficient	Study the genetic basis of melanomagenesis	(145)
Mouse	$NRAS^{Q61K}$; INK4a-deficient	Obtain a novel mouse model with melanotic and metastasizing melanoma	(146)
Mouse	$BRAF^{V600E}$, INK4A/Arf-deficient	Produce a pre-clinical model of mutant BRAF function in melanoma	(147)
Mouse	HGF/SF-Tg	Study the genetic basis of melanoma formation and progression	(148)
Mouse	$BRAF^{CA}$; $Cdkn2a^{lox/lox}$; $PTEN^{lox/lox}$	Study the mechanisms driving melanoma metastasis	(149)

over time. Interest in this model has been growing due to its rapid development, low cost, and minimal amounts of compounds and housing requirements (150). Added to this, similarities between human and zebrafish larvae in terms of genetics and the physiology of the innate immune system makes this model ideal for melanoma studies (151). Despite this, the model does have some limitations, including the route of compound delivery (dissolving the compound in egg water, diffusion through the skin and gills, or absorption via the gastrointestinal tract), and whether these compounds pass through the blood-brain barrier needs to be clarified (152). Some groups have started to investigate some of these concerns, as Fleming et al. who used fluorescent labels and capture compounds to assess blood-brain barrier permeability (153–155).

Zebrafish models can also be genetically engineered to closely recapitulate the genetic background and characteristics of human melanomas. In the same way that GEMMs are usually employed, genetic engineered zebrafish models are most commonly use to elucidate the genetic basis of melanoma initiation, development, and progression rather than for drug screening. Examples of genetically modified zebrafish models for melanoma are

provided in **Table 3**. However, there are examples of zebrafish genetic modified models that were first used to model genetic characteristics of melanoma (142) and later employed for *in vivo* validation of targeted melanoma treatments (156).

One more extremely relevant animal model is the swine. Swine are known to hold great resemblance toward humans in several aspects, including genetic, physiologic, and anatomic levels. A review from Bourneuf et al. discusses the advantages of using swine models to study the genetic basis of spontaneous melanoma, specially the MeLim minipig. He states that swine are an important model for studying spontaneous melanoma development because they recapitulate features of human melanoma, and that a spontaneous porcine melanoma model could be extremely valuable for investigating melanoma genetics. In addition to the above-mentioned similarities with humans, the location of the melanocytes is the same in both species, being found in the basal layer of the epidermis. This is in contrast to mice where the melanocytes are located in the dermis. As such, pig skin is expected to better reflect healthy and neoplastic human tissue (157).

The knowledge of the pig's genome sequence, which shows great similarity with humans (158, 159), combined with the advancement in genetic engineering techniques makes genetic engineering a powerful tool for developing transgenic porcine models for cancer drug discovery. These platforms represent a more robust model than swine that develop spontaneous melanomas because they can be engineered to express mutated genes frequently found in human tumor, allowing for generation of personalized models that closely mimics the human disease.

To this end, our group in partnership with collaborators has developed the genetically modified Oncopig cancer model, a transgenic pig harboring Cre recombinase inducible transgenes representing two of the most common genetic mutations found in human cancers ($TP53^{R167H}$ and $KRAS^{G12D}$) (160). This genetically defined porcine cancer model holds the potential for generating several types of cancer, including melanoma. In a review published by Segatto et al. pigs were proposed as a complementary model for phenotypic drug discovery (PDD) of new cancer therapies due to their metabolic, physiological, and genetic similarities with humans (161).

Section III
In silico Drug Assays for Melanoma

The use of alternative methodologies for the development of new compounds with potential antimelanoma activity has rarely been applied in recent years to complement currently used *in vitro* and *in vivo* approaches. These approaches have been developed in order to minimize the use of laboratory animals for experimental testing, as well as to provide additional safety evaluations for subsequent preclinical tests (162). Thus, the use of *in silico* methodologies, such as molecular docking, addresses the need for reduction, replacement, and refinement of animal use in research (3Rs). As we can see in **Table 1**, the drugs currently used for the treatment of melanoma did not undergo *in silico* testing as part of their development process. The inclusion of such tests represents a more rational approach to screening that can help reduce both the number of animals required and the time and money invested
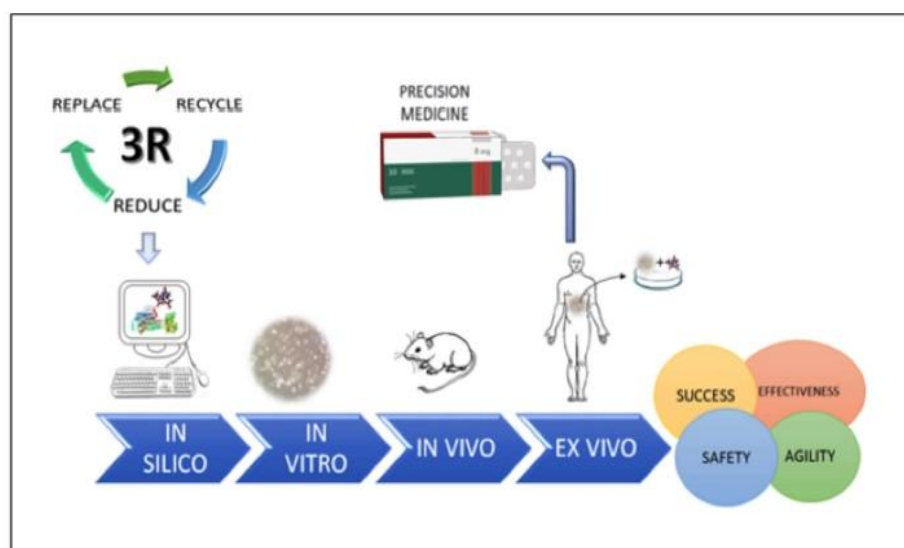
FIGURE 3 | Software most commonly used for melanoma drug screening. The most commonly used software is MOE (17%), followed by HTS (11%).

in each molecule. While it is well known that *in vivo* testing is still essential, there are ways to incorporate alternative processes prior to animal testing so that only promising compounds are advanced to animal studies. In addition, using docking studies that predict interactions between molecules and their receptors save time and money during the costly process of discovery and development of new drugs (163).

Researchers have focused on developing numerous software's to aid in this initial developmental process (164). Using these approaches, millions of molecules can be tested computationally to investigate the effectiveness of structure-activity relationships (binding affinity, prediction of the binder's conformation/orientation) and identify cell types it is likely to be most effective in Thiel and Hummer (165), Meng et al. (166). These "*in silico*" approaches therefore allow researchers to choose the best candidates to advance to *in vitro* and *in vivo* testing.

A literature search was performed to identify programs most frequently used for the development of compounds with potential antimelanoma activity over the past few decades (**Figure 3**). In this review, we will focus on MOE, HTS, GLIDE, and AutoDock. The Molecular Operating Environment (MOE) is one of the most widely used programs availablely by the research community. This software was developed and is available for purchase through the Chemical Computing Group (CCG). However, there are teaching licenses available on the group's website. This program is capable of performing many functions, including structure and fragment-based design, pharmacophore discovery, biological and medicinal chemistry applications, molecular modeling and simulations, and protein and antibody modeling, among others[3]. Ismail et al. (167) used this program to sharpen the joints of topoisomerase II DNA

gyrase (167). In addition, Al-Suwaidan et al. used this feature to verify whether their ligands were formed at the proposed receptors (EGFR-TK ATP binding site) (168, 169). Furthermore, Hassan et al. used this software to identify new candidates for cancer treatments with higher efficacy and lower toxicity, identifying the possible mechanisms of 13a binding in the CDK2 enzyme (170).

High throughput screening (HTS) is the second most widely used software for screening for melanoma treatments. It is a scientific experimental method that selects large libraries of compounds for activity against biological targets through automation, miniature assays, and even analyzes the data on a large scale. With the aid of HTS it is possible to quickly identify active compounds, antibodies, or genes that modulate a specific biomolecular pathway, providing starting points for drug design and an understanding of their role in biochemical processes (171). However, access to this software requires a high investment. To run the HTS requires a highly specialized screening laboratory, so in many cases, due to the high investment costs associated with this *in silico* tool, small to medium research institutions typically use the services of an existing HTS facility instead of developing one themselves. These facilities are typically run by companies, but some universities also have HTS facilities. Hwang et al. used the HTS tool to selectively activate p53 and inhibit NF-κB at the same time, as a strategy for anticancer activity (172). Zimmer et al. also used HTS to induce molecular inhibitors of the S100B protein for melanoma therapy (173). Although an interesting technology, there are some limitations, including a high number of false-positives. Because of this, virtual screening (VS), a totally *in silico* method, emerged as an alternative to HTS (174–176).

GLIDE and Auto-Dock are two other commonly used programs. GLIDE presents itself as complete software for determining anchoring between receptors and ligands. With the

---

[3]Information extracted from: https://www.chemcomp.com/MOE-Molecular_Operating_Environment.htm

FIGURE 4 | The steps necessary for safe, agile, and effective drug screening, which represent important steps for future development of precision medicine.

help of this tool, productivity increases considerably and the costs of drug development are reduced. What makes this tool even more interesting is that it has a high throughput virtual screening mode (HTVS) included in its system, as well as a standard precision (SP) mode so you can reliably anchor hundreds of thousands of libraries. Another important feature is its ability to reduce false positives using the "false-positive extra precision (XP)" mode. This software is also available through academic licensing[4]. Wang et al. (55) used this tool to identify and obtain molecular structures of potential inhibitors of B-Raf [V600E.] (177). Quirit et al. (178) aiming to inhibit the proliferation of human melanoma cells, performed *in silico* binding simulations with the crystallographic structure of NEDD4-1, showing that each of the indolecarbinol compounds bound to the catalytic HECT domain purified from NEDD4-1 (178).

AutoDock 4.0 is a free to download software featuring a set of automated docking tools. It is designed to predict how binding of small molecules, such as substrates or drug candidates, occurs to a receptor of known 3D structure. Easy access to this free software has stimulated its use by academic research groups, where basic and initial research is usually developed. AutoDock has already been distributed to more than 29,000 users worldwide. Among the advantages cited by the creators of the software include its speed and ability to provides high quality predictions and correlations between predicted and experimental inhibition constants[5]. Luo et al. (179) and Ruan et al. (59) used AutoDock to evaluate the antiproliferative activity of melanoma cell lines, in order to run a coupling simulation to insert a compound of interest into the crystal structure of tubulin to determine the likely binding pattern (41, 42). While it is clear that some programs are more complete than others, the cost to research groups must also be taken into consideration. In

this context, AutoDock software is a very interesting tool for researchers focused on the synthesis of new compounds.

In silico tools are undoubtedly of great value for the initial steps of drug screening. With the aid of these tools, thousands of compounds can be tested to effectively identify candidates for *in vitro* and *in vivo* testing while considering multiple endpoints during a single assessment. Thus, the inserted models can evaluate multiple effects, providing a more comprehensive prediction. However, these approaches, like all techniques, have limitations such as the high cost of commercially available software, the need for high performance processors, the high number of false-positives predicted by software like HTS, and additional uncertainties due to the absence of toxicological data. Although there are limitations, research groups have developed strategies to lessen their impact. There is no doubt that *in vitro* and *in vivo* testing is essential for drug development. Nothing thus far replaces pharmacokinetic and pharmacodynamic tests with such precision as that of a living organism. However, the available systems are based on validated models and well-established REA and QSTR information, which has tended to rationalize the testing, acceptance, recommendation and inclusion of *in silico* methods in several organizations around the world such as European Community, United States Environmental Protection Agency (USEPA) and Food and Drug Administration (FDA). Because of this, we believe that the results of *in silico* methodologies tends to make subsequent tests more effective and predictable and are essential for the screening of new molecules.

PERSPECTIVES AND CONCLUSIONS

Several approaches are available for melanoma drug screening, including *in silico*, *in vitro*, and *in vivo* methods, even though few studies have explored the union of these methodologies. *In silico* techniques represent a necessary first step in the screening

---

[4]Information extracted from: https://www.schrodinger.com/glide
[5]Information extracted from: http://autodock.scripps.edu/

process and a potential predictive test with the ability to evaluate thousands of molecules and identify the 5–10 with a greater chance of success. In addition to being able to better identify drug candidates, it is possible to exploit drug repositioning, which is a cheap and safe strategy for researchers. In the future, it would be ideal if these computational simulations could be applied more comprehensively using a single software that would simultaneously provide information on cell lines, proteins, and receptors.

The need to understand and mimic the tumor microenvironment *in vitro* has promoted the development of 3D culture models, aiming to reduce the limitations of other *in vitro* tests. We believe that the union of molecular docking with *in vitro* models, such as 3D cultivation, will provide more direct and reliable results. In the period analyzed by our group, few studies used the triad of tests that we consider essential, which demonstrates the need to evolve our future drug screening process in this direction.

Regarding *in vivo* screening, not much has changed regarding the xenograft models used for melanoma drug screening over the past four decades. Although other robust animal models have been developed recently, the "go to" graft model for *in vivo* screening of antimelanoma compounds continues to be the B16 mouse model, even though it represents an unsatisfactory model. Nowadays, *in vivo* drug screening is also performed using additional robust tools to test the efficiency of new molecules and therapies, such as human cell line xenograft models, patient-derived-xenograft models, zebra fish, and GEMs.

We conclude that in order to obtain reliable data when screening potential antimelanoma compounds, researchers should explore several of the currently available animal models options, since (i) one single model is not able to answers all the essential questions required for refined and reliable drug screening, and (ii) one approach usually complements the other. Therefore, by choosing the most promising compounds through initial *in silico* and *in vitro* approaches, it is possible to optimize and reduce animal use by testing a smaller number of potential compounds in multiple *in vivo* models in parallel.

In conclusion, we highlight that rational drug screening should respect the sequence of *in silico*/*in vitro*/*in vivo* testing, which will provide more promising drug candidates supported by robust data for preclinical trials, minimizing the unnecessary use of laboratory animals with regards to the 3R's. This sequence is of fundamental importance as we move toward an era of precise personalized medicine (**Figure 4**).

AUTHOR CONTRIBUTIONS

GC, NS, TO, FS, KS, and TC had an equal participation in writing and approving the present manuscript.

FUNDING

REFERENCES

1. WHO Cancer. *WHO*. (2018). Available onilie at: https://www.who.int/gho/publications/world_health_statistics/2018/en/ (accessed August 21, 2018).

2. Siegel RL, Miller KD, Jemal A. Cancer statistics, 2018. *CA Cancer J Clin*. (2018) 68:7–30. doi: 10.3322/caac.21442

3. Instituto Nacional do Câncer. Estimativa 2018: incidência de câncer no Brasil/Instituto Nacional de e Câncer José Alencar Gomes da Silva, Coordenação de Prevenção e Vigilância-Rio de Janeiro. *INCA*. (2018). p. 1–130.

4. Rozeman EA, Dekker TJA, Haanen J, Blank CU. Advanced melanoma: current treatment options, biomarkers, and future perspectives. *Am J Clin Dermatol*. (2018) 19:303–17. doi: 10.1007/s40257-017-0325-6

5. Gray-Schopfer V, Wellbrock C, Marais R. Melanoma biology and new targeted therapy. *Nature*. (2007) 445:851–7. doi: 10.1038/nature05661

6. Miele M, Bonassi S, Bonatti S, Martini E, Miglio L, Ottaggio L, et al. Micronucleus analysis in peripheral blood lymphocytes from melanoma patients treated with dacarbazine. *Anticancer Res*. (1998) 18:1967–71.

7. Serrone L, Zeuli M, Sega FM, Cognetti F. Dacarbazine-based chemotherapy for metastatic melanoma: thirty-year experience overview. *J Exp Clin Cancer Res*. (2000) 19:21–34.

8. Eton O, Legha SS, Bedikian AY, Lee JJ, Buzaid AC, Hodges C, et al. Sequential biochemotherapy versus chemotherapy for metastatic melanoma: results from a phase III randomized trial. *J Clin Oncol*. (2002) 20:2045–52. doi: 10.1200/JCO.2002.07.044

9. Middleton MR, Grob JJ, Aaronson N, Fierlbeck G, Tilgen W, Seiter S, et al. Randomized phase III study of temozolomide versus dacarbazine in the treatment of patients with advanced metastatic malignant melanoma. *J Clin Oncol*. (2000) 18:158–66. doi: 10.1200/JCO.2000.18.1.158

10. Quirt I, Verma S, Petrella T, Bak K, Charette M. Temozolomide for the treatment of metastatic melanoma. *Curr Oncol*. (2007) 14: 27–33. doi: 10.1634/theoncologist.12-9-1114

11. Hersh EM, Del Vecchio M, Brown MP, Kefford R, Loquai C, Testori A, et al. A randomized, controlled phase III trial of nab-Paclitaxel versus dacarbazine in chemotherapy-naïve patients with metastatic melanoma. *Ann Oncol*. (2015) 26:2267–74. doi: 10.1093/annonc/mdv324

12. Kottschade LA, Suman VJ, Amatruda T, McWilliams RR, Mattar BI, Nikcevich DA, et al. A phase II trial of nab-paclitaxel (ABI-007) and carboplatin in patients with unresectable stage IV melanoma : a North Central Cancer Treatment Group Study, N057E(1). *Cancer*. (2011) 117:1704–10. doi: 10.1002/cncr.25659

13. Tabernero J, Chiorean EG, Infante JR, Hingorani SR, Ganju V, Weekes C, et al. Prognostic Factors of Survival in a Randomized Phase III Trial (MPACT) of weekly nab-paclitaxel plus gemcitabine versus gemcitabine alone in patients with metastatic pancreatic cancer. *Oncologist*. (2015) 20:143–50. doi: 10.1634/theoncologist.2014-0394

14. Rosenberg B, VanCamp L, Trosko JE, Mansour VH. Platinum compounds: a new class of potent antitumour agents [24]. *Nature*. (1969) 222:385–6.doi: 10.1038/222385a0

15. Evans LM, Casper ES RR. Phase II trial of carboplatin in advanced malignant melanoma. *Cancer Treat Rep*. (1987) 71:171–2.

16. Flaherty KT, Lee SJ, Zhao F, Schuchter LM, Flaherty L, Kefford R, et al. Phase III trial of carboplatin and paclitaxel with or without sorafenib in metastatic melanoma. *J Clin Oncol*. (2013) 31:373–9. doi: 10.1200/JCO.2012.42.1529

17. Adams M, Kerby IJ, Rocker I, Evans A, Johansen K, Franks CR. A comparison of the toxicity and efficacy of cisplatin and carboplatin in advanced ovarian cancer. *Acta Oncol*. (1989) 28:57–60. doi: 10.3109/02841868909111182

18. Wang C, Thudium KB, Han M, Wang X-T, Huang H, Feingersh D, et al. *In vitro* characterization of the Anti-PD-1 antibody nivolumab, BMS-936558, and *in vivo* toxicology in non-human primates. *Cancer Immunol Res.* (2014) 2:846–56. doi: 10.1158/2326-6066.CIR-14-0040

19. Weber SJ, O'Day S, Urba W, Powderly J, Nichol G, Yellin M, et al. Phase I/II study of ipilimumab for patients with metastatic melanoma. *Am Soc Clin Oncol.* (2008) 26:5950–6. doi: 10.1200/JCO.2008.16.1927

20. Selby MJ, Engelhardt JJ, Johnston RJ, Lu LS, Han M, Thudium K, et al. Preclinical development of ipilimumab and nivolumab combination immunotherapy: mouse tumor models, In vitro functional studies, and cynomolgus macaque toxicology. *PLoS ONE.* (2016) 11:e0161779. doi: 10.1371/journal.pone.0167251

21. American Cancer Society. *Cancer Facts & Figures 2018.* American Cancer Society (2018).

22. Eggermont AMM, Spatz A, Robert C. Cutaneous melanoma. *Lancet.* (2014) 383:816–27. doi: 10.1016/S0140-6736(13)60802-8

23. Bass AS, Hombo T, Kasai C, Kinter LB, Valentin JP. A historical view and vision into the future of the field of safety pharmacology. *Handb Exp Pharmacol.* (2015) 229:3–45. doi: 10.1007/978-3-662-46943-9_1

24. Rodriguez B, Carusi A, Abi-Gerges N, Ariga R, Britton O, Bub G, et al. Human-based approaches to pharmacology and cardiology: an interdisciplinary and intersectorial workshop. *Europace.* (2016) 18:1287–98. doi: 10.1093/europace/euv320

25. Broussard, Lindsey Howland A, Ryu S, Song K, Norris D, Armstrong CA, et al. Melanoma cell death mechanisms. *Chonnam Med J.* (2018) 54:135–42. doi: 10.4068/cmj.2018.54.3.135

26. Morton DL, Eilber FR, Holmes EC, Hunt JS, Ketcham AS, Silverstein MJ, et al. BCG immunotherapy of malignant melanoma: summary of a seven-year experience. *Ann Surg.* (1974) 180:635–43. doi: 10.1097/00000658-197410000-00029

27. Triozzi PL, Tuthill RJ, Borden E. Re-inventing intratumoral immunotherapy for melanoma. *Immunotherapy.* (2011) 3:653–71. doi: 10.2217/imt.11.46

28. Homet B, Ribas A. New drug targets in metastatic melanoma. *J Pathol.* (2014) 232:134–41. doi: 10.1002/path.4259

29. Zaffaroni N, Villa R, Silvestro L, Sanfilippo O, Silvestrini R. Cytotoxic activity of azelaic acid against human melanoma primary cultures and established cell lines. *Anticancer Res.* (1990) 10:1599–602.

30. Hanauske AR, Degen D, Marshall MH, Hilsenbeck SG, McPhillips JJ, Von Hoff DD. Preclinical activity of ilmofosine against human tumor colony forming units *in vitro. Anticancer Drugs.* (1992) 3:43–6. doi: 10.1097/00001813-199202000-00008

31. Finlay GJ, Marshall E, Matthews JHL, Paull KD, Baguley BC. *In vitro* assessment of N-[2-(dimethylamino)ethyl]acridine-4-carboxamide, a DNA-intercalating antitumour drug with reduced sensitivity to multidrug resistance. *Cancer Chemother Pharmacol.* (1993) 31:401–6. doi: 10.1007/BF00686155

32. Schadendorf D, Worm M, Algermissen B, Kohlmus CM, Czarnetzki BM. Chemosensitivity testing of human malignant melanoma. A retrospective analysis of clinical response and *in vitro* drug sensitivity. *Cancer.* (1994) 73:103–8.

33. Dahl C, Guldberg P. The genome and epigenome of malignant melanoma. *APMIS.* (2007) 115:1161–76. doi: 10.1111/j.1600-0463.2007.apm_855.xml.x

34. Welch DR, Lobl TJ, Seftor EA, Wack PJ, Aeed PA, Yohem KH, et al. Use of the membrane invasion culture system (mics) as a screen for anti-invasive agents. *Int J Cancer.* (1989) 43:449–57. doi: 10.1002/ijc.2910430318

35. Chen KG, Leapman RD, Zhang G, Lai B, Valencia JC, Cardarelli CO, et al. Influence of melanosome dynamics on melanoma drug sensitivity. *J Natl Cancer Inst.* (2009) 101:1256–71. doi: 10.1093/jnci/djp259

36. Sharma KV, Davids LM. Depigmentation in melanomas increases the efficacy of hypericin-mediated photodynamic-induced cell death. *Photodiagnosis Photodyn Ther.* (2012) 9:156–63. doi: 10.1016/j.pdpdt.2011.09.003

37. Kudugunti SK, Vad NM, Whiteside AJ, Naik BU, Yusuf MA, Srivenugopal KS, et al. Biochemical mechanism of Caffeic Acid Phenylethyl Ester (CAPE) selective toxicity towards melanoma cell lines. *Chem Biol Interact.* (2010) 188:1–14. doi: 10.1016/j.cbi.2010.05.018

38. Melnikova VO, Bolshakov SV, Walker C, Ananthaswamy HN. Genomic alterations in spontaneous and carcinogen-induced murine melanoma cell lines. *Oncogene.* (2004) 23:2347–56. doi: 10.1038/sj.onc.1207405

39. Ediriweera MK, Tennekoon KH, Samarakoon SR. *In vitro* assays and techniques utilized in anticancer drug discovery. *J Appl Toxicol.* (2018) 39:38–71. doi: 10.1002/jat.3658

40. Abildgaard C, Guldberg P. Molecular drivers of cellular metabolic reprogramming in melanoma. *Trends Mol Med.* (2015) 21:164–71. doi: 10.1016/j.molmed.2014.12.007

41. Castro DJ, Ward PH. The effects of argon lasers on human melanoma cells sensitized with rhodamine-123 *in vitro. Am J Otolaryngol Head Neck Med Surg.* (1988) 9:18–29. doi: 10.1016/S0196-0709(88)80004-8

42. Mahgoub T, Eustace AJ, Collins DM, Walsh N, O'Donovan N, Crown J. Kinase inhibitor screening identifies CDK4 as a potential therapeutic target for melanoma. *Int J Oncol.* (2015) 47:900–8. doi: 10.3892/ijo.2015.3097

43. Vijayaraghavan S, Moulder S, Keyomarsi K, Layman RM. Inhibiting CDK in cancer therapy: current evidence and future directions. *Target Oncol.* (2018) 13:21–38. doi: 10.1007/s11523-017-0541-2

44. Jonsson A, Tuominen R, Grafström E, Hansson J, Egyhazi S. High frequency of p16 INK4A promoter methylation in NRAS-mutated cutaneous melanoma. *J Invest Dermatol.* (2010) 130:2809–17. doi: 10.1038/jid.2010.216

45. Held MA, Langdon CG, Platt JT, Graham-Steed T, Liu Z, Chakraborty A, et al. Genotype-selective combination therapies for melanoma identified by high-throughput drug screening. *Cancer Discov.* (2013) 3:52–67. doi: 10.1158/2159-8290.CD-12-0408

46. Parker KA, Glaysher S, Hurren J, Knight LA, McCormick D, Suovouri A, et al. The effect of tricyclic antidepressants on cutaneous melanoma cell lines and primary cell cultures. *Anticancer Drugs.* (2012) 23:65–9. doi: 10.1097/CAD.0b013e32834b1894

47. Hearing VJ, Ekel TM. Mammalian tyrosinase. A comparison of tyrosine hydroxylation and melanin formation. *Biochem J.* (1976) 157:549–57. doi: 10.1042/bj1570549

48. Kleemann B, Loos B, Scriba TJ, Lang D, Davids LM. St. John's Wort (Hypericum perforatum L.) photomedicine: Hypericin-photodynamic therapy induces metastatic melanoma cell death. *PLoS ONE.* (2014) 9:e103762. doi: 10.1371/journal.pone.0103762

49. Slominski A, Paus R, Mihm MC. Inhibition of melanogenesis as an adjuvant strategy in the treatment of melanotic melanomas: selective review and hypothesis. *Anticancer Res.* (1998) 18:3709–15.

50. Slominski A. Melanin pigmentation in mammalian skin and its hormonal regulation. *Physiol Rev.* (2004) 84:1155–228. doi: 10.1152/physrev.00044.2003

51. Riley PA, Cooksey CJ, Johnson CI, Land EJ, Latter AM, Ramsden CA. Melanogenesis-targeted anti-melanoma pro-drug development: effect of side-chain variations on the cytotoxicity of tyrosinase-generated ortho-quinones in a model screening system. *Eur J Cancer Part A.* (1997) 33:135–43. doi: 10.1016/S0959-8049(96)00340-1

52. Dooley TP, Gadwood RC, Kilgore K, Thomasco LM. Development of an *in vitro* primary screen for skin depigmentation and antimelanoma agents. *Skin Pharmacol.* (1994) 7:188–200.

53. Ping F, Shang J, Zhou J, Song J, Zhang L. Activation of neurokinin-1 receptor by substance P inhibits melanogenesis in B16-F10 melanoma cells. *Int J Biochem Cell Biol.* (2012) 44:2342–8. doi: 10.1016/j.biocel.2012.09.025

54. Zouboulis CC, Garbe C, Krasagakis K, Krüger S, Orfanos CE. A fluorometric rapid microassay to identify anti-proliferative compounds for human melanoma cells *in vitro. Melanoma Res.* (1991) 1:91–6. doi: 10.1097/00008390-199106000-00003

55. Wang L, Yin H, Jabed MA, Hetu M, Wang C, Monro S, et al. π-expansive heteroleptic ruthenium(ii) complexes as reverse saturable absorbers and photosensitizers for photodynamic therapy. *Inorg Chem.* (2017) 56:3245–59. doi: 10.1021/acs.inorgchem.6b02624

56. Viola E, Donzello MP, Sciscione F, Shah K, Ercolani C, Trigiante G. Tetra-2,3-pyrazinoporphyrazines with externally appended pyridine rings. 17. Photosensitizing properties and cellular effects of ZnIIoctacationic and ZnII/PtIIhexacationic macrocycles in aqueous media: perspectives of

multimodal anticancer potentialities. *J Photochem Photobiol B Biol.* (2017) 169:101–9. doi: 10.1016/j.jphotobiol.2017.03.005

57. Eng MS, Kaur J, Prasmickaite L, Engesæter B, Weyergang A, Skarpen E, et al. Enhanced targeting of triple-negative breast carcinoma and malignant melanoma by photochemical internalization of CSPG4-targeting immunotoxins. *Photochem Photobiol Sci.* (2018) 17:539–51. doi: 10.1039/C7PP00358G

58. Sun F, Liu JY, He F, Liu Z, Wang R, Wang DM, et al. *In-vitro* antitumor activity evaluation of hyperforin derivatives. *J Asian Nat Prod Res.* (2011) 13:688–99. doi: 10.1080/10286020.2011.584532

59. Ruan BF, Lu X, Li TT, Tang JF, Wei Y, Wang XL, et al. Synthesis, biological evaluation and molecular docking studies of resveratrol derivatives possessing curcumin moiety as potent antitubulin agents. *Bioorganic Med Chem.* (2012) 20:1113–21. doi: 10.1016/j.bmc.2011.11.017

60. Krishnegowda G, Prakasha Gowda AS, Tagaram HRS, Carroll KFSO, Irby RB, Sharma AK, et al. Synthesis and biological evaluation of a novel class of isatin analogs as dual inhibitors of tubulin polymerization and Akt pathway. *Bioorganic Med Chem.* (2011) 19:6006–14. doi: 10.1016/j.bmc.2011.08.044

61. Qin J, Xie P, Ventocilla C, Zhou G, Vultur A, Chen Q, et al. Identification of a novel family of BRAFV600Einhibitors. *J Med Chem.* (2012) 55:5220–30. doi: 10.1021/jm3004416

62. Saueressig S, Tessmann J, Mastelari R, da Silva LP, Buss J, Segatto NV, et al. Synergistic effect of pyrazoles derivatives and doxorubicin in claudin-low breast cancer subtype. *Biomed Pharmacother.* (2018) 98:390–8. doi: 10.1016/j.biopha.2017.12.062

63. Wagner MS, Schultze E, Oliveira TL, de Leon PMM, Thurow HS, Campos VF, et al. Revitalizing the AZT through of the selenium: an approach in human triple negative breast cancer cell line. *Front Oncol.* (2018) 8:525. doi: 10.3389/fonc.2018.00525

64. Pacheco BS, dos Santos MAZ, Schultze E, Martins RM, Lund RG, Seixas FK, et al. Cytotoxic activity of fatty acids from antartic macroalgae on the growth of human breast cancer cells. *Front Bioeng Biotechnol.* (2018) 6:185. doi: 10.3389/fbioe.2018.00185

65. Buss JH, Begnini KR, Bruinsmann FA, Ceolin T, Sonego MS, Pohlmann AR, et al. Lapatinib-loaded nanocapsules enhances antitumoral effect in human bladder cancer cell. *Front Oncol.* (2019) 9:203. doi: 10.3389/fonc.2019.00203

66. Tessmann JW, Buss J, Begnini KR, Berneira LM, Paula FR, de Pereira CMP, et al. Antitumor potential of 1-thiocarbamoyl-3,5-diaryl-4,5-dihydro-1H-pyrazoles in human bladder cancer cells. *Biomed Pharmacother.* (2017) 94:37–46. doi: 10.1016/j.biopha.2017.07.060

67. Begnini KR, Buss JH, Collares T, Seixas FK. Recombinant Mycobacterium bovis BCG for immunotherapy in nonmuscle invasive bladder cancer. *Appl Microbiol Biotechnol.* (2015) 99:3741–54. doi: 10.1007/s00253-015-6495-3

68. Begnini KR, Rizzi C, Campos VF, Borsuk S, Schultze E, Yurgel VC, et al. Auxotrophic recombinant Mycobacterium bovis BCG overexpressing Ag85B enhances cytotoxicity on superficial bladder cancer cells *in vitro.* *Appl Microbiol Biotechnol.* (2013) 97:1543–52. doi: 10.1007/s00253-012-4416-2

69. Morris SM, Mhyre AJ, Carmack SS, Myers CH, Burns C, Ye W, et al. A modified gene trap approach for improved high-throughput cancer drug discovery. *Oncogene.* (2018) 37:4226–38. doi: 10.1038/s41388-018-0274-4

70. Elder DE. Pathology of melanoma. *Surg Oncol Clin N Am.* (2015) 24:229–37. doi: 10.1016/j.soc.2014.12.002

71. Gurzu S, Beleaua MA JI. The role of tumor microenvironment in development and progression of malignant melanomas - a systematic review. *Rom J Morphol Embryol.* (2018) 1:23–28.

72. Pandya HJ, Dhingra K, Prabhakar D, Chandrasekar V, Natarajan SK, Vasan AS, et al. A microfluidic platform for drug screening in a 3D cancer microenvironment. *Biosens Bioelectron.* (2017) 94:632–42. doi: 10.1016/j.bios.2017.03.054

73. Tevis KM, Colson YL, Grinstaff MW. Embedded spheroids as models of the cancer microenvironment. *Adv Biosyst.* (2017) 1:1700083. doi: 10.1002/adbi.201700083

74. Vörsmann H, Groeber F, Walles H, Busch S, Beissert S, Walczak H, et al. Development of a human three-dimensional organotypic skin-melanoma spheroid model for *in vitro* drug testing. *Cell Death Dis.* (2013) 4:e719. doi: 10.1038/cddis.2013.249

75. Zhang H, Fang X, Meng Q, Mao Y, Xu Y, Fan T, et al. Design, synthesis and characterization of potent microtubule inhibitors with dual anti-proliferative and anti-angiogenic activities. *Eur J Med Chem.* (2018) 157:380–96. doi: 10.1016/j.ejmech.2018.07.043

76. FDA. Guidance on M3(R2) nonclinical safety studies for the conduct of human clinical trials and marketing authorization for pharmaceuticals. In: *International Conference Harmonisation.* Washington, DC (2010). p. 3471–2.

77. Oxenhandler R, Adelstein E, Haigh J, Hook R, Clark W. Malignant melanoma in the sinclair miniature swine: an autopsy study of 60 cases. *J Invest Dermatol.* (1974) 62:20–30. doi: 10.1111/1523-1747.ep12676714

78. Wanke R, Hein R, Ring J, Hermanns W. Munich miniature swine troll (UMline): a porcine model of hereditary cutaneous melanoma. *J Invest Dermatol.* (1998) 110:772.

79. Horak V, Fortyn K, Hruban V, Klaudy J. Hereditary melanoblastoma in miniature pigs and its successful therapy by devitalization technique. *Cell Mol Biol.* (1999) 45:1119–29.

80. Kuzu OF, Nguyen FD, Noory MA, Sharma A. Current State of Animal (Mouse) modeling in melanoma research. *Cancer Growth Metastasis.* (2015) 8:81–94. doi: 10.4137/CGM.S21214

81. Klarquist J, Janssen E. Melanoma-infiltrating dendritic cells: limitations and opportunities of mouse models. *Oncoimmunology.* (2012) 1:1584–93. doi: 10.4161/onci.22660

82. Miura S, Ueda T, Jimbow K, Ito S, Fujita K. Synthesis of cysteinylphenol, cysteaminylphenol, and related compounds, and *in vivo* evaluation of antimelanoma effect. *Arch Demartological Res.* (1987) 279:219–25. doi: 10.1007/BF00417318

83. Vila J, Thomasset N, Navarro C, Doré JF. *In vitro* and *in vivo* anti-tumor activity of L-glutamic acid gamma-monohydroxamate against L1210 leukemia and B16 melanoma. *Int J Cancer.* (1990) 45:737–43. doi: 10.1002/ijc.2910450428

84. Atassi G, Dumont P, Kabbe HJ, Yoder O. A new antitumour agent, batracylin, selected by a preclinical solid tumour model. *Drugs Exp Clin Res.* (1988) 14:571–4.

85. Kinet V, Nguyen NQ, Sabatel C, Blacher S, Noël A, Martial JA, et al. Antiangiogenic liposomal gene therapy with 16K human prolactin efficiently reduces tumor growth. *Cancer Lett.* (2009) 284:222–8. doi: 10.1016/j.canlet.2009.04.030

86. Kundu S, Fan K, Cao M, Lindner DJ, Zhao ZJ, Borden E, et al. Novel SHP-1 inhibitors tyrosine phosphatase inhibitor-1 and analogs with preclinical anti-tumor activities as tolerated oral agents. *J Immunol.* (2010) 184:6529–36. doi: 10.4049/jimmunol.0903562

87. Gopal M, Shahabuddin MS. Biological properties of 8-methoxypyrimido[4(1),5(1):4,5]thieno(2,3-b)quinoline-4(3H)-one, a new class of DNA intercalating drugs. *indian J Med Res.* (2004) 119:198–205.

88. Ivankovic S, Stojkovic R, Galic Z, Galic B, Ostojic J, Marasovic M, et al. *In vitro* and *in vivo* antitumor activity of the halogenated boroxine dipotassium-trioxohydroxytetrafluorotriborate (K2[B3O3F4OH]). *J Enzym Inhib Med Chem.* (2015) 30:354–9. doi: 10.3109/14756366.2014.926344

89. Overwijk WW, Restifo NP. B16 as a mouse model for human melanoma. *Curr Protoc Immunol.* (2001) Chapter 20: Unit 20.1. doi: 10.1002/0471142735.im2001s39

90. Houghton AN, Polsky D. Focus on melanoma. *Cancer Cell.* (2002) 2:275–8. doi: 10.1016/S1535-6108(02)00161-7

91. Agarwala SS. Current systemic therapy for metastatic melanoma. *Expert Rev.* (2009) 9:587–95. doi: 10.1586/era.09.25

92. Sullivan RJ, Flaherty KT. Resistance to BRAF-targeted therapy in melanoma. *Eur J Cancer.* (2013) 49:1297–304. doi: 10.1016/j.ejca.2012.11.019

93. Sharma BS, Balazs L, Jin A, Jolley WB, Robins RK. Successful immunotherapy of murine melanoma metastases with 7-thia-8-oxoguanosine. *Clin Exp Metastasis.* (1991) 9:429–39. doi: 10.1007/BF01785529

94. Harper DE, Welch DR. Isolation, purification, synthesis, and antiinvasive/antimetastatic activity of U-77863 and U-77864 from Streptomyces griseoluteus, strain WS6724. *J Antibiot.* (1992) 45:1827–36. doi: 10.7164/antibiotics.45.1827

95. Lai L, Jin J, Goldschneider I. *In vivo* antitumor activity of a recombinant IL-7/HGFbeta hybrid cytokine in mice. *Cancer Res.* (2011) 71:61–7. doi: 10.1158/0008-5472.CAN-10-3198

96. Lee K, Kim J, Choi J, Kim H, Chung Y, Roh S, et al. Inhibition of tumor invasion and metastasis by aqueous extract of the radix of Platycodon grandiflorum. *Food Chem Toxicol.* (2006) 44:1890–1896. doi: 10.1016/j.fct.2006.06.009

97. Ahmad I, Filep J, Franklin J, Janoff A, Masters G, Pattassery J, et al. Enhanced therapeutic effects of liposome-associated 1-O-octadecyl-2-O-methyl-sn-glycero-3-phosphocholine. *Cancer Res.* (1997) 57:1915–21.

98. Guo R, Liu Y, Lu W, Zhao J, Wang X, Zhang H, et al. A recombinant peptide, hirudin, potentiates the inhibitory effects of stealthy liposomal vinblastine on the growth and metastasis of melanoma. *Biol Pharm Bull.* (2008) 31:696–702. doi: 10.1248/bpb.31.696

99. Loch-Neckel G, Nemen D, Puhl A, Fernandes D, Stimamiglio M, Alvarez Silva M, et al. Stealth and non-stealth nanocapsules containing camptothecin: in-vitro and in-vivo activity on B16-F10 melanoma. *J Pharm Pharmacol.* (2007) 59:1359–64. doi: 10.1211/jpp.59.10.0005

100. Conesa C, Sánchez N, Ortega V, Reverte J, Carpe F, Aranda M. In vitro and *in vivo* effect of IFNalpha on B16F10 melanoma in two models: subcutaneous (C57BL6J mice) and lung metastasis (Swiss mice). *Biomed Pharmacother.* (2009) 63:305–12. doi: 10.1016/j.biopha.2008.07.092

101. Hamsa T, Kuttan G. Berberine inhibits pulmonary metastasis through down-regulation of MMP in metastatic B16F-10 melanoma cells. *Phyther Res.* (2012) 26:568–78. doi: 10.1002/ptr.3586

102. Aguzzi M, D'Arcangelo D, Giampietri C, Capogrossi M, Facchiano A. RAM, an RGDS analog, exerts potent anti-melanoma effects *in vitro* and *in vivo*. *PLoS ONE.* (2011) 6:e25352. doi: 10.1371/journal.pone.0025352

103. Lentini A, Tabolacci C, Nardi A, Mattioli P, Provenzano B, Beninati S. Preclinical evaluation of the antineoplastic efficacy of 7-(2-hydroxyethyl)theophylline on melanoma cancer cells. *Melanoma Res.* (2012) 22:133–9. doi: 10.1097/CMR.0b013e328350d228

104. Figueiredo C, Matsuo A, Massaoka M, Polonelli L, Travassos L. Anti-tumor activities of peptides corresponding to conserved complementary determining regions from different immunoglobulins. *Peptides.* (2014) 59:14–19. doi: 10.1016/j.peptides.2014.06.007

105. Reich R, Hoffman A, Suresh R, Shai O, Frant J, Maresca A, et al. Carbamoylphosphonates inhibit autotaxin and metastasis formation *in vivo*. *J Enzym Inhib Med Chem.* (2015) 30:767–72. doi: 10.3109/14756366.2014.968146

106. Lu Y, Chen T, Chang K, Chang C, Wei T, Liu J, et al. Synthesis of novel C4-benzazole naphthalimide derivatives with potent anti-tumor properties against murine melanoma. *Bioorg Med Chem.* (2017) 25:789–94. doi: 10.1016/j.bmc.2016.11.057

107. Yang X, Tu C, Luo P, Zhu H, Zhu D, Wu H, et al. Antimetastatic activity of MONCPT in preclinical melanoma mice model. *Invest New Drugs.* (2010) 28:800–11. doi: 10.1007/s10637-009-9323-8

108. Guimarães-Ferreira C, Rodrigues E, Mortara R, Cabral H, Serrano F, Ribeiro-dos-Santos R, et al. Antitumor effects *in vitro* and *in vivo* and mechanisms of protection against melanoma B16F10-Nex2 cells by fastuosain, a cysteine proteinase from Bromelia fastuosa. *Neoplasia.* (2007) 9:723–33. doi: 10.1593/neo.07427

109. Pereira F, Arruda D, Figueiredo C, Massaoka M, Matsuo A, Bueno V, et al. NCBINCBI logo skip to main content skip to navigation resources how to about NCBI accesskeys PubMed US National Library 1263 of medicine national institutes of health search databasesearch term 1264 search advancedhelp result filters format: abstractsend to Clinics. 1265 *Clinics.* (2013) 68:1018–27. doi: 10.1590/clin.v68i7.76934

110. Bechara A, Barbosa C, Paredes-Gamero E, Garcia D, Silva L, Matsuo A, et al. Palladacycle (BPC) antitumour activity against resistant and metastatic cell lines: the relationship with cytosolic calcium mobilisation and cathepsin B activity. *Eur J Med Chem.* (2014) 79:24–33. doi: 10.1016/j.ejmech.2014.03.073

111. Giavazzi R, Decio A. Syngeneic murine metastasis models: B16 melanoma. *Methods Mol Biol.* (2014) doi: 10.1007/978-1-4614-8244-4_10

112. Gay L, Baker A, Graham TA. Tumour cell heterogeneity [version 1; referees: 5 approved]. *F1000 Res.* (2016) 5:1–14. doi: 10.12688/f1000research.7210.1

113. Teicher BA. *Tumor Models in Cancer Research.* Humana Press (2010). doi: 10.1007/978-1-60761-968-0

114. Herlyn M, Fukunaga-Kalabis M. What is a good model for melanoma? *J Invest Dermatol.* (2010) 130:911–2. doi: 10.1038/jid.2009.441

115. Poste G, Doll J, Hart IR, Fidler IJ. *In vitro* selection of murine b16 melanoma variants with enhanced tissue-invasive properties. *Cancer Res.* (1980) 40:1636–44.

116. Ganapathi R, Grabowski D, Sweatman T, Seshadri R, Israel M. N-benzyladriamycin-14-valerate versus progressively doxorubicin-resistant murine tumours: cellular pharmacology and characterisation of cross-resistance *in vitro* and *in vivo*. *Br J Cancer.* (1989) 60:819–826. doi: 10.1038/bjc.1989.373

117. Li W, Song R, Fang X, Wang L, Chen W, Tang P, et al. SBF-1, a synthetic steroidal glycoside, inhibits melanoma growth and metastasis through blocking interaction between PDK1 and AKT3. *Biochem Pharmacol.* (2012) 84:172–81. doi: 10.1016/j.bcp.2012.04.006

118. Chen Y, Zhou L, Yuan L, Zhang Z, Liu X, Wu Q. Formulation, characterization, and evaluation of *in vitro* skin permeation and *in vivo* pharmacodynamics of surface-charged tripterine-loaded nanostructured lipid carriers. *Int J Nanomed.* (2012) 7:3023–32. doi: 10.2147/IJN.S32476

119. Lasek W, Wankowicz A, Kuc K, Feleszko W, Gołab J, Giermasz A, et al. Potentiation of antitumor effects of tumor necrosis factor alpha and interferon gamma by macrophage-colony-stimulating factor in a MmB16 melanoma model in mice. *Cancer Immunol Immunother.* (1995) 40:315–21. doi: 10.1007/BF01519632

120. Zagozdzon R, Golab J, Mucha K, Foroncewicz B, Jakobisiak M. Potentiation of antitumor effects of IL-12 in combination with paclitaxel in murine melanomamodel in vivo. *Int J Mol Med.* (1999) 4:645–8. doi: 10.3892/ijmm.4.6.645

121. Duś D, Matuszyk J, Kuśnierczyk H, Strzadała LRC. Tumorigenicity and metastatic ability of MmB16 mouse melanoma cell line and its two Aleuria aurantia agglutinin resistant variants. *Arch Immunol Ther Exp.* (1992) 40:263–9.

122. Ye Y, Wang C, Zhang X, Hu Q, Zhang Y, Liu Q, et al. A melanin-mediated cancer immunotherapy patch. *Sci Immunol.* (2017) 2: eaan5692. doi: 10.1126/sciimmunol.aan5692

123. Ye Y, Wang J, Hu Q, Hochu G, Xin H, Wang C, et al. synergistic transcutaneous immunotherapy enhances antitumor immune responses through delivery of checkpoint inhibitors. *ACS Nano.* (2016) 10:8956–63. doi: 10.1021/acsnano.6b04989

124. Chen Q, Wang C, Zhang X, Chen G, Hu Q, Li H, et al. In situ sprayed bioresponsive immunotherapeutic gel for post-surgical cancer treatment. *Nat Nanobiotechnology.* (2019) 14:89–97. doi: 10.1038/s41565-018-0319-4

125. Knight G, Laubscher K, Fore M, Clark D, Scallen T. Vitalethine modulates erythropoiesis and neoplasia. *Cancer Res.* (1994) 54:5623–35.

126. Rofstad E, Lyng H. Xenograft model systems for human melanoma. *Mol Med Today.* (1996) 2:394–403. doi: 10.1016/S1357-4310(96)10035-6

127. Flanagan S. 'Nude', a new hairless gene with pleiotropic effects in the mouse. *Genet Res.* (1966) 8:295–309. doi: 10.1017/S0016672300010168

128. Fischer A. Severe combined immunodeficiencies (SCID). *Clin Exp Immunol.* (2000) 122:143–9. doi: 10.1046/j.1365-2249.2000.01359.x

129. Mujoo K, Cheung L, Murray J, Rosenblum M. Pharmacokinetics, tissue distribution, and *in vivo* antitumor effects of the antimelanoma immunotoxin ZME-gelonin. *Cancer Immunol Immunother.* (1995) 40:339–45. doi: 10.1007/BF01519635

130. Li C, Wang Z, Lu Y, Ahn S, Narayanan R, Kearbey J, et al. Biological activity of 4-substituted methoxybenzoyl-aryl-thiazole: an active microtubule inhibitor. *Cancer Res.* (2011) 71:216–24. doi: 10.1158/0008-5472.CAN-10-1725

131. Amino N, Ideyama Y, Yamano M, Kuromitsu S, Tajinda K, Samizu K, et al. YM-201627: an orally active antitumor agent with selective inhibition of vascular endothelial cell proliferation. *Cancer Lett.* (2006) 238:119–227. doi: 10.1016/j.canlet.2005.06.037

132. Bhandarkar S, Bromberg J, Carrillo C, Selvakumar P, Sharma R, Perry B, et al. Tris (dibenzylideneacetone) dipalladium, a N-myristoyltransferase-1 inhibitor, is effective against melanoma growth *in vitro* and *in vivo*. *Clin Cancer Res.* (2008) 14:5743–8. doi: 10.1158/1078-0432.CCR-08-0405

133. Merlino G, Flaherty K, Pesantes NA, Aplin A, Holmen S. The future of preclinical mouse models in melanoma treatment is now. *Pigment Cell Melanoma Res.* (2013) 26:E8–14. doi: 10.1111/pcmr.12099

174. Andricopulo AD, Salum LB, Abraham DJ. Structure-based drug design strategies in medicinal chemistry. *Curr Top Med Chem.* (2009) 9:771–90. doi: 10.2174/156802609789207127

175. Ferreira RS, Oliva G, Andricopulo AD. Integrating virtual and high-throughput screening: opportunities and challenges in drug research and development. *Quim Nova.* (2011) 34:1770–8. doi: 10.1590/S0100-40422011001000010

176. Caraus I, Alsuwailem AA, Nadon R, Makarenkov V. Detecting and overcoming systematic bias in highthroughput screening technologies: a comprehensive review of practical issues and methodological solutions. *Brief Bioinform.* (2015) 16:974–86. doi: 10.1093/bib/bbv004

177. Wang GM, Wang X, Zhu JM, Bin Guo B, Yang Z, Xu ZJ, et al. Docking-based structural splicing and reassembly strategy to develop novel deazapurine derivatives as potent B-Raf V600E inhibitors. *Acta Pharmacol Sin.* (2017) 38:1059–68. doi: 10.1038/aps.2016.173

178. Quirit JG, Lavrenov SN, Poindexter K, Xu J, Kyauk C, Durkin KA, et al. Indole-3-carbinol (I3C) analogues are potent small molecule inhibitors of NEDD4-1 ubiquitin ligase activity that disrupt proliferation of human melanoma cells. *Biochem Pharmacol.* (2017) 127:13–27. doi: 10.1016/j.bcp.2016.12.007

179. Luo Y, Qiu KM, Lu X, Liu K, Fu J, Zhu HL. Synthesis, biological evaluation, and molecular modeling of cinnamic acyl sulfonamide derivatives as novel antitubulin agents. *Bioorganic Med Chem.* (2011) 19:4730–8. doi: 10.1016/j.bmc.2011.06.088

Conflict of Interest Statement: The authors declare that the research was conducted in the absence of any commercial or financial relationships that could be construed as a potential conflict of interest.

Os resultados que fazem parte desta tese de doutorado estão apresentados sob forma de artigo. Os itens materiais e métodos, resultados, discussão e referências bibliográficas encontram-se no próprio manuscrito.

4.3 Capítulo 3 (Artigo 3) - **Tetra-cationic platinum(II) porphyrins like a candidate photosensitizers to bind, selective and drug delivery for metastatic melanoma**

O Artigo foi publicado na revista **Journal of Photochemistry & Photobiology, B: Biology. F.I: 4.38**

Tetra-cationic platinum(II) porphyrins like a candidate photosensitizers to bind, selective and drug delivery for metastatic melanoma

Gabriela Klein Couto[a], Bruna Silveira Pacheco[a], Victoria Mascarenhas Borba[a],
João Carlos Rodrigues Junior[a], Thaís Larré Oliveira[a], Natália Vieira Segatto[a],
Fabiana Kommling Seixas[a], Thiago V. Acunha[b], Bernardo Almeida Iglesias[b,*], Tiago Collares[a,*]

[a] Molecular and Cellular Oncology Research Group, Cancer Biotechnology Laboratory, Technological Development Center, Federal University of Pelotas, Pelotas, Brazil
[b] Laboratory of Bioinorganic and Porphyrinoid Materials, Chemistry Department, Federal University of Santa Maria, Santa Maria, Brazil

ARTICLE INFO

ABSTRACT

Photodynamic therapy (PDT) is an expanding treatment modality due to its minimally invasive localized activity and few adverse effects. This therapy requires photosensitive compounds, which have high sensitivity to light exposure. Thus, in this work, the *in vitro* antitumor activity of *meso*-tetra(3- and 4-pyridyl)porphyrins (**3-TPyP** and **4-TPyP**) in metastatic melanoma cell (WM1366 line) and non-tumoral Ovarian lineage Chinese Hamster (CHO) was evaluated using photodynamic process. Cell viability tests, molecular docking, annexin V, confocal microscopy and qRT-PCR were performed. Our results show that both porphyrins inhibited the viability of metastatic melanoma cells when exposed to light and did not alter viability in the dark. In addition, they did not demonstrate cytotoxicity in non-tumor cells. Molecular coupling demonstrated platinum porphyrin affinity for the N-terminal region of APO B-100, LDL receptor, and therefore of the cells under study. Genes such as Caspase 3 and 9, P21, Bax / BCL2, MnSod and GSH showed increased expression. For *meta* isomer **3-PtTPyP** treatment, caspase-9 and caspase-3 expression levels showed a 4.89 and 3.23-fold increase, respectively, while for the para isomer **4-PtTPyP**, this change was 3.77 and 12.16-fold, respectively. We also observed an upregulated expression of p21, a protein well-known by its action in cell cycle arrest in a p53-dependent manner. Conclusion: **3-PtTPyP** and **4-PtTPyP** demonstrated antitumor effect on WM1366 cells, inducing apoptosis and significant alteration of cell cytoskeleton actin. Our work shows that platinum(II) porphyrins may be promising photosensitizers for the treatment of metastatic melanoma by PDT.

1. Introduction

Melanoma is considered the most aggressive type of skin cancer, due to its late diagnosis in most cases [1]. It can be cured when diagnosed in the early stages, however, it is very likely to develop metastases if this diagnosis is late. The treatment of this pathology is chosen depending on the tumor staging. The advanced stages are very difficult to be treated with the currently available therapies, including chemo and immunotherapy, highlighting the need for new and selective treatments [2–4]. According to World Cancer Research Fund, this neoplasy is the 19th most commonly occurring cancer. In 2018, nearly 300,000 new cases were diagnosed [5]. According to American Cancer Society, 96,480 new cases are estimated to be diagnosed in 2019 and 7230 deaths from melanoma are expected. And in Brazil, for biennium 2018/2019, an estimated 6260 new cases of skin cancer of the melanoma type [6].

In this context, alternative therapies have been studied to optimize the treatment of aggressive pathologies such as cancer [7]. Photodynamic therapy (PDT) has been shown to be a promising alternative in this regard. It has its action based on three main points, being: the use of sensitizers, light and oxygen molecule, to induce cellular damage. It is characterized by being a minimally invasive and a tumor-selective method, besides presenting a decrease of the adverse effects to the patient [8,9].

Currently, new molecules have been found that have ideal properties to be used as photosensitizers in PDT. In this sense, some specific characteristics need to be observed in these molecules so that they can be used as photosensitizers. Among these characteristics we highlight potentiated photostability, good solubility in physiological medium, high generation of reactive oxygen species (ROS), selectivity and high phototoxicity [10].

A widely studied example is the porphyrins due to their structure in

the form of a ring with 18 conjugated π electrons, which is why their porphyrin derivatives absorb light, proving their photophysical properties as well as their ability to accumulate in the tumor selectively [11]. In order to potentiate the action of these structures, associations with some inorganic compounds, such as platinum(II) complexes, have been described [12]. This association is justified by the fact that, in isolation, such metals demonstrate potent anti-tumor action properties, and thus, the union between porphyrins and metal-transition co-ordination compounds may offer the possibility of synergistic effects as well as decrease observed adverse effects for each drug separately [12]. Thus, the aim of this study was to analyze the anti-tumor action of isomeric tetra-cationic(pyridyl)porphyrins containing peripheral attached platinum(II) complexes at the *meta* and *para* positions on metastatic melanoma cell line using photoactivated compounds.

2. Materials and Methods

2.1. Tetra-cationic porphyrin photosensitizers 3-PtTPyP and 4-PtTPyP

The *meso*-tetra(3- and 4-pyridyl)porphyrins (3-TPyP and 4-TPyP) were purchased from Frontier Scientific® (Logan, Utah, USA). Peripheral platinated(II) porphyrin hexafluorophosphate compound (3-PtTPyP and 4-PtTPyP; Fig. 1) were synthesized, fully characterized and reported in some publications in the literature [12–15] (see *supplementary information section* – Figs. S1–S7 and Table S1). All Pt(II)-porphyrins tested in this study are soluble in DMSO and stable in this solution (see *supplementary information section* – Figs. S8-S9). Stock solutions were prepared in anhydrous dimethyl sulfoxide at concentration of 1 mg/mL (Sigma-Aldrich®).

2.2. Cell culture and reagents

The WM1366 cell line kindly provided by Universidade de Ribeirão Preto, SP-Brazil and a non-tumor cell line derived from the ovary of the Chinese hamster (CHO), were obtained from the Rio de Janeiro Cell Bank (PABCAM, Federal University of Rio de Janeiro, RJ, Brazil). They were grown in Dulbecco's Modified Eagle's Medium (DMEM) supplemented with 10% fetal bovine serum (FBS), respectively, obtained from Vitrocell Embriolife (Campinas, Brazil) and Gibco (Grand Island, NY, USA). Cells were grown under controlled atmosphere at 37 °C, 95% humidity and 5% CO_2.

2.3. Experimental groups and photodynamic assay

The cells were divided into two distinct groups: light and dark conditions. Each group was treated with five different concentrations (0.563, 1.125, 5.625, 11.25, 28.125 and 56.25 nM) of the two platinum (II) porphyrins, 3-PtTPyP and 4-PtTPyP. After adherence of the cells to the wells, they were divided into separate groups and treated with the different concentrations previously presented of the proposed compounds. As these compounds are activated by the incidence of light, these were divided into two groups (light and dark), where the light group was activated by phototherapy for 30 min. In the irradiation light conditions, the porphyrins were exposed to white-light (400 to 800 nm range, consisting of a 100 W LED lamp system) with a fluence rate of 50 mW/cm², for 30 min (total light dose of 45 J/cm²), according to a method in the literature [16]. After exposure to light for 30 min the plates were put back into the incubator and the following tests were performed 24 h after exposure to light (Fig. 2).

2.4. Cell proliferation assay

WM1366 and CHO cells were seeded in 96-well culture plates at a density of 2.0×10^4/well (200 μL/well) with different concentrations of the molecules. The negative control consisted in 200 μL/well of medium, and the control of the vehicle in 200 μL/well of medium and DMSO (with concentration < 0.5%). Cell proliferation was evaluated 24 h after the activation of the compounds by the light irradiation. After the incubation period, the MTT salt (tetrazolium salt [3- (4,5-dimethylthiazol-2-yl) -2,5-diphenyltetrazolium bromide]) was added to each well (5 mg MTT/ml). Then, absorbance was measured using a spectrophotometer (Thermo Plate TP-Reader) at a wavelength of at 495 nm. Percent of growth inhibition was determined by the formula:

$$\%\text{inhibition} = (\text{Abs}_{492} \text{ treated cells}/\text{Abs}_{492} \text{ control cells}) \times 100.$$

2.5. Molecular docking

Given the importance of the binding between our molecules (3-PtTPyP and 4-PtTPyP) in the mechanism of selectivity of tumor cells, molecular docking analyzes were performed. For the creation of the target receptor we used the sequence APOB_HUMAN (P04114) that was obtained from the UniProt website (Cathy H. Wu et al., 2006) and its domains were analyzed by the SMART platform (Ivica Letunic et al., 2004) to obtain the N-terminal domain amino acid sequence (LPD_N),
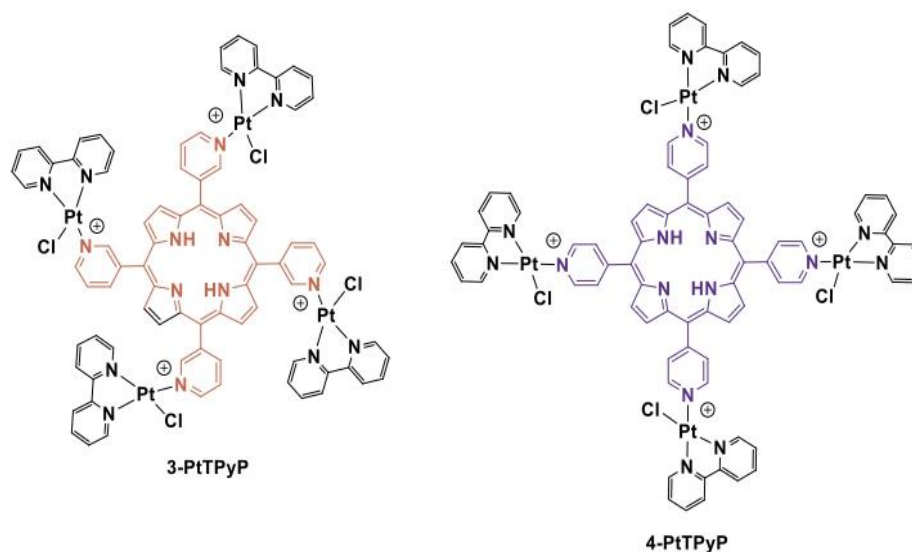

Fig. 1. Structural representation of free-base platinum(II) peripheral porphyrins 3-PtTPyP and 4-PtTPyP used in this study. The hexafluorophosphate counter-ions are omitted for more clarity.
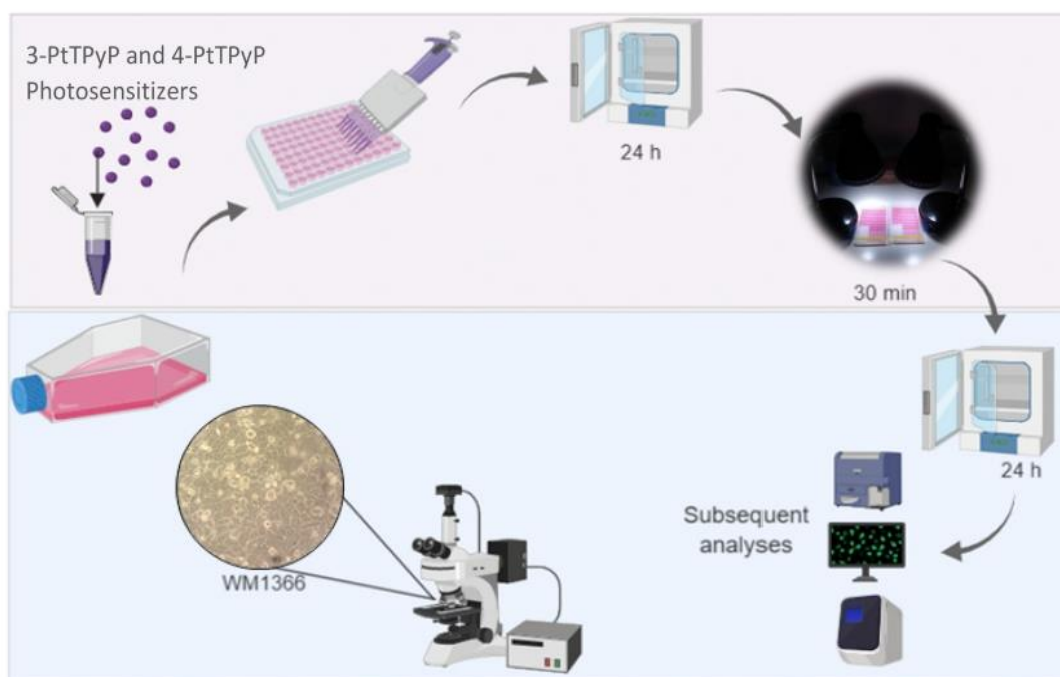
Fig. 2. Scheme of treatment protocol of WM1366 cells with **3-PtTPyP** and **4-PtTPyP** photosensitizers in photodynamic therapy.

which was predicted at the 46–598 position with its *E*-value of 6.97e-140. This represents a conserved region that has been found in several lipid carrier proteins, including vitellogenin, triglyceride microsomal transfer protein and Apolipoprotein B-100 [44]. The receptor was modeled by homology using CPHmodels-3.0 (Morten Nielsen et al., 2010) with its *Z*-score of 59.41. The model used was 1LSH protein refined lipovitelin molecular structure with a resolution of 1.9 Å, with its E-Value of 5e-05 and 99% convergence with BLAST-protein search. The preparation of the molecules began with the 2D creation of the molecules, prepared by ChemDraw 2018 software, the molecules were prepared as ligands for anchoring using the Molecular Operating Environment (MOE; Chemical computing Group, Montreal, Canada) software. The protonation state was adjusted to pH 7. Our ^{receptor} was prepared by the Schröndinger Maestro Protein Preparation Wizard (Protein Preparation Wizard, Schröndinger, LLC, New York, NY, 2015). Where hydrogens were added, completing the missing loops and finally minimizing their energy and optimizing the protein. Molecular anchoring was performed using the GOLD software (G. Jones, P. Willett, R. C. Glen, A. R. Leach, R. Taylor, J. Mol. Biol. 1997, 267, 727).

Anchoring results were obtained through fitness values, in which the higher the value, the better the interaction of anchoring with the complexes is defined. For this work we used the ChemPLP algorithm. To validate the results obtained by docking, we used a low-density lipoprotein (LDL) analog, which binds at the Apo B-100 site causing it to trigger the membrane LDL-R binding cycle. The analog chosen was amino acid sequence ^{0582}DLKKLVKEVLKESQLPTVMDFRKFSRNYQ^{0610} of name B0582 [17]. This amino acid sequence was taken from the N-terminal region of APO B-100 itself and was modeled by CPHmodels-3.0 (Morten Nielsen et al., 2010). After modeling, the GOLD molecular anchor program was used to simulate the binding of B0582 to our target protein. For this simulation was used the standard mode of the software, we used the target protein without solvent and with added hydrogen atoms.

2.6. Confocal microscopy analysis

Changes in cell membrane were identified using DAPI (4,6-diamidino-2-phenylindole) staining, which forms a fluorescent complex with double-stranded DNA, and Texas red that stains the cell's actin. Cells seeded in a 96-well plate were treated with 4.501 and 3.012 nM of **3-PtTPyP** and **4-PtTPyP** porphyrins, respectively. After 24 h of treatment

the white-light source was applied, and cells were incubated for 24 h. After treatment, the cells were washed three times in phosphate buffered saline (PBS), fixed and stained according to the manufacturer's protocol. Cell morphology was examined by SP8 confocal microscopy (Leica Microsystems ©). DAPI dye emission: ~460 nm. Texas red dye emission: ~615 nm. Cell morphology was examined by confocal microscopy at a magnification of 400×.

2.7. RNA extraction and qRT-PCR

Total mRNA was extracted of cells using TRIzol (Invitrogen™, Carlsbad, USA) followed by DNase treatment with DNA-free® kit (Ambion™, USA) and mRNA quantification by Nanovue Plus Spectrophotometer™ (GE®). The cDNA synthesis was performed using High Capacity cDNA Reverse Transcription kit (Applied Biosystems™, UK) according to the manufacturer's protocol. The amplification was made with UltraSYBR Mix (COWIN Bioscience Co., Pequim, China) using the Stratagene Mx3005P and the sequence of primers used are indicated in Table 1. Gene expression were normalized using glyceraldehyde 3-phosphate dehydrogenase (GAPDH) as a reference gene and the conditions for the reactions included 95 °C for 15 s, 60 °C for 60 s and 72 °C for 30 s. The 2ΔΔCT (Delta–Delta Comparative Threshold) method was used to normalize the fold change in gene expressions. Control used to calculate ΔΔCT was the group that received only DMEM, without porphyrin and without light.

2.8. Annexin V by flow cytometry

The ability of the different treatments to induce apoptosis against metastatic melanoma cells was assessed by flow cytometry using the Muse ™ Annexin V & Dead Cell Assay Kit (EMD Millipore Corporation). For this analysis, WM1366 cells were plated in 12-well plates at a density of 1.0×10^5 cells per well. After 24 h of adhesion, the cells were incubated with the IC_{50} concentrations of the porphyrin molecules. Twenty-four hours after treatment, the cells were treated with light for 30 min (the dark group stayed away from the light). After light exposure, the cells were washed with PBS, trypsinized and centrifuged at 1200 rpm for 10 min. After centrifugation, 1.0×10^5 cells were stained according to the manufacturer's instructions and analyzed using the Muse Cell Analyzer (EMD Millipore Corporation).

Table 1
Primer sequences for qRT-PCR used in this study.

Primer	Sequence 5′ → 3′
MnSod For	GGAAGCCATCAAACGTGACT
MnSod Rev	CTGATTTGGACAAGCAGCAA
P21 For	TGTCCGTCAGAACCCATGC
P21 Rev	AAAGTCGAAGTTCCATCGCTC
Casp 9 For	GTCTCAATGCCACAGTCCAG
Casp 9 Rev	TGTACATGCAGCAAACCTC
Casp 3 For	CAGTGGAGGCCGACTTCTTG
Casp 3 Rev	TGGCACAAAGCGATCGGAT
GSHR For	CCCGATGTATCACGCAGTTA
GSHR Rev	TTCACTGCAACAGCAAAACC
Bax For	ATGCGTCCACCAAGAAGC
Bax Rev	ACGGCGGCAATCATCCTC
BCL-2 For	GGTGGGGTCATGTGTGTGG
BCL-2 Rev	CCGTTCAGGTACTCAGTCATCC
iNOS For	ACAAGCCTACCCCTCCAGAT
iNOS Rev	TCCCGTCAGTTGGTAGGT
GAPDH For	GGATTTGGTCGTATTGGG
GAPDH Rev	TCGCTCCTGGAAGATGG

Table 2
IC$_{50}$ values of molecules **3-PtTPyP** and **4-PtTPyP** after 24 h of light exposition against WM1366 line.

Porphyrin	IC$_{50}$ (nM)
3-PtTPyP	4.501 ± 0.58
4-PtTPyP	3.012 ± 0.27

(Merck Millipore Corporation) and analyzed in the Muse Cell Analyzer (EMD Millipore Corporation).

2.10. Statistical analysis

Data are presented as mean and standard deviation (SD). Comparative analyzes were performed using one-way analysis of variance (ANOVA). Tukey's *post hoc* method was employed for multiple comparisons. All statistical analyzes were performed with GraphPad Prism and $p < .05$ was considered statistically significant. For the the cell cycle analysis, the bidirectional analysis of variance (ANOVA) was used. Bonferroni's *post hoc* method was used for multiple comparisons.

3. Results

3.1. Platinum(II) porphyrins as good candidates for photosensitizers

With the cell proliferation assay, it was observed that platinum (II) porphyrins were activated in the presence of light (Fig. 3A and B) at most concentrations tested. Cellular inhibition was more expressive for 3-PtTPyP and 4-PtTPyP molecules at the two highest concentrations (5.625 and 56.25 nM). In addition, we calculated the IC50 of the molecules for subsequent testing (Table 2). Also, we tested as porphyrins in the CHO cell at the same IC50 concentrations calculated for the 3-PtTPyP and 4-PtTPyP porphyrins. In addition to the IC50 concentration, we added a concentration above and below this value, and these

2.9. Cell cycle analysis

In order to assess possible mechanisms involved in the decreased cell viability, such as cell cycle arrest, we performed flow cytometry analysis with the objective of identifying cell populations at different stages of the cell cycle after different treatments. For this analysis, WM1366 cells were plated in 12-well plates at a density of 2.0×10^5 cells per well. After 24 h, the cells were incubated with the IC$_{50}$ concentrations of each of the molecules. After 24 h, the cells underwent photodynamic therapy for 30 min. After light irradiation process, cells were detached, fixed with 70% ethanol and stained according to the manufacturer's protocol. Measurement of DNA content was analyzed by propidium iodide staining using the Guava Cell Cycle reagent kit
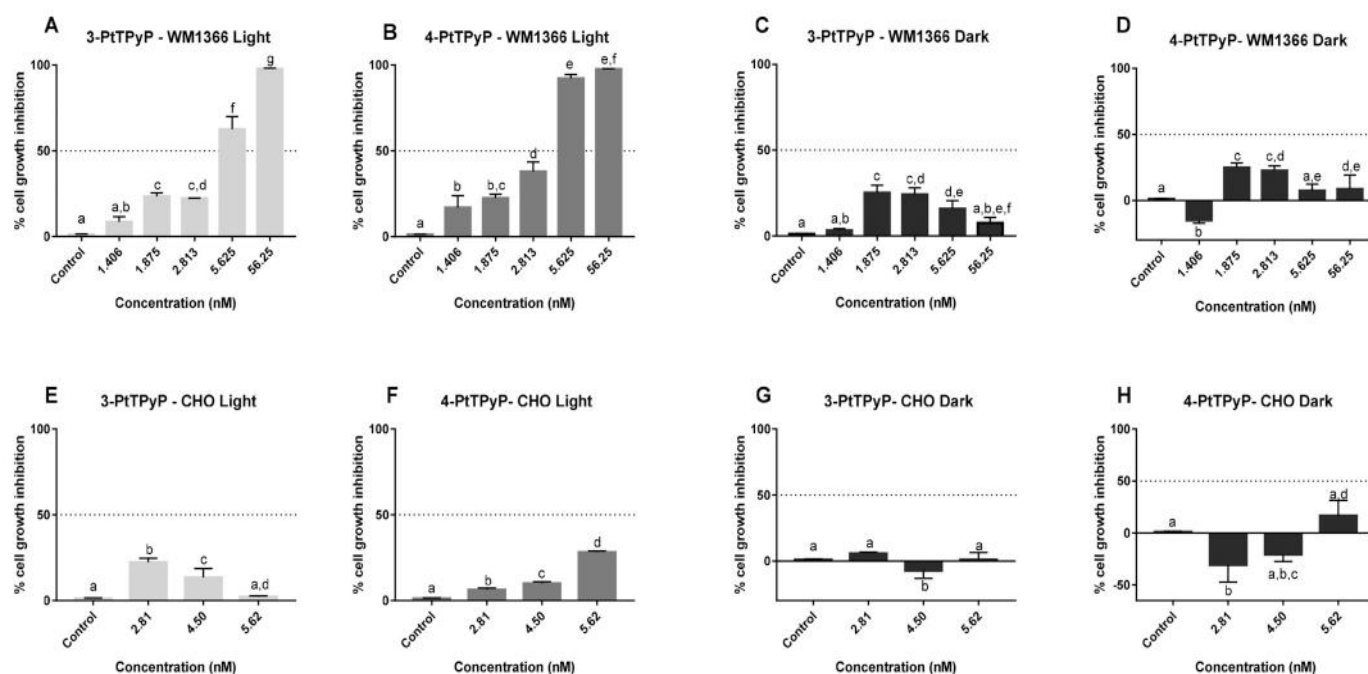

Fig. 3. Effect of light action on photosensitizing molecule on cell proliferation. Porphyrin-treated and untreated cells were irradiated for 30 min. Dark group went totally in the dark for the same time. The graph shows the comparison within the light and dark group of **3-PtTPyP** and **4-PtTPyP** porphyrins. Data are expressed as mean ± SD of three independent times performed in triplicate. Fig. 3A–D: WM1366 cell line was treated with **3-PtTPyP** (Fig. A and B) and **4-PtTPyP** (Fig.C and D) platinum (II) porphyrins at 5 different concentrations. Control group received no treatment with porphyrins. Fig. 3E–F: Effect of light on the photosensitizing molecule on cell proliferation of non-tumor cells. The CHO cell line was treated with **3-PtTPyP** (Fig. E and G) and **4-PtTPyP** (Fig. F and H) platinum (II) porphyrins at a concentration above the IC 50 and one below the predetermined IC 50 of each of the molecules. The concentrations used were: 5.62, 4.50 and 2.81 nM for 3-PtTPyP and 5.62, 3.01 and 2.81 for 4-PtTPyP. For comparison different letters in the chart denote significant difference between the groups. $p < .05$ was considered significant.

Table 3

Anchor results of APO B-100 E LDL receptor molecules.

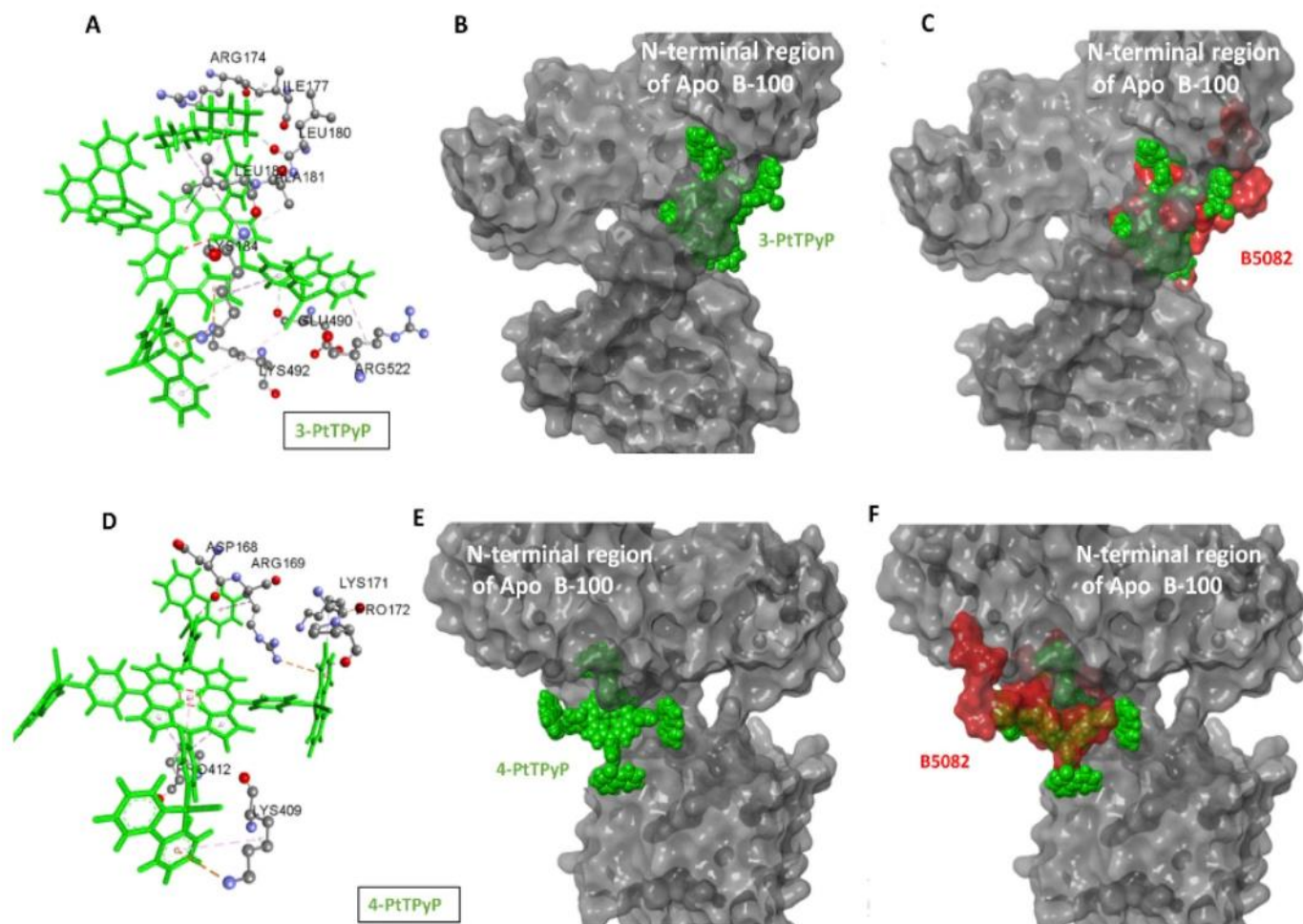| Molecule – protein	Amino acids	Fitness	Common amino acids with B0582
B0582 - Apo B-100	ASP168, PRO172, ARG174, LEU182, LYS184, LYS409, PRO412, LYS462, LYS488, LYS492	93.2881	–
3-PtTPyP - Apo B-100	ARG174, ILE177, LEU180, ALA181, LEU182, LYS184, GLU490, LYS492 e ARG522	90.7311	**ARG174, LEU182, LYS184 e LYS492**
4-PtTPyP -Apo B-100	ASP168, ARG169, LYS171, PRO172, LYS409, PRO412	68.5542	**ASP168, PRO172, LYS409 e PRO412**

Fig. 4. Molecular docking results. Fig. A and D represent the 3D molecular structure of platinum porphyrins **3-PtTPyP** and **4-PtTPyP** and their amino acid linkages of the B0582 LDL analog. Fig. B and E demonstrate the binding of platinum porphyrins to the N-terminal region of APO B-100. Fig. C and F demonstrate the similarity of B0582 anchoring of **3-PtTPyP** and **4-PtTPyP** molecules to the N-terminal region of APO B-100.

compounds were not toxic to normal cells (Figs. 3E–H). Graphs 3C-D and 3G-H show the test performed with porphyrins in the dark and we can see that all concentrations were well below 50% inhibition. In addition, due to the low solubility and aggregate formation, all assays without platinum (II) peripheral complexes could not be performed.

3.2. Peripheral platinum(II) porphyrins bind to LDL receptor

After running the molecular docking tests, we recognized as better the position of the analog B0582 that obtained the highest fitness which was 93.2881 with the ChemPLP algorithm. Based on these values, we chose the positions with the closest proximity of this score to the **3-PtTPyP** and **4-PtTPyP** molecules. It was also taken into consideration the pose in which it had greater interaction with lysines, because according to Guevara et al. this analog has high affinity for lysines. We anchored the **3-PtTPyP** and **4-PtTPyP** molecules in the region of the binding site that B0582 was anchored to, having amino acid residues at a distance of 20 Å considered. Anchoring results can be seen in Table 3 and Figs. 4A–F. For this study of docking molecular we use the

algorithms in the default mode directly in the GOLD software, we use the fitness function like parameters for screening poses. This function indicates the ability of the ligand compound interact directly with the target protein, the higher this value better they are because they indicate the affinity of bond of these poses and the protein. This score was calculated by the forces of the bonds between the ligand and the protein for example, van der Waals forces, electrostatics and hydrophobics interactions.

We used as valid the poses of the compounds in which they obtained a high fitness score and obtained bonds with amino acids present in the active site of the protein.

3.3. Platinum(II) porphyrins alter cellular actin organization

To analyze the morphological alterations of the treated WM1366 cells with a cytotoxic concentration of the **3-PtTPyP** and **4-PtTPyP** porphyrins, we observed that in the control group (without treatment) the stress fibers appeared thin and diffuse (Fig. 5A). After being treated, the cells appeared to be rounded, a general thickening of the membrane
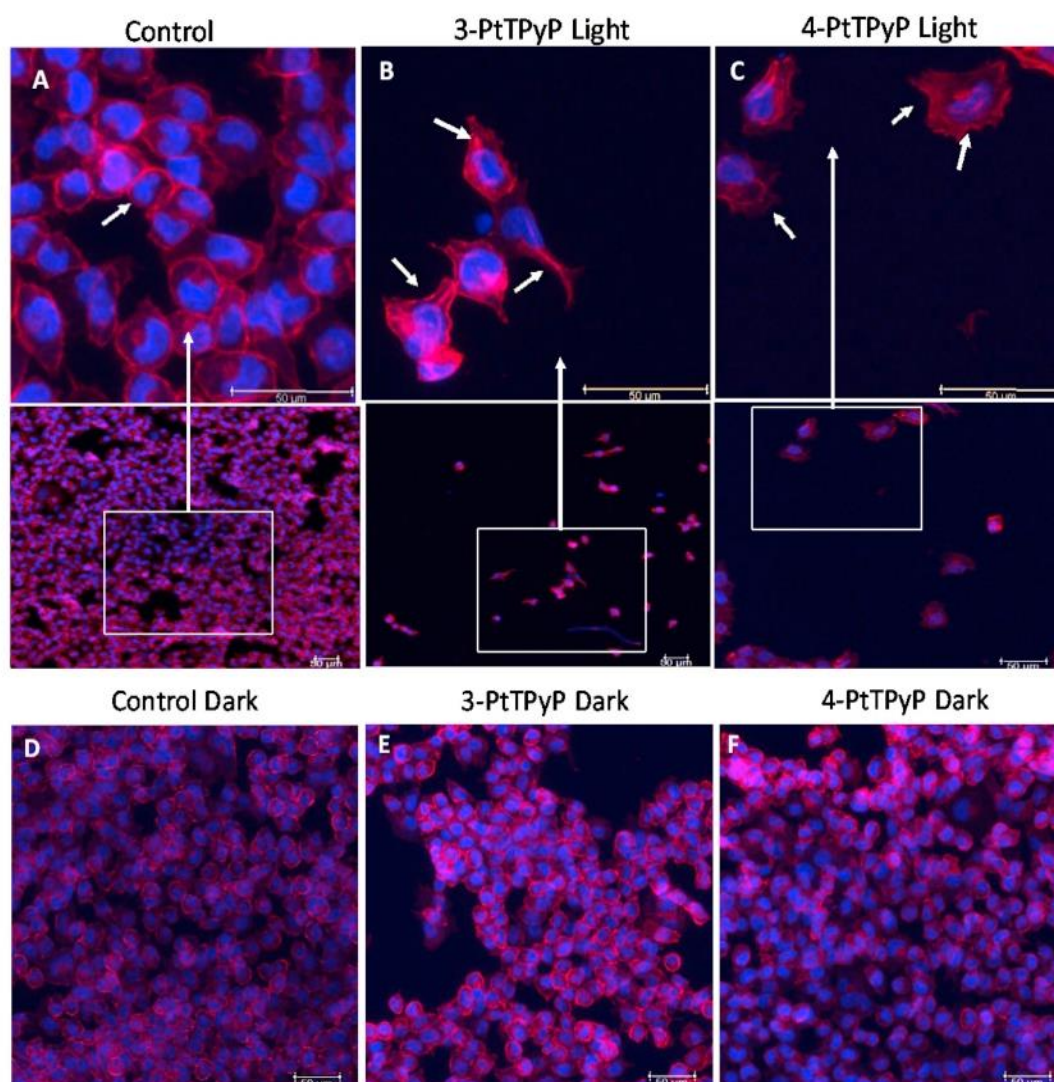
Fig. 5. (A–F): Morphological analysis after treatment with **3-PtTPyP** and **4-PtTPyP** photosensitizers. WM1366 cells were stained Texas Red and DAPI-cytoplasm and nucleus, respectively. In the image we can observe a uniform cytoplasm in the control group (Figs. 5A and D) and in the treatments (**3-PtTPyP** and **4-PtTPyP**) we observe a reorganization of actin filaments (arrows Fig. 5B). A general thickening of actin fibers in the membrane, ruffling occurred at the border of its plasma membrane (arrows Fig. 5B) and microspikes (arrows Fig. 5C) was observed on the cell surface of some cells. These changes were not identified in dark group cells (Figs. 5D, E and F), respectively.

actin fibers (Figs. 5B and C) and significant ruffling occurred at the edge of their plasma membrane was also observed. Additional morphological changes as microspikes were observed (Fig. 5C) on the cell surface of some cells. Such changes mentioned above were not identified in dark group cells (Figs. 5D, E and F).

3.4. Pt(II)-porphyrins induces apoptosis

We use annexin V to detect apoptotic cells because of its ability to bind to phosphatidylserine, an apoptosis marker when it is on the outer leaflet of the plasma membrane. The annexin V double staining assay and dead cells allow to differentiate between early apoptosis, late apoptosis, dead / debris and living cell populations. Early or late apoptosis rates (Fig. 6A–D and 7A–D) assessed by flow cytometry showed that **3-PtTPyP** and **4-PtTPyP** porphyrins at concentrations of 4.50 and 3012 nM induced a percentage of the total. of apoptotic cells of 37.18% and 13.5%, respectively (total apoptosis = early and late apoptosis), indicating that the photodynamic process using Pt (II)-pyrphyrins as photosensitizers is efficient. In addition, we observed that the dark, light control and light control groups did not significantly induce apoptosis in both molecules (Figs. 6 and 7) ($P < .05$).

3.5. Tetra-cationic platinum(II) porphyrins alter expression level of genes related to apoptosis and oxidative stress

In order to further investigate the platinum(II) porphyrins photodynamic therapy mechanisms of apoptosis induction in the melanoma cell line, evidenced by the annexin V assay, the relative mRNA expression of the p21, BAX, Bcl-2, caspase 9, caspase 3, MnSOD, iNOS and Glutathione reductase (GSHR) genes were assessed by qRT-PCR. As shown in Figs. 8–10, both porphyrins (**3-PtTPyP** and **4-PtTPyP**) significantly altered the expression levels of all genes analyzed in metastatic melanoma cell (WM1366) after photodynamic conditions (exposure to light) ($p < .001$). Interestingly, we also obtained a discrete increase in GSHR expression in the dark group of **3-PtTPyP** porphyrin ($p < .001$), Fig. 8G. As expected, the increased relative expression of caspase 3, caspase 9 and P21 genes as well as the upregulated Bax/Bcl-2 ratio corroborate with the apoptotic results obtained in the annexin V test. Further, elevated iNOS levels in porphyrin **4-PtTPyP** (Fig. 10B) indicate that oxidative stress may be related to a possible cause of apoptosis and cell death.

3.6. Peripheral platinum(II) porphyrins don't arrest the cell cycle

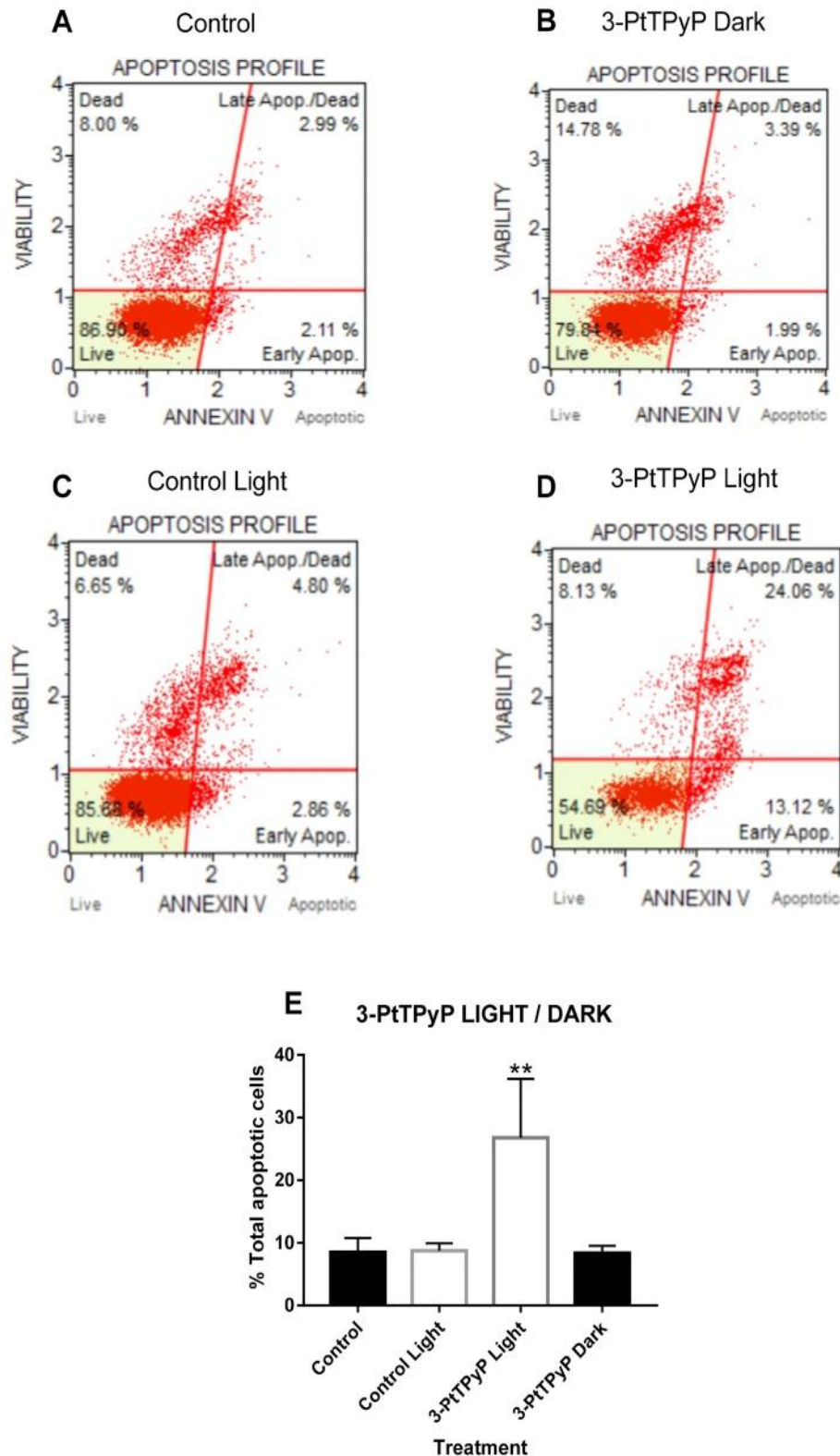Cells at the different stages of the cell cycle (G0/ 1, S and G2/M)

Fig. 6. Induction of apoptosis by porphyrin **3-PtTPyP**. WM1366 cells were evaluated for apoptosis by annexin V staining under light and dark group conditions at the IC 50 concentration of the compound. The graph (Fig. E) shows the total percentage of apoptotic cells. Figs. A–D show % late and recent apoptosis in each of the groups. Porphyrin **3-PtTPyP** with white light dosage had a significant increase in apoptosis when compared to all other groups (**) denotes $p < .007$.

were analyzed by flow cytometry and are shown in Fig. 11. The results showed that although an increased expression of the P21 gene (involved in the cell cycle) was observed in the qRT-PCR, we did not have a significant stop in the G0/G1, S and G2/M cycle between the groups evaluated.

4. Discussion

Results obtained in WM1366 after treatment with **3-PtTPyP** and **4-PtTPyP** showed that both porphyrins were not toxic to non-tumor cells (CHO cell line), as they showed low levels of inhibition in the
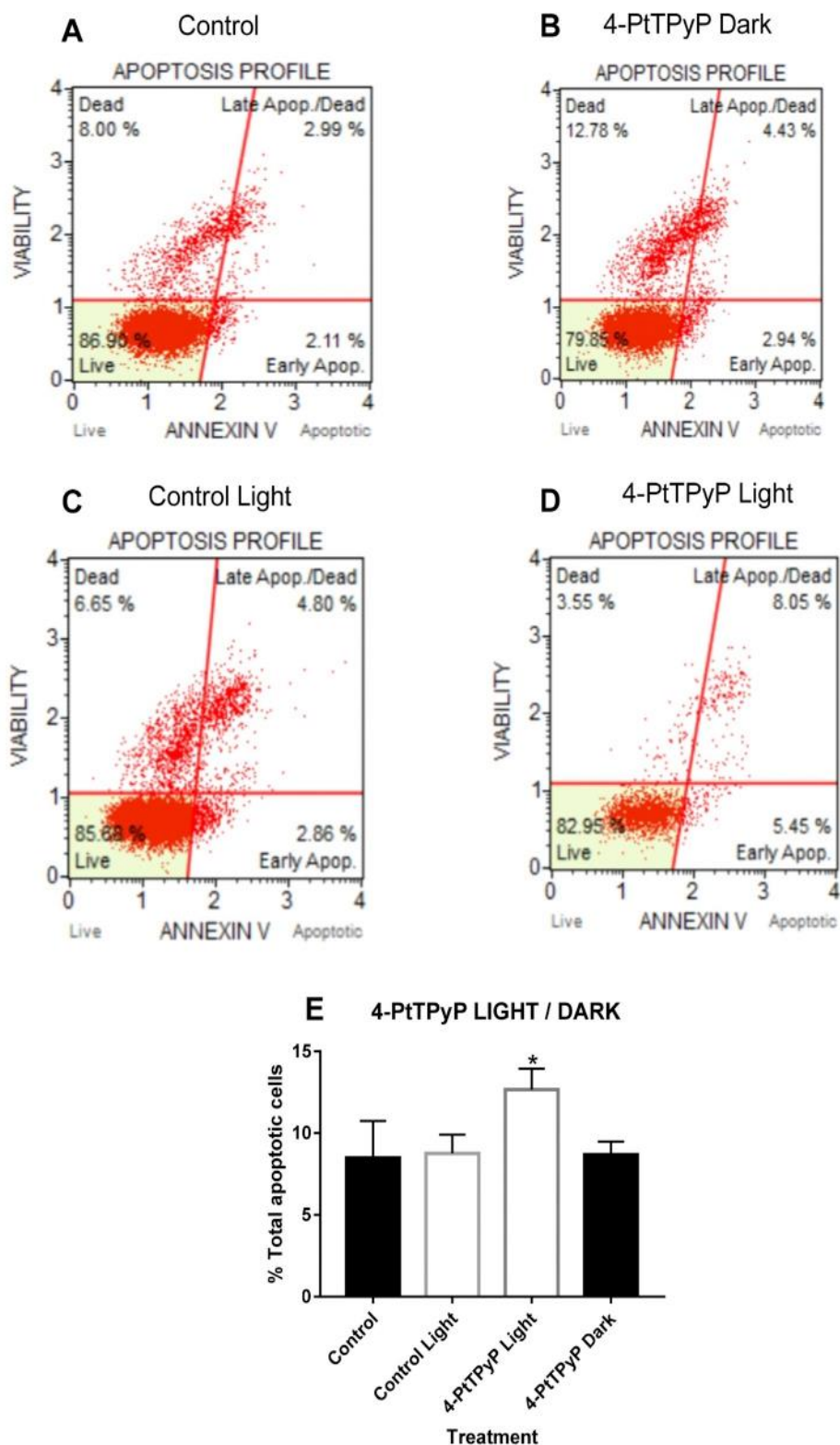
Fig. 7. Porphyrin **4-PtTPyP** apoptosis induction. WM1366 cells were evaluated for apoptosis by annexin V staining under light and dark group conditions at the IC 50 concentration of the compound. The graph (Fig. E) shows the total percentage of apoptotic cells. Figs. A–D show % of late and recent apoptosis in each of the groups. Porphyrin **4-PtTPyP** with white light dosage had a significant increase in apoptosis when compared to all other groups (*) denotes $p < .03$.

cytotoxicity test. These findings suggest a possible selectivity of porphyrin compounds towards tumor cells, which could be explained by the tendency of binding of the photosensitizers, preferably, with low density lipoproteins (LDL) [18,19]. Firestone et al. demonstrated that neoplastic cells have higher uptake of LDL and with this a greater expression of these receptors [20]. Our molecular docking data corroborate this suggestion as our **3-PtTPyP** and **4-PtTPyP** porphyrins demonstrated a binding profile with the target. This protein was chosen because an important part of the circulating LDL binds to Apo B-100 to

bind to the LDL receptor present on the cell membrane. The peptide sequence called B0582 (analogous to LDL) showed the binding of the N-terminal region of APO B-100 + B0582 and allowed us to compare the interaction of porphyrins with this target [17]. Our results demonstrate that platinum porphyrins **3-PtTPyP** and **4-PtTPyP** bound very similarly to B0582 in the target protein, especially **3-PtTPyP**, which had a fitness score of 90.73 (very close to the B0582 score that was 93.28) and amino acid binding: ARG174, ILE177, LEU180, ALA181, LEU182, LYS184, GLU490, LYS492 and ARG522. Of which four of these amino acids were
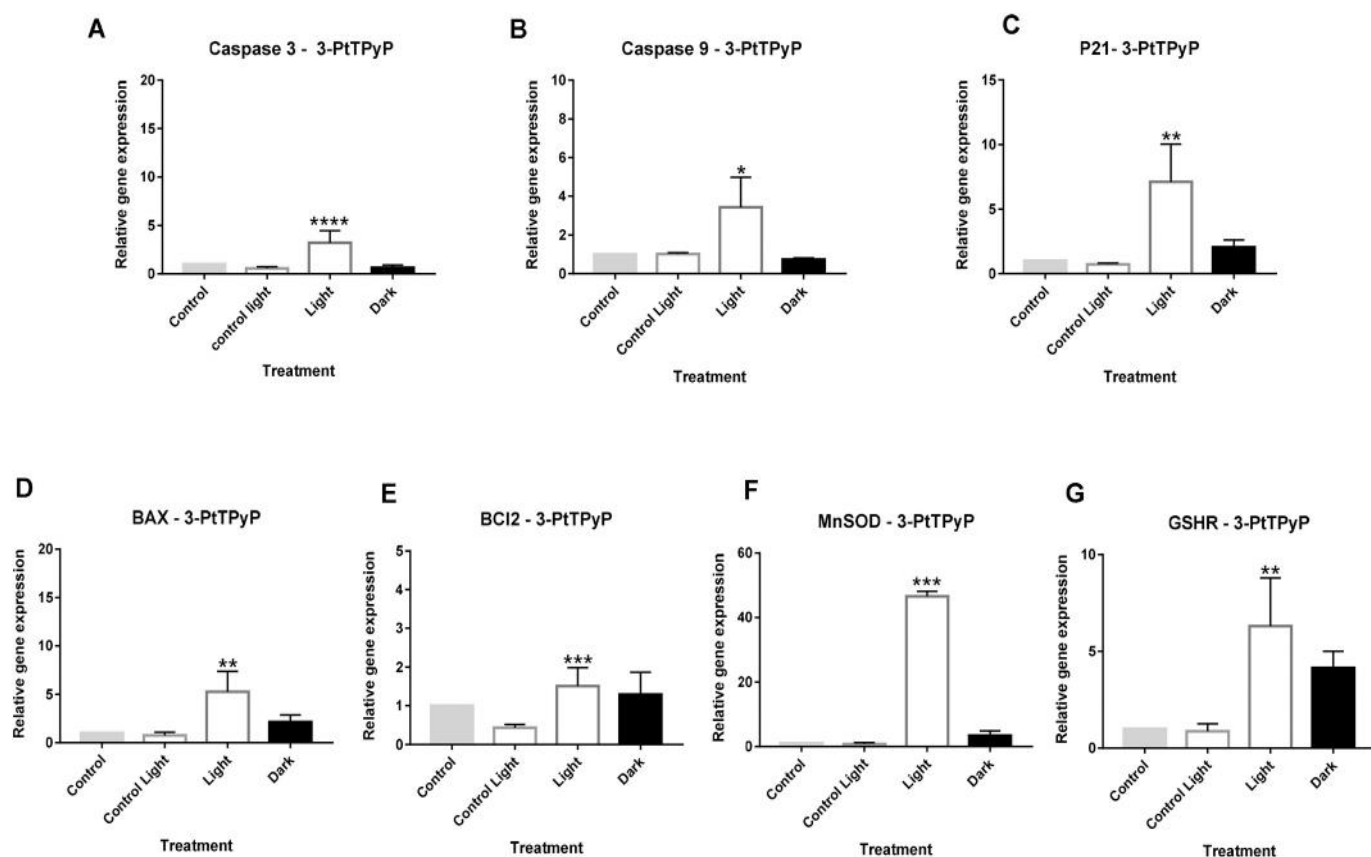
Fig. 8. Platinum(II) porphyrin **3-PtTPyP** increased expression of Caspase 3, Caspase 9, P21, BAX, BCL2, MnSOD and GSHR genes in metastatic melanoma line WM1366 24 h after being submitted to white-light irradiation. The gene expression profile was determined by qRT-PCR and the data were normalized using the GAPDH levels. **3-PtTPyP** had a significant increase in the expression of all evaluated genes when compared to the other groups. (****) denotes $p < .0001$, (***) denotes $p < .0005$, (**) denotes $p < .004$, (*) $p < .04$. when compared to the light and dark group of the same molecule. Three independent experiments were performed in triplicate.

the same in the binding of B0582 to N-terminal region (ARG174, LEU182, LYS184 and LYS492).

Porphyrin **4-PtTPyP** had a score of 68.55 fitness and amino acid binding ASP168, ARG169, LYS171, PRO172, LYS409, PRO412. In this platinum porphyrin we also find four amino acids in common with B0582 (ASP168, PRO172, LYS409 and PRO412). These results corroborate our *in vitro* findings, described above, where we observed a selectivity for the tumor lineage. As with 3-PtTPyP we can suggest that 4-PtTPyP platinum porphyrin is a photosensitizer-like candidate due to the stability of hydrophobic bonds with amino acids. These molecular anchor studies have also been described in the same vein to predict specific receptor affinities in order to improve drug delivery or induce possible selectivity. Bazcaran and co-workers conducted anchor studies with the ALK gene for non-small-cell lung cancer to try to improve the action of drugs for this cancer. [21]. Similarly, Xu et al. Evaluated by molecular anchorage the receptor RXR as a pharmacological route for acute promyelocytic leukemia [22]. Still a review published by our group demonstrated the importance of using molecular docking to predict interactions between molecules and their receptors in the development of new drug candidates [4].

It is still important to highlight the fact that the molecules did not present cytotoxicity in all dark groups confirming the action of the molecules **3-PtTPyP** and **4-PtTPyP** only when exposed to light. In addition, other evidence leads us to believe that one of the main acting species may be singlet oxygen ($^1O_2$) produced by the light action in the presence of Pt(II)-porphyrins studied here [12,23], as reported in the literature on photoinactivation processes of microorganisms by the same platinum(II) porphyrins [16,24].

Morphological changes were observed in WM1366 cells treated with **3-PtTPyP** and **4-PtTPyP** porphyrins. The reorganization of actin fibers can be observed after treatment with photodynamic therapy,

such as microspikes on the surface of the membrane and formation of filopodia. It can be said that these modifications in actin from the cytoskeleton of the cell are important for the defense mechanism and cell death [25]. Garg and collaborators in a study with retinal pigmented epithelium cells obtained findings corroborating ours [26]. As well as Zhao and co-workers who observed such modifications in the actin in bovine pulmonary artery endothelial cells (BPAEC), which underwent stress caused by hydrogen peroxide (H_2O_2), stress similar to that caused by anti-cancer drugs such as cisplatin [27–29]. Other studies in lung cells (A549 and H460) have also confirmed our findings related to actin cytoskeleton rearrangement [30]. In our study these changes were observed only in the light-exposed groups treated with porphyrins **3-PtTPyP** and **4-PtTPyP**, probably by ROS generation. In the light/dark and **3-PtTPyP** and **4-PtTPyP** dark control groups we did not observe these modifications. With these results we can state that the molecules are activated only in white-light conditions and that only light exposure has no action on the cells.

We accessed the effect of porphyrins **3-PtTPyP** and **4-PtTPyP** in the apoptosis induction of metastatic melanoma cells *in vitro*. Treatments with both Pt(II)-porphyrins after light exposure increased the number of total apoptotic cells evidenced by their phosphatidylserine externalization, when compared to the control group and to the groups in the dark conditions. This evidence of phosphatidylserine externalization taken together with the finds towards cytoskeleton actin reorganization demonstrated by Texas red staining strongly indicate that porphyrins **3-PtTPyP** and **4-PtTPyP** induce apoptosis in metastatic melanoma cells *in vitro* after light activation. In addition, the fact that porphyrins **3-PtTPyP** and **4-PtTPyP** treatments did not have an effect in the cell cycle of WM1366 cells could further indicate that the mechanism of growth inhibition of these compounds is linked to apoptosis induction rather than cell cycle arrest. Deregulations in the apoptotic
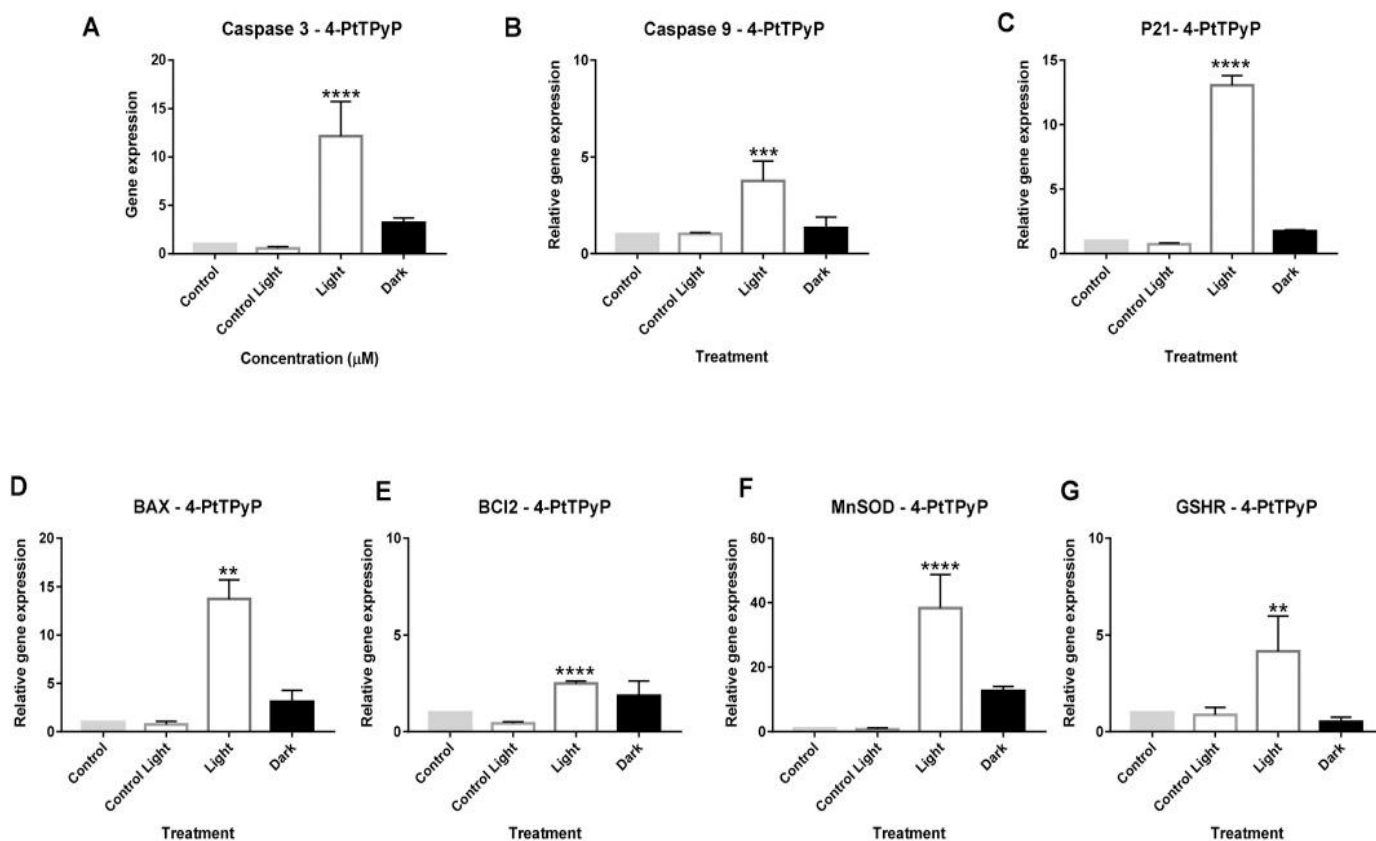
Fig. 9. Platinum(II) porphyrin **4-PtTPyP** increased expression of Caspase 3, Caspase 9, P21, BAX, BCL2, MnSOD and GSHR genes in metastatic melanoma line WM1366 24 h after being submitted to white-light irradiation. The gene expression profile was determined by qRT-PCR and the data were normalized using the GAPDH levels. **4-PtTPyP** had a significant increase in the expression of all evaluated genes when compared to the other groups. (****) denotes $p < .0001$, (***) denotes $p < .0005$, (**) denotes $p < .004$, (*) $p < .04$. when compared to the light and dark group of the same molecule. Three independent experiments were performed in triplicate.

process can generate cellular disorders that are related to several pathologies, such as cancer [31,32]. Thus, the ability to modulate this cellular death mechanism presents great potential in the development of new oncological therapies. Cells undergoing death by apoptosis experience some cellular alterations known as apoptotic hallmarks, that include actin reorganization, phosphatidylserine externalization, chromatin condensation and membrane permeabilization [33].

Our results corroborate with finds in the literature, where the apoptotic activity of different porphyrins as photosensitizers in photodynamic therapy has been demonstrated in several human cell lines, including lung carcinoma [34], tongue squamous carcinoma [35], breast adenocarcinoma [36] and gastric cancer [37]. The mechanisms involved in porphyrin's induction of apoptosis are usually related to increased ROS production and caspase activation [35,36]. Hematoporphyrin monomethyl ether, for instance, caused apoptosis by increased production of intracellular reactive oxygen species as well as caspase 3 activity in human tongue squamous cell carcinoma (Tca8113) after photodynamic therapy [35].

Gene expression profile observed through qPCR in WM1366 cells exposed to platinum(II) porphyrin derivatives followed by white-light activation also indicate induction of programmed cell death by apoptosis, corroborating with results obtained by confocal microscopy and annexin V analysis. Apoptosis intrinsic pathway is related with mitochondrial damage and oxidative stress, both induced by photosensitizer molecules [38]. Initiator and executor caspases involved in this pathway [39] were upregulated in response to porphyrin treatments when compared with negative control group that received only medium. For *meta* isomer **3-PtTPyP** treatment, caspase-9 and caspase-3 expression levels showed a 4.89 and 3.23-fold increase, respectively, while for the *para* isomer **4-PtTPyP**, this change was 3.77 and 12.16-fold, respectively. We also observed an upregulated expression of p21, a

protein well-known by its action in cell cycle arrest in a p53-dependent manner. Despite no cell cycle arrest has been induced by tetra-platinated(II) porphyrins, several authors have reported a direct involvement of p21 in apoptosis induction in a p53-independent mechanism [40].

Mitochondrial permeability and cytochrome *c* liberation, involved in apoptosis intrinsic pathway, are regulated by proteins from Bcl-2 family [39]. We observed an increased expression of both anti-apoptotic and pro-apoptotic regulators, BCL-2 and BAX, respectively, in WM1366 cells treated with porphyrins. However, when we analyzed the BAX/BCL-2 ratio, an up-regulation was observed, indicating a proapoptotic response induced by photodynamic therapy, also in accordance with other analyses performed here. Considering that the Bcl-2 family comprises 25 proteins, and among them, BAX and BCL-2 represent its major members, the ratio BAX/BCL-2 has been used as one of the hallmarks in the apoptotic process as well as a predictive and prognostic marker for cancer treatments [35].

Upregulation of MnSOD expression profile is in accordance with low levels of nitrite and nitrate, molecules that act inactivating this enzyme. High levels of MnSOD are reported as a marker of oxidative stress; direct or indirectly, through ROS detoxification, this enzyme prevents formation of nitrites and nitrates [41]. Unchanged levels of iNOS may be related with cytoskeletal reorganization during apoptosis [42] and also could explain the stable rates observed for NOx. Similarly, oxidative stress is also marked by an increased rate of oxidized glutathione [43], which may explain high levels of glutathione reductase observed in our study as a defense mechanism against cell redox imbalance. Although most of our results are concordant, it is important to highlight that besides transcriptional regulation, several targets that we have evaluated in this study are also subject to post-transcriptional and translational regulations.
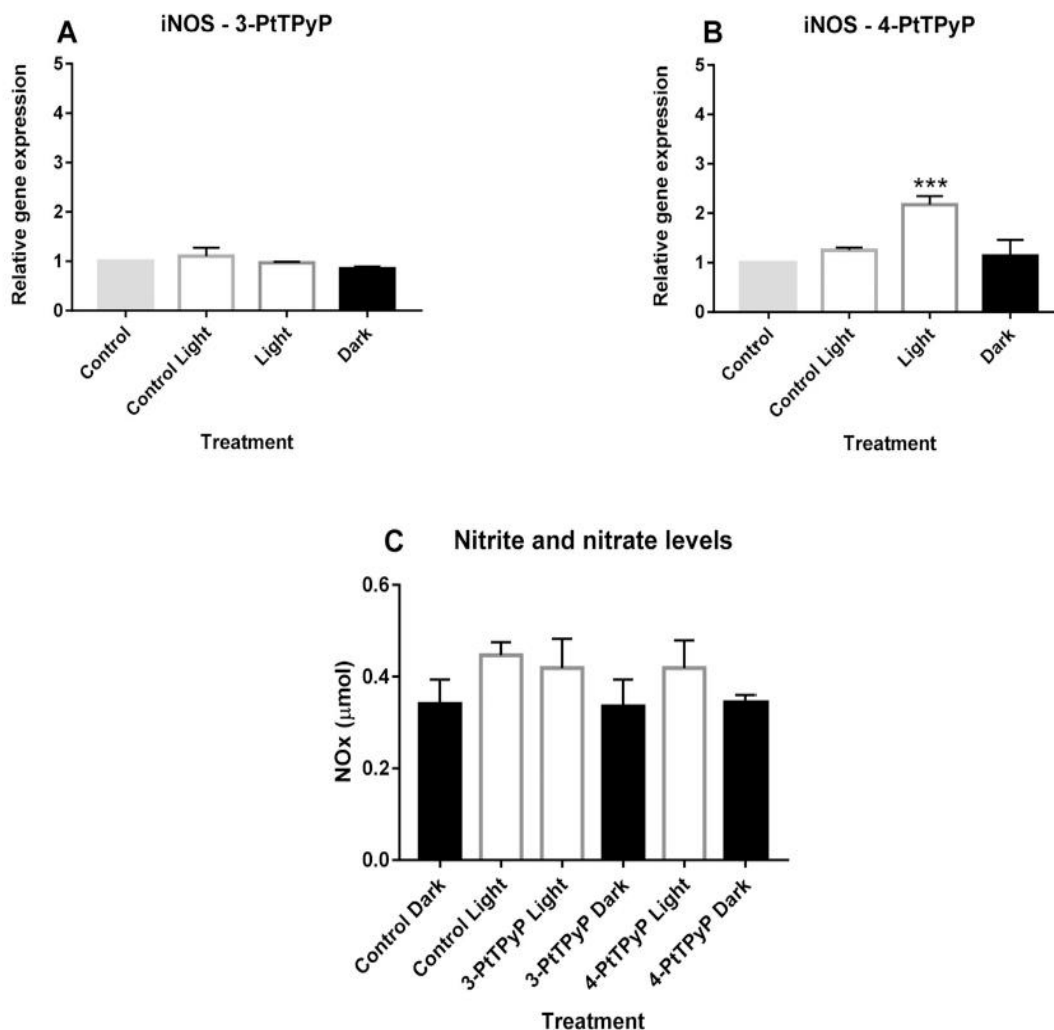
Fig. 10. The platinum(II) porphyrins **3-PtTPyP** and **4-PtTPyP** did not alter the expression of the iNOS gene (Figs. 10A and B) in the metastatic melanoma line WM1366 and did not induce production of nitric oxide in the cell medium (Fig. 10C) 24 h after submitted to white-light irradiation. The concentration tested was that of the IC$_{50}$ of each of the molecules. Data are expressed as mean $\pm$ SD of three independent times, performed in triplicate. There was no significant difference in the light and dark groups.
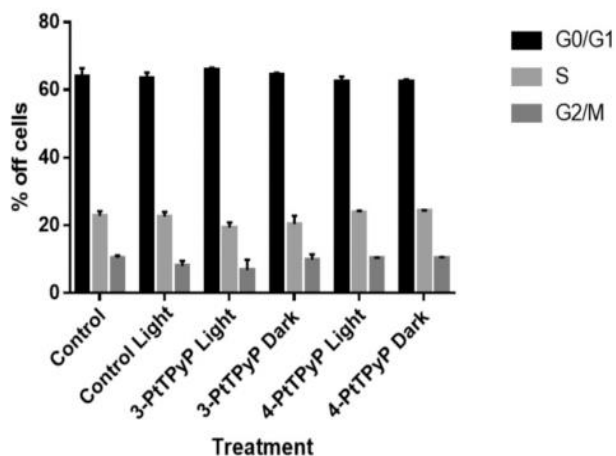

Fig. 11. The platinum(II) porphyrins **3-PtTPyP** and **4-PtTPyP** did not alter the cell cycle. The groups had no significant difference in cell cycle arrest.

5. Conclusion

In this article we investigate possible mechanisms of action involved in the anti-tumor activity of tetra-cationic porphyrins **3-PtTPyP** and **4-PtTPyP**, submitted to white-light irradiation conditions. Our results suggest that both platinum(II) porphyrins induced apoptosis *via*

activation of caspases 3 and 9. This cell death by apoptosis was confirmed by the Annexin V assay. In addition, the reorganization of actin observed in the groups treated with porphyrins corroborates with death by apoptosis. Moreover, the *in silico* study indicated that both platinum (II) porphyrins are promisors as drug-delivery strategy, since they presented affinity to *N*-terminal region of ApoB-100. Additional assays will be performed on different cell lines in order to further extend the application spectrum of platinum porphyrins. Also, modifications in the chemical structure of these porphyrins, as different metallic centers and new platinum derivatives will be studied.

Appendix A. Supplementary Data

Supplementary data to this article can be found online at https://doi.org/10.1016/j.jphotobiol.2019.111725.

References
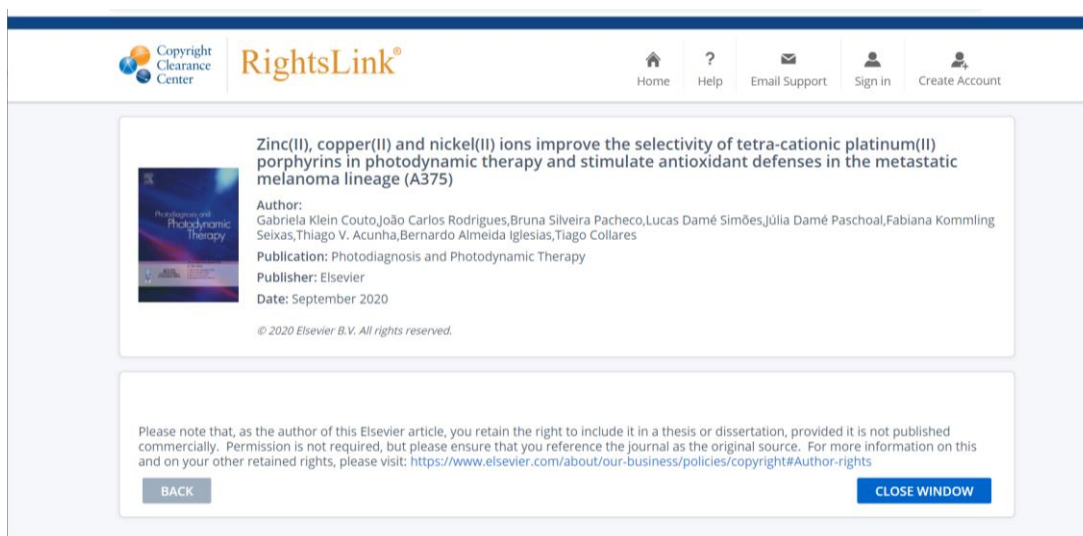
[1] L. Broussard, A. Howland, S. Ryu, K. Song, D. Norris, C.A. Armstrong, P.I. Song, 543135, Chonnam Med. J. 54 (2018) 135–142.

[2] Organização Mundial de Saúde - OMS, Guide To Cancer Early Diagnosis, (2017).

[3] M. Lucia, R. Benitez, C.B. Bender, T.L. Oliveira, K.M. Schachtschneider, T. Collares, F.K. Seixas, *Mycobacterium bovis* BCG in metastatic melanoma therapy, (2019).

[4] G.K. Couto, N.V. Segatto, T.L. Oliveira, F.K. Seixas, K.M. Schachtschneider, T. Collares, The melding of drug screening platforms for melanoma, Front. Oncol. 9 (2019) 1–20.

[5] F. Bray, J. Ferlay, I. Soerjomataram, R.L. Siegel, L.A. Torre, A. Jemal, Global cancer statistics 2018: GLOBOCAN estimates of incidence and mortality worldwide for 36 cancers in 185 countries, CA Cancer J. Clin. 68 (2018) 394–424.

[6] Instituto Nacional do Câncer, Estimativa 2018: incidência de câncer no Brasil / Instituto Nacional de e Câncer José Alencar Gomes da Silva, Coordenação de Prevenção e Vigilância-Rio de Janeiro, INCA, 2018, pp. 1–130.

[7] American Cancer Society, Cancer Facts and Figures 2018, (2018), p. 2018.

[8] S.B. Brown, E.A. Brown, I. Walker, The present and future role of photodynamic therapy in cancer treatment, Lancet Oncol. 5 (2004) 497–508.

[9] R. Saini, C.F. Poh, Photodynamic therapy: a review and its prospective role in the management of oral potentially malignant disorders, Oral Dis. 19 (2013) 440–451.

[10] A.E. O'Connor, W.M. Gallagher, A.T. Byrne, Porphyrin and nonporphyrin photo-sensitizers in oncology: preclinical and clinical advances in photodynamic therapy, Photochem. Photobiol. 85 (2009) 1053–1074.

[11] A.M. Rkein, D.M. Ozog, Photodynamic therapy, Dermatol. Clin. 32 (2014) 415–425.

[12] T.T. Tasso, T.M. Tsubone, M.S. Baptista, L.M. Mattiazzi, T.V. Acunha, B.A. Iglesias, Isomeric effect on the properties of tetraplatinated porphyrins showing optimized phototoxicity for photodynamic therapy, Dalt. Trans. 46 (2017) 11037–11045.

[13] J.A. Naue, S.H. Toma, J.A. Bonacin, K. Araki, H.E. Toma, Probing the binding of tetraplatinum(pyridyl)porphyrin complexes to DNA by means of surface plasmon resonance, J. Inorg. Biochem. 103 (2009) 182–189.

[14] L.M.O. Lourenço, B.A. Iglesias, P.M.R. Pereira, H. Girão, R. Fernandes, M.G.P.M.S. Neves, J.A.S. Cavaleiro, J.P.C. Tomé, Synthesis, characterization and biomolecule-binding properties of novel tetra-platinum(ii)-thiopyridylporphyrins, Dalt. Trans. 44 (2015) 530–538.

[15] A. Naik, R. Rubbiani, G. Gasser, B. Spingler, Visible-light-induced annihilation of tumor cells with platinum-porphyrin conjugates, Angew. Chemie - Int. Ed. 53 (2014) 6938–6941.

[16] E.F.F. and B.A.I. Giovana Basso, Juliana F. Cargnelutti, Amanda L. Oliveira, Thiago V. Acunha, Rudi Weiblen, Photodynamic inactivation of selected bovine viruses by isomeric cationic tetra-platinated porphyrins, J. Porphyr. Phthalocyanines 23 (2019) 1041–1046.

[17] J. Guevara, J. Romo, E. Hernandez, N.V. Guevara, Identification of receptor ligands in Apo B100 reveals potential functional domains, Protein J. 37 (2018) 548–571.

[18] P.M.R. Cruz, H. Mo, W.J. McConathy, N. Sabnis, A.G. Lacko, The role of cholesterol metabolism and cholesterol transport in carcinogenesis: a review of scientific findings, relevant to future cancer therapeutics, Front. Pharmacol 4 (SEP) (2013).

[19] M.R. Hamblin, E.L. Newman, Photosensitizer targeting in photodynamic therapy II conjugates of haematoporphyrin with serum lipoproteins, J. Photochem. Photobiol. B Biol. 26 (1994) 147–157.

[20] R.A. Firestone, Low-density lipoprotein as a vehicle for targeting antitumor compounds to cancer cells, Bioconjug. Chem. 5 (1994) 105–113.

[21] C. Baskaran, M. Ramachandran, Computational molecular docking studies on anticancer drugs, Asian Pacific J. Trop. Dis. 8 (2012) 463–465.

[22] H. Xu, Y. Wang, J. Zhao, P.W. Jurutka, D. Huang, L. Liu, L. Zhang, S. Wang, Y. Chen, S. Cheng, Triterpenes from *Poria cocos* are revealed as potential retinoid X receptor selective agonists based on cell and *in silico* evidence, Chem. Biol. Drug Des. (2019) cbdd.13610, , https://doi.org/10.1111/cbdd.13610.

[23] L.H.Z. Cocca, F. Gotardo, L.F. Sciuti, T.V. Acunha, B.A. Iglesias, L. de Boni, Investigation of excited singlet state absorption and intersystem crossing mechanism of isomeric meso-tetra(pyridyl)porphyrins containing peripheral polypyridyl platinum(II) complexes, Chem. Phys. Lett. 708 (2018) 1–10.

[24] L.Q. Soares Lopes, A.P. Ramos, P.M. Copetti, T.V. Acunha, B.A. Iglesias, R.C. Vianna Santos, A.K. Machado, M.R. Sagrillo, Antimicrobial activity and safety applications of meso-tetra(4-pyridyl)platinum(II) porphyrin, Microb. Pathog. 128 (2019) 47–54.

[25] R.W. Leopardi, E, amigo DS, target cell lysis: ultrastructural and cytoskeletal alterations, J. Immunol. 133 (1984) 3429–3436.

[26] T.K. Garg, J.Y. Chang, Oxidative stress causes ERK phosphorylation and cell death in cultured retinal pigment epithelium: prevention of cell death by AG126 and 15-deoxy-delta 12, 14-PGJ2, BMC Ophthalmol. 3 (2003) 1–15.

[27] I.M. Lee Ju, R. Hosotani, M. Wada, R. Doi, T. Kosiba, K. Fujimoto, Y. Miyamoto, C. Mori, N. Nakamura, K. Shiota, Mechanism of apoptosis induced by cisplatin and VP-16 in PANC-1 cells, Anticancer Res. 17 (1997) 3445–3450.

[28] J.L. Jacques Huot, F. Houle, S. Rousseau, R.G. Deschesnes, G.M. Shah, SAPK2/p38-dependent F-actin reorganization regulates early membrane blebbing during stress-induced apoptosis, J. Cell Biol. 143 (1998) 1361.

[29] Y. Zhao, H.W. Davis, Hydrogen peroxide-induced cytoskeletal rearrangement in cultured pulmonary endothelial cells, J. Cell. Physiol. 174 (1998) 370–379.

[30] H. Zhao, Y. Jiao, Z. Zhang, Deguelin inhibits the migration and invasion of lung cancer A549 and H460 cells via regulating actin cytoskeleton rearrangement, Int. J. Clin. Exp. Pathol. 8 (2015) 15582–15590.

[31] M.O. Hengartner, The biochemistry of apoptosis, Nature 407 (2000) 770–776.

[32] X. Pu, S.J. Storr, Y. Zhang, E.A. Rakha, A.R. Green, I.O. Ellis, S.G. Martin, Caspase-3 and caspase-8 expression in breast cancer: caspase-3 is associated with survival, Apoptosis 22 (2017) 357–368.

[33] S. Elmore, Apoptosis: a review of programmed cell death, Toxicol. Pathol. 35 (2007) 495–516.

[34] D. Sengupta, Z.H. Mazumdar, A. Mukherjee, D. Sharma, A.K. Halder, S. Basu, T. Jha, Benzamide porphyrins with directly conjugated and distal pyridyl or pyridinium groups substituted to the porphyrin macrocycles: study of the photo-sensitising abilities as inducers of apoptosis in cancer cells under photodynamic conditions, J. Photochem. Photobiol. B Biol. 178 (2018) 228–236.

[35] X. Lai, F. Ning, X. Xia, D. Wang, L. Tang, J. Hu, J. Wu, J. Liu, X. Li, HMME combined with green light-emitting diode irradiation results in efficient apoptosis on human tongue squamous cell carcinoma, Lasers Med. Sci. 30 (2015) 1941–1948.

[36] S. Rangasamy, H. Ju, S. Um, D.C. Oh, J.M. Song, Mitochondria and DNA targeting of 5,10,15,20-tetrakis(7-sulfonatobenzo[b]thiophene) porphyrin-induced photo-dynamic therapy via intrinsic and extrinsic apoptotic cell death, J. Med. Chem. 58 (2015) 6864–6874.

[37] J.J. Chen, L.J. Gao, T.J. Liu, Photodynamic therapy with a novel porphyrin-based photosensitizer against human gastric cancer, Oncol. Lett. 11 (2016) 775–781.

[38] A. P., B. K., C. Ka., F. T.H., G. a.W., G. S.O., H. S.M., H. M.R., J. A., K. D., K. M., M. J., M. P., N. D., P. J., W. B.C., G. J, Photodynamic therapy of cancer: An update, CA Cancer J. Clin. Densitom. 61 (2011) 250–281.

[39] S. Goldar, M.S. Khaniani, S.M. Derakhshan, B. Baradaran, Molecular mechanisms of apoptosis and roles in cancer development and treatment, Asian Pacific J. Cancer Prev. 16 (2015) 2129–2144.

[40] M.T. Piccolo, S. Crispi, The dual role played by p21 may influence the apoptotic or anti-apoptotic fate in cancer, J. Can. Res. Updates 1 (2012) 189–202.

[41] D. Candas, J.J. Li, MnSOD in oxidative stress response-potential regulation via mitochondrial protein influx, Antioxid. Redox Signal. 20 (2013) 1599–1617.

[42] D.K, E.R.B. Yunchao Su, Cytoskeletal regulation of nitric oxide synthase, Cell Biochem. Biophys. 43 (2005) 439–449.

[43] M.L. Circu, T.Y. Aw, Glutathione and apoptosis, Free Radic. Res. 42 (2008) 689–706.

[44] A.H. Khan, A. Prakash, D. Kumar, A.K. Rawat, R. Srivastava, S. Srivastava, Virtual screening and pharmacophore studies for ftase inhibitors using Indian plant anticancer compounds database, Bioinformation 5 (2) (2010) 62–66.
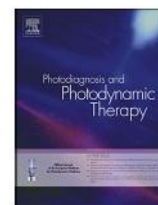
Os resultados que fazem parte desta tese de doutorado estão apresentados sob forma de artigo. Os itens materiais e métodos, resultados, discussão e referências bibliográficas encontram-se no próprio artigo.

4.4 Capítulo 4 (Artigo 4) - **Zinc(II), copper(II) and nickel(II) ions improve the selectivity of tetra-cationic platinum(II) porphyrins in photodynamic therapy and stimulate antioxidant defenses in the metastatic melanoma lineage (A375)**

O artigo foi publicado na revista **Photodiagnosis and Photodynamic therapy. F.I: 2,894**

Zinc(II), copper(II) and nickel(II) ions improve the selectivity of tetra-cationic platinum(II) porphyrins in photodynamic therapy and stimulate antioxidant defenses in the metastatic melanoma lineage (A375)

Check for updates

Gabriela Klein Couto[a], João Carlos Rodrigues Junior[a], Bruna Silveira Pacheco[a], Lucas Damé Simões[a], Júlia Damé Paschoal[a], Fabiana Kommling Seixas[a], Thiago V. Acunha[b], Bernardo Almeida Iglesias[b],*, Tiago Collares[a],*

[a] Molecular and Cellular Oncology Research Group, Cancer Biotechnology Laboratory, Technological Development Center, Federal University of Pelotas, Pelotas, Brazil
[b] Laboratory of Bioinorganic and Porphyrinoid Materials, Chemistry Department, Federal University of Santa Maria, Santa Maria, Brazil

ABSTRACT

Tetra-cationic porphyrins with peripheral Pt (II) -bipyridyl complexes demonstrated a potential as photosensitizers to be used in photodynamic therapy (PDT). First-line transition metals, such as zinc (II), copper (II) and nickel (II), can be incorporated into the porphyrin nucleus, making this molecule more selective and more effective for this therapy in combating to tumor cells, such as metastatic melanoma. We characterized these derivatives to verify the improvement in selectivity of platinum (II) 4-PtTPyP porphyrins. Receptors such as LDL and endothelin (ERT-B) were investigated, as well as the binding affinity of two antioxidants: catalase model enzymes and superoxide dismutase. Human serum albumin (SAH) HSA binding properties have been verified. In addition, we evaluated the antitumor action of such metalloporphyrins in an in vitro cell viability. Our results demonstrated that porphyrins have significant antitumor potential when exposed to white light conditions. The affinity for the LDL receptor was better when compared to platinum porphyrin 4-PtTPyP without addition of metals and the affinity for the endothelin receptor was higher than the control used in this study. Still, the interaction with the HSA showed the possibility of this connection taking photosensitizers to places of interest, such as the delivery of medicines.

1. Introduction

Tetra-cationic porphyrins with peripheral platinum(II)-polypyridyl complexes have been widely studied in order to be applied to the treatment of pathologies such as cancer and have had good results *in vitro* in the treatment of metastatic melanoma [1–4]. Metastatic melanoma that has had an increase in its incidence and worry because it is the most aggressive type of skin cancer, especially when diagnosed late [5]. Platinum(II) derivatives is already present in antineoplastic agents, such as cisplatin, oxaliplatin and carboplatin [6]. Even though be an alternative as a treatment with a high initial response to various types of cancer, some patients end up relapsing with cisplatin-resistant disease and other drugs [7,8]. Associating transition metals with porphyrins such as platinum(II) compounds at the peripheral positions seems to be a good strategy for using them as photosensitizers in

photodynamic therapy (PDT) [2].

Photodynamic Therapy (PDT) appears in this context as an alternative, with less adverse effects, local and more selective action [9]. In our previous study we demonstrated the interesting action of this treatment of metastatic melanoma cells (WM1366) with platinum porphyrins [2]. Using other metals ions coordinated in the porphyrin core with platinum(II)-polypyridyl complexes such as Zn(II), Cu(II) or Ni(II) ions can make these molecules even more effective [10–15].

Studies have shown that zinc(II) derivatives can be a good anti-cancer agent [16–19]. Still, zinc complexes play important roles as radioprotective agents [10,20], photosensitizers for tumors and anti-microbial agents [21]. In this context, zinc(II) ions is interesting to associate with photodynamic therapy due to the preference in generating singlet oxygen – $^1O_2$ (directly involved to the PDT mechanism of action), as it is a full-shell d metal (d^{10} configuration) and with that the

photodynamic processes are not negatively affected [22]. In addition to the reasons already mentioned, due to its homeostatic mechanism - responsible for the entry and exit of zinc(II) species, its distribution and excretion of cells, there are no known changes in the body due to excessive accumulation [23].

On the other hand, nickel(II) porphyrins are d^8 configuration system, so it has a moderate tendency to generate singlet oxygen, but a greater number of radical species, another mechanism involved in PDT (Type I – electron transfer) [24,25]. Still, with respect to transition metals, studies show that copper(II) ions can serve as a limiting factor for multiple aspects of tumor progression, including growth, angiogenesis and metastasis. This factor deserves attention in the current scenario of developing new compounds for the treatment of cancer [26].

Another important aspect in the selection of photosensitizer candidates is the binding to overexpressed receptors in tumor cells, as is the case of the LDL receptor, already described in the previous study of the group [2] and the endothelin receptor that also appears to be overexpressed in tumor cells, such as metastatic melanoma and responsible for cell proliferation, anti-apoptotic action and metastasis [27]. Thus, the objective of this study was to verify, using tetra-cationic platinum (II) porphyrins, the formation of $^1O_2$, preliminary HSA-binding properties, selectivity and, consequently, the antitumor action of platinum (II) porphyrin **4-PtTPyP**, coordinated to the transition metals Zn(II) (**Zn-4-PtTPyP**), Cu(II) (**Cu-4-PtTPyP**) and Ni(II) (**Ni-4-PtTPyP**) metal center ions (Fig. 1).

2. Materials and methods

2.1. Tetra-cationic porphyrin photosensitizers Zn-4-PtTPyP, Cu-4-PtTPyP and Ni-4-PtTPyP

Metalloporphyrins were prepared slightly methodology modification by Hahn da Silveira and co-workers [28] reacting free-base tetracationic **4-PtTPyP** (0.020 g, 0.07 mmol; 1.0 equiv.) with 5.0 equivalents of metal acetate (zinc, copper and nickel), in DMF reflux system (10 mL), for 24 h period time. The solvent was removed in an evaporator and the solid washed with cold distilled water and diethyl ether, recrystallized, filtered and dried in a vacuum desiccators system. Elemental analysis (CHN%) and spectroscopic data (absorption and emission spectra) are presented in the *supplementary information section* (*supplementary information section* – Table S1 and Figs. S1 and S2). All metalloporphyrins tested in this study are soluble in DMSO and stable in this solution (see *supplementary information section* – Figs. S3–S5).

2.2. Irradiation experiments

In the irradiation light conditions, the porphyrins were exposed to white-light lamp source (400–800 nm range, consisting of a 100 W LED lamp system) with a fluence rate of 50 mW/cm^2, for 30 min (total light dose of 45 J/cm^2), according to a method in the literature [2].

2.3. Photostability and $^1O_2$ generation

The photostability of metalloporphyrins **Zn-4-PtTPyP**, **Cu-4-PtTPyP** and **Ni-4-PtTPyP** ([] =2.0 μM each) was determined by

M = Zn(II): Zn-4-PtTPyP
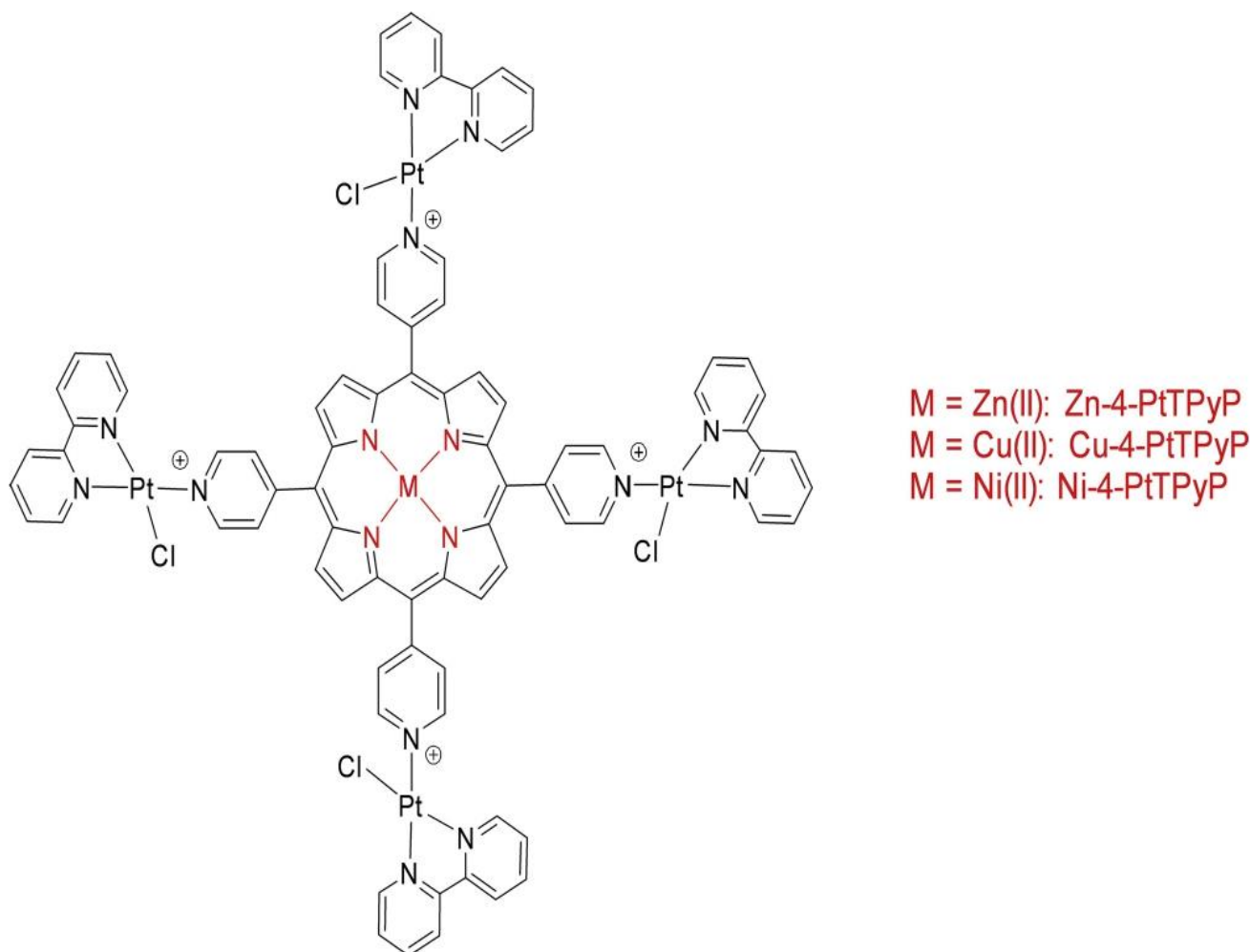M = Cu(II): Cu-4-PtTPyP
M = Ni(II): Ni-4-PtTPyP

Fig. 1. Representative molecular structures of Pt(II) metalloporphyrins used in this study. The counter-ion hexafluorophosphate (PF$_6$⁻) was omitted for more clarity.

measuring the absorbance at Soret band in DMSO(2 %)–phosphate-buffered saline (PBS) mixture solution before and after white-light LED lamp irradiation (100 W; 400–800 nm) at fluence of 50 mW/cm^2 for 30 min.

For the determination of $^1O_2$ production, solutions containing 1,3-diphenylisobenzofuran (DPBF) (20 μM) with or without metalloporphyrins at 2.0 μM were prepared in dimethylformamide (DMF) solution in a 1.0 cm × 1.0 cm quartz cuvette. The solutions were irradiated at room temperature and under gentle magnetic stirring, with a red-light LED array system (λ = 635 nm) at fluence of 26 mW/cm^2 for 600 s (total light dose of 7.8 J/cm^2), monitoring the decrease in absorbance at 416 nm (photo-oxidation of DBPF scavenger). All experiments were performed in duplicate and independently.

2.4. Cell culture and reagents

The A375 cell line and a non-tumor cell line derived from the human skin fibroblast (HFF-1), were obtained from the Rio de Janeiro Cell Bank (PABCAM, Federal University of Rio de Janeiro, RJ, Brazil). They were grown in Dulbecco's Modified Eagle's Medium (DMEM) supplemented with 10 % fetal bovine serum (FBS) for A375 cell line and High-glucose Dulbecco's Modified Eagle's Medium (DMEM) supplemented with 15 % fetal bovine serum (FBS), respectively, obtained from Vitrocell Embriolife (Campinas, Brazil) and Gibco (Grand Island, NY, USA). Cells were grown under controlled atmosphere at 37 °C, 95 % humidity and 5 % CO$_2$.

2.5. Experimental groups and photodynamic assay

The cells were divided into two distinct groups: light and dark conditions. Each group was treated with six different concentrations (1.75, 3.5, 7.0, 14.0, 28.0 e 56.0 nM) of the three platinum(II) porphyrins, **Zn-4-PtTPyP**, **Cu-4-PtTPyP** and **Ni-4-PtTPyP**. After adherence of the cells to the wells, they were divided into separate groups and treated with the different concentrations previously presented of the proposed compounds. As these compounds are activated by the incidence of light, these were divided into two groups (light and dark), where the light group was activated by phototherapy according to protocol established by Couto et al. 2020 [2].

2.6. Cell proliferation assay

A375 cell were seeded in 96-well culture plates at a density of 2.0 × 10^4/well (200 μL/well) with different concentrations of the molecules. The negative control consisted in 200 μL/well of medium, and the control of the vehicle in 200 μL/well of medium and DMSO (with concentration less than 0.5 %). Cell proliferation was evaluated 24 h after the activation of the compounds by the light irradiation. After the incubation period, the MTT salt (tetrazolium salt [3-(4,5-dimethylthiazol-2-yl)-2,5-diphenyltetrazolium bromide]) was added to each well (5.0 mg MTT/mL). Then, absorbance was measured using a spectrophotometer (Thermo Plate TP-Reader) at a wavelength of at 495 nm. Percent of growth inhibition was determined by the Eq. 1:

$$\% \ inhibition = (Abs_{492} \ treated \ cells \ / \ Abs_{492} \ control \ cells) \times 100 \tag{1}$$

2.7. HSA-binding properties of metalloporphyrins

The interaction of HSA with the metalloporphyrins **Zn-4-PtTPyP**, **Cu-4-PtTPyP** and **Ni-4-PtTPyP** was studied by steady-state fluorescence emission at room temperature (298 K) in a Tris-HCl buffer solution (pH 7.4). A stock solution was prepared in DMSO (≈ 10^{-6} M range) and successive aliquots of each porphyrin added into the HSA solution (10 μM) in order to get concentrations ranging from 0 to

100 μM. The samples were excited at λ = 290 nm and the fluorescence emission evaluated in the range of 300–550 nm. The inner filter effect of each metalloporphyrin was considered in the HSA-binding assays. Generally, fluorescence quenching can occur by static or dynamic mechanisms, and the fluorescence quenching experiments data analyzed using the Stern–Volmer Eq. 2:

$$\frac{F_0}{F} = 1 + k_q \tau_0 [Q] = 1 + K_{SV} [Q] \tag{2}$$

where F_0 and F are the fluorescence intensities in the absence and presence of the quencher, whereas K_{SV}, k_q, τ_0 and $[Q]$ denote the Stern–Volmer constant, the bimolecular quenching rate constant, the fluorescence lifetime of HSA ($\tau_0 = 5.67 \times 10^{-9}$ s) [29] and the concentration of quencher, respectively. According to Eq. 2, the Stern-Volmer constant (K_{SV}) was calculated from the slope and k_q is equal to K_{SV}/τ_0.

For static fluorescence quenching mechanism, it is expected lower k_q values with increasing temperatures since the stability of the complex tend to decrease whilst the opposite effect is expected for the dynamic fluorescence quenching mechanism Diffusion-controlled quenching typically results in values of $k_{diff} \approx 7.40 \times 10^9$ M^{-1}s^{-1}, according to Smoluchowski-Stokes-Einstein theory at 298 K, which is considered to be the largest as possible value in aqueous solution for macromolecules [30]. Smaller k_q values can result from steric shielding of the Pt(II)-metalloporphyrins, and larger apparent k_q values usually indicate some type of binding interaction.

In order to estimate the association constant value (K_a) and the number of binding sites (n) the double logarithmic approximation was applied, as represented by Eq. 3:

$$\log\left(\frac{F_0 - F}{F}\right) = \log K_a + n \log [Q] \tag{3}$$

where F_0 and F represent fluorescence intensities in the absence and presence of the quencher, respectively, and $[Q]$ the concentration of the porphyrin. According to Eq. 3, the K_a value can be calculated from the intercept (linear coefficient) of the plot, while n value is given by the slope.

Moreover, the standard Gibbs free-energy (ΔG°) of metalloporphyrin-HSA adducts was calculated from the values of K_a using the Eq. 4:

$$\Delta G^\circ = -RT \ln K_a \tag{4}$$

where R and T is the gas constant (1.987 kcal/K mol) and the temperature (298 K), respectively.

2.8. Molecular docking

The porphyrins **4-PtTPyP**, **Zn-4-PtTPyP**, **Cu-4-PtTPyP** and **Ni-4-PtTPyP** molecular structure were created in 2D by the ChemDraw software (PerkinElmer ChemOffice 2018), converted into 3D ligands by the Molecular Operating Environment software [31] where the Quick-Prep tool was used to correct the bonds of the molecule atoms and add hydrogens. Their charges were assimilated in each atom and the structure had its energy minimized by MMFF94x, gradient: 0.01. Molecular coupling was performed using GOLD 5.5 software [32]. Where all the water was removed and hydrogen atoms were added to the receptors according to the program. The active site of each receptor was defined based on the position of the Co-crystallized ligands, and was given a distance of up to 15 Å from the initial position of the ligand due to the size of our molecules. The results of the best connections were obtained through the values of "fitness" (fitness plp), in which the higher the value, the better the interaction with the complexes is defined. For this work, the ChemPLP algorithm was used, which has already proved to be one of the most reliable algorithms in the program [33]. The images generated from the best poses were created using the Discovery Studio 2019 software [34] and the Schröndinger Maestro

software [59].

In this work we evaluate the connection of metalloporphyrins to Apolipoprotein B-100 (APOB-100), Endothelin receptor (ERT-B), Superoxide dismutase (SOD), Catalase (CAT) and Human Serum Albumin (HSA). For APO B-100 we validate the results obtained by docking, an LDL analogue was used, in which it binds at the APO B-100 site causing it to trigger the binding cycle in the membrane LDL-R. The analogue chosen was B0582 [35] which was modeled after the previous work [2].

For ERT analysis, select the use of the endothelin B receptor (ETR-B), which is already showing the important route of cell proliferation of metastatic melanoma [36]. To evaluated the receptor ERT-B, the crystallographic structure of the human B endothelin receptor with endothelin-3 in its complex was used. The crystallized structure was removed from the Protein Data Bank (PDB code: 6IGK) [37]. For validation, we use the fitness value of crystallized Endothelin 3 as a benchmark of success and compare it with that of our molecules together with the connection of similar amino acids between them. For evaluated the HSA protein, we use the HSA crystallographic structure obtained from the Protein Data Bank website (PDB code: 1N5U) was used [38]. As a form of control, the redocking technique was used using the crystallized structure of the protoporphyrin IX in which there was already in the structure, the fitness result of the redocking was noted and will be used for comparison with the result of our molecules. According to Chaves and co-authors (2019), one of the best sites of HSA for platinum(II) porphyrin **4-PtTPyP** would be the subunit IB, so we use this HSA subunit as an active site for this study [39].

Finally, to analyze the impact of our molecules on oxidative stress, we chose the proteins Superoxide Dismutase I (hSOD1) and the human red cell catalase (CAT). The crystallized structures were removed from the Protein Data Bank in which the code 5YTO [40] was used for hSOD1 and the code 1DGF for CAT [41].

2.9. Statistical analysis

Data are presented as mean and standard deviation (SD). Comparative analyzes were performed using one-way analysis of variance (ANOVA). Tukey's post hoc method was employed for multiple comparisons. All statistical analyzes were performed with GraphPad Prism and $p < 0.05$ was considered statistically significant.

3. Results

3.1. Platinum(II) metalloporphyrins

Free-base **4-PtTPyP** and metallo-derivatives **Zn-4-PtTPyP**, **Cu-4-PtTPyP** and **Ni-4-PtTPyP** were prepared by synthetic methodology as described previously [28,42]. Novel metalloporphyrins contain Zn(II), Cu(II) and Ni(II) metal center ions were characterized by standard characterization methods (see *supplementary information section*).

3.2. Photostability and singlet oxygen production assays

It is of interest to know if these molecules are photostable and if they generate reactive oxygen species (ROS) [43–49]. For this, photostability and $^1O_2$ generation experiments were performed for metalloporphyrins **Zn-4-PtTPyP**, **Cu-4-PtTPyP** and **Ni-4-PtTPyP**. The photostability behavior of metalloporphyrins was studied by monitoring the decrease of absorbance of Soret bands, after different times of white-light LED lamp irradiation (visible range), delivered by an illumination system at a fluence rate of $50\,mW/cm^2$. In DMSO(2 %)–PBS mixture solution both metallo-derivatives **Zn-4-PtTPyP**, **Cu-4-PtTPyP** and **Ni-4-PtTPyP** at a concentration of 2.0 μM showed high to moderate photostability over the investigated irradiation period (30 min; Fig. 2).

The ability of porphyrins **Zn-4-PtTPyP**, **Cu-4-PtTPyP** and **Ni-4-PtTPyP** to generate $^1O_2$ in DMF solution was determined using a

photochemical method with DPBF as the $^1O_2$ scavenger. Porphyrin derivative *meso*-tetrakis[(4-*N*-methylpyridyl)porphyrinate]zinc(II) (**ZnTMePyP**) was used as reference. Metalloporphyrins at a concentration of 2.0 μM were able to photo-oxidize DPBF at a concentration of 20 μM (Fig. 3). Porphyrin **Zn-4-PtTPyP** was the best generator of $^1O_2$, following by **Ni-4-PtTPyP** and **Cu-4-PtTPyP**, after 30 min of red-light irradiation ($\lambda = 635\,nm$). At this concentration, metalloporphyrins decompose between 5–35 % range of DPBF, respectively. **Zn-4-PtTPyP** derivatives have a similar photo-oxidation effect on DPBF when compared to the corresponding reference **ZnTMeTPyP**, but much more effective than Ni(II) and Cu(II) porphyrins. The ability of these compounds to photo-oxidize DPBF decreases in the order **ZnTMePyP** ≈ **Zn-4-PtTPyP** > **Ni-4-PtTPyP** > **Cu-4-PtTPyP**. The good photostability and ability to generate $^1O_2$ after being exposed to light irradiation and oxygen allowed us to envisage them as potential photodynamic sensitizers.

3.3. Zinc and nickel associated with platinum (II) porphyrins decrease cell viability and proliferation in PDT

After exposure to phototherapy the porphyrins **Zn-4-PtTPyP**, **Cu-4-PtTPyP** and **Ni-4-PtTPyP**, they inhibited the cell growth of the A375 strain in most of its concentrations, drawing attention to porphyrins coordinated with zinc(II) and nickel(II) (Fig. 4B and F). It was also possible to observe (Fig. 4A, C and E) that the same porphyrins in the dark group had a low inhibition in cell proliferation (all below 50 %). It is also important to note that the vehicle in which the porphyrins were solubilized (DMSO) was not toxic to the cells. In addition, we calculated the IC_{50} of **Zn-4-PtTPyP** and **Ni-4-PtTPyP** porphyrins (Table 1) noting that the concentrations were on the nanomolar scale. It was not possible to calculate the IC_{50} of Cu(II)-porphyrin due to its action, in the tested concentrations, reaching a maximum of around 60 % inhibition.

3.4. Zinc(II), nickel(II) and copper(II) ions coordinated with tetra-cationic platinum(II) porphyrin have affinity for APO B-100 and endothelin receptors

In a previous study, we demonstrated the affinity, and thus, possible selectivity of platinum(II) porphyrins for the APO B-100 receptor overexpressed in tumor cells [2,50]. The porphyrin **4-PtTPyP** showed a lower fitness than the other porphyrin tested. One of the reasons that made us associate other transition metals to it, in order to better this interaction with the receiver. When zinc and nickel metals are included, this value is better, especially with the inclusion of zinc(II) ions in the porphyrin core (Table 2), fitness reached 87.6885. The compound **Zn-4-PtTPyP** located in a region of the site with its highest value, obtained 4 amino acid bonds in common with B0582 (LDL analog). In addition, we included in this study an evaluation of the molecular photosensitizer ALA (aminolevulinic acid) standard in photodynamic therapy and also used to treat other types of cancer in this same therapy [51]. The results showed a fitness plp of 40.1348, apparently this molecule does not demonstrate a good interaction with the protein in question. Several tests were carried out with no changes significant between them. These bindings can be seen in Fig. 5.

Another receptor that we addressed in this study was the endothelin receptor B (ETR-B). The evaluation of this receptor is important, since the endothelin (ET) and ETR comprise the ET axis, and it has a tumor-promoting role in a variety of tumors, including metastatic melanoma [36]. Biological effects mediated by the ET axis: tumor growth induction, anti-apoptotic effects, increased invasion and metastasis [52]. In addition, ETR-B appears to be overexpressed in metastatic melanoma [27].

We therefore chose the ETR-B receptor and endothelin 3 (ET3), as studies have shown that the induction, development, proliferation and migration of precursor melanocytic cells depend on the interaction of ET3 and ETR-B [36]. Our results show that the amino acid most
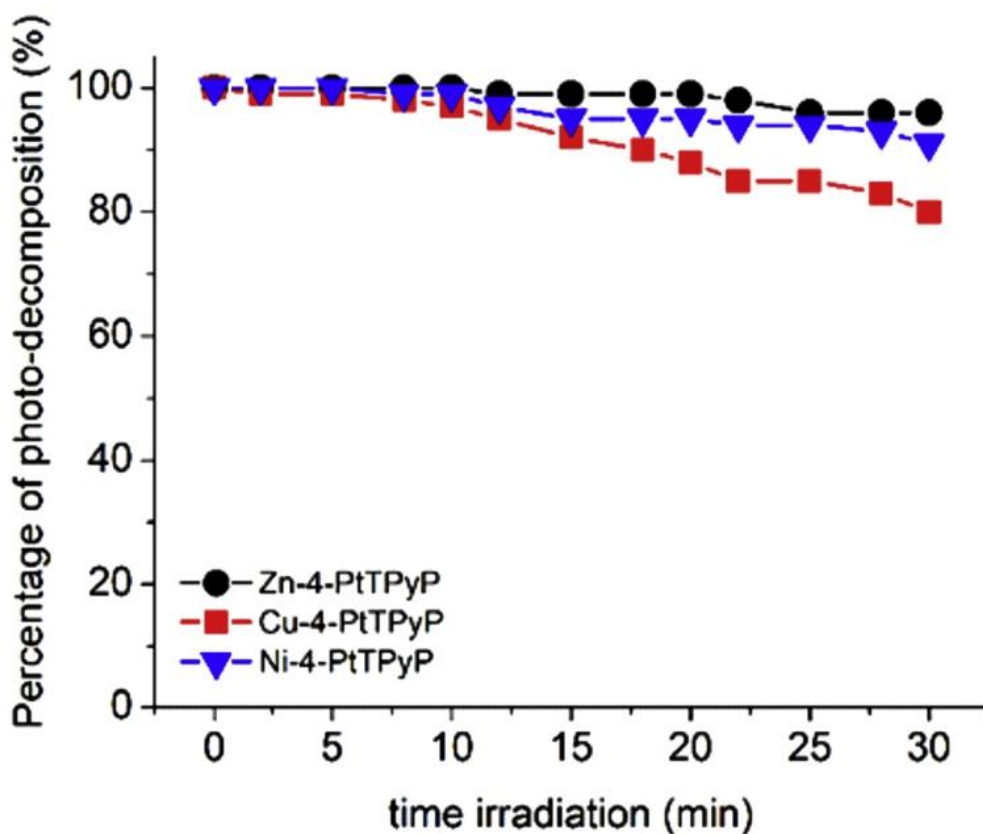
Fig. 2. Photostability of metalloporphyrin derivatives **Zn-4-PtTPyP**, **Cu-4-PtTPyP** and **Ni-4-PtTPyP**, after irradiation with white-light LED lamp source (100 W; 400-800 nm) at a fluence rate of 50 mW/cm^2 for different periods of time (0–30 min).
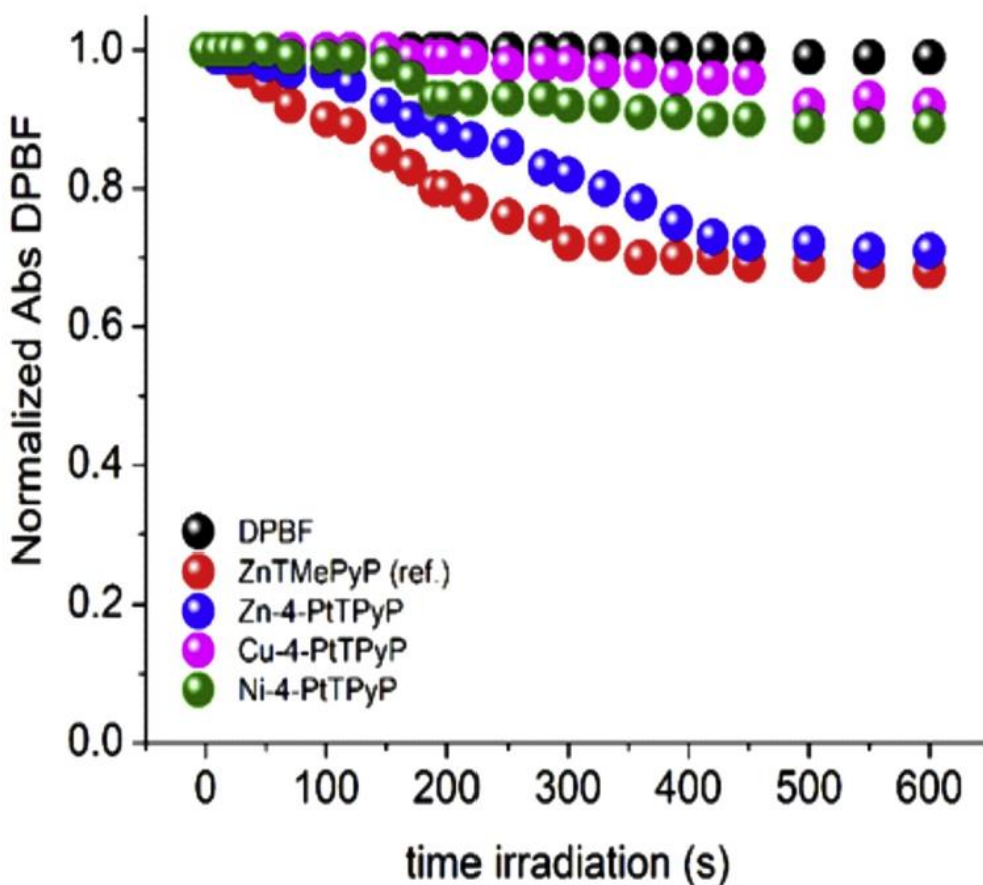
Fig. 3. DPBF photo-degradation assay (20 μM) in DMF solution with or without metalloporphyrin derivatives at 2.0 μM, after red-light irradiation (LED array system) at a potency of 26 mW/cm^2. The DPBF absorbance was recorded at 416 nm.
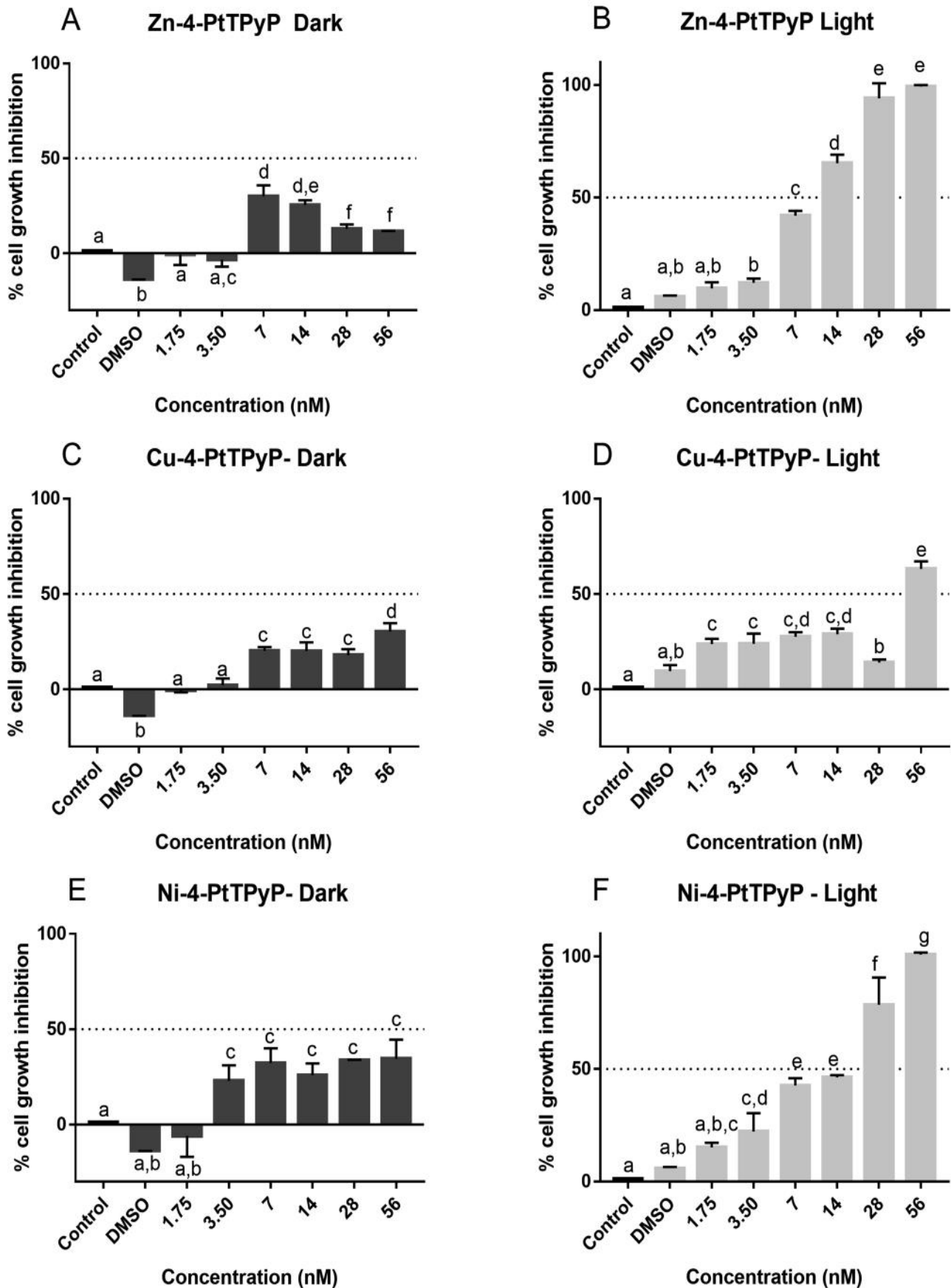
Fig. 4. Effect of light action on photosensitizing molecule on cell proliferation. Porphyrin-treated and untreated cells were irradiated for 30 min. Dark group went totally in the dark for the same time. Comparisons were made within the white-light and dark groups, separately, for each porphyrin. Control group received no treatment with porphyrins. DMSO was the vehicle used to solubilize porphyrins. Data are expressed as mean ± SD of three independent times performed in triplicate. Fig. 4B, D and F: A375 cell line was treated with **Zn-4-PtTPyP** (Fig. B), **Cu-4-PtTPyP** (Fig. D) and **Ni-4-PtTPyP** (Fig. F) and platinum (II) porphyrins at 6 different concentrations and exposed at photodynamic therapy, for 30 min. Fig. 4A, 4C and 4E: A375 cell line was treated with **Zn-4-PtTPyP** (Fig. A), **Cu-4-PtTPyP** (Fig. C) and **Ni-4-PtTPyP** (Fig. E) and platinum(II) porphyrins at 6 different concentrations, but the groups were kept in the dark. For this evaluation we used the MTT technique. For comparison different letters in the chart denote significant difference between the groups. $p < 0.05$ was considered significant.

Table 1
IC$_{50}$ values of porphyrins **Zn-4-PtTPyP** and **Ni-4-PtTPyP** after 24 h of white-light exposition against A375 line.

Porphyrin	IC$_{50}$ (nM)
Zn-4-PtTPyP	8.89 ± 0.87
Ni-4-PtTPyP	11.03 ± 2.10

common among all bonds actually is ILE94, which are shown in all tests. It is also possible to note that the **Zn-4-PtTPyP** and **Cu-4-PtTPyP** porphyrins seem to be attracted by the amino acid proline, interacting in 3 and 2 cases, respectively, with an aptitude plp of 87.3270 and 85.8910, respectively. The nickel molecule, on the other hand, shares more common bonds with ET3 with an aptitude plp of 86.2139. Both values were superior to the connection of the ETR-B receptor with the ET3, which was 59.1418 and, in this context, it was used as a control (Table 3). The connections can be seen in Fig. 6.

3.5. Zinc(II), copper(II) and nickel(II) ions coordinated with tetra-cationic platinum(II) porphyrin increase antioxidant power with increased interaction with enzyme CuZn-SOD (SOD1)

When we investigated the antioxidant action of our tetra-cationic metalloporphyrins with [Pt(bpy)Cl]$^+$ units, we observed a strong connection with the active site of the enzyme CuZn-SOD (SOD1) - region B- fitness plp with nickel(II) porphyrin **Ni-4-PtTPyP** reached 94.1585 while that of zinc(II) derivative **Zn-4-PtTPyP** 97,0192 expressive values, about 79 % more than the connection with the control, which was 54.4633 fitness plp. Although copper(II) porphyrin **Cu-4-PtTPyP** had a lower fitness plp (68.9688), it still had a value 26 % higher than that of the control (crystallographic molecule) (Table 4).

In parallel to the results of SOD1, we evaluate binding of porphyrins to catalase (CAT) in its reduced form, that is, we use only one protein A chain. It results in a relatively lower fitness plp than our control (87.2729), 70.1889, 65.5986 and 78.5041 for zinc(II), copper(II) and nickel(II) porphyrins, respectively (Table 5).

3.6. HSA-binding assays with metalloporphyrins

Interactions between molecules and macromolecules such as proteins can be investigated by emission fluorescence studies. As a result of their interaction, fluorescence quenching, molecular reorganizations, and energy transfer processes can be occurred [53]. The main responsible for the HSA intrinsic fluorescence is its tryptophan residue (single unit), located in the subdomain IIA [37].

The fluorescence emission from HSA is usually obtained exciting the protein at λ_{exc} =290 nm due to the high contribution of tryptophan residues (Trp^{214}). As example, Fig. 7 shows the fluorescence emission spectra of HSA without and in the presence of successive additions of metalloporphyrin **Zn-4-PtTPyP**, **Cu-4-PtTPyP** and **Ni-4-PtTPyP**. The HSA solution presents a strong fluorescence emission peak around 340 nm and the quenching of this fluorescence peak can be used to investigate the interaction of albumin with the metalloporphyrin

derivatives.

In this assay, the fluorescence emission intensity of HSA decreased gradually upon increasing the concentrations of derivatives in the albumin solution indicating that the metalloporphyrin derivatives interacts with the protein. The quenching of the HSA fluorescence can be induced by different mechanisms [54], which are in general classified in dynamic, static or combined quenching mechanisms. The behavior of the fluorescence quenching mechanism induced by the metalloporphyrin **Zn-4-PtTPyP**, **Cu-4-PtTPyP** and **Ni-4-PtTPyP**, was examined using the well-known Stern–Volmer Eq. 2 (see Experimental section). The results have shown a good linear relationship and the Stern-Volmer quenching and bimolecular rate constants (K_{SV} and k_q) at room temperature (298 K) were calculated for the HSA-porphyrin complex. The results shown in Table 6 clearly indicate that the quenching occurs by static collision quenching mechanism (k_q values are higher than k_{diff}) upon association of HSA with a metalloporphyrin in the ground state.

The association constant K_a and the number of binding sites (n) values were calculated using Eq. 3 (see Experimental section). The number of the binding sites for each metalloporphyrin and HSA was observed in the range between 1.10–1.60, indicating that in addition to the tryptophan residue, other residues may have a contribution in this interaction, probably are interacting with different binding sites of HSA, or by different modes, where can occupy more than one subdomain at the same time, mainly due to the large volume of the tetra-cationic metalloporphyrin molecules under study. Moreover, the K_a association constants determined by the fluorescence quenching experiments showed a good correlation with the K_{SV} data (both constants are in the same or close order of magnitude), suggesting that the porphyrins can interact with human serum albumin, but probably present weak binding ability [29]. The thermodynamic analysis via ΔG° values (negative values), indicated that all porphyrins tend to form a more or less stable adduct with HSA, especially the tetra-cationic porphyrins presenting [Pt(bpy)Cl]$^+$ units and different metal center coordinated into the porphyrin core.

3.7. Zinc(II),copper(II) and nickel(II) ions coordinated with tetra-cationic platinum(II) porphyrin increase binding to human serum albumin (HSA)

We evaluated the binding potential of tetra-cationic platinum(II) metallo-derivatives coordinated with the transition metals as zinc(II), copper(II) and nickel(II) ions in possible binding processes to human serum albumin (HSA) due to the possibility of this protein transporting molecules throughout the body. We can observe that, by adding zinc (II), nickel(II) and copper(II) compounds, we obtained fitness plp of 100.7534, 102.3533 and 100.1382, respectively, and both values were higher than free-base porphyrin **4-PtTPyP** (99.3098). In this molecular arrangement, we use the IB region in the HSA protein (Table 7).

Theoretical calculations through molecular docking approach are widely used to model the interaction between a target molecule and macromolecule. This provides important information that may increase interest in experimental studies at a molecular level [29]. Thus, in order to analyze the main intermolecular interactions between each studied compound and the amino acid residues present in the interaction cavity located in site IB (the main binding site suggested by drug-binding

Table 2
Anchor Results of APO B-100 E LDL Receptor Molecules.

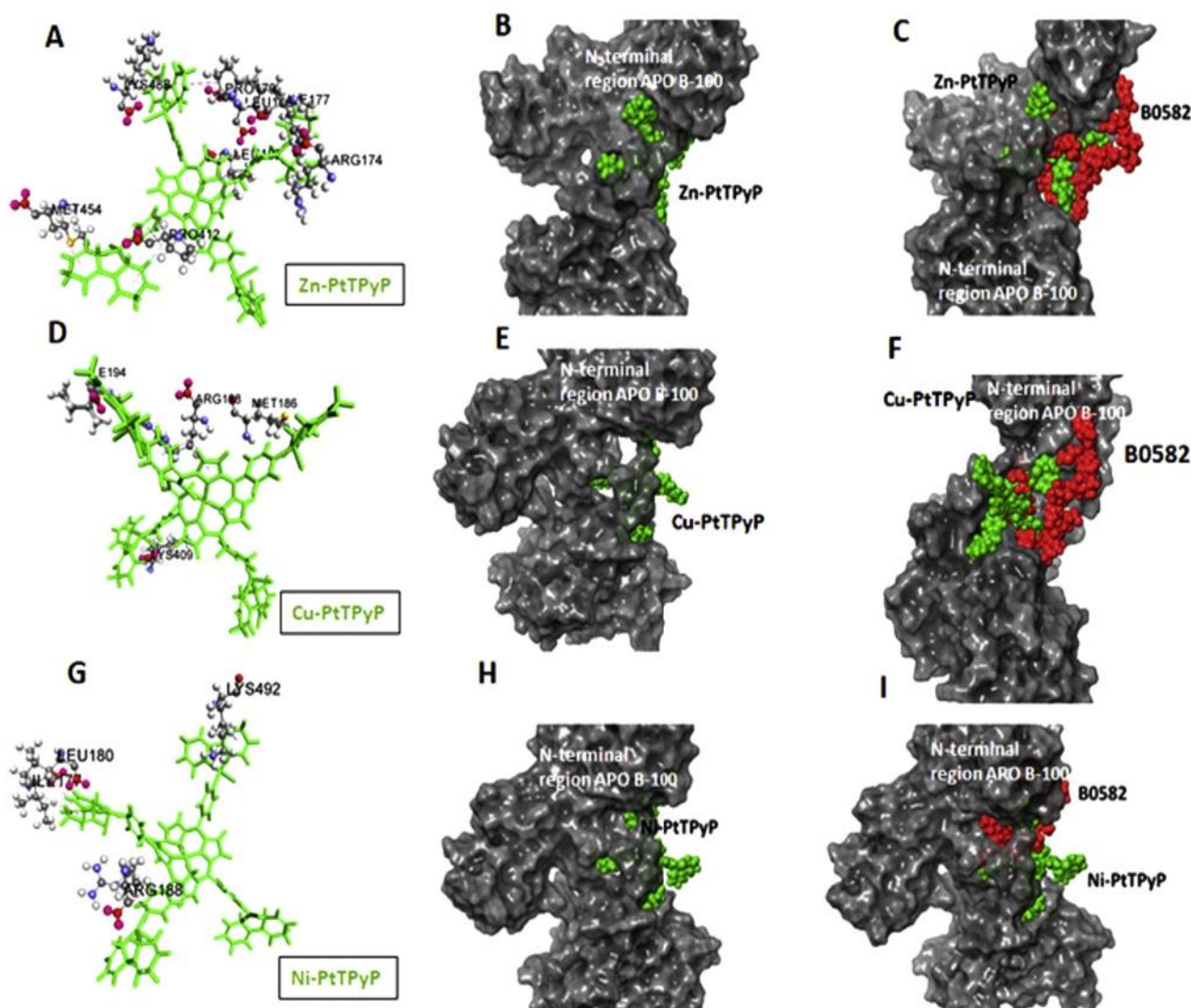| Porphyrin/Protein	Amino acid residues	Fitness plp	Common amino acids with B0582
B0582/ Apo B-100	ASP168, PRO172, ARG174, LEU182, LYS184, LYS409, PRO412, LYS462, LYS488, LYS492.	93.2881	–
4-PtTPyP/ Apo B-100	ASP168, ARG169, LYS171, PRO172, LYS409, PRO412.	68.5542	ASP168, PRO172, LYS409 e PRO412
Zn-4-PtTPyP/ Apo B-100	ARG174, ILE177, LEU179, ALA18, LEU182, PRO412, MET454, LYS488,	87.6885	ARG174, LEU182, PRO412, LYS488
Cu-4-PtTPyP/ Apo B-100	MET186, ARG188, ILE194, LYS409	62.8786	LYS409
Ni-4-PtTPyP/ Apo B-100	ILE177, LEU180, LEU188, LYS492	69.1085	LYS492
Aminolevulinic Acid (ALA) / Apo B-100	LYS171	40.1348	–

Fig. 5. A-I – Image of the molecular arrangement of **Zn-4-PtTPyP**, **Cu-4-PtTPyP** and **Ni-4-PtTPyP** porphyrins with the AP-B-100 N-terminal region. In A, D and G we observe the 3D structure of platinum(II) porphyrins with zinc(II), copper(II) and nickel(II), respectively, and their bindings with amino acids. In B, E and H we observe the coupling of porphyrin with zinc(II), copper(II) and nickel(II), respectively and the N-terminal region of Apo B-100. In C, F and I, we can see that the coupling between B0582 and the Apo B-100 region occurs in a similar way to that of zinc(II), copper(II) and nickel(II), respectively derivative. We can observe that the coupling between B0582 and the Apo B-100 region occurs in a similar way to that of zinc(II), copper(II) and nickel(II).

Table 3
Anchor Results of ET3 and ETR-B Receptor Molecules.

Protein/Porphyrin	Amino acid residues	Fitness plp	Common amino acids with ET3
ETR-B + ET3	ILE94, LYS161, TYR247, TYR251, ILE254, LEU256, ARG343, GLN352, LEU361, LEU365	59.1418	–
ETR-B + Zn-4-PtTPyP	PRO87, PRO93, ILE94, PRO178, PHE240, CYS255, ARG343, LEU347	87.3270	ILE94
ETR-B + Cu-4-PtTPyP	PRO89, ILE94, LEU252, ILE254, LEU257, PRO259, LYS273	85.8910	ILE94, ILE254
ETR-B + Ni-4-PtTPyP	ILE94, TYR247, LEU256, VAL260, ALA270	86.2139	ILE94, TYR247, LEU256

displacement described above), molecular docking calculations were performed.

The superposition of the best docking pose for each metalloporphyrin in site IB (Fig. 8) suggests that although both porphyrins present high volumes, they can be accommodated in this protein pocket. Molecular docking results suggested H-bonding and hydrophobic interactions as the main binding forces involved in the interaction between HSA and each metalloporphyrin (Table 8). Regarding specifically the type of bond of each of the porphyrins, we have that **Zn-4-PtTPyP**, had a large part of its intermolecular interactions based on hydrophobic interactions, having a hydrogen bond made by the SER517 residue at a distance of 2.94 Å. As for **Cu-4-PtTPyP**, most of its intermolecular interactions were based on hydrophobic interactions and on the donation of hydrogen molecules to the oxygen atoms of the amino acid residues.

The amino acids received hydrogens from a heterocyclic region. Residues TYR138 and ASN429 formed bonds with a distance of 3.17 and 1.86 Å, residue ASP187 received two hydrogens thus forming two bonds with distances of 2.56 and 2.61 Å. As well as **Ni-4-PtTPyP**, which also had a large part of its intermolecular interactions, hydrophobic interactions and the donation of hydrogen molecules to oxygen atoms of amino acid residues. Amino acids receive hydrogens from a heterocyclic region. Residues LEU115, ARG117 and GLU425 form connections with distances of 2.05, 2.33 and 2.96 respectively. The common position of coupling for HSA with metalloporphyrins is shown in Fig. 9. For instance, for the zinc(II) derivative **Zn-4-PtTPyP**, the guanidinium group in the amino acid residues Arg-113, Arg-116, and Arg-196 interacts via electrostatic forces with the porphyrin structure within distance of 3.40, 3.70 and 2.30 Å, respectively. On the other hand, one of
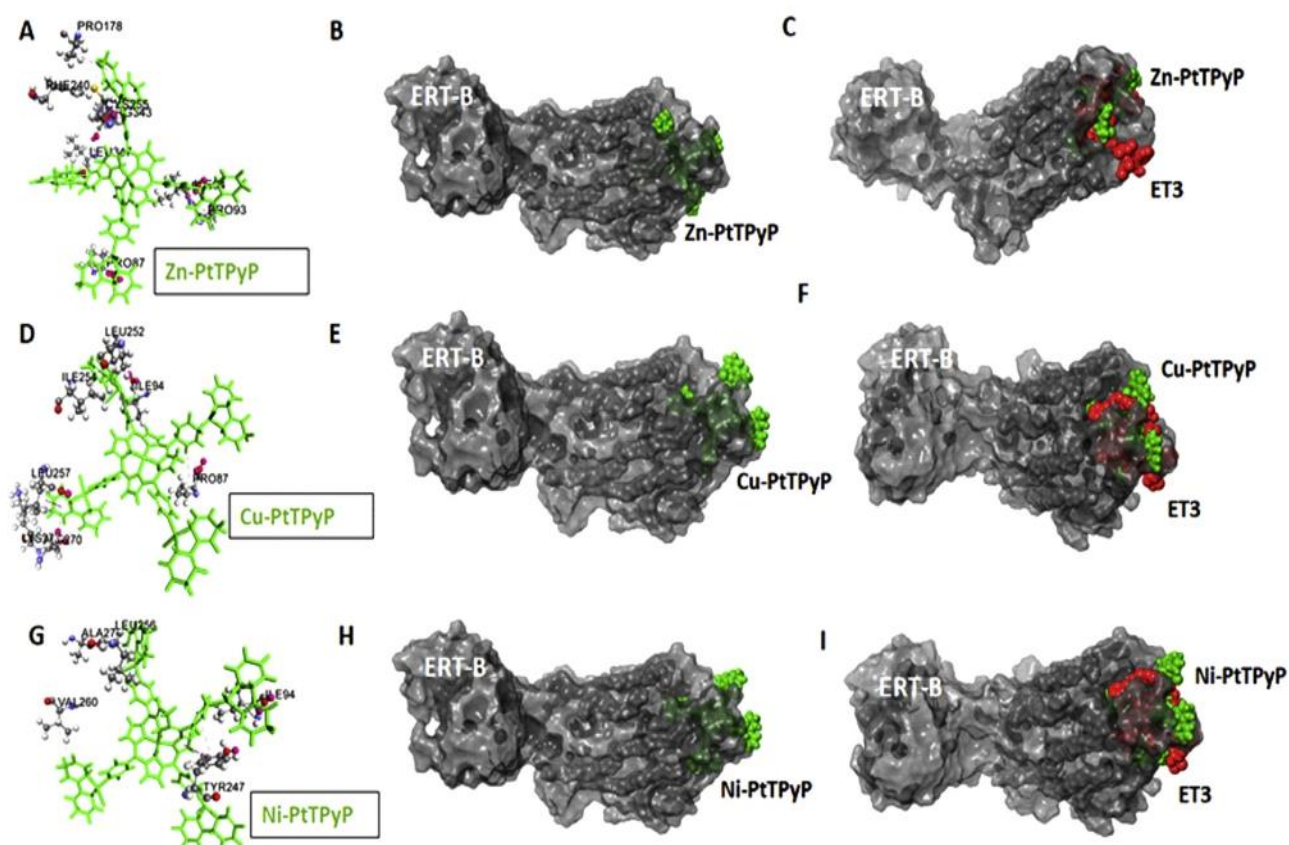
Fig. 6. A-I – Image of the molecular arrangement of **Zn-4-PtTPyP**, **Cu-4-PtTPyP** and **Ni-4-PtTPyP** porphyrins with the endothelin B receptor (ERT-B). In A, D and G we observe the 3D structure of platinum(II) porphyrins with zinc(II), copper(II) and nickel(II), respectively, and their bindings with amino acids. In B, E and H we observe the coupling of porphyrin with zinc(II), copper(II) and nickel(II) respectively, and the endothelin B receptor. In C, F and I we can see that the coupling between ET3 and the ERT-B region occurs in a similar way to that of zinc(II), copper(II) and nickel(II) derivative, respectively. we can observe that the coupling between ET3 and the ERT-B region occurs in a similar way for zinc(II), copper(II) and nickel(II).

Table 4
Molecular anchoring results of the CuZn-SOD (SOD1) enzyme with metalloporphyrins.

Protein/Porphyrin	Amino acid residues	Fitness plp	Common amino acids with SOD1
SOD1 + crystallographic molecule	REGION B: PRO28, LYS30, TRP32	54.4633	–
SOD1 + Zn-4-PtTPyP	REGION B: ILE17, LYS23, LYS30, TRP32, SER34 REGION H: TRP32	97.0192	REGION B: LYS30, TRP32
SOD1 + Cu-4-PtTPyP	REGION B: ILE17, LYS30, TRP32. REGION C: HIS80, LYS136 REGION H: TRP32	68.9688	REGION B: LYS30, TRP32
SOD1 + Ni-4-PtTPyP	REGION B: THR2, LYS3, PRO28, LYS30, TRP32 REGION H: LYS30, TRP32	94.1588	REGION B: PRO28, LYS30, TRP32

Table 5
Molecular anchoring results of the catalase (CAT) enzyme with metalloporphyrins.

Protein/Porphyrin	Amino acid residues	Fitness plp	Common amino acids with CAT
CAT + crystallographic molecule	PHE198, ARG203, LYS243, ASN244	87.2729	–
CAT + Zn-4-PtTPyP	LYS237, ILE242, ALA445	65.5986	
CAT + Cu-4-PtTPyP	LYS237, LYS243, VAL450	78.5041	LYS243
CAT + Ni-4-PtTPyP	ILE242, LYS243, ASN244	70.1889	LYS243

the aromatic rings in the 2,2′-bipyridine group complexed with ruthenium in the porphyrin structure can interact with the amino acid residue His-145 via π-π stacking within a distance of 3.20 Å. Finally, hydrophobic interactions were also detected between copper(II) derivative **Cu-4-PtTPyP** and **Ni-4-PtTPyP** structures with Leu-114, Pro-117, Ile-141, Leu-153, Phe- 164, Leu-178, and Leu-181 residues. Overall, molecular docking results are in accordance with the experimental data previously described above.

4. Discussion

In this study, we chose the A375 metastatic melanoma amelanotic cell line because of a previous study published by our the group, which demonstrated after 7 decades of analysis (1960–2019) that amelanotic cell lines, especially A375 and SKMEL-28, have been used with the objective of identifying drugs capable of improving therapeutic efficacy and avoiding resistance related to the melanin elimination capacity [55].
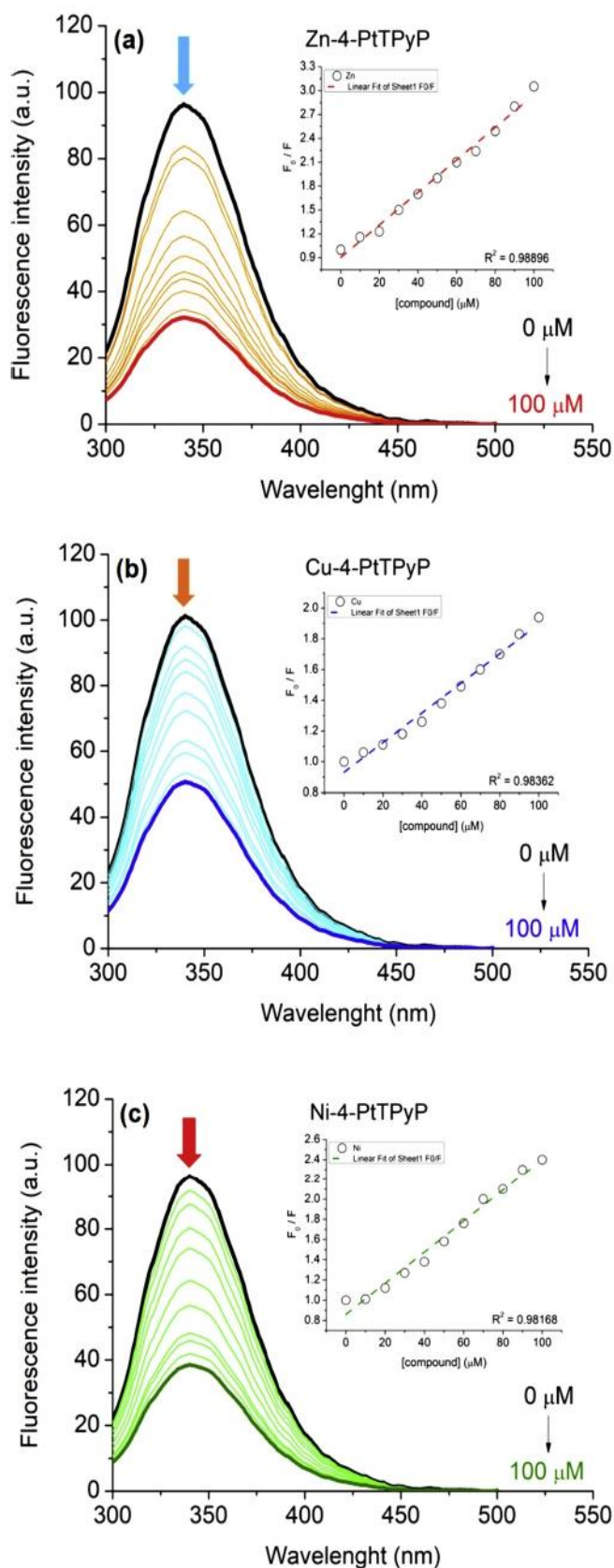
Fig. 7. The HSA steady-state fluorescence emission spectra without and as a function of metalloporphyrin (a) **Zn-4-PtTPyP**, (b) **Cu-4-PtTPyP** and (c) **Ni-4-PtTPyP**, in a Tris-HCl buffer (pH = 7.4). The concentration of HSA is 10 μM and porphyrin concentrations ranged from 0 to 100 μM. *Inset:* plot of F_0/F *versus* [porphyrin].

Our results obtained in the A375 metastatic melanoma strain demonstrated a good anti-proliferative effect of the compounds **Zn-4-PtTPyP** and **Ni-4-PtTPyP**. Both significantly reduce cell viability only

when exposed to the photodynamic system. These *in vitro* results corroborate the results of the previous study, when we evaluated the **4-PtTPyP** platinum without the presence of other transition metals [2]. Thus, the presence of zinc(II) and nickel(II) ions does not alter the antitumor potential of the porphyrin under study, what is positive.

It is important to note that *in silico* methodologies, such as molecular docking, were used here, as the inclusion of such tests represents a more rational approach to screening which has the precision of predicting interactions between molecules and their receptors saving time and money during the expensive process discovery and development of new compounds [55]. These tools are of great value for the initial stages of screening compounds.

The insertion of these metals was used in the idea of improving selectivity via affinity for receptors, which were found with increased expression in tumor cells. We to evaluate the LDL receptor, since **4-PtTPyP** porphyrin without the presence of metals demonstrated a lower affinity for this receptor. This receptor is an important ally for both drug delivery and guided diagnosis [56], moreover, this increased expression has been associated with a shorter relapse-free survival [57]. Therefore, using the LDL receptor as an ally to anti-tumor therapies becomes an interesting alternative.

This binding affinity is evident in our study when we added zinc and nickel to porphyrin, significantly improving the interaction with the LDL receptor, especially with that of zinc, which presented a fitness plp of 87.6885, an increase of approximately 30 % when compared to free-base Pt(II)-porphyrin. Another advantage of zinc(II) compounds is the fact that this metal does not accumulate significantly *in vivo* [23], important data when we think about this porphyrin for further studies with greater complexity.

In addition, we evaluated the endothelin B receptor, due to the overexpression of ETR-B associated with the development of various diseases, such as cardiovascular disorders and cancers [58]. Thus, ETR-B seems to be relevant for the treatment or diagnosis of high-prevalence human diseases. Our data demonstrated that both porphyrins overcome the control group's affinity for the receptor (endothelin B receptor with endothelin 3) with a 50 % greater response in fitness plp. As we know that the activation of the ERT-B receptor occurs with the ET3 binding [36], to have porphyrins that bind with a greater affinity for this receptor than ET3, they end up competing with an ET3 for receptor and we can infer that proliferative activity, anti-apoptotic, metastatic of ERT-B is compromised, which is favorable in therapy for metastatic melanoma. Still, we can see that the shared binding amino acids are not exactly the same, indicating a different action than ET3.

The insertion of zinc(II) or nickel(II) ions in the tetra-cationic porphyrin core favors the mechanism of action - type II - of photodynamic therapy due to the preference by the formation of $^1O_2$ (Fig. 4 – ROS generation), because zinc(II) ions is a full *d*-shell (all orbitals with electrically filled) and nickel is d^8-low spin specie and thus the photodynamic processes are not negatively affected. Because of the stimulus triggered of the type II mechanism, the excited photosensitizers do not damage cell structures, they react only with oxygen molecules that separate dissolved in the cytoplasm [59]. In view of this panorama, it is understood that the type II mechanism is the most important process conditioning the efficiency of the PDT [60].

We evaluated the enzymes superoxide dismutase and catalase because oxidative stress is present in cancer cells and modulating this process can be a key part in this context [61]. Our results also demonstrated that, mainly, porphyrins with zinc and nickel metals have a strong connection with the active site of the enzyme CuZn-SOD (SOD-1), an enzyme important in the antioxidant process. Antioxidants such as superoxide dismutase (SOD) are known to be important for the treatment of pathologies such as cancer [62]. Other studies show that increased SOD2 activity has been found to suppress the malignant phenotype of human melanoma cells [62,63]. Increasing antioxidant defenses can be an ally in anticancer therapy [62]. Although the results of catalase are lower than the control, the nickel shows a fitness plp of

Table 6

The HSA-binding parameters with metalloporphyrins **Zn-4-PtTPyP**, **Cu-4-PtTPyP** and **Ni-4-PtTPyP**.

Porphyrin	Q (%)[a]	K_{SV} (M^{-1})[b]	k_q (M^{-1} s^{-1})[c]	K_a (M^{-1})[d]	n[e]	ΔG^o (kcal mol^{-1})[f]
Zn-4-PtTPyP	66.70	2.04×10^4	3.60×10^{12}	4.87×10^4	1.14	-6.39
Cu-4-PtTPyP	50.05	9.65×10^3	1.70×10^{12}	6.00×10^3	1.50	-5.15
Ni-4-PtTPyP	60.00	1.54×10^4	2.71×10^{12}	6.46×10^3	1.57	-5.20

[a] $Q(\%) = (\text{Emission}_{initial} - \text{Emission}_{final})/(\text{Emission}_{initial}) \times 100$.

[b] Stern-Volmer quenching constants.

[c] Bimolecular quenching rate constant determined by steady-state fluorescence emission spectra (τ_0 HSA $= 5.67$ ns).

[d] Association equilibrium constant of porphyrin with HSA determined by steady-state emission spectra.

[e] Number of binding sites.

[f] Free-energy value obtained using T $= 298$ K and R $= 1.987$ kcal/K mol.

Table 7

Molecular anchoring results of the human serum albumin (HSA) with metalloporphyrins.

| Protein/Porphyrin	Amino acid residues	Fitness plp	Common amino acids with porphyrin
HSA + crystallographic porphyrin	ARG117, PRO118, MET123, PHE134, LEU135, TYR138, LEU139, ILE142, PHE149, LEU154, ALA158, TYR161, PHE165, ARG186	133.1563	–
HSA + 4-PtTPyP	LEU115, VAL116, ARG117, PRO118, MET123, ILE142, TYR161, LEU182, ARG186, LYS190, PRO421, GLN459	99.3098	ARG117, PRO118, MET123, ILE142, TYR161, ARG186
HSA + Zn-4-PtTPyP	ARG117, PRO118, VAL120, MET123, TYR138, ALA175, LEU179, LYS190, ALA194, PRO421, SER517	100.7534	ARG117, PRO118, MET123, TYR138
HSA + Cu-4-PtTPyP	ARG114, VAL116, ARG117, PRO118, MET123, TYR138, ARG186, ASP187, PRO421, ASN429, LYS432	100.1382	ARG117, PRO118, MET123, TYR138, ARG186
HSA + Ni-4-PtTPyP	ARG114, LEU115, VAL116, ARG117, TYR138, ILE142, ALA158, TYR161, LEU179, ARG186, VAL424, GLU425, ILE523	102.3533	ARG117, TYR138, ILE142, ALA158, TYR161, ARG186
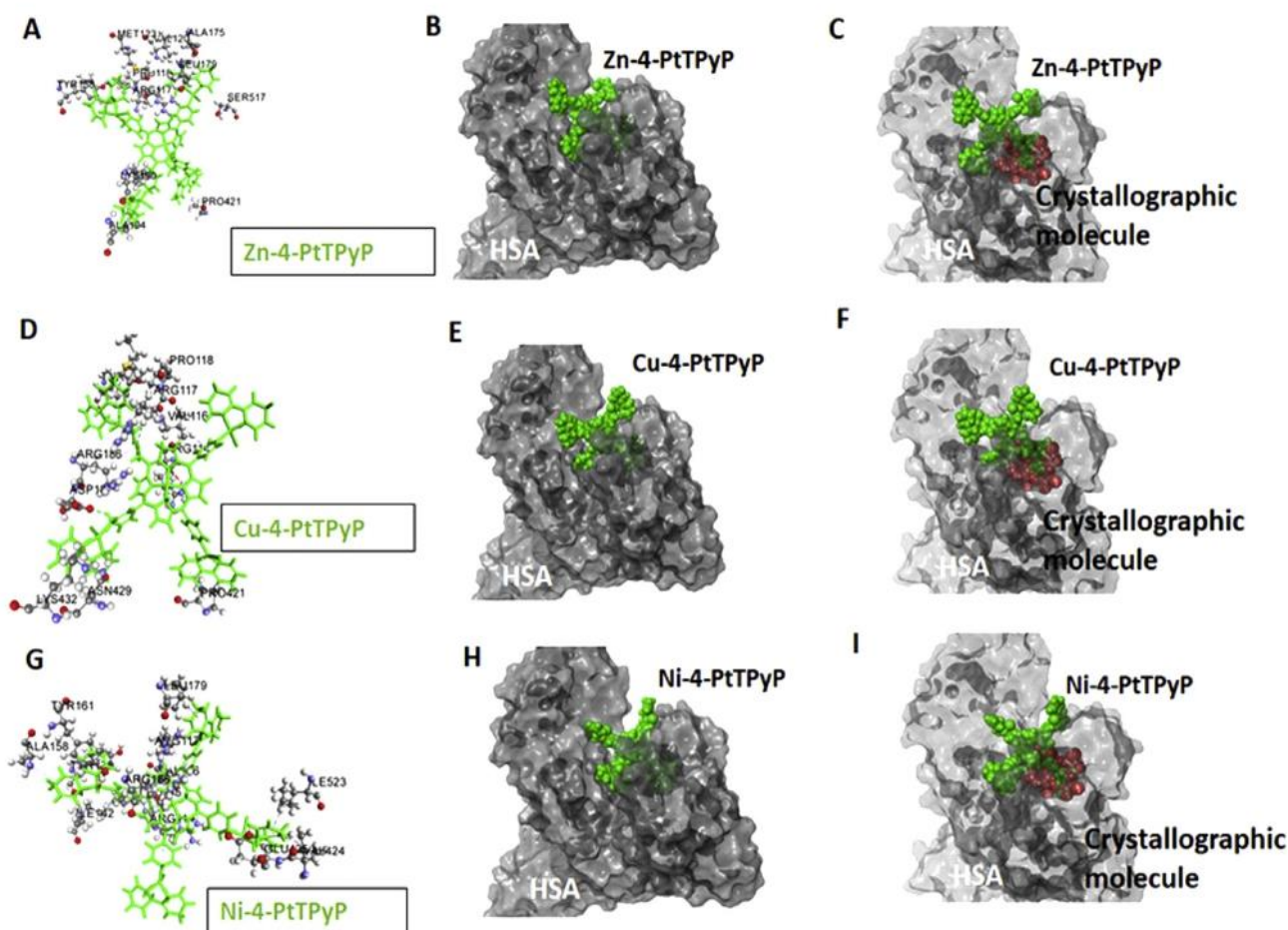
Fig. 8. A-I – Image of the molecular arrangement of **Zn-4-PtTPyP**, **Cu-4-PtTPyP** and **Ni-4-PtTPyP** porphyrins with the protein Human serum albumin (HSA). In A, D and G we observe the 3D structure of platinum (II) porphyrins with zinc, copper and nickel, respectively, and their bindings with amino acids. In B, E and H we observe the coupling of porphyrin with zinc, copper and nickel, respectively and HSA protein. In C, F and I we can see that the coupling between crystallographic ligand and the HSA protein region occurs in a similar way to that of zinc, copper and nickel, respectively. We can observe that the coupling between the crystallographic ligand and the HSA protein region occurs in a similar way for zinc, copper and nickel.

Table 8

Amino acid residues participating in the interaction HSA:metalloporphyrin derivatives in the site IB.

Porphyrin	Amino acid residues	Interaction	Distance (Å)
Zn-4-PtTPyP	ARG117	Hydrophobic Alkyl	5.18
	PRO118	Hydrophobic Alkyl	5.38
	VAL120	Hydrophobic Alkyl	5.43
	MET123	Hydrophobic Alkyl	5.21
	TYR138	Hydrophobic Pi-Alkyl	4.21
	ALA175	Hydrophobic Alkyl	5.43
	LEU179	Hydrophobic Alkyl	4.16
	LYS190	Hydrophobic Alkyl	4.68
	ALA194	Hydrophobic Alkyl	4.92
	PRO421	Hydrophobic Alkyl	4.34
	SER517	Carbon Hydrogen-Bond	2.94
Cu-4-PtTPyP	ARG114	Unfavorable Donor-Donor	2.74
	VAL116	Hydrophobic Pi-Alkyl	5.26
	ARG117 2x	Hydrophobic Alkyl, Hydrophobic Alkyl	5.35, 5.15
	PRO118	Hydrophobic Alkyl	5.33
	MET123	Hydrophobic Alkyl	5.05
	TYR138 2x	Hydrophobic Pi-Alkyl, Pi-Donor Hydrogen-Bond	4.30, 3.17
	ARG186	Hydrophobic Alkyl	5.25
	ASP187 2x	Conventional Hydrogen-Bond, Carbon Hydrogen-Bond	2.56, 2.61
	PRO421 2x	Hydrophobic Alkyl, Hydrophobic Alkyl	4.25, 3.74
	ASN429	Conventional Hydrogen-Bond	1.86
	LYS432	Unfavorable Donor-Donor	2.44
Ni-4-PtTPyP	ARG114	Hydrophobic Alkyl	5.0
	LEU115 2x	Conventional Hydrogen-Bond, Hydrophobic Pi-Alkyl	2.05, 5.46
	VAL116	Hydrophobic Pi-Alkyl	5.43
	ARG117 3x	Carbon Hydrogen-Bond, Hydrophobic Pi-Alkyl, Hydrophobic Pi-Alkyl	2.33, 4.14, 4,61
	TYR138	Hydrophobic Pi-Alkyl	4.36
	ILE142	Hydrophobic Alkyl	4.54
	ALA158	Hydrophobic Alkyl	5.15
	TYR161 3x	Unfavorable Donor-Donor, Hydrophobic Pi-Alkyl, Hydrophobic Pi-Alkyl	1,64, 3.65, 4.64
	LEU179	Hydrophobic Pi-Alkyl	5.16
	ARG186 2x	Hydrophobic Pi-Alkyl, Hydrophobic Pi-Alkyl	4.41, 5.41
	VAL424	Hydrophobic Alkyl	4.51
	GLU425	Carbon Hydrogen-Bond	2.96
	ILE523	Hydrophobic Alkyl	4.36

Fig. 9. In this image, we can see the main common interactions of amino acids and porphyrins. In image A, B and C we see that the most important connections are the same in both porphyrins TYR138 and ARG117, for **Zn-4-PtTPyP**, **Cu-4-PtTPyP** and **Ni-4-PtTPyP**.

around 70 and that is significant. Cancer cells to some extent depend on the highly unstable and mutagenic environment of oxidative stress [61], that's why the management of antioxidant species is interesting.

In this work, we evaluated the possible interaction of zinc(II), nickel (II) and copper(II) metallo-derivatives with human serum albumin (HSA), considering that it is the protein in greater abundance in blood plasma and also a negatively charged and highly soluble protein, it helps in maintaining the oncotic pressure in the human circulatory system, in addition to being responsible for the distribution of organic and inorganic components through their endogenous (fatty acids) and exogenous (drugs) interactions [64].

Thus, HSA-binding properties plays a crucial role in the pharmacokinetic process of commercial drugs and potential drugs in development, since these proteins linked to compounds of interest could be transported in the bloodstream [65]. In this context, our *in silico* studies have shown a small improvement when we add transition center metals to porphyrins when compared to free-base platinum(II) porphyrin **4-PtTPyP**. In general, when analyzing their amino acid residues interactions, we can see that they were composed mainly of hydrophobic forces accompanied by hydrogen bonds. In this sense, hydrophobic forces are important for the recognition of the molecule by the receptor,
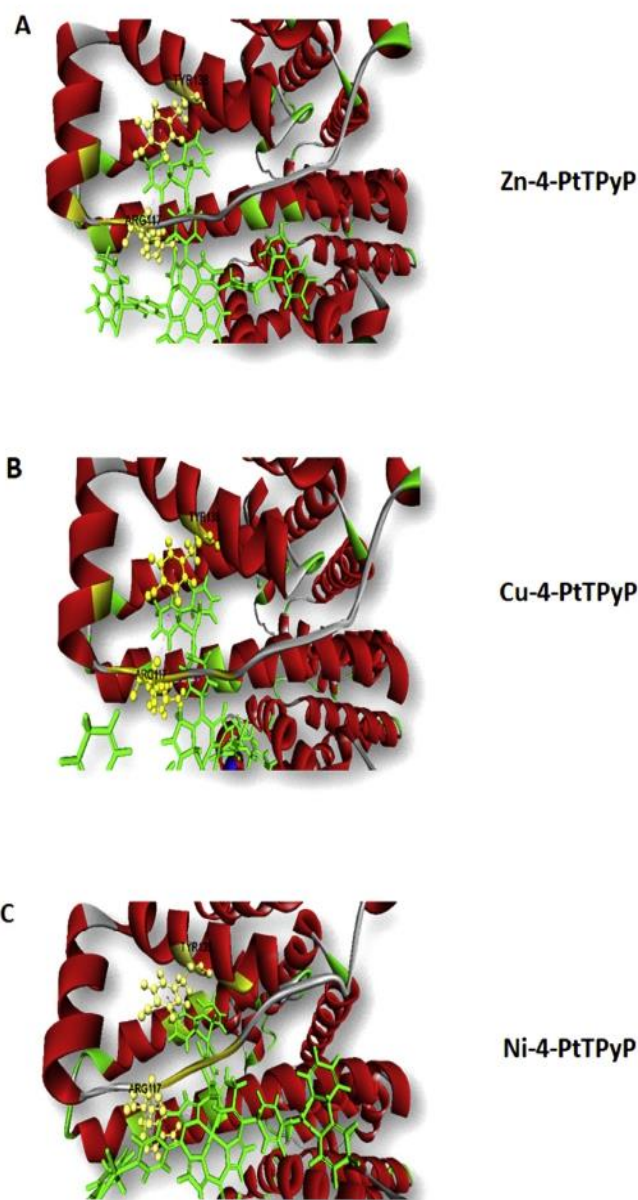
while hydrogen bonds are important for maintaining the stability of the molecule. We also observed that all porphyrins have the ability to accommodate themselves within the protein, so we understand that HSA has the ability to transport them through the bloodstream.

Thus, as a common point among all the results, the ARG117 and TYR138 residues stand out, which make hydrophobic forces in the three molecules, thus being able to serve as a fitting flag in the protein site (Fig. 9).

5. Conclusion

In this article, we investigate the consequences of the inclusion of transition metals (II) - zinc, copper and nickel on the antitumor activity of metastatic melanoma cells (A375) and their action on the connection between APO B-100 and ERT-B, HSA receptors and antioxidants like SOD and CAT. Our results suggest that, mainly, porphyrins **Zn-4-PtTPyP** and **Ni-4-PtTPyP** of platinum (II) inhibit cell proliferation of metastatic melanoma when exposed to the photodynamic system. In addition, the *in silico* study indicated that tetra-cationic platinum(II) porphyrins are promising as a drug administration strategy, as they

showed an improvement in affinity with the N-terminal region of ApoB-100 when adding metals. Still, the affinity for the endothelin receptor was higher than the control used in this study. Thus, our metalloporphyrins show promise as an antitumor and in the strategy of selectivity, delivery and inhibition of tumor metastasis.

Funding and acknowledgments

References

[1] T.T. Tasso, T.M. Tsubone, M.S. Baptista, L.M. Mattiazzi, T.V. Acunha, B.A. Iglesias, Isomeric effect on the properties of tetraplatinated porphyrins showing optimized phototoxicity for photodynamic therapy, Dalton Trans. 46 (2017), https://doi.org/10.1039/c7dt01205e.

[2] G.K. Couto, B.S. Pacheco, V.M. Borba, J.C.R. Junior, T.L. Oliveira, N.V. Segatto, F.K. Seixas, T.V. Acunha, B.A. Iglesias, T. Collares, Tetra-cationic platinum(II) porphyrins like a candidate photosensitizers to bind, selective and drug delivery for metastatic melanoma, J. Photochem. Photobiol. B Biol. 222 (2020), https://doi.org/10.1016/j.jphotobiol.2019.111725.

[3] A. Naik, R. Rubbiani, G. Gasser, B. Spingler, Visible-light-induced annihilation of tumor cells with platinum-porphyrin conjugates, Angew. Chemie - Int. Ed. 53 (2014), https://doi.org/10.1002/anie.201400533.

[4] V. Rapozzi, S. Zorzet, M. Zacchigna, E. Della Pietra, S. Cogoi, L.E. Xodo, Anticancer activity of cationic porphyrins in melanoma tumour-bearing mice and mechanistic in vitro studies, Mol. Cancer 13 (2014), https://doi.org/10.1186/1476-4598-13-75.

[5] Instituto Nacional do Câncer, Estimativa Incidência de Câncer no Brasil - Biênio 2018-2019, (2018) doi:978-85-7318-194-4.

[6] N.J. Wheate, S. Walker, G.E. Craig, R. Oun, The status of platinum anticancer drugs in the clinic and in clinical trials, Dalton Trans. 39 (2010), https://doi.org/10.1039/c0dt00292e.

[7] B. Stordal, M. Davey, Understanding cisplatin resistance using cellular models, IUBMB Life 59 (2007), https://doi.org/10.1080/15216540701636287.

[8] M.E. Rodríguez, C. Catrinacio, A. Ropolo, V.A. Rivarola, M.I. Vaccaro, A novel HIF-1α/VMP1-autophagic pathway induces resistance to photodynamic therapy in colon cancer cells, Photochem. Photobiol. Sci. 16 (2017), https://doi.org/10.1039/c7pp00161d.

[9] M.J. Lamberti, A.B. Morales Vasconsuelo, M. Chiaramello, V.F. Ferreira, M. Macedo Oliveira, S. Baptista Ferreira, V.A. Rivarola, N.B. Rumie Vittar, NQO1 induction mediated by photodynamic therapy synergizes with β-Lapachone-halogenated derivative against melanoma, Biomed. Pharmacother. 108 (2018), https://doi.org/10.1016/j.biopha.2018.09.159.

[10] Q. Huang, Z. Pan, P. Wang, Z. Chen, X. Zhang, H. Xu, Zinc(II) and copper(II) complexes of β-substituted hydroxylporphyrins as tumor photosensitizers, Bioorganic Med. Chem. Lett. 16 (2006), https://doi.org/10.1016/j.bmcl.2005.02.094.

[11] P.M. Antoni, A. Naik, I. Albert, R. Rubbiani, S. Gupta, P. Ruiz-Sanchez, P. Munikorn, J.M. Mateos, V. Luginbuehl, P. Thamyongkit, U. Ziegler, G. Gasser, G. Jeschke, B. Spingler, (Metallo)porphyrins as potent phototoxic anti-cancer agents after ir-radiation with red light, Chem. - A Eur. J. 20 (2015), https://doi.org/10.1002/chem.201405470.

[12] E. Barragán, B. Gordillo, G. Vargas, L. Velazco, The role of cobalt, copper, nickel, and zinc in the DNA replication inhibitory activity of p-aminophenyl triphe-nylporphyrin, Appl. Organomet. Chem. 18 (2004), https://doi.org/10.1002/aoc.649.

[13] E.R. Milaeva, O.A. Gerasimova, Z. Jingwei, D.B. Shpakovsky, S.A. Syrbu, A.S. Semeykin, O.I. Koifman, E.G. Kireeva, E.F. Shevtsova, S.O. Bachurin, N.S. Zefirov, Synthesis and antioxidative activity of metalloporphyrins bearing 2,6-di-tert-butylphenol pendants, J. Inorg. Biochem. 102 (2008), https://doi.org/10.1016/j.jinorgbio.2008.01.022.

[14] R. Socoteanu, G. Manda, R. Boscencu, G. Vasiliu, A.S. Oliveira, Synthesis, spectral analysis and preliminary in vitro evaluation of some tetrapyrrolic complexes with 3d metal ions, Molecules 20 (2015), https://doi.org/10.3390/molecules200915488.

[15] L. Fouani, S.V. Menezes, M. Paulson, D.R. Richardson, Z. Kovacevic, Metals and metastasis: Exploiting the role of metals in cancer metastasis to develop novel anti-metastatic agents, Pharmacol. Res. 115 (2017), https://doi.org/10.1016/j.phrs.2016.12.001.

[16] S.N. Loh, The missing zinc: P53 misfolding and cancer, Metallomics (2010), https://doi.org/10.1039/c003915b.

[17] E.I. Yslas, C. Prucca, S. Romanini, E.N. Durantini, M. Bertuzzi, V. Rivarola, Biodistribution and phototherapeutic properties of Zinc (II) 2,9,16,23-tetrakis (methoxy) phthalocyanine in vivo, Photodiagnosis Photodyn. Ther. 6 (2009), https://doi.org/10.1016/j.pdpdt.2009.03.001.

[18] Edith Inés Yslas, Laura Natalia Milla, Silvia Ro manini, Edgardo N.éstor Durantini, Comparative photodynamic therapy study using two phthalocyanine derivatives, Exp. Ther. Med. 1 (2010) 713–718, https://doi.org/10.3892/etm_00000110.

[19] Luis Exequiel Ibarra, Gabriela Valeria Porcal, Lorena Paola Macor, V. Ponzio3, 4, Ramiro Martin Spada, Carolina Lorente, Carlos Alberto Chesta, A.R. & R.E. Palacios, Metallated porphyrin-doped conjugated polymer nanoparticles for efficient photo-dynamic therapy of brain and colorectal tumor cells, 13 (2018). doi:10.2217 / nnm-2017-0292.

[20] S.K. Mantena, M.K. Unnikrishnan, K. Chandrasekharan, Radioprotection by copper and zinc complexes of 5-aminosalicylic acid: a preliminary study, J. Environ. Pathol. Toxicol. Oncol. 27 (2008), https://doi.org/10.1615/JEnvironPatholToxicolOncol.v27.i2.50.

[21] A. Nakayama, M. Hiromura, Y. Adachi, H. Sakurai, Molecular mechanism of anti-diabetic zinc-allixin complexes: regulations of glucose utilization and lipid meta-bolism, J. Biol. Inorg. Chem. 13 (2008), https://doi.org/10.1007/s00775-008-0352-0.

[22] C. Pavani, A.F. Uchoa, C.S. Oliveira, Y. Iamamoto, M.S. Baptista, Effect of zinc in-sertion and hydrophobicity on the membrane interactions and PDT activity of porphyrin photosensitizers, Photochem. Photobiol. Sci. 8 (2009), https://doi.org/10.1039/b810313e.

[23] B.X. Hoang, B. Han, D.G. Shaw, M. Nimni, Zinc as a possible preventive and ther-apeutic agent in pancreatic, prostate, and breast cancer, Eur. J. Cancer Prev. 00 (2016), https://doi.org/10.1097/CEJ.0000000000000194.

[24] E.C. Johnson, T. Niem, D. Doolphin, Electron transport via metalloporphyrins, Can. J. Chem. 56 (1978) 1381–1388, https://doi.org/10.1139/v78-229.

[25] S. Boisvert, D. Joly, S. Leclerc, S. Govindachary, J. Harnois, R. Carpentier, Inhibition of the oxygen-evolving complex of photosystem II and depletion of ex-trinsic polypeptides by nickel, BioMetals. 20 (2007), https://doi.org/10.1007/s10534-007-9081-z.

[26] D. Denoyer, S. Masaldan, S. La Fontaine, M.A. Cater, Targeting copper in cancer therapy: "copper that cancer,", Metallomics 7 (2015), https://doi.org/10.1039/c5mt00149h.

[27] S. Sandhu, C.M. McNeil, P. LoRusso, M.R. Patel, O. Kabbarah, C. Li, S. Sanabria, W.M. Flanagan, R.F. Yeh, F. Brunstein, D. Nazzal, R. Hicks, V. Lemahieu, R. Meng, O. Hamid, J.R. Infante, Phase I study of the anti-endothelin B receptor antibody-drug conjugate DEDN6526A in patients with metastatic or unresectable cutaneous, mucosal, or uveal melanoma, Invest. New Drugs 3 (2019), https://doi.org/10.1007/s10637-019-00832-1.

[28] C. Hahn da Silveira, E.N. Garoforo, O.A. Chaves, P.F.B. Gonçalves, L. Streit, B.A. Iglesias, Synthesis, spectroscopy, electrochemistry and DNA interactive studies of meso-tetra(1-naphthyl)porphyrin and its metal complexes, Inorganica Chim. Acta 482 (2018), https://doi.org/10.1016/j.ica.2018.06.052.

[29] O.A. Chaves, T.V. Acunha, B.A. Iglesias, C.S.H. Jesus, C. Serpa, Effect of peripheral platinum(II) bipyridyl complexes on the interaction of tetra-cationic porphyrins with human serum albumin, J. Mol. Liq. 301 (2020), https://doi.org/10.1016/j.molliq.2020.112466.

[30] M. Montalti, A. Credi, L. Prodi, M.T. Gandolfi, Handbook of Third Edition 3 (2006).

[31] C.Q.U.L.C. G. de, Ambiente Operacional Molecular (MOE), (2013) 08, (2018).

[32] G. Jones, P. Willett, R.C. Glen, A.R. Leach, R. Taylor, Development and validation of a genetic algorithm for flexible docking, J. Mol. Biol. (1997), https://doi.org/10.1006/jmbi.1996.0897.

[33] O. Korb, T. Stützle, T.E. Exner, Empirical scoring functions for advanced Protein-Ligand docking with PLANTS, J. Chem. Inf. Model. (2009), https://doi.org/10.1021/ci800298z.

[34] D.S. BIOVIA, Discovery Studio Modeling Environment, Release 2017, Dassault Systèmes, San Diego, 2016.

[35] J. Guevara, J. Romo, E. Hernandez, N.V. Guevara, Identification of receptor ligands in apo B100 reveals potential functional domains, Protein J. 6 (2018), https://doi.org/10.1007/s10930-018-9792-8.

[36] N. Lin, C. Huang, J. Tian, J. Tao, J. Zhang, L. Yang, Y. Li, Y. Liu, S. Chen, G. Shen, J. Li, C. Wang, Y. Tu, The expression of endothelin receptor B in melanoma cells A375 and Sk-mel-1 and the proliferative effects of endothelin 3 on A375 cells, J. Huazhong Univ. Sci. Technol. - Med. Sci. 27 (2007), https://doi.org/10.1007/s11596-007-0535-x.

[37] M. Wardell, Z. Wang, J.X. Ho, J. Robert, F. Ruker, J. Ruble, D.C. Carter, The atomic structure of human methemalbumin at 1.9 Å, Biochem. Biophys. Res. Commun. 291 (2002), https://doi.org/10.1006/bbrc.2002.6540.

[38] O.A. Chaves, C.S.H. Jesus, P.F. Cruz, C.M.R. Sant'Anna, R.M.M. Brito, C. Serpa, Evaluation by fluorescence, STD-NMR, docking and semi-empirical calculations of the o-NBA photo-acid interaction with BSA, Spectrochim. Acta - Part A Mol. Biomol. Spectrosc. 169 (2016), https://doi.org/10.1016/j.saa.2016.06.028.

[39] O.A. Chaves, L.B. Menezes, B.A. Iglesias, Multiple spectroscopic and theoretical investigation of meso-tetra-(4-pyridyl)porphyrin-ruthenium(II) complexes in HSA-binding studies. Effect of Zn(II) in protein binding, J. Mol. Liq. 294 (2019), https://doi.org/10.1016/j.molliq.2019.111581.

[40] R. Manjula, G.S.A. Wright, R.W. Strange, B. Padmanabhan, Assessment of ligand binding at a site relevant to SOD1 oxidation and aggregation, FEBS Lett. 592 (2018), https://doi.org/10.1002/1873-3468.13055.

[41] C.D. Putnam, A.S. Arvai, Y. Bourne, J.A. Tainer, Active and inhibited human cat-alase structures: ligand and NADPH binding and catalytic mechanism, J. Mol. Biol. 296 (2000), https://doi.org/10.1006/jmbi.1999.3458.

[42] J.A. Naue, S.H. Toma, J.A. Bonacin, K. Araki, H.E. Toma, Probing the binding of tetraplatinum(pyridyl)porphyrin complexes to DNA by means of surface plasmon resonance, J. Inorg. Biochem. 103 (2009), https://doi.org/10.1016/j.jinorgbio.2008.10.005.

[43] B.L. Auras, S. De Lucca Meller, M.P. da Silva, A. Neves, L.H.Z. Cocca, L. De Boni, C.H. da Silveira, B.A. Iglesias, Synthesis, spectroscopic/electrochemical character-ization and DNA interaction study of novel ferrocenyl-substituted porphyrins, Appl. Organomet. Chem. 32 (2018) 1–12, https://doi.org/10.1002/aoc.4318.

[44] V.A. Oliveira, B.A. Iglesias, B.L. Auras, A. Neves, H. Terenzi, Photoactive: meso

-tetra(4-pyridyl)porphyrin-tetrakis-[chloro(2,2′bipyridine)platinum(II) derivatives recognize and cleave DNA upon irradiation, Dalton Trans. 46 (2017) 1660–1669, https://doi.org/10.1039/c6dt04634g.

[45] B.L. Auras, V.A. Oliveira, H. Terenzi, A. Neves, B.A. Iglesias, Meso-Mono-[4-(1,4,7-triazacyclononanyl)]-tri(phenyl)]porphyrin and the respective zinc(ii)-complex: complete characterization and biomolecules binding abilities, Photochem. Photobiol. Sci. 15 (2016), https://doi.org/10.1039/c6pp00016a.

[46] L.M.O. Lourenço, B.A. Iglesias, P.M.R. Pereira, H. Girão, R. Fernandes, M.G.P.M.S. Neves, J.A.S. Cavaleiro, J.P.C. Tomé, Synthesis, characterization and biomolecule-binding properties of novel tetra-platinum(ii)-thiopyridylporphyrins, Dalton Trans. 44 (2015) 530–538, https://doi.org/10.1039/c4dt02697g.

[47] G. Basso, J.F. Cargnelutti, A.L. Oliveira, T.V. Acunha, R. Weiblen, E.F. Flores, B.A. Iglesias, Photodynamic inactivation of selected bovine viruses by isomeric cationic tetra-platinated porphyrins, J. Porphyr. Phthalocyanines 23 (2019), https://doi.org/10.1142/S1088424619500767.

[48] B.A. Iglesias, J.F.B. Barata, P.M.R. Pereira, H. Girão, R. Fernandes, J.P.C. Tomé, M.G.P.M.S. Neves, J.A.S. Cavaleiro, New platinum(II)-bipyridyl corrole complexes: synthesis, characterization and binding studies with DNA and HSA, J. Inorg. Biochem. 159 (2015), https://doi.org/10.1016/j.jinorgbio.2015.08.016.

[49] R.C. Pivetta, B.L. Auras, B. de Souza, A. Neves, F.S. Nunes, L.H.Z. Cocca, L. De Boni, B.A. Iglesias, Synthesis, photophysical properties and spectroelectrochemical characterization of 10-(4-methyl-bipyridyl)-5,15-(pentafluorophenyl)corrole, J. Photochem. Photobiol. A Chem. 332 (2017), https://doi.org/10.1016/j.jphotochem.2016.09.008.

[50] J. Golab, P. Agostinis, K. Berg, K.A. Cengel, T.H. Foster, A.W. Girotti, S.O. Gollnick, S.M. Hahn, M.R. Hamblin, A. Juzeniene, D. Kessel, M. Korbelik, J. Moan, P. Mroz, D. Nowis, J. Piette, B.C. Wilson, Photodynamic therapy of cancer: an update, Ca-a Cancer J. Clin. 61 (2011), https://doi.org/10.3322/caac.20114.

[51] S.W. Cramer, C.C. Chen, Photodynamic therapy for the treatment of glioblastoma, Front. Surg. 6 (2020) 1–11, https://doi.org/10.3389/fsurg.2019.00081.

[52] A.G. Baynash, K. Hosoda, A. Giaid, J.A. Richardson, N. Emoto, R.E. Hammer, M. Yanagisawa, Interaction of endothelin-3 with endothelin-B receptor is essential for development of epidermal melanocytes and enteric neurons, Cell 79 (1994), https://doi.org/10.1016/0092-8674(94)90018-3.

[53] J.R. Lakowicz, Principles of Fluorescence Spectroscopy, (2006), https://doi.org/10.1007/978-0-387-46312-4.

[54] S.S. Kalanur, J. Seetharamappa, V.K.A. Kalalbandi, Characterization of interaction and the effect of carbamazepine on the structure of human serum albumin, J. Pharm. Biomed. Anal. 53 (2010), https://doi.org/10.1016/j.jpba.2010.05.025.

[55] G.K. Couto, N.V. Segatto, T.L. Oliveira, F.K. Seixas, K.M. Schachtschneider, T. Collares, The melding of drug screening platforms for melanoma, Front. Oncol. 9

(2019), https://doi.org/10.3389/fonc.2019.00512.

[56] G.M. Favero, J.L. Paz, A.H. Otake, D.A. Maria, E.G. Caldini, R.S.S. de Medeiros, D.F. Deus, R. Chammas, R.C. Maranhão, S.P. Bydlowski, Cell internalization of 7-ketocholesterol-containing nanoemulsion through LDL receptor reduces melanoma growth in vitro and in vivo: a preliminary report, Oncotarget 9 (2018), https://doi.org/10.18632/oncotarget.24389.

[57] E.J. Gallagher, Z. Zelenko, B.A. Neel, I.M. Antoniou, L. Rajan, N. Kase, D. LeRoith, Elevated tumor LDLR expression accelerates LDL cholesterol-mediated breast cancer growth in mouse models of hyperlipidemia, Oncogene 36 (2017), https://doi.org/10.1038/onc.2017.247.

[58] B. Allard, A. Wijkhuisen, A. Borrull, F. Deshayes, F. Priam, P. Lamourette, F. Ducancel, D. Boquet, J.Y. Couraud, Generation and characterization of re-ndomab-B1, a monoclonal antibody displaying potent and specific antagonism of the human endothelin B receptor, MAbs 36 (2013), https://doi.org/10.4161/mabs.22696.

[59] S.M. Fonseca, J. Pina, L.G. Arnaut, J.S. De Melo, H.D. Burrows, N. Chattopadhyay, L. Alcácer, A. Charas, J. Morgado, A.P. Monkman, U. Asawapirom, U. Scherf, R. Edge, S. Navaratnam, Triplet-state and singlet oxygen formation in fluorene-based alternating copolymers, J. Phys. Chem. B 110 (2006) 8278–8283, https://doi.org/10.1021/jp060251f.

[60] A.P. Castano, T.N. Demidova, M.R. Hamblin, Mechanisms in photodynamic therapy: Part two - Cellular signaling, cell metabolism and modes of cell death, Photodiagnosis Photodyn. Ther. 2 (2005) 1–23, https://doi.org/10.1016/S1572-1000(05)00030-X.

[61] L. Andrisic, D. Dudzik, C. Barbas, L. Milkovic, T. Grune, N. Zarkovic, Short overview on metabolomics approach to study pathophysiology of oxidative stress in cancer, Redox Biol. 14 (2018), https://doi.org/10.1016/j.redox.2017.08.009.

[62] V. Sosa, T. Moliné, R. Somoza, R. Paciucci, H. Kondoh, M.E. LLeonart, Oxidative stress and cancer: an overview, Ageing Res. Rev. 12 (2013), https://doi.org/10.1016/j.arr.2012.10.004.

[63] S.L. Church, J.W. Grant, L.A. Ridnour, L.W. Oberley, P.E. Swanson, P.S. Meltzer, J.M. Trent, Increased manganese superoxide dismutase expression suppresses the malignant phenotype of human melanoma cells, Proc. Natl. Acad. Sci. U. S. A. 90 (1993), https://doi.org/10.1073/pnas.90.7.3113.

[64] M. Poór, S. Kunsági-Máté, M. Bálint, C. Hetényi, Z. Gerner, B. Lemli, Interaction of mycotoxin zearalenone with human serum albumin, J. Photochem. Photobiol. B Biol. 170 (2017), https://doi.org/10.1016/j.jphotobiol.2017.03.016.

[65] T. Mukherjee, J.C. Pessoa, A. Kumar, A.R. Sarkar, Formation of an unusual pyridoxal derivative: characterization of Cu(II), Ni(II) and Zn(II) complexes and eva-luation of binding to DNA and to human serum albumin, Inorganica Chim. Acta 426 (2015), https://doi.org/10.1016/j.ica.2014.11.033.

5. DISCUSSÃO

A TFD é uma área de interesse não só biomédica - aplicada a saúde humana - como também, da saúde animal, da indústria e da agricultura. Esta terapia correlaciona-se de forma integrada com a biotecnologia e as ciências biológicas. Foram essas as perspectivas que obtivemos em nosso artigo de revisão que buscou entender o estado da arte desta terapia (COUTO et al., 2020a).

Nossa "*invited review*" observou que a TFD pode ser utilizada com sucesso não só para o tratamento de câncer que possuem resistência aos quimioterápicos convencionais (KHDAIR et al., 2010; ZHEN et al., 2019), , como também, para diagnóstico desta patologia, além de proporcionar a diminuição dos efeitos adversos que, muitas vezes, comprometem o tratamento, como – por exemplo - a aderência a ele (MICHY et al., 2019; MOKOENA; GEORGE; ABRAHAMSE, 2019; WANG et al., 2020).

Abordamos ainda novas tecnologias relacionadas a TFD: (i) correlacionamos terapias imunológicas com a TFD (RAMÍREZ-GARCÍA et al., 2019); (ii) o uso de nanopartículas (NPs) para atingir alvos de interesse específicos, aumentando a seletividade da terapia (SHI et al., 2017); (iii) descrevemos a utilização de além das NPs, como os polissomos, NPs biodegradáveis, micelas, entre outros (MESQUITA et al., 2018).

Além da utilização da TFD em câncer, citamos ainda o uso na saúde animal como no tratamento de mastites bovinas (MOREIRA et al., 2018) e otite canina (SEEGER MG, RIES AS, GRESSLER LT, BOTTON SA; JF, 2020), sem esquecer da utilização desta terapia na indústria e agricultura. A aplicação da TFD no aumento do tempo de prateleira de determinados produtos, merece destaque aqui (KIM et al., 2017).

Existem desafios em torno da TFD no campo da biotecnologia como o desenvolvimento de fotossensibilizadores eficazes e não tóxicos ou menos

tóxicos para humanos, animais e plantas. Nossos resultados demonstraram que o foco deve ser na terceira geração moléculas, que incluem as características necessárias ao funcionamento da TFD, como o aumento e seletividade na geração de espécies reativas de oxigênio e eficiência. Acreditamos que existe potencial atual e futuro para a terapia fotodinâmica em diferentes campos da biotecnologia, devido a já demanda existente. A necessidade de tratamentos mais eficazes, com menos efeitos adversos efeitos, direcionados, com menor incidência de resistência (a drogas e microrganismos) tanto na área da saúde humana e animal, bem como na área agrícola.

Conhecer melhor a TFD nos fez entender que seria uma terapia interessante para aplicarmos às linhagens de melanoma metastático, foco desta tese. Dessa forma, revisamos na literatura a forma como novos compostos candidatos ao tratamento futuro do melanoma vinham sendo triados ao longo das últimas seis décadas (1960 – dias atuais) (COUTO et al., 2019). Demonstramos neste artigo de revisão as plataformas que têm sido utilizadas para desenvolver da melhor forma a triagem de tais compostos. Modelos *in silico, in vitro e in vivo* foram bastante discutidos.

Ao longo da revisão discutimos modelos convencionais, modelos 3D, abordagens moleculares, com o intuito de determinar os mecanismos de citotoxicidade, como danos à membrana, bloqueio da síntese de DNA, produção de espécies reativas de oxigênio (ROS e absorção de drogas) (ABILDGAARD; GULDBERG, 2015; CASTRO; WARD, 1988; EDIRIWEERA; TENNEKOON; SAMARAKOON, 2018); além das abordagens *in vivo e ex vivo,* como os modelos de xenoenxerto de linhagens celular (ROFSTAD; LYNG, 1996).

Estudos *in sílico*, como ancoragem molecular, foram discutidos ao longo de uma sessão por entendermos a importância da inserção de tais ensaios. A inclusão destes testes representa uma abordagem mais racional para a

triagem podendo auxiliar na redução do número de animais necessários, do tempo e dinheiro investidos em cada molécula (FU; CHEN; SUN, 2018). Atualmente existem bons softwares que auxiliam pesquisadores de todo o mundo na busca da previsão de ligação de moléculas a receptores, análise de farmacocinética, bem como triagem de inúmeros compostos com o intuito de predizer aquele no qual deve-se investir foco total. Auto-Dock Vina, MOE, GLIDE, GOLD, foram os softwares mais citados em nossa busca (COUTO et al., 2019).

Assim, entendemos que ferramentas *in silico* são, sem dúvida, de grande valor para as etapas iniciais de rastreamento de drogas. Com a ajuda desses dispositivos, milhares de compostos podem ser testados para identificar com eficácia os candidatos para os ensaios *in vitro* e *in vivo* enquanto consideramos vários *endpoints* durante uma única avaliação. Somado a isso, tais técnicas também podem ser aliadas na busca por respostas relacionadas a seletividades e mecanismo de ação de determinados compostos.

Nesta linha, juntando a TFD e o conhecimento que obtivemos da triagem de novos compostos, obtivemos excelentes resultados que serão discutidos na sequência (COUTO et al., 2020b). O *paper "Tetra-cationic platinum(II) porphyrins like a candidate photosensitizers to bind, selective and drug delivery for metastatic melanoma"*, buscou bioprospectar fotossensibilizadores (**3-PtTPyP** e **4-PtTPyP**) para serem utilizados na TFD e utilizar testes *in sílico* para justificar a possível seletividade dos compostos pelas células de melanoma metastático.

Os resultados obtidos na linhagem de melanoma metastático WM1366 após tratamento com **3-PtTPyP** e **4-PtTPyP** mostraram que ambas as porfirinas de platina(II) não foram tóxicas para células não tumorais (linhagem CHO), pois apresentaram baixos níveis de inibição no teste de citotoxicidade. Esses achados sugerem uma possível seletividade dos compostos porfirínicos em relação às células tumorais, o que poderia ser explicado pela

tendência de ligação dos fotossensibilizadores, preferencialmente, às lipoproteínas de baixa densidade (LDL) (CRUZ et al., 2013; HAMBLIN; NEWMAN, 1994). Firestone et al. demonstraram que as células neoplásicas apresentam maior captação de LDL e com isso maior expressão desses receptores (FIRESTONE, 1994).

Nossos estudos de *docking* molecular, demonstraram uma forte ligação dos nossos composto de platina(II), principalmente pela porfirina **3-PtTPyP** a APOB-100, molécula responsável por carrear grande parte do colesterol LDL ao receptor (LDLR). Esses estudos de ancoragem molecular também foram descritos na mesma linha para prever afinidades de receptores específicos, a fim de melhorar a distribuição de drogas ou induzir uma possível seletividade. Bazcaran e colaboradores conduziram estudos com o gene ALK para câncer de pulmão de células não pequenas para tentar melhorar a ação de drogas para esse tipo de câncer (BASKARAN; RAMACHANDRAN, 2012). Da mesma forma, Xu et al. avaliaram por meio da ancoragem molecular o receptor RXR como uma via farmacológica para leucemia promielocítica aguda (XU et al., 2019).

Além da importância de demonstrarmos efetividade dos compostos contra as células tumorais, é interessante entendermos a via pela qual a morte celular está sendo desencadeada. Nossos resultados demonstraram uma morte induzida por apoptose via caspase 9 e 3, desencadeada por Bax/BCL2, genes avaliados por PCR em tempo real, sendo a morte por apoptose confirmada por ensaios de citometria de fluxo e microscopia confocal (Figura 9). Somado a isso, eles corroboram com achados na literatura, onde a atividade apoptótica de diferentes porfirinas como fotossensibilizadores na terapia fotodinâmica foi demonstrada em várias linhas de células humanas, incluindo carcinoma de pulmão (SENGUPTA et al., 2018), carcinoma escamoso de língua (LAI et al., 2015), adenocarcinoma de mama (RANGASAMY et al., 2015) e câncer gástrico (CHEN; GAO; LIU, 2016). Os

mecanismos envolvidos na indução da apoptose porfirina estão geralmente relacionados ao aumento da produção de ROS e ativação da caspase (LAI et al., 2015; RANGASAMY et al., 2015).
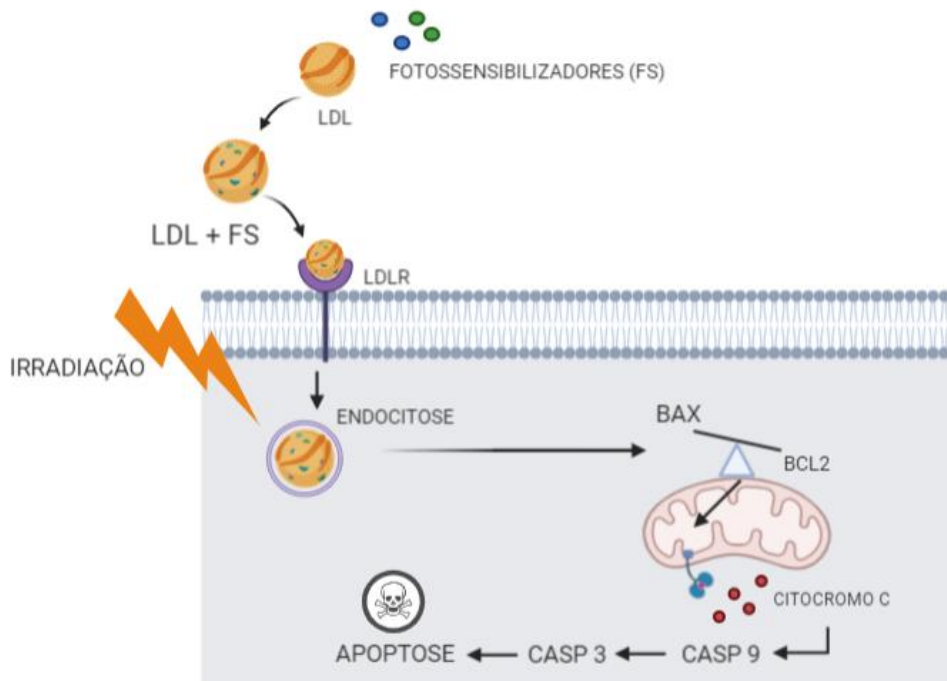

Figura 9: Representação esquemática do mecanismo de morte induzido por apoptose.

Convencidos do potencial antitumoral das porfirinas de platina que foram bioprospectadas nesta tese, buscamos melhorar a afinidade da porfirina **4-PtTPyP**, pois esta apresentou afinidade menos intensa pela APOB-100. Para isso, íons de metais de transição (zinco, cobre e níquel) foram adicionados a esta porfirina. Assim, além da ligação a APOB-100, foram avaliados receptor ERT-B (um dos responsáveis pelas metástases, ação anti-apoptótica e atividade proliferativa), receptores antioxidantes como SOD e CAT e a

ligação a proteína Albumina Soro Humano (HSA), responsável por carrear grande parte dos fármacos pela corrente sanguínea.

Faveiro e colaboradores ao avaliarem LDLR demonstraram por meio de seus achados que essa expressão aumentada, deste receptor, foi associada a uma maior sobrevida livre de recidiva (FAVERO et al., 2018). Portanto, usar o receptor de LDL como um aliado para terapias antitumorais torna-se uma alternativa interessante. Esta afinidade de ligação é evidente em nosso estudo quando adicionamos zinco e níquel para porfirina, melhorando significativamente a interação com o receptor de LDL, principalmente com o de zinco, que apresentou um aumento de aproximadamente 30% quando comparado com a base livre Pt(II). Somado a isso, cabe ressaltar que Hoang e colaboradores já haviam demonstrado em seus estudos que o zinco não se acumula significativamente *in vivo* (HOANG et al., 2016).

Nossos resultados ainda constataram que os metais de transição permitem uma ligação forte ao receptor ERT-B, o qual está super expresso em patologias como o câncer e distúrbios cardiovasculares (ALLARD et al., 2013), dessa maneira o manejo deste receptor torna-se relevante para o tratamento ou diagnóstico de alta prevalência doenças humanas. Como sabemos que a ativação do receptor ERT-B ocorre com a ligação ET3 (LIN et al., 2007), por terem porfirinas que se ligam com maior afinidade por esse receptor do que ET3, elas acabam competindo com o ET3 pelo receptor e, desta forma, podemos inferir que a atividade proliferativa, antiapoptótica, metastática de ERT-B está comprometido, o que é favorável na terapia para melanoma metastático.

Entendemos que a avaliação das enzimas SOD e CAT seria relevante, pois o estresse oxidativo está presente nas células cancerosas e modular este processo pode ser uma parte fundamental no tratamento (ANDRISIC et al., 2018). Nossos resultados demonstraram que, principalmente, porfirinas com zinco e níquel apresentaram uma forte ligação com o sítio ativo da

enzima CuZn-SOD (SOD1), importante no processo antioxidante. Outros estudos como o de Church e colaboradores e o de Sosa e colaboradores, mostram que aumento da atividade de SOD2 foi encontrado para suprimir a malignidade fenótipo de células de melanoma humano. Dessa forma, o aumento das defesas antioxidantes pode ser um aliado na terapia anticâncer (CHURCH et al., 1993; SOSA et al., 2013).

Por fim, escolhemos testar nossas porfirinas com íons metálicos na ligação com a HSA, por ser a proteína em maior abundância no plasma, ser carregada negativamente e altamente solúvel, que ajuda a manter a pressão oncótica no sistema circulatório humano, além de ser responsável pela distribuição de componentes orgânicos e inorgânicos através de suas interações endógenas (ácidos graxos) e exógenas (drogas) (POÓR et al., 2017). Assim, as propriedades de ligação de HSA desempenham um papel crucial no processo farmacocinético de drogas comerciais e drogas potenciais em desenvolvimento, uma vez que essas proteínas ligadas a compostos de interesse podem ser transportadas pela corrente sanguínea [65].

Nossos estudos *in silico* sinalizam que na presença de metais adicionados ao centro de transição da porfirina quando comparadas à porfirina de platina (II) de base livre **4-PtTPyP** houve um aumento da força de ligação. Somado a isso, ao analisar suas interações de resíduos de aminoácidos, observamos que eles foram compostos, principalmente, por forças hidrofóbicas acompanhadas por ligações de hidrogênio. Dentro deste contexto, forças hidrofóbicas são importantes para o reconhecimento da molécula pelo receptor, enquanto as ligações de hidrogênio são importantes para manter a estabilidade da molécula. Também observamos que todas as porfirinas têm a capacidade de se acomodar dentro da proteína, desta forma, entendemos que HSA tem a capacidade de transportá-los através da corrente sanguínea.

6. CONSIDERAÇÕES FINAIS

Ao longo desta Tese buscamos apontar o potencial da terapia fotodinâmica (TFD) aplicada ao melanoma metastático por meio de testes *in vitro* e *in silico* em linhagens celular de melanoma metastático (WM1366 e A375). Propusemos que a inserção de testes *in silico* pode ser uma abordagem racional para a triagem de novos compostos, levando a uma escolha mais assertiva de moléculas candidatas aos testes subsequentes. Gerando, dessa forma, uma economia de tempo e dinheiro.

Demonstramos, ainda que as porfirinas tetracatiônicas de platina(II) são boas candidatas a fotossensibilizadores e que metais de transição como zinco, cobre e níquel melhoram a seletividade das porfirinas às células tumorais, sem mexer em sua atividade antiproliferativa.
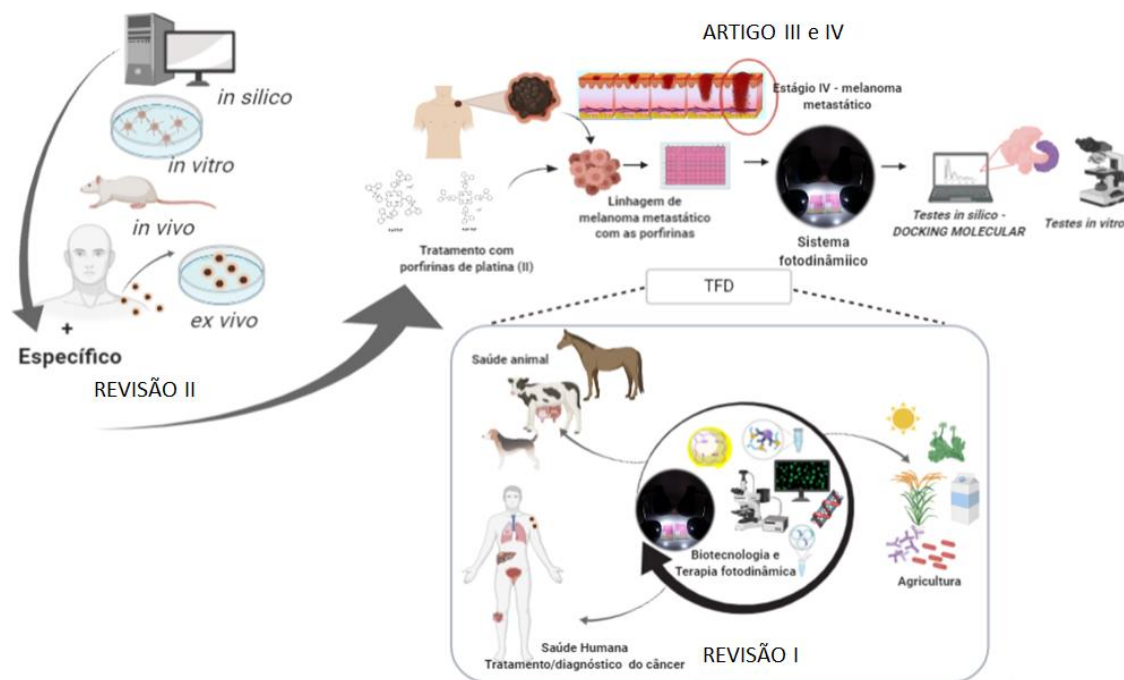
7. PERSPECTIVAS

Abordamos, ao longo deste estudo, testes *in silico* e *in vitro* para comprovarmos uma hipótese que havíamos criado. Com eles conseguimos justificar o mecanismo de ação provável que está por trás da morte celular. Obtivemos como resultados que o possível mecanismo de morte se da por apoptose via caspases 9 e 3 induzidas por Bax/BCL2 e ainda conseguimos explicar a possível seletividade dos fotossensibilizadores que foram utilizados pelas células tumorais.

Futuramente, serão necessários testes *in vivo* e – posteriormente – *ex vivo* para que se aumente a complexidade dos organismos em estudo para mais adiante ter a possibilidade de ser extrapolado para seres humanos. Ainda, sugerimos que tecnologias como a nanotecnologia sejam somadas a TFD para melhorar ainda mais a entrega dos fotossensibilizadores, bem como termos a possibilidade de incluirmos a TFD como diagnóstico do câncer, além de tratamento.

110
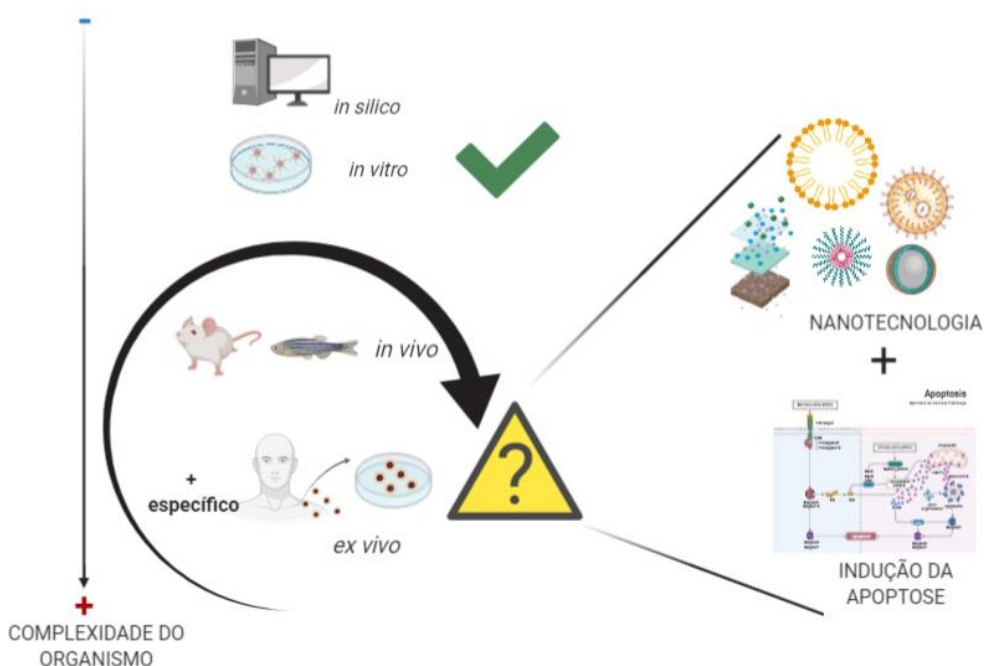
8. REFERÊNCIAS

ABILDGAARD, C.; GULDBERG, P. Molecular drivers of cellular metabolic reprogramming in melanomaTrends in Molecular Medicine, 2015.

ABRAHAMSE, H. et al. New photosensitizers for photodynamic therapy. The Biochemical journal, v. 473, n. 4, p. 347–64, 2016.

ABRAHAMSE, H.; HAMBLIN, M. R. New photosensitizers for photodynamic therapy. Biochemical Journal, v. 473, n. 4, p. 347–364, 2016.

ALLARD, B. et al. Generation and characterization of rendomab-B1, a monoclonal antibody displaying potent and specific antagonism of the human endothelin B receptor. mAbs, 2013.

AMERICAN CANCER SOCIETY. Cancer Facts & Figures 2016. Cancer Facts & Figures 2016, p. 1–9, 2016.

AMERICAN CANCER SOCIETY. Cancer Facts and Figures 2018. 2018, 2018a.

AMERICAN CANCER SOCIETY. Cancer Facts & Figures 2018Atlanta: American Cancer Society. [s.l: s.n.]. Disponível em: <https://www.cancer.org/content/dam/cancer-org/research/cancer-facts-and-statistics/annual-cancer-facts-and-figures/2017/cancer-facts-and-figures-2017.pdf>.

ANDRISIC, L. et al. Short overview on metabolomics approach to study pathophysiology of oxidative stress in cancerRedox Biology, 2018.

BASKARAN, C.; RAMACHANDRAN, M. Computational molecular docking studies on anticancer drugs. Asian Pacific Journal of Tropical Disease, 2012.

BONNETT, R.; BERENBAUM, M. Porphyrins as photosensitizers. Ciba Foundation symposium, v. 146, p. 53; discussion 53, 1989.

BRAUNA, S.; BITTON-WORMS, K.; LE ROITH, D. The link between the metabolic syndrome and cancerInternational Journal of Biological Sciences, 2011.

BROUSSARD, L. et al. 54.3.135 Ⓒ. Chonnam Medical Journal, v. 54, p. 135–142, 2018.

BROWN, S. B.; BROWN, E. A.; WALKER, I. The present and future role of photodynamic therapy in cancer treatmentLancet Oncology, 2004.

BUZZÁ, H. H. et al. Photodynamic therapy: Progress toward a scientific and clinical network in Latin America. Photodiagnosis and Photodynamic Therapy, v. 13, p. 261–266, 2016.

CANNAVÒ, S. P. et al. The role of oxidative stress in the biology of melanoma: A systematic reviewPathology Research and Practice, 2019.

CASTANO, A. P.; DEMIDOVA, T. N.; HAMBLIN, M. R. Mechanisms in photodynamic therapy: Part two - Cellular signaling, cell metabolism and modes of cell deathPhotodiagnosis and Photodynamic Therapy, 2005.

CASTRO, D. J.; WARD, P. H. The effects of argon lasers on human melanoma cells sensitized with rhodamine-123 in vitro. American Journal of Otolaryngology - Head and Neck Medicine and Surgery, v. 9, n. 1, p. 18–29, 1988.

CHATTERJEE, D. K.; FONG, L. S.; ZHANG, Y. Nanoparticles in photodynamic therapy: An emerging paradigmAdvanced Drug Delivery Reviews, 2008.

CHEN, J. J.; GAO, L. J.; LIU, T. J. Photodynamic therapy with a novel porphyrin-based photosensitizer against human gastric cancer. Oncology Letters, v. 11, n. 1, p. 775–781, 2016.

CHURCH, S. L. et al. Increased manganese superoxide dismutase expression suppresses the malignant phenotype of human melanoma cells. Proceedings of the National Academy of Sciences of the United States of America, 1993.

COMPREHENSIVE, N.; NETWORK, C. NCCN Clinical Practice Guidelines in Oncology (NCCN Guidelines®) Melanoma. Journal of the National Comprehensive Cancer Network : JNCCN, 2020.

COUTO, G. K. et al. Profile of pterostilbene-induced redox homeostasis modulation in cardiac myoblasts and heart tissue. Journal of Biosciences, 2018.

COUTO, G. K. et al. The Melding of Drug Screening Platforms for Melanoma. Frontiers in Oncology, 2019.

COUTO, G. K. et al. Perspectives of photodynamic therapy in biotechnology. Journal of Photochemistry and Photobiology B: Biology, v. 213, n. September, p. 112051, 2020a.

COUTO, G. K. et al. Tetra-cationic platinum(II) porphyrins like a candidate photosensitizers to bind, selective and drug delivery for metastatic melanoma. Journal of Photochemistry and Photobiology B: Biology, 2020b.

CRUZ, P. M. R. et al. The role of cholesterol metabolism and cholesterol transport in carcinogenesis: A review of scientific findings, relevant to future cancer therapeuticsFrontiers in Pharmacology, 2013.

DE ROSA, F. S.; BENTLEY, M. V. Photodynamic therapy of skin cancers: sensitizers, clinical studies and future directives. Pharmaceutical research, v. 17, n. 12, p. 1447–55, 2000.

DE SILVA, P. et al. Photodynamic therapy, priming and optical imaging: Potential co-conspirators in treatment design and optimization — a Thomas Dougherty Award for Excellence in PDT paper. Journal of Porphyrins and Phthalocyanines, 2020.

DENAT, L. et al. Melanocytes as instigators and victims of oxidative stressJournal of Investigative Dermatology, 2014.

DOBSON, J.; DE QUEIROZ, G. F.; GOLDING, J. P. Photodynamic therapy and diagnosis: Principles and comparative aspectsVeterinary Journal, 2018.

DRÖGE, W. Free radicals in the physiological control of cell functionPhysiological Reviews, 2002.

EDIRIWEERA, M. K.; TENNEKOON, K. H.; SAMARAKOON, S. R. In vitro assays and techniques utilized in anticancer drug discovery. Journal of Applied Toxicology, 2018.

EMERSON, H.; MEMBER, F. A. P. H. A. L. Heaith *. 1932.

FAVERO, G. M. et al. Cell internalization of 7-ketocholesterol-containing nanoemulsion through LDL receptor reduces melanoma growth in vitro and in vivo: A preliminary report. Oncotarget, 2018.

FIRESTONE, R. A. Low-Density Lipoprotein as a Vehicle for Targeting Antitumor Compounds to Cancer Cells. Bioconjugate Chemistry, v. 5, n. 2, p. 105–113, 1994.

FISCHER, J.; ROBIN GANELLIN, C. Analogue-based Drug Discovery. [s.l: s.n.].

FONSECA, S. M. et al. Triplet-state and singlet oxygen formation in fluorene-based alternating copolymers. Journal of Physical Chemistry B, v. 110, n. 16, p. 8278–8283, 2006.

FONSECA TEIXEIRA, A.; ALVES, J. R. Title: Low power blue LED exposure increases effects of doxorubicin on MDA-MB-231 breast cancer cells. Photodiagnosis and Photodynamic Therapy, 2018.

FU, Y.; CHEN, Z.; SUN, J. Random drift particle swarm optimisation algorithm for highly flexible protein-ligand docking. Journal of Theoretical Biology, v. 457, p. 180–189, 2018.

GOMES, A. T. P. C.; NEVES, M. G. P. M. S.; CAVALEIRO, J. A. S. Cancer, photodynamic therapy and porphyrin-type derivatives. Anais da Academia

Brasileira de Ciencias, v. 90, n. 1, p. 993–1026, 2018.

HAMBLIN, M. R.; NEWMAN, E. L. Photosensitizer targeting in photodynamic therapy II. Conjugates of haematoporphyrin with serum lipoproteins. Journal of Photochemistry and Photobiology, B: Biology, v. 26, n. 2, p. 147–157, 1994.

HIROTO, S.; MIYAKE, Y.; SHINOKUBO, H. Synthesis and Functionalization of Porphyrins through Organometallic MethodologiesChemical Reviews, 2017.

HOANG, B. X. et al. Zinc as a possible preventive and therapeutic agent in pancreatic, prostate, and breast cancer. European Journal of Cancer Prevention, 2016.

HORLINGS, R. K.; TERRA, J. B.; WITJES, M. J. H. MTHPC mediated, systemic photodynamic therapy (PDT) for nonmelanoma skin cancers: Case and literature review. Lasers in Surgery and Medicine, v. 47, n. 10, p. 779–787, 2015.

HORNE, T. K.; CRONJÏ¿½, M. J. Mechanistics and photo-energetics of macrocycles and photodynamic therapy: An overview of aspects to consider for research. Chemical Biology and Drug Design. Anais...2017

INCA. Estimativa 2018-Incidência de câncer no Brasil. Instituto Nacional de Câncer José Alencar Gomes da Silva, p. 130, 2017.

INCA. Brasil - estimativa dos casos novos.

INSTITUTO NACIONAL DEL CANCER. Instituto Nacional del Cáncer. Manual de Enfermeria Oncologiaca, 2016.

INSTITUTO NACIONAL DO CâNCER. Estimativa 2018: incidência de câncer no Brasil / Instituto Nacional de e Câncer José Alencar Gomes da Silva, Coordenação de Prevenção e Vigilância-Rio de Janeiro.. INCA, p. 1–130, 2018a.

INSTITUTO NACIONAL DO CâNCER. Estimativa Incidência de Câncer no Brasil - Biênio 2018-2019. [s.l: s.n.].

JOSEFSEN, L. B.; BOYLE, R. W. Photodynamic therapy: Novel third-generation photosensitizers one step closer?British Journal of Pharmacology, 2008.

JUZENIENE, A.; MOAN, J. The history of PDT in Norway. Photodiagnosis and Photodynamic Therapy, v. 4, n. 1, p. 3–11, 2007.

KADISH, K. M.; CAEMELBECKE, E. VAN; ROYAL, G. The Porphyrin Handbook Volume 8. In: The Porphyrin Handbook vol. 8. [s.l: s.n.].

KANDA, T. et al. Low-density lipoprotein receptor expression is involved in the beneficial effect of photodynamic therapy using talaporfin sodium on gastric cancer cells. Oncology Letters, 2019.

KATAOKA, H. et al. New photodynamic therapy with next-generation photosensitizers. Annals of Translational Medicine, v. 5, n. 8, p. 183–183, 2017.

KESSEL, D.; OLEINICK, N. L. Photodynamic therapy and cell death pathways. Methods in molecular biology (Clifton, N.J.), v. 635, p. 35–46, 2010.

KHARKWAL, G. B. et al. Photodynamic therapy for infections: Clinical applications. Lasers Surg Med, v. 43, n. 7, p. 755–767, 2011.

KHDAIR, A. et al. Nanoparticle-mediated combination chemotherapy and photodynamic therapy overcomes tumor drug resistance. Journal of Controlled Release, 2010.

KIM, M. J. et al. Antibacterial effect of 405 ± 5 nm light emitting diode illumination against Escherichia coli O157:H7, Listeria monocytogenes, and Salmonella on the surface of fresh-cut mango and its influence on fruit quality. International Journal of Food Microbiology, 2017.

KLEIN COUTO, G. et al. Zinc(II), copper(II) and nickel(II) ions improve the selectivity of tetra-cationic platinum(II) porphyrins in photodynamic therapy and stimulate antioxidant defenses in the metastatic melanoma lineage (A375). Photodiagnosis and Photodynamic Therapy, 2020.

KLEMENT, R. J.; KÄMMERER, U. Is there a role for carbohydrate restriction in the treatment and prevention of cancer?Nutrition and Metabolism, 2011.

KNIEBÜHLER, G. et al. Photodynamic therapy for cholangiocarcinoma using low dose mTHPC (Foscan®). Photodiagnosis and Photodynamic Therapy, v. 10, n. 3, p. 220–228, 2013.

KWIATKOWSKI, S. et al. Photodynamic therapy – mechanisms, photosensitizers and combinationsBiomedicine and Pharmacotherapy, 2018.

LAI, X. et al. HMME combined with green light-emitting diode irradiation results in efficient apoptosis on human tongue squamous cell carcinoma. Lasers in Medical Science, v. 30, n. 7, p. 1941–1948, 2015.

LEHNINGER. Principles of Biochemistry, 6th ed. [s.l: s.n.].

LIN, N. et al. The expression of endothelin receptor B in melanoma cells A375 and Sk-mel-1 and the proliferative effects of endothelin 3 on A375 cells. Journal of Huazhong University of Science and Technology - Medical Science, 2007.

LINARES-ESPINÓS, E. et al. New technologies and techniques for prostate cancer focal therapyMinerva Urologica e Nefrologica, 2018.

LØKSE, M. Encyclopædia Britannica Online. Ravnetrykk, 2018.

LUCIA, M. et al. Mycobacterium bovis BCG in metastatic melanoma therapy.

2019.

LUO, D. et al. Chemophototherapy: An Emerging Treatment Option for Solid TumorsAdvanced Science, 2017.

MAUSKOPF, S. H.; MCDONALD, D.; HUNT, L. B. A History of Platinum and Its Allied Metals. Technology and Culture, 1984.

MEEKS, N.; LA NIECE, S.; ESTÉVEZ, P. The technology of early platinum plating: A gold mask of the La Tolita culture, Ecuador. Archaeometry, 2002.

MEHRABAN, N.; FREEMAN, H. S. Developments in PDT sensitizers for increased selectivity and singlet oxygen productionMaterials, 2015.

MEIERJOHANN, S. Oxidative stress in melanocyte senescence and melanoma transformationEuropean Journal of Cell Biology, 2014.

MESQUITA, M. Q. et al. An insight on the role of photosensitizer nanocarriers for photodynamic therapy. Anais da Academia Brasileira de Ciencias, 2018.

MICHY, T. et al. Verteporfin-loaded lipid nanoparticles improve ovarian cancer photodynamic therapy in vitro and in vivo. Cancers, 2019.

MILGROM, L. R. What porphyrins are and what they do. In: The colours of life: an introduction to the chemistry of porphyrinas and related compounds. [s.l: s.n.].

MILLER, K. D. et al. Cancer treatment and survivorship statistics, 2016. CA: A Cancer Journal for Clinicians, v. 66, n. 4, p. 271–289, 2016.

MOKOENA, D. R.; GEORGE, B. P.; ABRAHAMSE, H. Enhancing breast cancer treatment using a combination of cannabidiol and gold nanoparticles for photodynamic therapyInternational Journal of Molecular Sciences, 2019.

MOREIRA, L. H. et al. Use of photodynamic therapy in the treatment of bovine subclinical mastitis. Photodiagnosis and Photodynamic Therapy, 2018.

MORTON, C. A. The emerging role of 5-ALA-PDT in dermatology: is PDT superior to standard treatments? The Journal of dermatological treatment, v. 13 Suppl 1, p. S25–S29, 2002.

MUEHLMANN, L. A. et al. Aluminum-phthalocyanine chloride associated to poly(methyl vinyl ether-co-maleic anhydride) nanoparticles as a new third-generation photosensitizer for anticancer photodynamic therapy. International Journal of Nanomedicine, 2014.

NISHIDA, S. et al. Immune adjuvant therapy using Bacillus Calmette–Guérin cell wall skeleton (BCG-CWS) in advanced malignancies. Medicine, 2019.

NOWAK-STEPNIOWSKA, A.; PERGOL, P.; PADZIK-GRACZYK, A.

Photodynamic Method of Cancer Diagnosis and Therapy--Mechanisms and Applications. Postepy biochemii, v. 59, n. 1, p. 53–63, 2013.

O'CONNOR, A. E.; GALLAGHER, W. M.; BYRNE, A. T. Porphyrin and nonporphyrin photosensitizers in oncology: Preclinical and clinical advances in photodynamic therapyPhotochemistry and Photobiology, 2009.

OMS. Lista Modelo de Medicamentos esenciales de la OMS. Oms, 2013.

ORGANIZAÇÃO MUNDIAL DE SAÚDE - OMS. Guide To Cancer Early DiagnosisWorld Health Organization. [s.l: s.n.]. Disponível em: <http://apps.who.int/iris/bitstream/10665/254500/1/9789241511940-eng.pdf?ua=1>.

PELLOSI, D. S. et al. Magneto low-density nanoemulsion (MLDE): A potential vehicle for combined hyperthermia and photodynamic therapy to treat cancer selectively. Materials Science and Engineering C, v. 92, p. 103–111, 2018.

POÓR, M. et al. Interaction of mycotoxin zearalenone with human serum albumin. Journal of Photochemistry and Photobiology B: Biology, 2017.

RAMÍREZ-GARCÍA, G. et al. Controlling trapping states on selective theranostic core@shell (NaYF4:Yb,Tm@TiO2-ZrO2) nanocomplexes for enhanced NIR-activated photodynamic therapy against breast cancer cells. Dalton Transactions, 2019.

RANGASAMY, S. et al. Mitochondria and DNA Targeting of 5,10,15,20-Tetrakis(7-sulfonatobenzo[b]thiophene) Porphyrin-Induced Photodynamic Therapy via Intrinsic and Extrinsic Apoptotic Cell Death. Journal of Medicinal Chemistry, v. 58, n. 17, p. 6864–6874, 2015.

RKEIN, A. M.; OZOG, D. M. Photodynamic therapy. Dermatologic Clinics, v. 32, n. 3, p. 415–425, 2014.

ROBERTSON, C. A.; EVANS, D. H.; ABRAHAMSE, H. Photodynamic therapy (PDT): A short review on cellular mechanisms and cancer research applications for PDTJournal of Photochemistry and Photobiology B: Biology, 2009.

ROCHA, C. R. R. et al. DNA repair pathways and cisplatin resistance: An intimate relationshipClinics, 2018.

ROFSTAD, E.; LYNG, H. Xenograft model systems for human melanoma. Molecular Medicine Today, v. 2, n. 9, p. 394–403, 1996.

SAINI, R.; POH, C. F. Photodynamic therapy: A review and its prospective role in the management of oral potentially malignant disordersOral Diseases, 2013.

SAVELLANO, M. D.; HASAN, T. Targeting cells that overexpress the epidermal

growth factor receptor with polyethylene glycolated BPD verteporfin photosensitizer immunoconjugates. Photochemistry and photobiology, v. 77, n. 4, p. 431–439, 2003.

SCHMITT, F.; JUILLERAT-JEANNERET, L. Drug targeting strategies for photodynamic therapy. Anticancer Agents Med Chem, v. 12, n. 5, p. 500–525, 2012.

SEEGER MG, RIES AS, GRESSLER LT, BOTTON SA, I. B.; JF, C. In vitro antimicrobial photodynamic therapy using tetra-cationic porphyrins against multidrug-resistant bacteria isolated from canine otitis. Photodiagnosis and Photodynamic Therapy, 2020.

SENGUPTA, D. et al. Benzamide porphyrins with directly conjugated and distal pyridyl or pyridinium groups substituted to the porphyrin macrocycles: Study of the photosensitising abilities as inducers of apoptosis in cancer cells under photodynamic conditions. Journal of Photochemistry and Photobiology B: Biology, v. 178, p. 228–236, 2018.

SETH, R. et al. Systemic Therapy for Melanoma: ASCO Guideline. Journal of Clinical Oncology, 2020.

SHI, J. et al. Cancer nanomedicine: Progress, challenges and opportunitiesNature Reviews Cancer, 2017.

SILVA, A. P. et al. Effects of methylene blue-mediated photodynamic therapy on a mouse model of squamous cell carcinoma and normal skin. Photodiagnosis and Photodynamic Therapy, v. 23, 2018.

SILVA, A. A. DA; GONÇALVES, R. C. Espécies reativas do oxigênio e as doenças respiratórias em grandes animais. Ciência Rural, 2010.

SOSA, V. et al. Oxidative stress and cancer: An overviewAgeing Research Reviews, 2013.

SPERANDIO, F. F.; HUANG, Y.-Y.; HAMBLIN, M. R. Antimicrobial Photodynamic Therapy to Kill Gram-negative Bacteria. Recent Pat Antiinfect Drug Discov, v. 8, n. 2, p. 1–23, 2013.

STORDAL, B.; DAVEY, M. Understanding cisplatin resistance using cellular modelsIUBMB Life, 2007.

TASSO, T. T. et al. Isomeric effect on the properties of tetraplatinated porphyrins showing optimized phototoxicity for photodynamic therapy. Dalton Transactions, v. 46, n. 33, p. 11037–11045, 2017.

to existing neoplasms treatment is fascinating . It is mentioned that porphyrins. p. 1972, 1972.

VROUENRAETS, M. B. et al. Basic principles, applications in oncology and improved selectivity of photodynamic therapyAnticancer Research, 2003.

WANG, D.; LIPPARD, S. J. Cellular processing of platinum anticancer drugsNature Reviews Drug Discovery, 2005.

WANG, X. et al. Photodynamic therapy is an effective adjuvant therapy for image-guided surgery in prostate cancer. Cancer Research, 2020.

WHEATE, N. J. et al. The status of platinum anticancer drugs in the clinic and in clinical trials. Dalton Transactions, 2010.

WHO. WHO _ Cancer.

WILLYARD, C. Risk factors: riddle of the rays. Nature, v. 515, n. 7527, p. S112–S113, 2014.

WITTGEN, H. G. M.; VAN KEMPEN, L. C. L. T. Reactive oxygen species in melanoma and its therapeutic implicationsMelanoma Research, 2007.

XU, H. et al. Triterpenes from *Poria cocos* are revealed as potential retinoid X receptor selective agonists based on cell and *in silico* evidence. Chemical Biology & Drug Design, p. cbdd.13610, 2019.

YOON, I.; LI, J. Z.; SHIM, Y. K. Advance in photosensitizers and light delivery for photodynamic therapy. Clinical Endoscopy, v. 46, n. 1, p. 7–23, 2013.

ZHANG, J. et al. An updated overview on the development of new photosensitizers for anticancer photodynamic therapyActa Pharmaceutica Sinica B, 2018.

ZHEN, S. et al. Drug delivery micelles with efficient near-infrared photosensitizer for combined image-guided photodynamic therapy and chemotherapy of drug-resistant cancer. Biomaterials, 2019.